

DISSERTATION

SYNTHETIC AND DNA CROSS-LINKING STUDIES OF BIOXALOMYCIN  $\alpha_2$

Submitted by

Bradley James Herberich

Department of Chemistry

In partial fulfillment of the requirements  
for the degree of Doctor of Philosophy

Colorado State University

Fort Collins, Colorado

Fall 1999

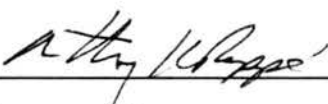
COLORADO STATE UNIVERSITY

July 13, 1999

WE HEREBY RECOMMEND THAT THE DISSERTATION PREPARED UNDER OUR SUPERVISION BY BRADLEY JAMES HERBERICH ENTITLED SYNTHETIC AND DNA CROSS-LINKING STUDIES OF BIOXALOMYCIN  $\alpha_2$  BE ACCEPTED AS FULFILLING IN PART REQUIREMENTS FOR THE DEGREE OF DOCTOR OF PHILOSOPHY.

Committee on Graduate Work

  
\_\_\_\_\_

  
\_\_\_\_\_

  
\_\_\_\_\_

  
\_\_\_\_\_

  
\_\_\_\_\_

Advisor

  
\_\_\_\_\_

Department Head

## ABSTRACT OF DISSERTATION

### SYNTHETIC AND DNA CROSS-LINKING STUDIES OF BIOXALOMYCIN $\alpha_2$

The preparation of a [3 + 2] cycloaddition precursor towards the total synthesis of bioxalomycin  $\alpha_2$  is presented. The route contains four key steps. These include a Staudinger reaction that sets the required *syn* stereochemistry at C-13a and C-13b, a stereoselective Pictet-Spengler reaction, an intramolecular transamidation to open a  $\beta$ -lactam ring, and a regioselective reduction of a diketopiperazine. The cycloaddition product afforded by this route though not amenable to the total synthesis of bioxalomycin  $\alpha_2$ , may be an entry into analogs of bioxalomycin  $\alpha_2$ .

Evidence for interstrand DNA cross-linking induced by bioxalomycin  $\alpha_2$  is outlined. The sequence specificity for the cross-link formation and the alkylated residue of DNA is identified. The requirement of reductive activation of cyanocycline A for DNA cross-linking is presented.

The synthesis of quinocarcin analogs, which contain the *epi* stereochemistry at C-11a, was completed. The analogs were designed to alkylate DNA without any undesired indiscriminate DNA strand scission. When evaluated the analogs demonstrated no evidence of DNA strand scission nor DNA alkylation. From these efforts a new quinocarcin analog, which may have the capacity to alkylate DNA, has been proposed.

Bradley J. Herberich  
Department of Chemistry  
Colorado State University  
Ft. Collins, Colorado 80523  
Fall 1999

## Acknowledgments

The author would like to take this opportunity to thank the faculty and staff of the Department of Chemistry at Colorado State University for supporting him during his tenure as a graduate student. The author would also like to thank Dr. George Ellestad for providing bioxalomycin  $\alpha_2$  and Professor Steve Gould of Oregon State University for a sample of cyanocycline A. A special token of gratitude is extended to Brian Brown, Curt Dvorak, and Dave Hennings for critiquing this dissertation.

The author acknowledges Professor Robert M. Williams for providing lab space and maintaining an intellectual environment conducive to independent thought and creativity.

The author wishes to extend a token of gratitude to all of his colleagues (past and present) in the Williams' research group for their friendship and for creating an intellectual stimulating work environment. The following individuals made significant contributions to this body of work through many helpful scientific discussions: Mark Flanagan, Scott Rajski, Steve Rubenstein, Samuel J. Rollins, Jack Scott, Dave Bender, Jeffrey Cao, Chester Yuan and Dave Hennings.

A special thanks goes out to all of my fellow labmates of B316 ("The Dungeon"). This group endured my occasional singing in close quarters with patience and for this I am very grateful. Although many lessons on chemistry were gained from my labmates, the discussions entertained by this collection of individuals were not only confined to worthy intellectual pursuits, but included conversations that ranged from tedious daily observations to ones that concerned the absurd and outlandish. The most spirited and unusual conversations were often led by Jack Scott and Dave Bender, while Samuel J. Rollins, among others, tried in vain to keep the conversation civilized.

The author would also like to acknowledge his undergraduate advisor, Professor Raymond J. Giguere, whose exceptional teaching made organic chemistry not only

accessible but also entertaining. In addition, Professor Giguere constructed a very strong foundation for a challenging and rewarding graduate career.

Lastly, the author would like to give a special thanks to his parents who were patient and tried to understand the unpredictability of graduate school. In particular, the author's mother attempted to comprehend the frustrations of research and often developed complex theories for an unusual result from just a rough description of an experiment. Although these ideas are not presented in this dissertation, they were very much appreciated.

<u>Contents</u>	<u>page</u>
<b>Chapter 1 Bioxalomycins, Naphthyridinomycin and Cyanocycline</b>	1
1.1 Introduction	1
1.2 Biochemical and Mechanistic Studies of the Bioxalomycins	3
1.3 Synthetic Studies of Naphthyridinomycin and Cyanocycline A	8
1.3.1 Danishefsky's Synthetic Studies of Naphthyridinomycin	9
1.3.2 Evans' Synthesis of ( $\pm$ )-Cyanocycline	12
1.3.3 Fukuyama's Synthesis of ( $\pm$ )-Cyanocycline	15
<b>Chapter 2 DNA Alkylation Studies of Quinocarcin Analogs</b>	21
2.1 Introduction and Design of Quinocarcin Analogs	21
2.2 Synthesis of Water-Soluble <i>epi</i> -Quinocarcin Analogs	29
2.3 Evaluation of <i>epi</i> -Quinocarcin Analogs	33
2.4 Future Work	37
<b>Chapter 3 DNA Cross-Linking Studies of Bioxalomycin <math>\alpha_2</math></b>	39
3.1 Introduction	39
3.2 DNA-Bioxalomycin $\alpha_2$ Interstrand Cross-Link Formation	41
3.3 DNA Cross-Linking Induced by Cyanocycline A	46
3.4 Conclusion	48
<b>Chapter 4 Synthetic Studies Towards Bioxalomycin <math>\alpha_2</math></b>	52
4.1 Introduction and Initial Strategy	52
4.2 Synthesis of Isoquinoline 180	55

4.3 Mannich Reaction Attempts	60
4.4 Aldol and $\beta$ -Lactam Routes	62
4.5 Second Generation $\beta$ -Lactam Route	70
4.6 Intramolecular [3 + 2] Cycloaddition Attempts	74
4.7 Alternate Routes	79
4.8 Asymmetric Route	82
4.9 Conclusion	86
<b>References</b>	90
<b>Experimental Section</b>	97
5.1 General procedures	97
5.2 Preparation of compounds	101
<b>Appendix 1 Nuclear Overhauser Effect Experiments</b>	222
<b>Appendix 2 Crystal Structure of <math>\beta</math>-Lactam 204</b>	233
<b>Appendix 3 Mass Spectra of Bioxalomycin <math>\alpha_2</math>-DNA Adduct</b>	240
<b>Appendix 4 Molecular Modeling of Bioxalomycin <math>\alpha_2</math>-DNA Binding</b>	242
<b>Appendix 5 Publication List</b>	245
<b>Appendix 6 Research Proposal</b>	248

There is a fine line between stupid and clever.

- David St. Hubbins

## Chapter 1

### Bioxalomycins, Naphthyridinomycin and Cyanocycline A

#### 1.1 Introduction

The bioxalomycins (**1-4**) are a class of anti-tumor antibiotics produced by *Streptomyces viridostaticus* ssp. "litoralis",<sup>1</sup> which are structurally similar to naphthyridinomycin (**5**)<sup>2</sup> and cyanocycline A(**6**) (Figure 1).<sup>3</sup> The bioxalomycins are characterized by a congested heptacyclic core containing two oxazolidine rings, a bridged piperazine ring, and an aromatic ring at the hydroquinone (**1, 2**) or non-aromatic quinone (**3, 4**) oxidation states. Naphthyridinomycin (**5**) and cyanocycline A (**6**) differ from the bioxalomycins by having one of the oxazolidine rings hydrolyzed and an alcohol or cyano substituent at C-7 for **5** and **6**, respectively.

Naphthyridinomycin was isolated from *Streptomyces lusitanus* as a ruby red crystalline compound that decomposes upon storage. The structure of naphthyridinomycin was determined by x-ray analysis by Sygusch, *et al.* in 1974 and later revised to the structure depicted in Figure 1.<sup>4</sup> In the isolation paper of the bioxalomycins, Ellestad and co-workers postulated that bioxalomycin  $\beta_2$  (**4**) is the actual biosynthetic product of *Streptomyces lusitanus* and the diol structure assigned to **5** is an artifact of the original acidic isolation technique.<sup>1</sup> To investigate this possibility, the isolation protocol used for the bioxalomycins by Ellestad and co-workers was used to isolate naphthyridinomycin from *S. lusitanus*. Instead of isolating naphthyridinomycin, the only compound isolated was bioxalomycin  $\beta_2$ , which led Ellestad and co-workers to conclude that naphthyridinomycin is an artifact of the earlier isolation protocol. Cyanocycline A(**6**) was isolated from *Streptomyces flavogriseus* as orange needles and can be prepared from

bioxalomycin  $\beta_2$  by the addition of KCN.<sup>1</sup> Due to the lack of stability of naphthyridinomycin, Zmijewski, Jr. and Goebel demonstrated that the more stable cyanocycline can also be prepared from naphthyridinomycin by the addition of NaCN.<sup>5</sup>

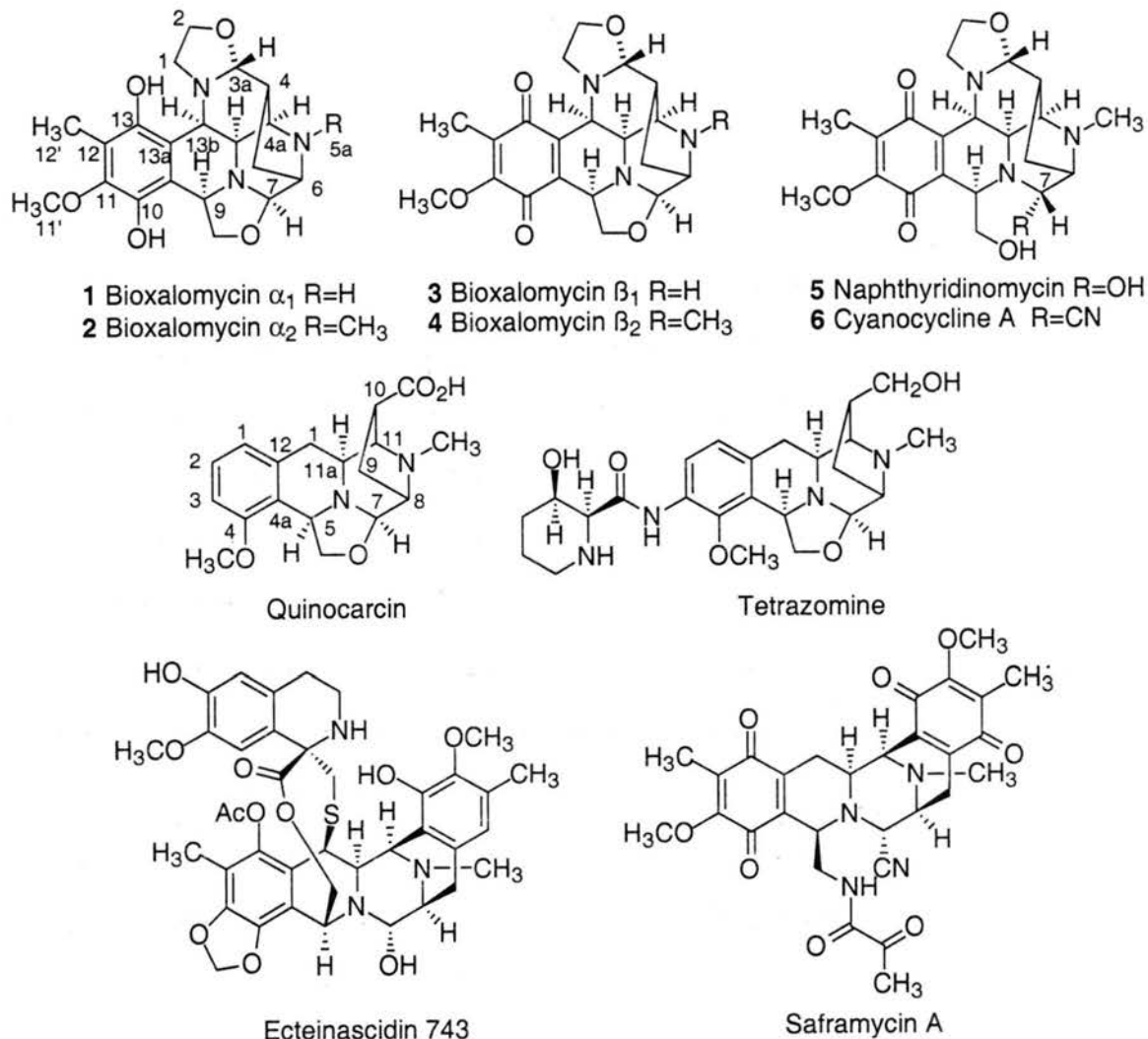


**Figure 1.** The bioxalomycins and related compounds.

Due to the interesting molecular framework of the bioxalomycins and its similarity to quinocarcin, an antitumor antibiotic that has been investigated in the Williams' group, the total synthesis and biological assays of bioxalomycin  $\alpha_2$  were examined.

Starting with the synthetic knowledge gained from the syntheses of quinocarcin and its analogs (Chapter 2), a route was proposed towards the bioxalomycin framework. The

key step in the route towards quinocarcin is a [3+2] cycloaddition reaction between an azomethine ylide and an activated olefin to form the bridged piperazine framework. After numerous revisions, an efficient synthesis of a [3+2] precursor to bioxalomycin  $\alpha_2$  has been developed (Chapter 4). In addition to these synthetic efforts, the binding of bioxalomycin  $\alpha_2$  to DNA has been investigated and is discussed in Chapter 3.

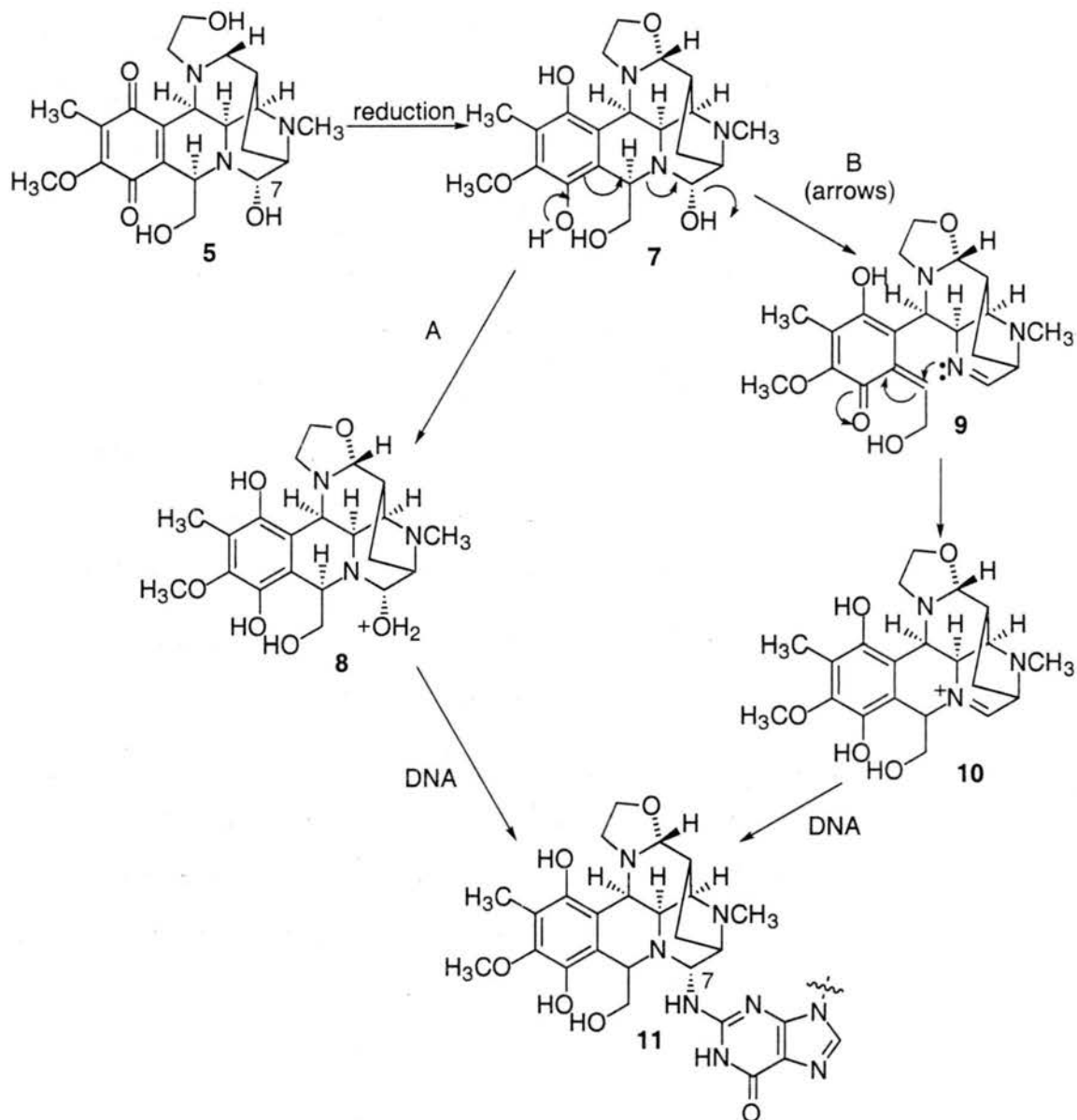
## 1.2 Biochemical and Mechanistic Studies of the Bioxalomycins

Naphthyridinomycin demonstrated antimicrobial activity against gram-positive and gram-negative bacteria.<sup>2</sup> It inhibited growth of *E. coli* and *S. epidermis* at low concentrations, while leakage of cellular material (lysis) only occurred at high levels of the antibiotic.<sup>6</sup> The incorporation of radiolabeled leucine, thymidine and uridine into *E. coli* was carried out to see the effect of **5** on macromolecular synthesis.<sup>6,7</sup> At low levels of **5** (<0.05  $\mu\text{g/ml}$ ), only the incorporation of thymidine was inhibited. At higher levels of the antibiotic (>0.5  $\mu\text{g/ml}$ ), the incorporation of radiolabelled leucine and uridine was also inhibited. From these studies the antibacterial activity of naphthyridinomycin was concluded to be a manifestation of its ability to inhibit DNA synthesis.

Similar studies using radiolabelled leucine, thymidine and uridine have been carried out with cyanocycline A and bioxalomycin  $\alpha_2$ ; inhibition of DNA synthesis, was again concluded to be the major effect of these two antibiotics on *E. coli*.<sup>8</sup>

More extensive *in vitro* studies of naphthyridinomycin's reactivity towards DNA were initiated by Zmijewski, *et al.*<sup>7</sup> Dialysis experiments with [<sup>3</sup>H]naphthyridinomycin and calf thymus DNA under neutral conditions showed only small amounts of covalently bound [<sup>3</sup>H]naphthyridinomycin. However under reducing conditions with dithiothreitol or acidic conditions (pH=5), irreversible binding of [<sup>3</sup>H]naphthyridinomycin was observed. Experiments with poly(dG)- poly(dC) and poly (dA)- poly(dT) polydeoxyribonucleic acids showed that **5** bound most effectively to GC-rich regions of DNA. In subsequent studies it was found that **5** does not bind to poly(dI)- poly(dC) polydeoxyribonucleic acids. Since

inosine lacks the exocyclic amine of guanine, the authors concluded that **5** alkylated the exocyclic amine of guanine in the minor groove of DNA.<sup>9</sup> From these experiments two mechanisms for the alkylation of DNA by **5** were postulated (Scheme 1).



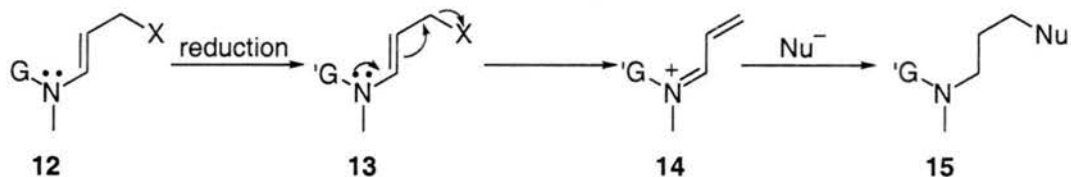
**Scheme 1.** Proposed mechanisms of binding of naphthyridinomycin with DNA.<sup>9</sup>

These mechanisms are based on an earlier proposed mechanism for DNA alkylation by a structurally related isoquinoline anti-tumor drug, saframycin A (Figure 1).<sup>10</sup> For the two proposed mechanisms for **5**, the first step is reductive activation resulting in

hydroquinone **7**. In the first mechanism, protonation of the alcohol moiety at C-7 followed by nucleophilic attack by guanine would give the DNA-naphthyridinomycin adduct **11** (path A, Scheme 1).

The second mechanism involves deprotonation of the hydroquinone and elimination of the alcohol moiety to form imine **9** (path B, Scheme 1). Imine **9** could then attack the quinone methide to furnish the highly reactive iminium ion **10**, which could then be alkylated by DNA. Protonation of the carbinolamine of **5**, and elimination would give the same iminium species **10** and may account for the activity of **5** under non-reducing, acidic conditions. Interestingly, studies on cyanocycline A showed no dependence on reductive activation prompting the authors to conclude that the mechanism for binding to DNA for cyanocycline A differs from that of naphthyridinomycin.<sup>8a</sup>

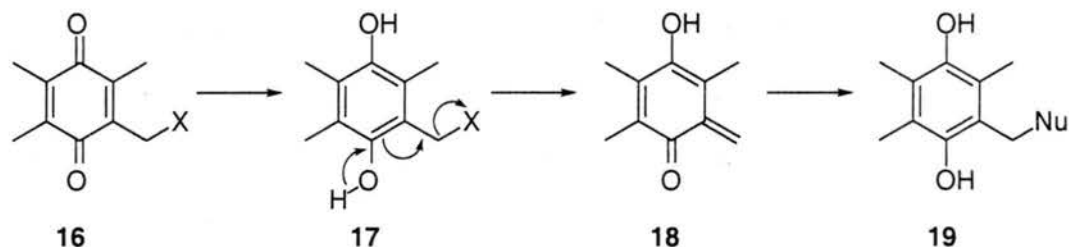
Another mechanism for the alkylation of DNA was proposed by Moore in a brief review on the bioactivation of drugs, in which he emphasized the importance of bioreduction as an important *in vivo* mode of activation for alkylating agents.<sup>11</sup> In this concept, an electron-deficient functional group is reduced, becoming electron-rich thus reversing the polarity of the drug. An example is shown in Scheme 2, where the lone pair of electrons of the enamine in **12** is tied up in G, an electron sink. After reduction of G to 'G, the nitrogen lone pair can displace leaving group X, forming electrophilic iminium ion **14**. A nucleophilic center on a biomolecule can then be alkylated to form **15**.



**Scheme 2.** General scheme of bioreductive activation.<sup>11</sup> Key: G= electron sink, G'= electron releasing group, X= leaving group, Nu= nucleophilic center on a biomolecule.

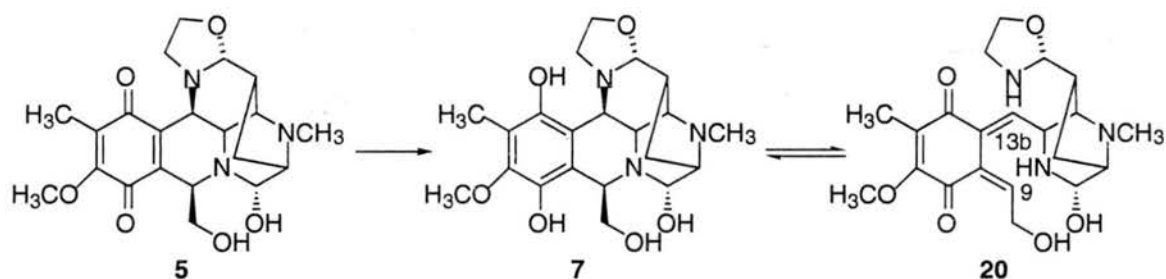
The quinone methide model, which has been suggested and investigated by Sartorelli, Lin and co-workers, follows the bioreductive concept.<sup>12</sup> In this model, a

benzoquinone, which has a leaving group at the benzyl position, is reduced to hydroquinone **17** (Scheme 3). Subsequent loss of HX would give quinone methide **18**, which would act as an alkylating agent via a conjugate addition reaction.



**Scheme 3.** Quinone methide model presented by Sartorelli, Lin and coworkers.<sup>12</sup>

Using the quinone methide model, Moore postulated a mechanism for the alkylation at two sites of naphthyridinomycin. In this mechanism, reductive activation of the quinone gives hydroquinone **7**, which can be deprotonated and displace the oxazolidine and amine resulting in the bis-ortho quinone methide **20**. The amino moieties of **20** could then add to the quinone methide giving back **7** or DNA could attack at C-9 or C-13b to give the alkylated product.

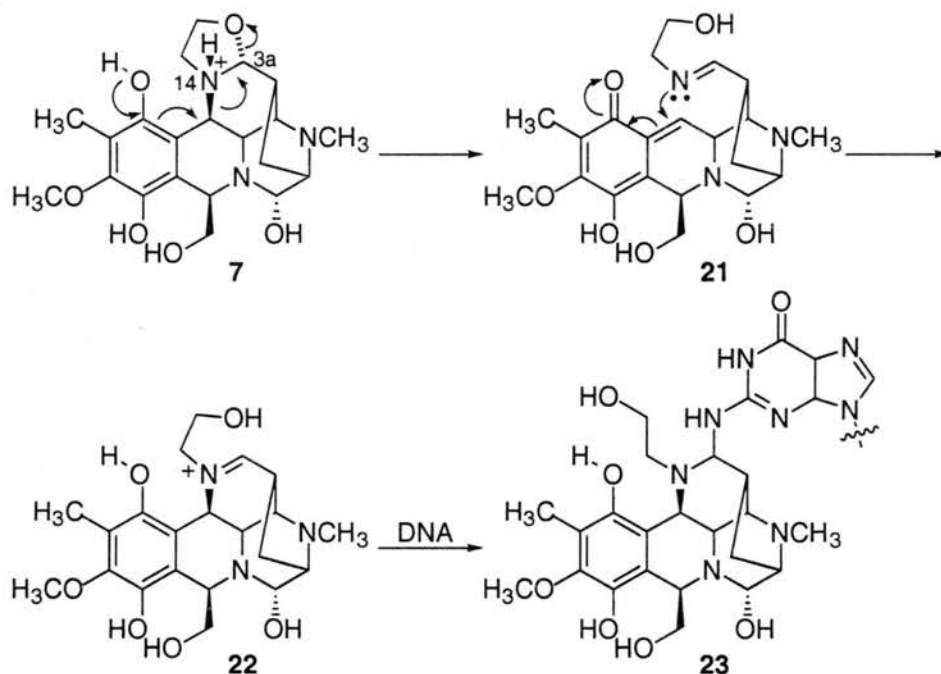


**Scheme 4.** Mechanism of DNA alkylation by naphthyridinomycin at C-9 and C-13b proposed by Moore.<sup>11</sup>

Two molecular modeling studies simulated the binding of **5** at C-7 and C-3a to the exocyclic amine of guanine in the minor groove, which was suggested earlier by Zmijewski and co-workers (Scheme 1).<sup>13</sup> Unfortunately, neither of these studies were concerned with the potential electrophilic sites at C-13b and C-9 of **5** proposed by Moore.

In one study, Cox, *et al.* visually docked **5** and various analogs with 16 different DNA heptamers via a partial intercalation approach.<sup>13a</sup> Both enantiomers of the drug were used and covalently bound between C-7 of **5** and the exocyclic amine of the guanine residue and the resulting structure minimized using an Amber force field. The authors found that the drug with the revised structure,<sup>4b</sup> and the *R* configuration at C-7 formed a better adduct with DNA. The authors also calculated a preference for the sequence 5'-ATGCAT-3' in net binding energy and helix distortion energy.

The other study conducted by Remers and co-workers, examined the possibility of DNA alkylation by **5** at C-3a.<sup>13b</sup> The authors postulated that the mechanism for DNA alkylation at C-7 by Zmijewski could be extended to C-3a of **5**. In this analogous mechanism (Scheme 5), the hydroquinone of **7** is deprotonated, which results in opening of the oxazolidine and formation of imine **21**. The imine could then add to the quinone methide moiety, forming iminium ion **22**, which is then alkylated by the exocyclic amine of guanine.



**Scheme 5.** Proposed mechanism of alkylation of C-3a of naphthyridinomycin.<sup>13b</sup>

Before modeling the bonding of **5** to DNA, it was important to know the extent and the site of protonation at pH 7. Remers established the pKa of cyanocycline A to be 6.6, which indicated that there would be 25% protonation at pH 7. NMR experiments demonstrated that N-14 of **6** is protonated preferentially over the other amines, and is shown protonated in the previous mechanism (Scheme 5).

In all of the modeling studies the DNA sequence 5'-ATGCAT-3' was used. Alkylation at C-7 and C-3a of **5** was modeled and it was found that it was not only physically feasible for **5** to be alkylated by DNA at C-7 but also at C-3a. The modeling showed that the possibility of DNA cross-linking by **5** at C-7 and C-3a was not permitted due to the geometry of **5**.

The three proposed mechanisms for DNA alkylation by Zmijewski, Moore, and Remers gave a total of four different electrophilic carbons (Figure 2). The possibility of DNA cross-linking by naphthyridinomycin was concluded to be not permitted geometrically and not investigated experimentally.

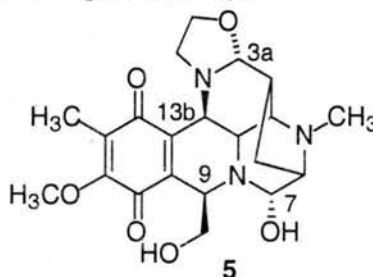


**Figure 2.** Possible alkylation sites, C-3a, C-7, C-9, and C-13b, of naphthyridinomycin identified in previous mechanisms.<sup>9, 11, 13b</sup>

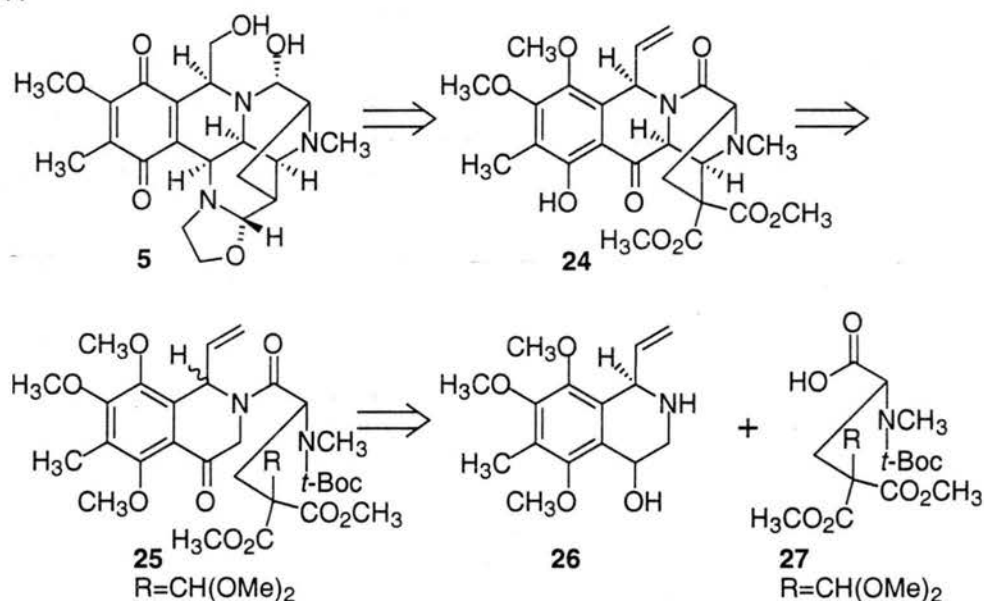
### 1.3 Synthetic Studies of Naphthyridinomycin and Cyanocycline A

In addition to the studies of the mechanism of action of these antibiotics, total syntheses have been attempted. The framework poses a formidable synthetic challenge to the organic chemist due to its congested ring system, its numerous stereocenters and its functionality.

Total syntheses of naphthyridinomycin have been attempted by the Fukuyama, Evans, and Danishefsky research groups.<sup>14</sup> None of these syntheses were successful due to the high instability of naphthyridinomycin. On the other hand, Fukuyama and Evans were able to prepare ( $\pm$ )-cyanocycline A (**6**) following similar strategies used in their attempts to synthesize naphthyridinomycin.<sup>15</sup>

### 1.3.1 Danishefsky's Synthetic Studies of Naphthyridinomycin

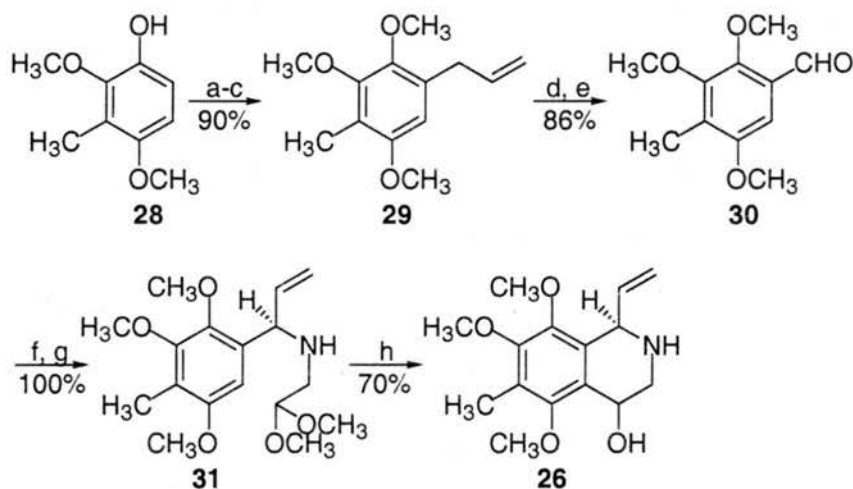
Although Danishefsky was not able to synthesize naphthyridinomycin, the route is interesting and merits discussion. The synthesis is based on an intramolecular Mannich reaction of **25** in which two rings are formed and two stereocenters are set (Scheme 6). Ketone **25** is prepared via the coupling between tetrahydroisoquinoline **26** and carboxylic acid **27**.



**Scheme 6.** Retrosynthetic analysis of Danishefsky's approach to ( $\pm$ )-naphthyridinomycin.<sup>14d, 14e</sup>

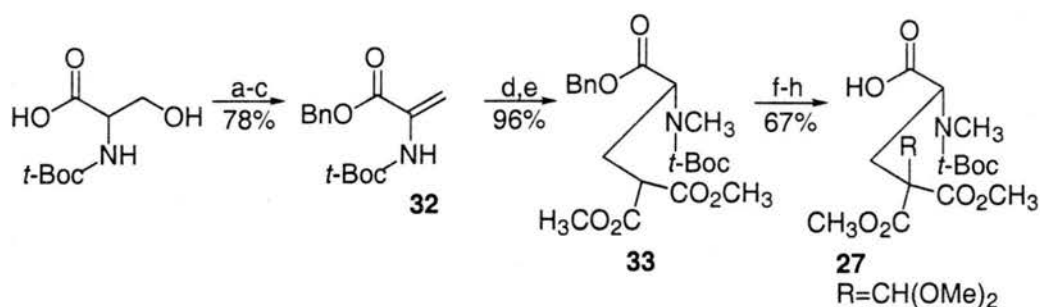
The preparation of **26** started with the formation of the allyl ether of phenol **28**, which underwent a Claisen rearrangement upon heating (Scheme 7). The resulting phenol was protected as the methyl ether to yield **29**. The double bond was isomerized using

$\text{PdCl}_2(\text{CH}_3\text{CN})_2$  to give the more substituted olefin, which underwent ozonolysis to prepare aldehyde **30** in 5 steps from **28** in 77% yield. In the presence of aminoacetaldehyde dimethylacetal under dehydrating conditions, the imine of **30** was made, and then underwent 1,2-addition with vinyl magnesium bromide to give **31**. Under acidic conditions, **31** was converted into **26** in 70% yield.



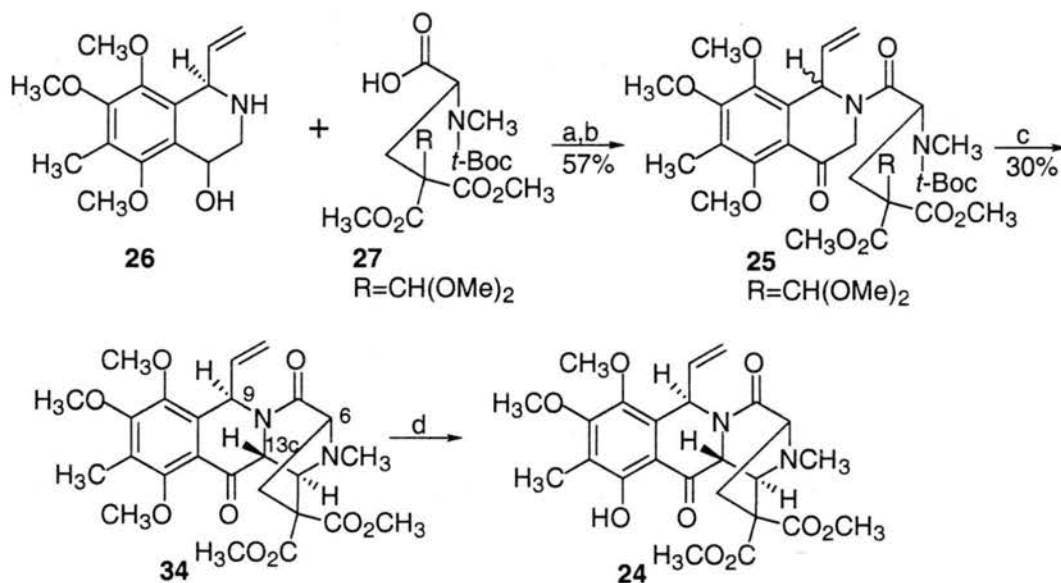
**Scheme 7.** Synthesis of tetrahydroisoquinolinol **26**.<sup>14d</sup> Key: (a) NaH, allyl bromide, DMF; (b) *N,N*-dimethylaniline, 180 °C; (c) NaH, MeI, DMF; (d)  $\text{PdCl}_2(\text{CH}_3\text{CN})_2$ ,  $\text{CH}_2\text{Cl}_2$ ; (e)  $\text{O}_3$ , MeOH, -78 °C; (f)  $\text{NH}_2\text{CH}_2\text{CH}(\text{OCH}_3)_2$ , benzene, reflux, Dean-Stark trap; (g)  $\text{CH}_2\text{CHMgBr}$ ; (h) 6M HCl.

The synthesis of carboxylic acid **27** started with commercially available *t*-Boc serine (Scheme 8). The benzyl ester of *t*-Boc serine was prepared under basic conditions with benzyl bromide and the alcohol activated as the tosylate and eliminated to give dehydroalanine benzyl ester **32**. Methylation of the nitrogen of the carbamate followed by a Michael addition of sodium dimethyl malonate led to **33**. The critical protected aldehyde moiety was added by alkylating the enolate of **33** with 2-chloro-1,3-dithiane. The dithiane was re-protected as the dimethyl acetal with the addition of NBS and  $\text{AgNO}_3$  in MeOH, and the benzyl ester was hydrogenated to give carboxylic acid **27**.



**Scheme 8.** Synthesis of intermediate **27**.<sup>14d</sup> Key: (a) BnBr, NEt<sub>3</sub>, acetone, reflux; (b) TsCl, pyr., -5 °C; (c) HNEt<sub>2</sub>, Et<sub>2</sub>O-EtOAc; (d) KH, MeI, Et<sub>2</sub>O; (e) (CO<sub>2</sub>CH<sub>3</sub>)<sub>2</sub>CHNa; (f) LDA, THF, then 2-chloro-1,3-dithiane; (g) NBS, AgNO<sub>3</sub>, MeOH; (h) H<sub>2</sub>, Pd/C, EtOAc.

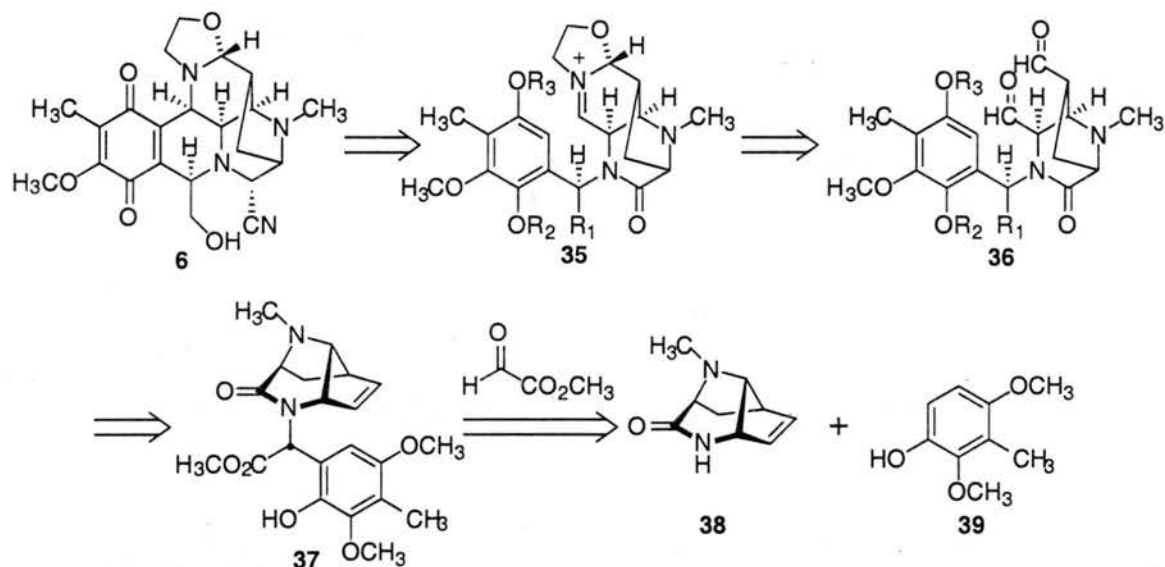
Danishefsky found that BOPCl was the only coupling reagent to form the amide bond between **26** and **27** (Scheme 9).<sup>16</sup> The crude acylation product was then oxidized to the ketone using Collins reagent resulting in a 1:1 mixture of diastereomers of **25**. The next step was the key intramolecular Mannich reaction, in which BF<sub>3</sub>·OEt<sub>2</sub> was added to **25** in CHCl<sub>3</sub> and the reaction heated at reflux. The only tetracyclic compound isolated was **34**, which has the *epi*-stereochemistry at C-13c. Interestingly, of the two diastereomers of **25**, only the stereoisomer with the correct stereochemistry at C-6 and C-9 underwent the cyclization. The methyl ether was then deprotected to give phenol **24**, whose X-ray crystal structure established the relative stereochemistry of the cyclization.



**Scheme 9.** Danishefsky's route to naphthyridinomycin.<sup>14e</sup> Key: (a) BOPCl, NEt<sub>3</sub>; (b) CrO<sub>3</sub>, pyridine; (c) BF<sub>3</sub>·OEt<sub>2</sub>, CHCl<sub>3</sub>, reflux; (d) BBr<sub>3</sub>, CH<sub>2</sub>Cl<sub>2</sub>.

### 1.3.2 Evans' Synthesis of (±)-Cyanocycline A

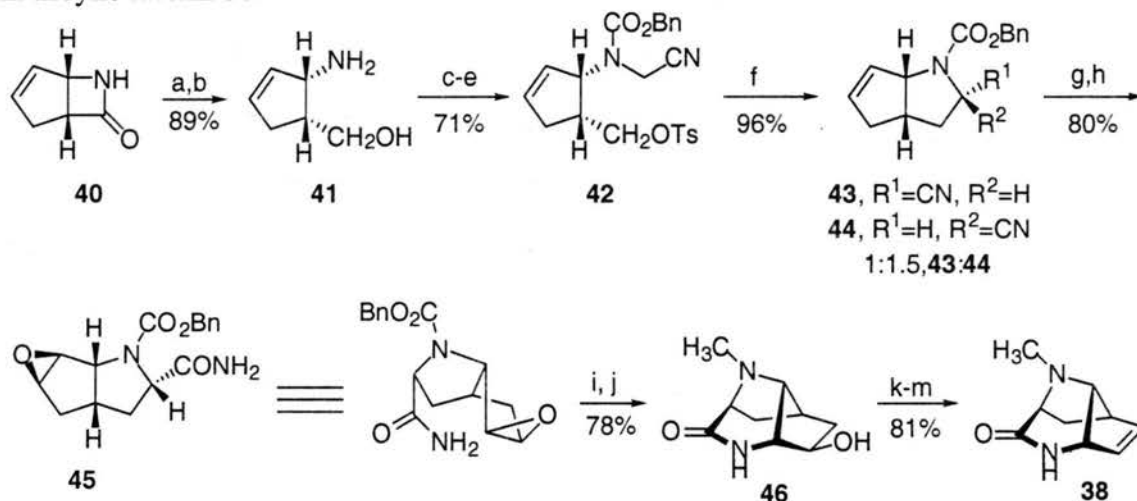
The first total synthesis of (±)-cyanocycline A was reported by Evans, *et al.*, in 1986.<sup>15b</sup> In this synthesis, Evans uses tricyclic lactam **38**,<sup>14b</sup> which was prepared earlier in his attempt to synthesize naphthyridinomycin (Scheme 10). In the first key step, tricyclic lactam **38** was envisioned to be coupled with methyl glyoxylate and 3-methyl-2,4-dimethoxyphenol to give **37**. The olefin could then be oxidized to unmask dialdehyde **36**, which could then undergo a Pictet-Spengler reaction in the presence of *O*-TBS-protected ethanolamine to give the hexacyclic core of cyanocycline. Reduction of the lactam and oxidation of the aromatic ring would then finish the synthesis of (±)-cyanocycline A.



**Scheme 10.** Retrosynthetic Analysis of Evans' Approach to (±)-cyanocycline A.<sup>15b</sup>

The synthesis of the tricyclic lactam **38** started with  $\beta$ -lactam **40**<sup>17</sup> which was opened under acidic conditions and the resulting methyl ester reduced using  $\text{LiAlH}_4$  to afford **41** (Scheme 11). A cyanomethyl moiety was added ( $\text{NaCN}$ ,  $\text{CH}_2\text{O}\cdot\text{NaHSO}_3$ ), and the resulting secondary amine was protected with a benzyloxycarbonyl group. The primary alcohol was then activated as a tosylate group. The tosylate of **42** was displaced

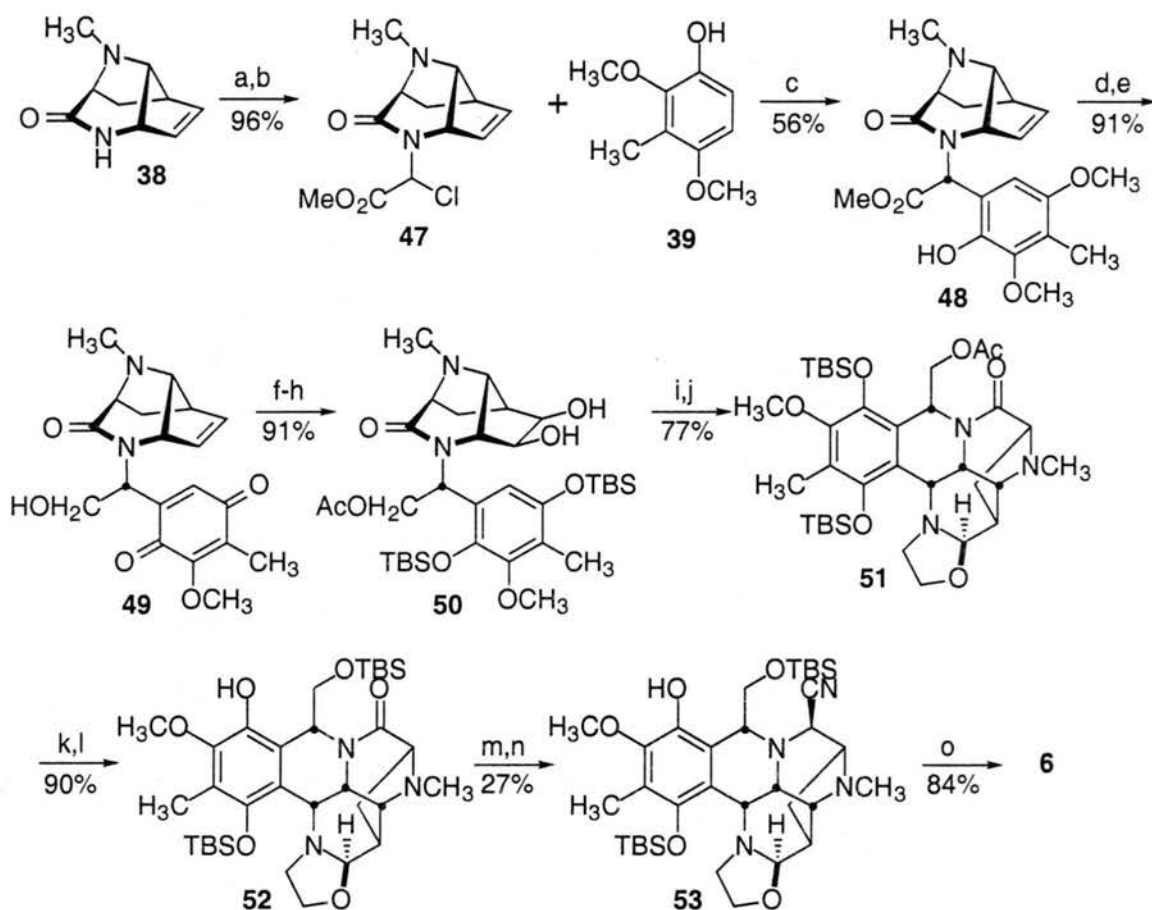
intramolecularly by generation of the anion  $\alpha$ - to the nitrile, generated by addition of KO $t$ -Bu to give the [3.3.0] ring system as a 1:1.5 mixture of diastereomers (**43** and **44**). The epoxide was formed regioselectively from the less hindered convex face of **43** using MCPBA and the nitrile was hydrolyzed to the primary amide to afford **45** in 80% yield. The amine was deprotected and methylated in one step under hydrogenolysis conditions in the presence of formaldehyde. At this point, epoxide **45** was opened intramolecularly via the attack of the amide anion to give the tricyclic core of **46**. The alcohol had to be eliminated, and this was accomplished by first transforming it to the mesylate, which was displaced by phenylselenide. The phenylselenide was then oxidatively eliminated resulting in tricyclic lactam **38**.



**Scheme 11.** Synthesis of tricyclic lactam **38**.<sup>14b</sup> Key: (a) MeOH, HCl; (b) Na<sub>2</sub>CO<sub>3</sub>, H<sub>2</sub>O, LiAlH<sub>4</sub>, Et<sub>2</sub>O; (c) NaCN, CH<sub>2</sub>O·NaHSO<sub>3</sub>, MeOH, H<sub>2</sub>O.; (d) CbzCl, Et(*i*-Pr)<sub>2</sub>N, CH<sub>2</sub>Cl<sub>2</sub>, 0 °C; (e) TsCl, pyr, 5 °C; (f) *t*-BuOK, *t*-BuOH, THF, 25 °C; (g) MCPBA, CH<sub>2</sub>Cl<sub>2</sub>; (h) H<sub>2</sub>O<sub>2</sub>, acetone, reflux; (i) H<sub>2</sub>, Pd/C, CH<sub>2</sub>O; (j) *t*-BuOK, *t*-BuOH; (k) MeSO<sub>2</sub>Cl, Et<sub>3</sub>N, CH<sub>2</sub>Cl<sub>2</sub>; (l) PhSeSePh, NaBH<sub>4</sub>, EtOH, 80 °C; (m) *t*-BuOOH, CHCl<sub>3</sub>.

Tricyclic lactam **38** was condensed with methyl glyoxylate, forming an iminium ion which was treated with SOCl<sub>2</sub> to furnish **47** (Scheme 12). In a key carbon-carbon bond-forming reaction, SnCl<sub>4</sub> was added to **47** in the presence of phenol **39** resulting in a mixture of products including **48** in 56% yield. The ester was then reduced (LiBEt<sub>3</sub>H, THF) and the phenol oxidized using DDQ to afford quinone **49**. The primary alcohol was

acylated ( $\text{Ac}_2\text{O}$ , pyridine, DMF), and the quinone was reduced and protected as the bis-TBS protected hydroquinone in one step using  $\text{ZnCl}_2$  and TBSCl. The olefin moiety was then dihydroxylated with  $\text{OsO}_4$  to yield diol **50**. Oxidation to dialdehyde **36** was difficult due to the instability of **36**, so instead the workers chose to oxidize to the dialdehyde in the presence of *O*-TBS-protected ethanolamine to give an amino diol, which underwent a Pictet-Spengler reaction under acidic conditions to produce hexacyclic lactam **51** in 77% yield. At this point, removal of the acetate protecting group using  $\text{LiEt}_3\text{BH}$  followed by a silyl migration under basic conditions was carried out to furnish phenol **52**. The free phenol was necessary to suppress an unwanted Birch reduction in the next step. A number of reducing agents were tried, but only lithium in ammonia reduced the lactam of **52** resulting in the desired unstable carbinolamine, which was immediately reacted with NaCN to afford nitrile **53**. The hydroquinone moiety was then deprotected (HF, pyridine) and oxidized in the presence of oxygen to complete the synthesis of **6**. Thus the total synthesis of ( $\pm$ )-cyanocycline A was accomplished in 29 steps and 1.1% overall yield.

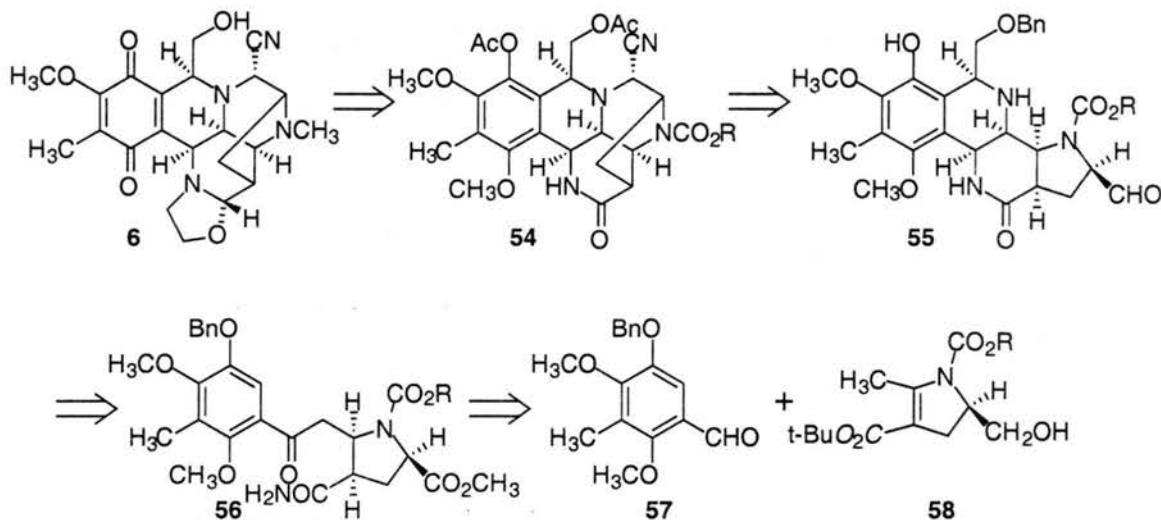


**Scheme 12.** Completion of (±)-cyanocycline by Evans. Key: (a) Methyl glyoxylate,  $\text{CH}_2\text{Cl}_2$ ; (b) Thionyl chloride,  $\text{CH}_2\text{Cl}_2$ ; (c)  $\text{SnCl}_4$ ,  $\text{CH}_2\text{Cl}_2$ ,  $0^\circ\text{C}$  to  $25^\circ\text{C}$ ; (d)  $\text{LiBEt}_3\text{H}$ , THF; (e) DDQ,  $\text{CH}_3\text{CN}-\text{H}_2\text{O}$ ,  $-5^\circ\text{C}$ ; (f)  $\text{Ac}_2\text{O}$ , Pyr, DMAP,  $0^\circ\text{C}$ ; (g) Zn dust, *i*- $\text{Pr}_2\text{NEt}$ , TBSCl,  $\text{CH}_2\text{Cl}_2$ ; (h)  $\text{OsO}_4$ , NMO, acetone; (i)  $\text{Et}_4\text{NIO}_4$ ,  $\text{H}_2\text{NCH}_2\text{CH}_2\text{OTBS}$ ,  $\text{CH}_2\text{Cl}_2$ ; (j) TFA; (k)  $\text{LiBEt}_3\text{H}$ , THF; (l)  $\text{KN}(\text{Me}_3\text{Si})_2$ , THF,  $0^\circ\text{C}$ ; (m) Li,  $\text{NH}_3$ -THF,  $-33^\circ\text{C}$ ; (n) NaCN, pH 8.0 Tris buffer,  $\text{CH}_3\text{CN}$ ; (o)  $(\text{HF})_x\text{.pyr}(x_s)$ ,  $\text{CH}_3\text{CN}$ ; then  $\text{Na}_2\text{CO}_3$  to pH 10,  $\text{O}_2$ .

### 1.3.3 Fukuyama's Synthesis of (±)-Cyanocycline A

Shortly after the Evans' synthesis, Fukuyama, *et al.*, completed a total synthesis of (±)-cyanocycline A in 1987.<sup>15a</sup> The retrosynthetic analysis is shown in Scheme 13. The first key step in Fukuyama's synthesis is the addition of the  $\gamma$ -enolate of **58**, to benzaldehyde **57** (Scheme 13).<sup>18</sup> Formation of the lactam and a Pictet-Spengler reaction would give **55**. The aldehyde of **55** could then be condensed with the free amine to form

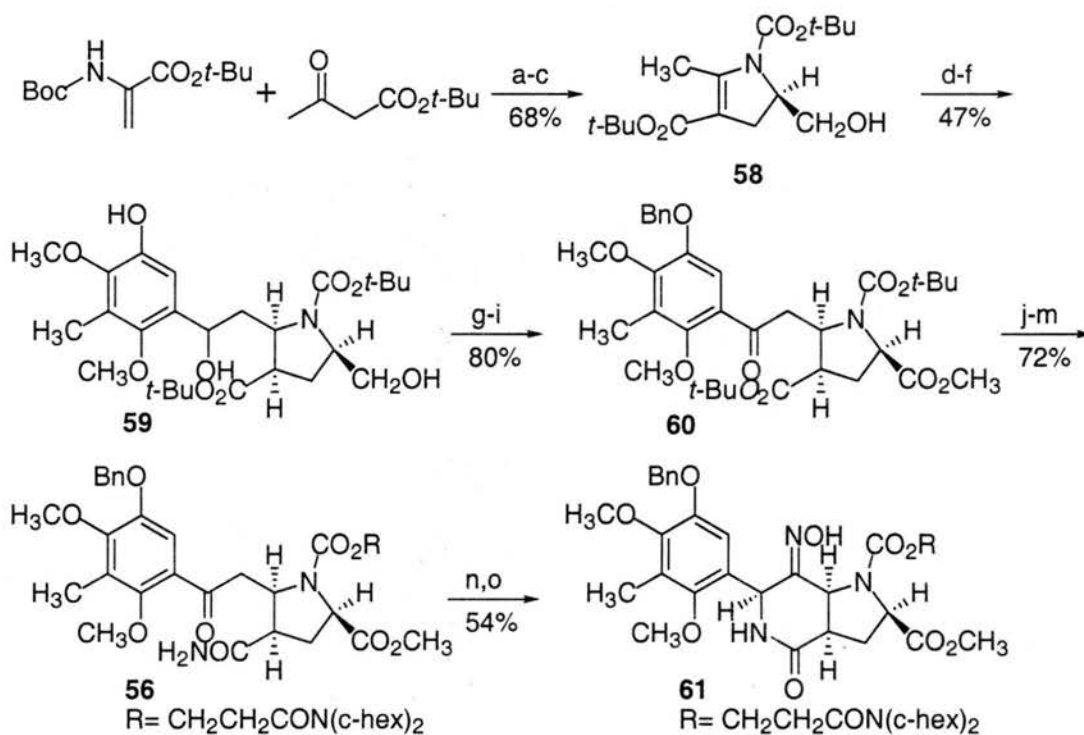
the main pentacyclic structure (**54**) of cyanocycline. From **54**, all that was needed to prepare **6** was to construct the oxazolidine ring and oxidize the aromatic ring to the quinone.



**Scheme 13.** Retrosynthetic analysis of Fukuyama's approach to (±)-cyanocycline A.<sup>15a</sup>

Dihydropyrrole **58** was constructed in a 3-step sequence starting with *N*-*t*-Boc-dehydroalanine-*t*-butyl ester, which underwent a Michael addition by the enolate of *t*-butyl acetoacetate (Scheme 14). The resulting ketone was condensed under acidic conditions (*p*-TsOH, toluene) to afford the dihydropyrrole ring. The *t*-butyl ester was reduced to afford alcohol **58**. The addition of the zinc dienolate of **58** to aldehyde **57**, followed by hydrogenolysis of the benzyl protecting group using Pd/C, followed by hydrogenation of the tetra-substituted olefin with Rh/C furnished the desired *syn*-stereochemistry of **59**. The free phenol was then reprotected as the benzyl ether and the secondary and primary alcohols oxidized to the ketone and carboxylic acid respectively, under Jones oxidation conditions. The carboxylic acid moiety was esterified to the methyl ester under basic conditions to give **60**. The *t*-Boc protecting group on the amine was removed and the *t*-butyl ester hydrolyzed using TFA in one step. At this point a unique protecting group was used for the protection of the amine. The protecting group had to be stable to acidic, basic

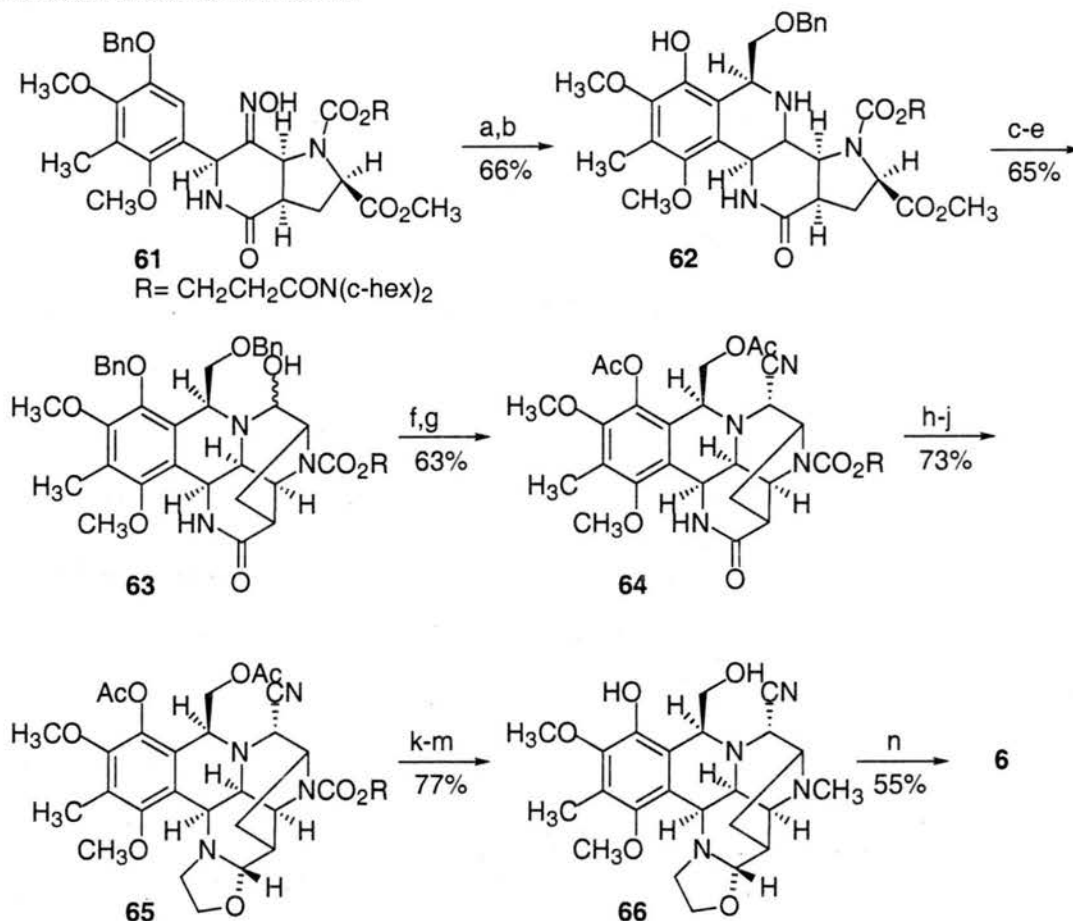
and reductive conditions, yet removed under mild conditions. Fukuyama chose to protect the amine by treating it with *N,N*-dicyclohexyl-3-chlorocarboxy-propanamide. After protection of the amine, the amide of the carboxylic acid was formed by the addition of ammonia to the mixed anhydride of the acid to prepare **56**. Under acidic conditions, attack of the amide on the ketone moiety produced an ene lactam, which was oxidized with nitrosyl chloride, and the resultant  $\alpha$ -chloro oxime was reduced to afford oxime **61**.



**Scheme 14.** Key: (a) NaOEt, EtOH; (b) *p*-TsOH, quinoline, toluene, reflux, Dean-Stark trap; (c) LiBEt<sub>3</sub>, THF; (d) LDA, THF, -78 °C, then ZnCl<sub>2</sub>, then **57**; (e) H<sub>2</sub> (1000 psi), 10% Pd/C, EtOH; (f) H<sub>2</sub> (1500 psi), 5% Rh/C, EtOAc, 80 °C; (g) BnBr, K<sub>2</sub>CO<sub>3</sub>, acetone, reflux; (h) Jones oxidation, acetone, 0 °C; (i) MeI, K<sub>2</sub>CO<sub>3</sub>, acetone, reflux; (j) 2% TFA, CH<sub>2</sub>Cl<sub>2</sub>, reflux; (k) ClCO<sub>2</sub>CH<sub>2</sub>CH<sub>2</sub>CON(c-hex)<sub>2</sub>, *i*-Pr<sub>2</sub>NEt, CH<sub>2</sub>Cl<sub>2</sub>, 0 °C; (l) TFA (m) ClCO<sub>2</sub>Et, NEt<sub>3</sub>, CH<sub>2</sub>Cl<sub>2</sub>, 0 °C, then NH<sub>3</sub>; (n) CSA, quinoline, benzene, reflux; (o) NOCl, CH<sub>2</sub>Cl<sub>2</sub>-CH<sub>3</sub>CN, -35 °C, then NaBH<sub>3</sub>CN, -20 °C.

To set up the Pictet-Spengler reaction, the oxime moiety of **61** was reduced under high pressure hydrogenation conditions (Scheme 15). Heating of the resulting amine in the presence of benzyloxyacetaldehyde and acetic acid gave the correct diastereomer of **62**. Reduction of the methyl ester to the alcohol, followed by Swern oxidation produced the aldehyde, which immediately condensed with the amine moiety to give unstable

carbinolamine **63**. Addition of TMS-CN to **63** yielded a single diastereomer of the amino nitrile. Deprotection of the benzyl protecting groups using  $\text{BCl}_3$ , and then re-protection of the free alcohols furnished **64**.



**Scheme 15.** Completion of synthesis of ( $\pm$ )-cyanocycline A. Key: (a)  $\text{H}_2$  (1500psi), Ra-Ni,  $\text{NEt}_3$ , EtOH, 100 °C; (b)  $\text{BnOCH}_2\text{CHO}$ , AcOH, MeOH, 60 °C; (c)  $\text{BnBr}$ ,  $\text{K}_2\text{CO}_3$ , DMF, 50 °C; (d)  $\text{LiBEtH}_3$ , TMEDA, THF, 0 °C; (e) Swern oxidation; (f)  $\text{Me}_3\text{SiCN}$ ,  $\text{ZnCl}_2$ ,  $\text{CH}_2\text{Cl}_2$ ; (g)  $\text{BCl}_3$ ,  $\text{CH}_2\text{Cl}_2$ , 0 °C, then  $\text{Ac}_2\text{O}$ , pyr.; (h) Lawesson's reagent, benzene, 80 °C; (i) Ra-Ni, acetone; (j) ethylene oxide- MeOH, 60 °C; (k) 3M NaOH, MeOH; (l) *t*-BuOK, *t*-BuOH, 18-crown-6, THF, 0 °C; (m) MeI, *i*-Pr<sub>2</sub>NEt,  $\text{CH}_3\text{CN}$ , 60 °C; (n)  $\text{Mn}(\text{OAc})_3$ , 0.3%  $\text{H}_2\text{SO}_4$ -  $\text{CH}_3\text{CN}$ .

The oxazolidine ring was then constructed via an imine by the procedure of Pelletier.<sup>19</sup> The imine was prepared from the lactam by first transforming the lactam to the thiolactam using Lawesson's reagent, and then removal of the sulfur with the addition of Raney nickel. The stable imine was stirred with ethylene oxide in MeOH at 60 °C to form the oxazolidine in 73% yield for the three steps. Hydrolysis of the acetate groups,

deprotection of the amine protecting group followed by methylation of the amine furnished **65**. Oxidation of the aromatic ring using  $\text{Mn}(\text{OAc})_3$  to the quinone completes the synthesis of ( $\pm$ )-cyanocycline A. Thus the Fukuyama synthesis was achieved in 30 steps in 0.8% overall yield.

The two syntheses of cyanocycline by Fukuyama and Evans are very similar in number of steps and overall yield. Evans was able to complete the synthesis of cyanocycline in one less step and a slightly higher overall yield. The synthesis of cyanocycline by Evans was more convergent and three of the stereocenters were set in the preparation of a key intermediate, tricyclic lactam **38** (Scheme 11). In the synthesis of **38**, the intramolecular displacement of the tosylate of **42** gave the [3.3.0] ring system as a mixture of diastereomers in a 1.5:1 ratio of the undesired to the desired diastereomer. The poor stereoselectivity of this transformation was the major drawback in this route. The total synthesis had three more key steps. The major intermolecular coupling was between **47** and phenol **39**, which gave **48** as a mixture of diastereomers at C-9 (Scheme 12). The most impressive transformation was the oxidative cleavage of the diol in **50**, followed by an intramolecular Pictet-Spengler reaction to afford **51** as a single diastereomer, which possessed the desired configuration at C-3a and C-13b. The last key step was the reduction of the lactam in **52**. A number of different reducing agents were screened and the transformation was achieved using dissolving metal conditions resulting in  $\alpha$ -aminonitrile **53** after the addition of NaCN.

The advantage of the Fukuyama route to cyanocycline was the complete control of the stereochemistry. The relative stereochemistry at C-4, C-4a, and C-6 was set by hydrogenation of the dihydropyrrole to afford **59** with the *cis*-relationship at these three stereocenters (Scheme 14). Reduction of oxime **61** to the amine, followed by a Pictet-Spengler reaction gave **62** as a single diastereomer with the correct configuration at C-9 (Scheme 15). An intramolecular condensation between an amine and an aldehyde resulted in the desired aminal (**63**), which was transformed to  $\alpha$ -aminonitrile **64** with the correct

configuration at C-7.

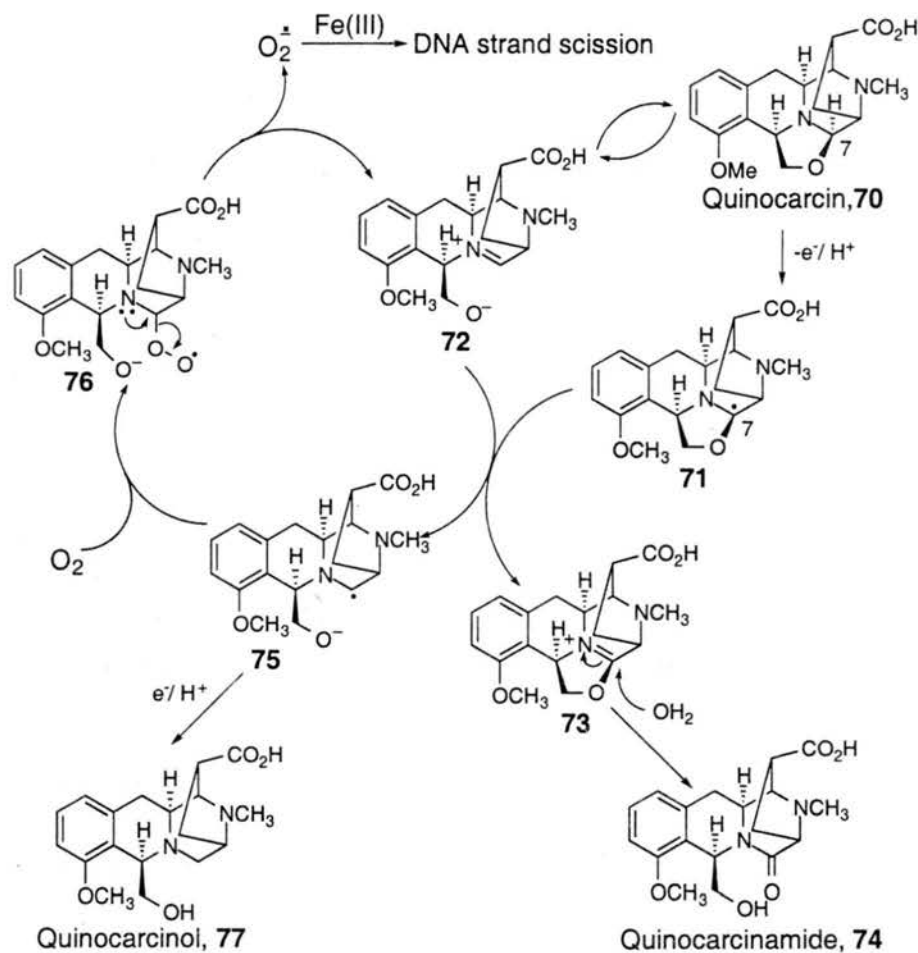
## Chapter 2

### Synthesis and DNA Alkylation Studies of Quinocarcin Analogs

#### 2.1 Introduction and Design of Quinocarcin Analogs

Quinocarcin (**70**) is a secondary metabolite isolated from *Streptomyces melanovinaceus*, and is structurally similar to the bioxalomycins.<sup>20</sup> Quinocarcin displays activity against a range of solid mammalian carcinomas.<sup>21</sup> Its antibiotic activity in *Bacillus subtilis* comes from its ability to inhibit DNA synthesis. A possible rationalization for quinocarcin's bioactivity was first offered by Tomita, *et al.* who reported that **70** cleaved plasmid DNA in an O<sub>2</sub>-dependent fashion.<sup>20a</sup> This report was intriguing since quinocarcin does not contain any recognizable functionality that would be associated with the capacity for oxidative DNA damage, such as metal chelation sites, quinones, or ene-dienes. Since this initial report, the Williams group has established that **70** activates molecular oxygen through a Cannizzaro reaction (Scheme 16).<sup>22</sup> The initial evidence for this self-redox disproportionation reaction came from the identification of quinocarcinamide (**74**) and quinocarcinol (**77**) when quinocarcin was allowed to stand in deoxygenated water at 25 °C.

In the first step of this self-redox cycle, single electron transfer from **70** with concomitant proton loss from the oxazolidine nitrogen to ring-opened tautomer **72** would furnish radical anion **75** and the oxazolidinyl radical **71**. Radical **71** should be capable of reducing a second equivalent of **72**, becoming iminium ion **73**, which should hydrolyze to quinocarcinamide (**74**). Evidence for the existence of iminium **73** was secured when the disproportionation reaction was run anaerobically in 98% <sup>18</sup>O<sub>2</sub>. When **74** was isolated from this reaction, incorporation of <sup>18</sup>O was observed at the amide carbonyl of **74**.

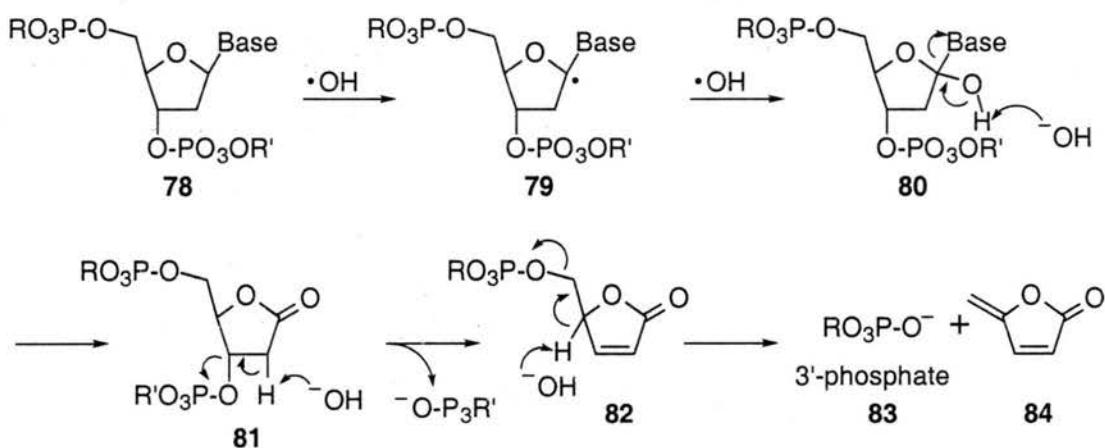


**Scheme 16.** Proposed self-redox cycle for quinocarcin that leads to DNA strand scission.<sup>22</sup>

Under aerobic conditions, the proposed cycle has radical anion **75** (and/or **71**) reacting with oxygen to furnish peroxy radical anion **76**, which, with nitrogen participation, expels 1 equivalent of superoxide. Superoxide is well documented to mediate DNA strand breakage via dismutation to hydrogen peroxide followed by Fenton-mediated generation of a hydroxy radical.<sup>23</sup> Hydroxy radicals could also be formed by homolytic cleavage of the O-O bond to give a hydroxy radical and **74**. If this were the case, running the reaction in water under an atmosphere of  $^{18}O_2$  would give incorporation of  $^{18}O$  in **74**. However, after running the  $^{18}O_2$  experiment, **74** did not demonstrate any incorporation of

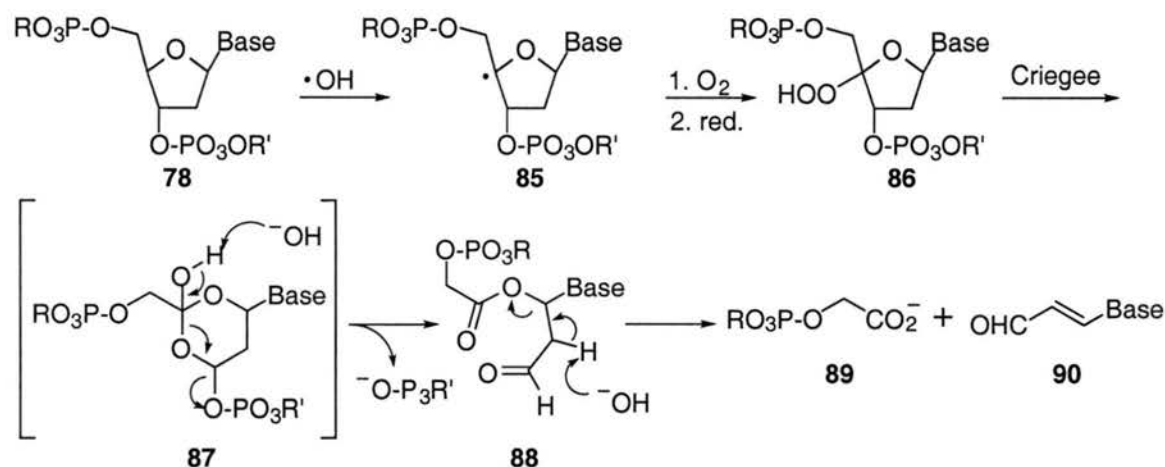
$^{18}\text{O}$  by mass spectral analysis. It has been established that hydroxy radical can then cleave DNA by hydrogen atom abstraction at the C-1' and C-4' of the deoxyribose.<sup>24</sup>

The first pathway that leads to DNA strand scission results from hydrogen abstraction from C-1' to produce radical **79** (Scheme 17). Capture of **79** with another equivalent of hydroxy radical forms **80**. The base on **80** is released in a pH-dependent step to give lactone **81**, which is deprotonated causing strand scission. In the final base-mediated step, the 3'phosphate product (**83**) is afforded in addition to the putative intermediate **84** (never actually isolated as a result of its high reactivity).



**Scheme 17.** DNA strand scission by C-1' hydrogen atom abstraction.

In the other pathway, hydrogen abstraction of the C-4' hydrogen forms radical **85**, which results in hydroperoxide **86** by reaction with oxygen followed by single electron reduction (Scheme 18). This species undergoes a Criegee reaction to give alkaline labile **87**, which rearranges to aldehyde **88** resulting in strand scission. In the final base-mediated step, aldehyde **88** decomposes to 3'-phosphoglycolate **89** and the base propenal (**90**).



**Scheme 18.** DNA strand scission by C-4' hydrogen atom abstraction.

In this self redox disproportionation cycle, the first step is radical generation at C-7 of **70** to furnish **71**. Quinocarcin can exist in two conformers, **91** and **92**. Calculations suggest that **91** with the piperazine in a chair-like confirmation is the lowest energy conformer by  $\sim 10$  kcal/mol.<sup>28</sup> Ring opening of the oxazolidine to iminium species **72** requires nitrogen pyramidal inversion to a higher energy boat conformation (**92**). It was suspected that **91**, which has the nitrogen lone pair *anti*-periplanar to the C-7-hydrogen bond (Figure 3), was responsible for generation of the radical and subsequent superoxide production.<sup>25</sup>

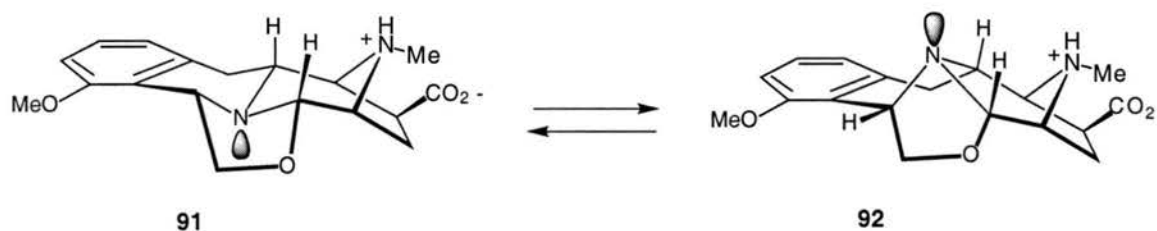


**Figure 3.** Two possible conformers of quinocarcin.

To test this hypothesis, analogs of quinocarcin that would model the two conformers were designed and synthesized by the Williams' group.<sup>25</sup> The X-ray crystal structures of **93** and **94** demonstrated that **93** has the nitrogen lone pair *anti*-periplanar to

the C-H bond and modeled conformer **91**. On the other hand, **94** has the nitrogen lone pair positioned *syn*-periplanar to the C-H bond and modeled conformer **92**.

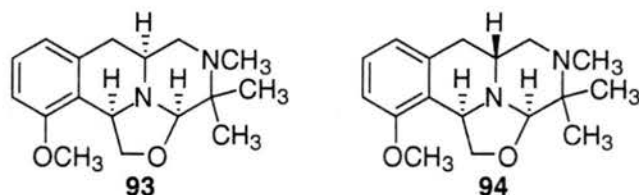


**Figure 4.** Quinocarcin conformer analogs.

When tested for superoxide production, only **93** demonstrated the ability to produce superoxide. Unfortunately, **93** was only slightly soluble in water and cleaved DNA to a lesser extent when compared to quinocarcin, while **94** did not show any DNA strand scission.

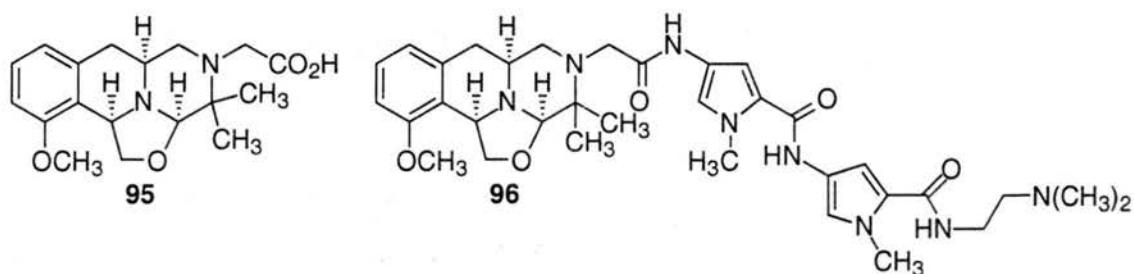
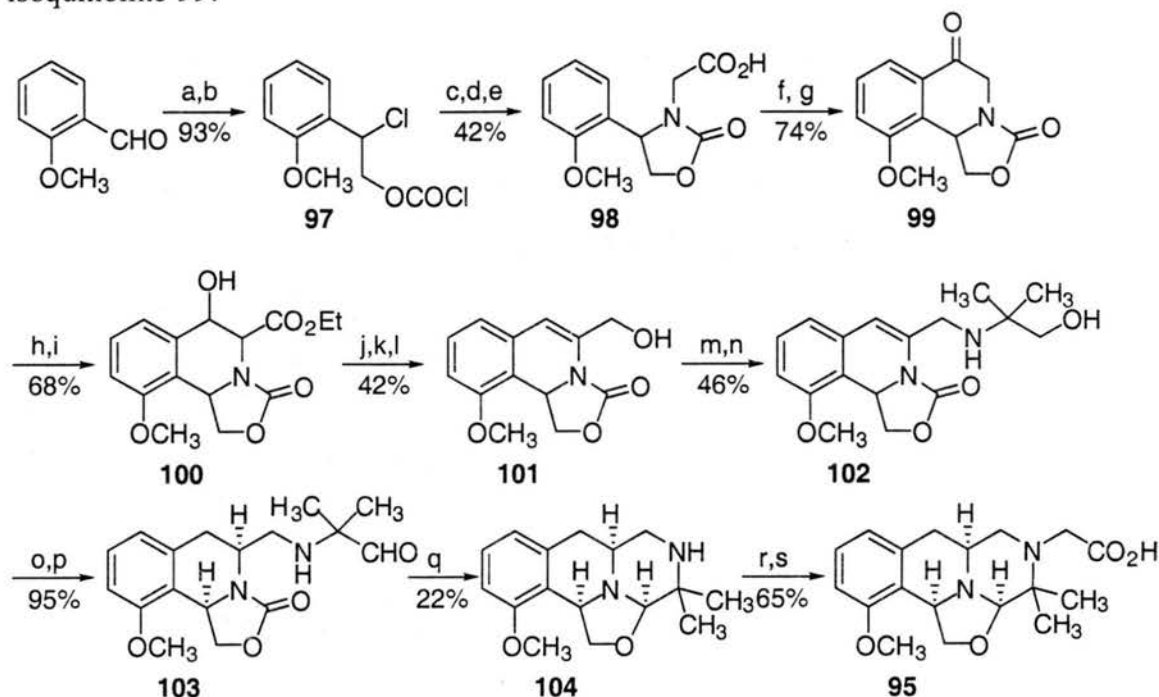


**Figure 5.** Water-soluble quinocarcin analogs.

By attaching a carboxylic acid moiety to the amine, the preparation of water-soluble analog **95** was achieved by the Williams' group (Figure 5).<sup>27</sup> Additionally, in the hope of cleaving DNA sequence selectively, a DNA binding moiety was tethered to the tetracyclic core to furnish **96**. The syntheses of these compounds were extensions of the syntheses of earlier analogs **93** and **94**.

The syntheses of **95** and **96** started with *o*-anisaldehyde, which was epoxidized using a sulfur ylide under phase transfer conditions (Scheme 19).<sup>27</sup> The epoxide was then opened regioselectively with phosgene to furnish chloroformate **97**. Nucleophilic attack of **97** with the amine of glycine ethyl ester, then closure of the oxazolidinone ring with KO<sup>t</sup>-

Bu, followed by saponification of the ethyl ester gave carboxylic acid **98** in 42% yield after recrystallization. A Friedel-Crafts acylation closed the six-membered ring to yield isoquinoline **99**.

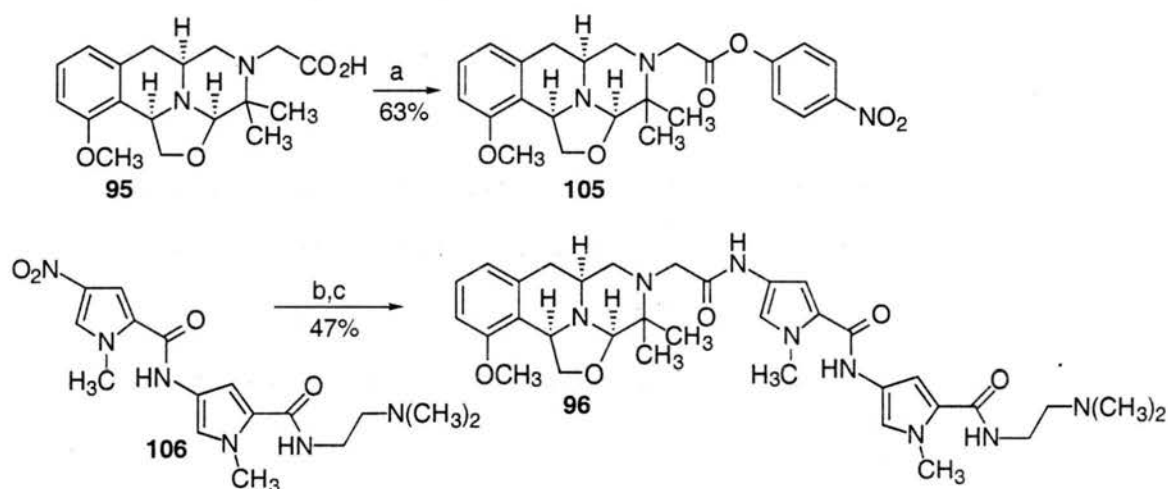


**Scheme 19.** Synthesis of water soluble analog **95**.<sup>27</sup> Key: (a)  $\text{Me}_3\text{S}^+\text{I}^-$ ,  $n\text{-Bu}_4\text{NBr}$ ,  $\text{NaOH}$ ,  $\text{CH}_2\text{Cl}_2$ ; (b)  $\text{COCl}_2$ , toluene; (c) glycine ethyl ester  $\cdot\text{HCl}$ ,  $\text{NaHCO}_3$ ,  $\text{CH}_2\text{Cl}_2$ ; (d)  $\text{KO}t\text{-Bu}$ , THF; (e)  $\text{LiOH(aq)}$ , EtOH; (f)  $(\text{ClCO})_2$ , DMF,  $\text{CH}_2\text{Cl}_2$ ; (g)  $\text{AlCl}_3$ ,  $\text{CH}_2\text{Cl}_2$ ; (h)  $\text{NaH}$ ,  $\text{EtO}_2\text{CCN}$ ; (i)  $\text{NaBH}_3\text{CN}$ , HOAc; (j)  $\text{LiOH(aq)}$ , EtOH; (k)  $\text{SOCl}_2$ , toluene, reflux; (l)  $\text{NaBH}_4$ ,  $\text{CH}_2\text{Cl}_2/\text{EtOH}$ ; (m)  $\text{MsCl}$ ,  $\text{NEt}_3$ ,  $\text{CH}_2\text{Cl}_2$ ; (n) 2-amino-2-methyl-1-propanol; (o)  $\text{PdCl}_2$ ,  $\text{H}_2$  (1 atm), EtOH; (p) DMSO,  $(\text{ClCO})_2$ ,  $-78^\circ\text{C}$ ; (q)  $\text{LiOH(aq)}$ , EtOH, reflux; (r) ethylbromo acetate,  $\text{NaHCO}_3$ , DMF; (s)  $\text{LiOH(aq)}$ , EtOH.

The enolate of **99** generated using  $\text{NaH}$ , was alkylated with ethyl cyanofornate to give the  $\beta$ -keto ester, whose ketone moiety was selectively reduced using  $\text{NaBH}_3\text{CN}$  to prepare  $\beta$ -hydroxy ester **100** as one diastereomer. Saponification of the ester, followed by treatment with thionyl chloride and  $\text{NaBH}_4$  furnished allylic alcohol **101**. The mesylate of **101** was prepared, and then displaced with 2-amino-2-methyl-1-propanol resulting in amino alcohol **102**. To set the *syn*-stereochemistry, the olefin was reduced using hydrogenation conditions with  $\text{PdCl}_2$ . The alcohol was then oxidized to aldehyde **103** using oxalyl chloride and DMSO. The critical cyclization of **103** was realized under basic

conditions to give tetracycle **104** in 22% yield. In this reaction, the oxazolidinone of **103** was hydrolyzed to the amino alcohol, which then condenses with the aldehyde to form the oxazolidine ring of **104**. The carboxylic acid moiety was easily attached to the secondary amine first by alkylation of **104** with ethyl bromoacetate, and then hydrolysis of the ester completed the synthesis of water-soluble analog **95**.

To prepare netropsin conjugate **96**, the carboxylic acid of **95** was first activated using *p*-nitrophenol to give **105** (Scheme 20). The nitro group of **106**<sup>26</sup> was reduced to the amine (5% Pd/C, H<sub>2</sub>) and coupled to **105** to give **96** in 47% yield.

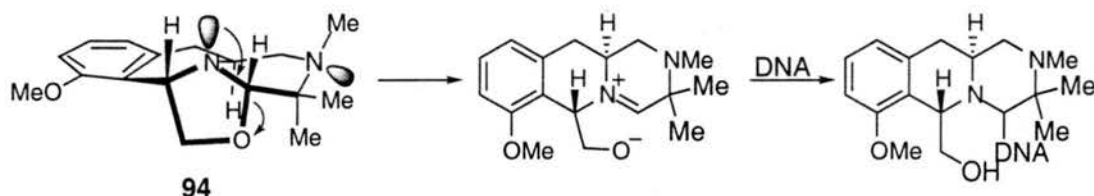


**Scheme 20.** Synthesis of netropsin conjugate **96**.<sup>27</sup> Key: (a) *p*-nitrophenol, DCC, CH<sub>2</sub>Cl<sub>2</sub>; (b) 5% Pd/C, H<sub>2</sub> (1 atm), DMF; (c) **105**, NEt<sub>3</sub>, DMF.

Analog **95** demonstrated superoxide production and non-specific DNA strand scission.<sup>27</sup> Netropsin conjugate **96** selectively cleaved DNA around 5'-d(ATTT)-3' sequences. Thus through the use of a DNA-binding moiety, selective cleavage of DNA has been achieved with this class of compounds. It was now of interest to switch the mode of action of these analogs from the cleavage of DNA to the alkylation of DNA.

The design of an analog of quinocarcin that will only alkylate DNA has to meet two criteria: 1) elimination of superoxide production; 2) formation of an electrophilic species. Using the tetracyclic core of **94** (Figure 4) would meet the first requirement since **94** does

not produce superoxide. For the second requirement, it has been postulated that quinocarcin may alkylate DNA in the same fashion as proposed for **5** through iminium **72** (Scheme 16).<sup>28</sup> The structure of **94** has the nitrogen lone pair of electrons trans-antiperiplanar to the C7-oxygen bond (Scheme 21), which should facilitate iminium ion formation. Nucleophilic attack of DNA upon the iminium ion would form the DNA adduct.



**Scheme 21.** Proposed mechanism of DNA alkylation.

Since *epi*-analog **94** fulfills the two requirements, the tetracyclic core of **94** would be a good model for this proposal. As in the earlier synthesis of water-soluble analog **95**, a carboxylic acid moiety could be tethered to the core structure to furnish **107** (Figure 6). In addition, netropsin conjugate **108** could be used to investigate the possibility of alkylation for a specific sequence of DNA.

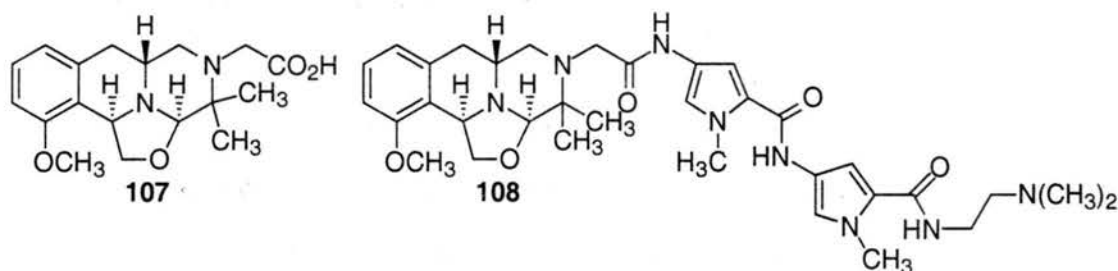
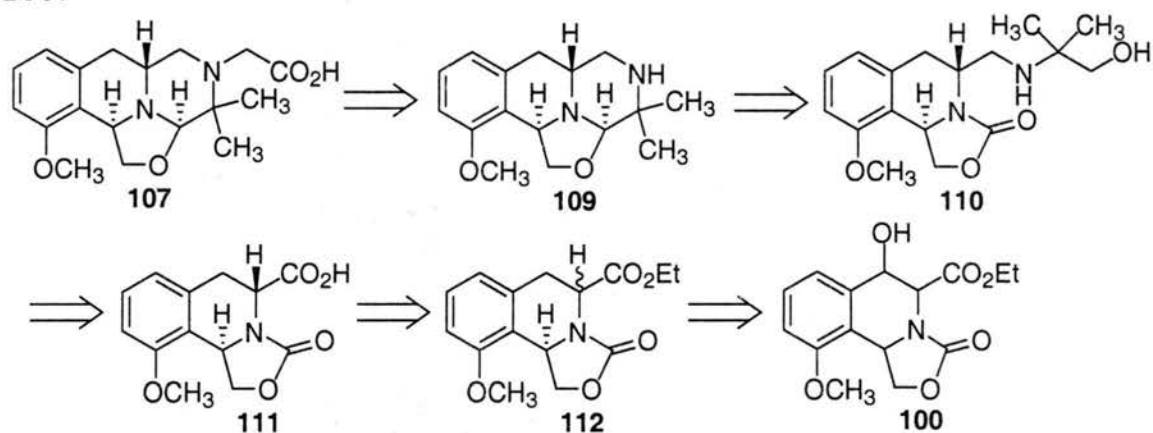


**Figure 6.** Water-soluble *epi*-quinocarcin analogs.

Production of superoxide could be analyzed by nitroblue tetrazolium (NBT) reduction experiments and the DNA alkylation abilities of **107** and **108** could be evaluated by band shift assays using gel electrophoresis.

## 2.2 Synthesis of Water-Soluble *epi*-Quinocarcin Analogs

The retrosynthetic plan for the synthesis of **107** was similar to the earlier quinocarcin analogs and involves introduction of the carboxylic acid moiety in the last step (Scheme 22). The tetracyclic core was envisioned to be formed using the same cyclization conditions as used to prepare **104**, to furnish **109**. To set the *anti*-stereochemistry, saponification of **112** should give the thermodynamically more stable diastereomer **111**. Saturated ester **112** should be available from the previously reported  $\beta$ -hydroxy ester **100**.<sup>25</sup>

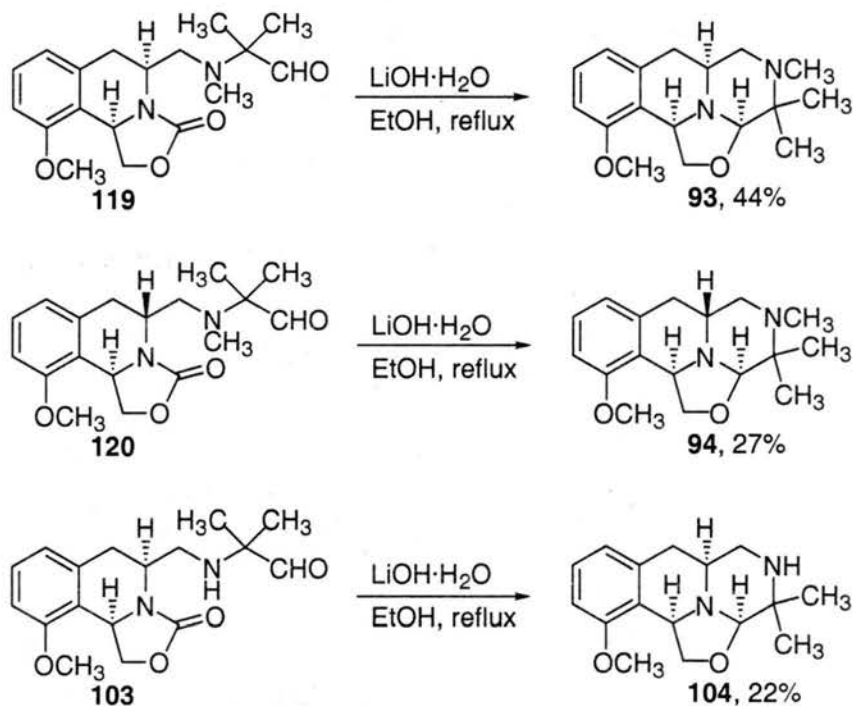


**Scheme 22.** Retrosynthetic analysis of quinocarcin analog **107**.

The  $\beta$ -chloride of  $\beta$ -hydroxy ester **100** was prepared by the addition of oxalyl chloride and DMF and eliminated to give  $\alpha, \beta$ -unsaturated ester **113** in 94% yield (Scheme 23). Hydrogenation of the olefin gave a 1:1 mixture of diastereomers of the saturated ester. In the key stereocenter-setting reaction, the ethyl ester moiety was saponified to provide carboxylic acid **111** as the only diastereomer. Carboxylic acid **111** was reduced to the alcohol, by first transforming the acid to the acid chloride, followed by reduction using NaBH<sub>4</sub> to furnish **114** in 98% yield. The mesylate of **114** was prepared and displaced using 2-amino-2-methyl-1-propanol (**115**) to afford amino alcohol **110**. Amino alcohol **117** was prepared to confirm the *anti*-stereochemistry, by displacement of the tosylate with 2-methylamino-2-methyl-1-propanol (**116**). Amino alcohol **117** had been synthesized



By examining previous work on the cyclization of related substrates, two trends became apparent (Scheme 25).<sup>25,27</sup> The cyclization worked better with a tertiary amine and when the relative stereochemistry of the two stereocenters are *syn*-. Unfortunately, aldehyde **118** lacks both of these features.

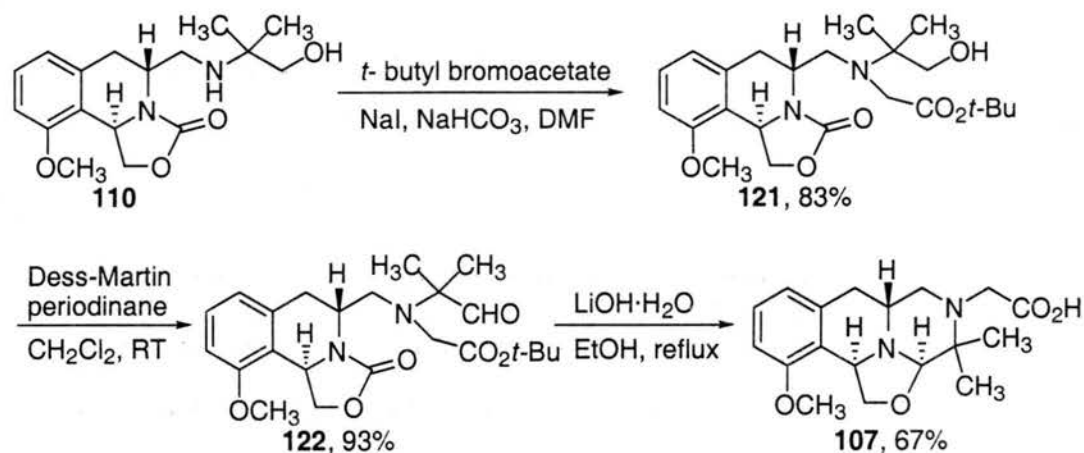


**Scheme 25.** Earlier cyclization attempts to give tetracyclic core.<sup>25,27</sup>

One possible solution to this problem was to attach a protected carboxylic acid to the amine, rendering it tertiary and thus, potentially increasing the chances for cyclization. A *t*-butyl ester was chosen for the protected carboxylic acid (Scheme 26). This particular group was selected based on past experiments on alkylating the amine with ethyl bromoacetate. In these instances the amine was alkylated, but the ethyl ester underwent transesterification to give a lactone. It was hoped that the *t*-butyl ester would preclude this unwanted lactonization.

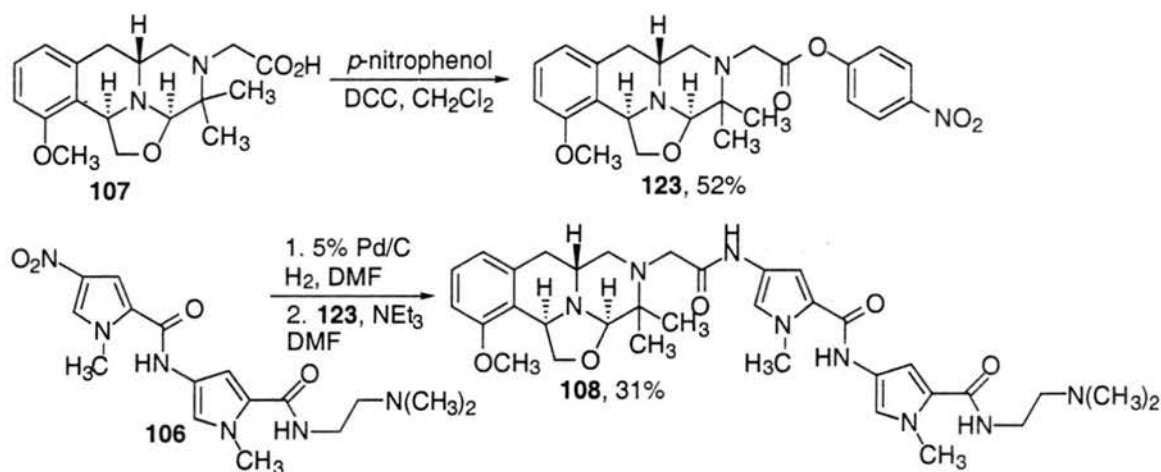
Amino alcohol **110** was alkylated with *t*-butyl bromoacetate to afford ester **121** in 83% yield with none of the undesired lactone (Scheme 26). The alcohol was oxidized

using Dess-Martin periodinane to give aldehyde **121** in 93% yield. Using the same reaction conditions employed for the cyclization of **105** not only resulted in the desired tetracyclic core, but also resulted in saponification of the ester to give analog **107** in 67% yield. The yield of this cyclization is the highest obtained for this group of compounds. In addition, this cyclization reaction in the past has always given a number of decomposition products, resulting in a very difficult separation. The cyclization to **107** was very clean and essentially gave a single new compound, which simplified the purification.



**Scheme 26.** Completion of synthesis of quinocarcin analog **107**.

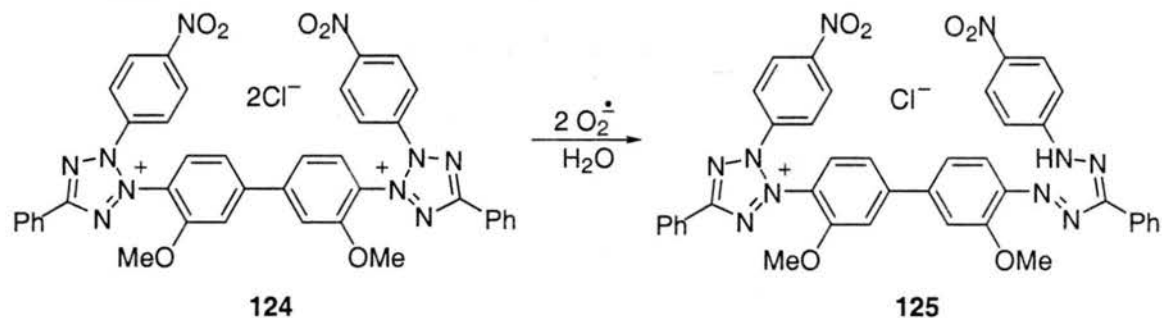
With **107** in hand, the same protocol used to prepare **96** was followed to synthesize netropsin conjugate **108** (Scheme 27). The carboxylic acid moiety of **107** was first activated as the *p*-nitrophenyl ester. The nitro group of known peptide **106**<sup>29</sup> was reduced under hydrogenation conditions with 5% Pd/C in DMF to the amine, which was coupled to **123** to furnish netropsin conjugate **108**.



**Scheme 27.** Synthesis of netropsin conjugate **108**.

### 2.3 Evaluation of *epi*-Quinocarcin Analogs

The ability of **107** to produce superoxide was measured by following the reduction of nitroblue tetrazolium (**124**, NBT).<sup>30</sup> In the reduction process NBT is reduced to the monoformazan compound **125**, which can be detected spectrophotometrically in the visible range ( $\lambda_{\text{max}} = 540 \text{ nm}$ ).



**Scheme 28.** Two electron reduction of NBT (**124**) by superoxide.

The assay was carried out as described previously in measuring the superoxide production of quinocarcin and analogs **93-96**.<sup>22,25</sup> Analog **107** was added to an aerated solution of NBT (0.12 mM) in a 20 mM phosphate buffer (pH= 7) such that the final concentration of **107** was 2.0 mM. The optical absorbance was recorded over 15 minutes and the change in optical density was the average slope for the linear change in optical

density over the reaction time. The rates of superoxide production were calculated from the molar extinction coefficient of **125** at 500 nm (12,200) and by assuming the reaction is pseudo first order in O<sub>2</sub>. Nitroblue tetazolium in the presence of **107** was not reduced, demonstrating the inability of **107** to produce superoxide. By comparison, under the same conditions water soluble analog **95** had a rate of superoxide production of  $0.82 \times 10^{-9} \text{ M s}^{-1}$ , while a 1.0 mM solution of quinocarcin exhibits a rate of  $4.2 \times 10^{-9} \text{ M s}^{-1}$  and a 0.1 mM solution of bioxalomycin  $\alpha_2$  demonstrates a rate of  $3.88 \times 10^{-8} \text{ M s}^{-1}$ .

To assay the DNA alkylating abilities of **107** and **108**, band shift assays were conducted. In these experiments solutions of the analogs and 5'-<sup>32</sup>P-labeled DNA were incubated at 37 °C for 12 hours. The DNA was then precipitated with ethanol and dried. The samples were suspended in water and loading dye, and loaded onto a denaturing or non-denaturing electrophoresis gel. After the gels were run, they were exposed to photographic film at -80 °C for 12 hours. If alkylation did occur, the mobility of the alkylated DNA should be retarded due to the increased mass.

Unfortunately, when **107** was incubated under a wide range of concentrations (5  $\mu\text{M}$ -5 mM) with a number of DNA templates (Templates A-C, Figure 7) at different concentrations (0.1-10  $\mu\text{M}$ ), no evidence for DNA alkylation was observed. As expected from the earlier NBT reduction experiments, no DNA strand scission occurred.



**Figure 7.** DNA templates incubated with **94**.

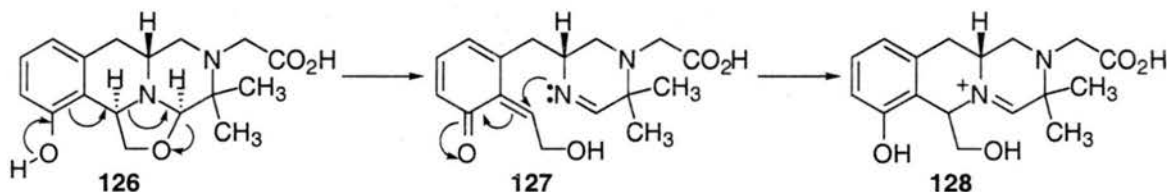
The netropsin conjugate **108** was incubated (at high concentrations (2.0-4.0 mM)) with DNA templates D-G (0.85- 2.45 mM), which contained netropsin binding sequences

(Figure 8). There were no band shifts of the DNA, indicative of no DNA alkylation with netropsin conjugate **108**.



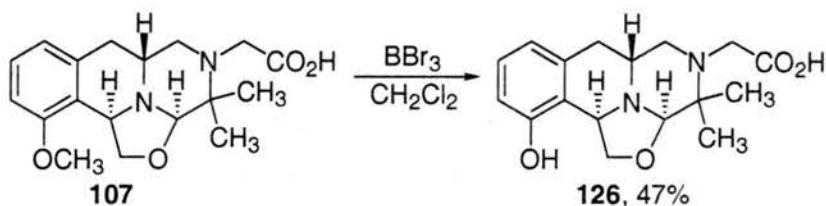
**Figure 8.** DNA templates incubated with **95**. The netropsin binding region is in bold face.

Due to these results, second generation analogs were designed based on the proposed mechanism of DNA alkylation by naphthyridinomycin (Scheme 1, Chapter 1). A similar mechanism could be proposed for analog **126**, if the methoxy group on the aromatic ring of **107** were replaced by a hydroxy moiety (Scheme 29).



**Scheme 29.** Proposed generation of iminium **128** from phenol **126**.

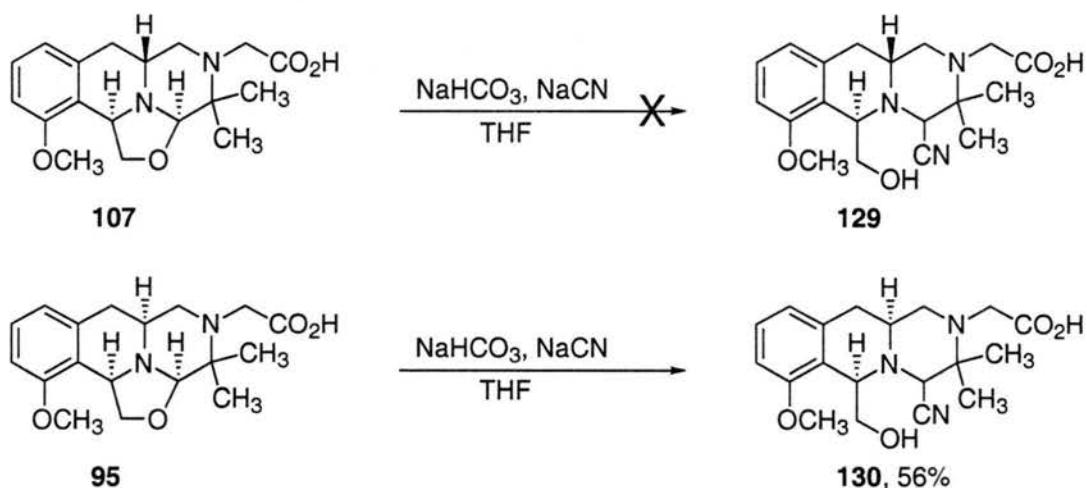
In this mechanism the phenol of **126** would be deprotonated, resulting in opening of the oxazolidine ring and formation of imine **127**. The lone pair of electrons on the nitrogen of the imine could then add to the electrophilic quinone methide to restore aromaticity and form iminium ion **128**, which is the proposed DNA alkylating agent.



**Scheme 30.** Synthesis of phenol **126**.

The demethylation of **107** to produce phenol **126** was easily achieved using  $\text{BBr}_3$ . To assay for DNA alkylation, phenol **126** and DNA templates were incubated at  $37^\circ\text{C}$  in a phosphate buffer (pH=8) for 12 hours. The samples were evaluated as described earlier using gel electrophoresis, and **126** demonstrated no evidence of DNA alkylation.

Next, to place a good leaving group at C-7, reactions were carried out to open the oxazolidine ring and place a cyano substituent at C-7 (Scheme 31). The reaction conditions that were used were developed earlier in the synthesis of cyano analogs of quinocarcin.<sup>31</sup> Interestingly, stirring **107** with  $\text{NaCN}$  under basic conditions gave mostly recovered starting materials with a small amount of new unidentifiable compounds. Conversely, the same reaction with **95** cleanly afforded the cyano product **130** (stereochemistry unassigned). This difference in reactivity between the two analogs raises questions of the ability of **107** to be alkylated at C-7.

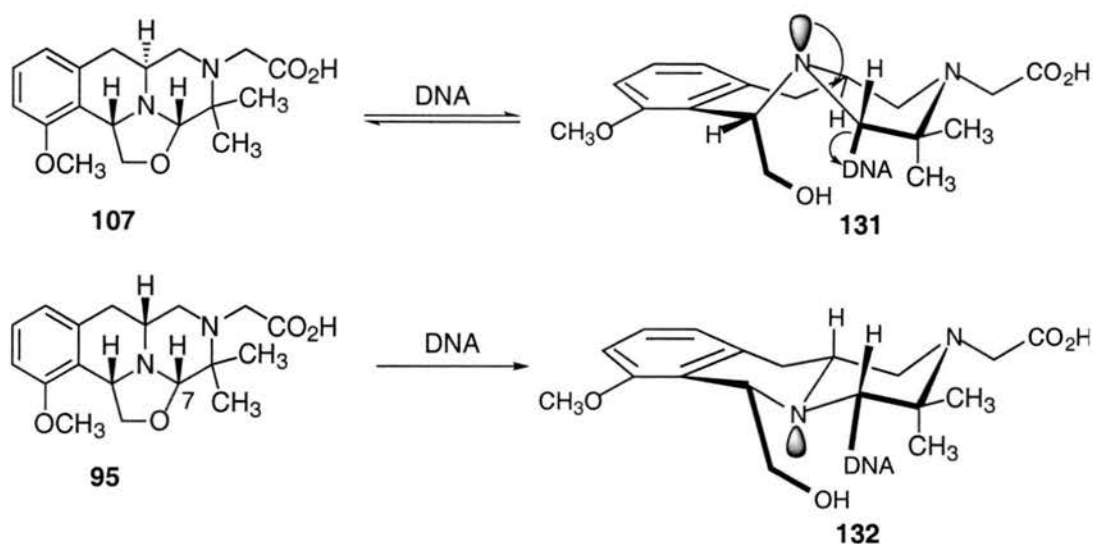


**Scheme 31.** Synthesis of cyano-quinocarcin analog **130**.

## 2.4 Future Work

The lack of DNA alkylation products with analogs that have *epi*-quinocarcin stereochemistry (**107**, **108**, and **126**) may be due to their steric congestion around C-7 or the instability of the alkylated product. The proximity of the reaction center (C-7) to a *gem*-dimethyl group may make the alkylation difficult due to steric interactions. On the other hand, the bioxalomycins, which are sterically congested around C-7, alkylate DNA. In addition, analog **96**, which contains the same *gem*-dimethyl group as the *epi*-quinocarcin analogs, cleaves DNA in a sequence specific manner. An explanation given by the authors for this specificity is that **96** is operating via a direct hydrogen abstraction mechanism.<sup>27</sup> If this is indeed the case, the steric argument due to the *gem*-dimethyl groups for the absence of DNA alkylation for **107**, **108**, and **126** would not be correct. Finally, since both **95** and **107** contain *gem*-dimethyl groups, the steric argument cannot explain the absence of the cyano adduct when **107** is exposed to NaCN, while these same conditions afford cyano adduct **130** from **95** (Scheme 31).

Another explanation for the absence of alkylation by the *epi*-quinocarcin analogs is shown in Scheme 32. If **107** is alkylated from the  $\alpha$  face by DNA, the resulting product (**131**) would have the nitrogen lone pair *anti*-periplanar to the DNA. In this configuration the DNA can be easily expelled to give back **107**. This equilibrium would also explain the failure to prepare cyano product **129** from **107**.



**Scheme 32.** DNA alkylated products of **107** and **95**.

Using the same model with **95**, produces an alkylated product (**132**) that may be more stable since the nitrogen pair is not *anti*-periplanar to the C-7-DNA bond.

The ability of quinocarcin to alkylate DNA is only a proposal based on molecular modeling,<sup>23</sup> and to date there has been no evidence to support this claim. Nonetheless, if this mode of action is going to be probed through the use of an analog, the analog should have the same relative stereochemistry as quinocarcin. This would obviate the equilibrium shown for **107** in Scheme 31. Unfortunately, this also means that superoxide production, and hence DNA strand scission will still occur with any of these analogs. A first generation analog would be phenol **133**, which could be prepared from **107** by demethylation with  $\text{BBr}_3$ . The mechanism of DNA alkylation by **133** may be similar to the postulated mechanism for DNA alkylation by naphthyridinomycin.

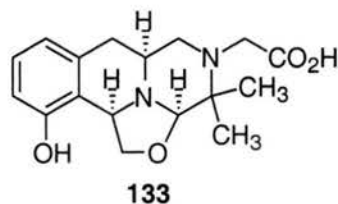


**Figure 9.** Possible DNA-alkylating quinocarcin analog.

## Chapter 3

### DNA Cross-Linking Studies of Bioxalomycin $\alpha_2$

#### 3.1 Introduction

Deoxyribonucleic acid (DNA), whose sequence codes for RNA synthesis via transcription and protein/enzyme synthesis via translation, is the main source of information within a living organism. Structurally, DNA consists of two 2'-deoxyribose phosphate backbones with a nucleotide substituted at the 1' position. The four nucleotides are deoxyadenosine, deoxyguanosine, deoxycytidine and deoxythymidine (dA, dG, dC and dT, respectively). The most common form of DNA, B-DNA, has the two strands wound around one another in a right-handed twist to form a double helix. In the helix, the phosphate backbone is on the periphery while the nucleotides hydrogen bond to one another in a specific Watson-Crick pairing (Figure 10).

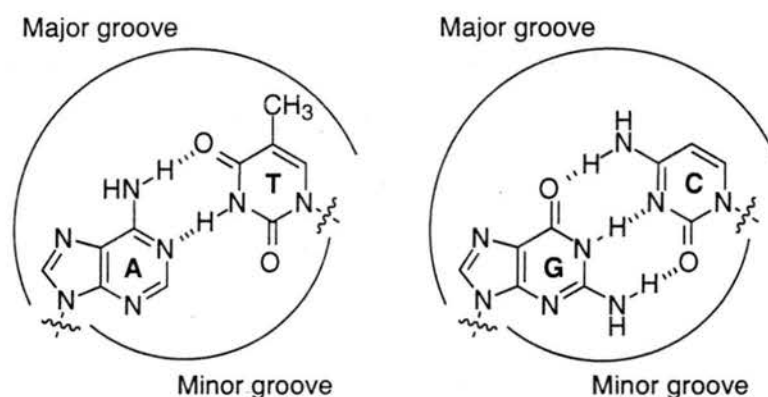
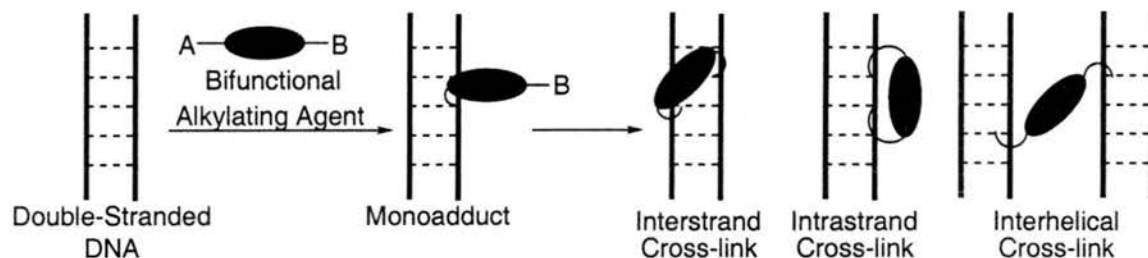


**Figure 10.** Depiction of hydrogen bonds between deoxyadenosine-deoxythymidine and deoxyguanosine-deoxycytidine pairs.

In a simplified version of DNA replication and transcription, the two polynucleotide strands separate, and then DNA polymerases use a single strand as a template upon which

the complementary DNA or RNA is synthesized. In the event of DNA replication or transcription, it is essential that the two strands separate and blocking this process inflicts catastrophic events in the cell.



**Scheme 32.** Diagram of different DNA products resulting from reaction with a bifunctional alkylating agent. After monoalkylation the DNA can be alkylated a second time to form an interstrand cross-link, an intrastrand cross-link or an interhelical cross-link.

One strategy in the treatment of cancers is to subject the rapidly dividing cells to compounds that are capable of DNA interstrand cross-linking. There are a number of different DNA alkylation products that could be produced with bisalkylation drugs (Scheme 32). Although the knowledge of the effects of these different alkylations is incomplete, it is generally accepted that interstrand cross-linking is by far the most toxic of all them since it results in the seizure of the separation of the two DNA strands.

In a recent review on DNA cross-linking agents, the drugs were divided into categories depending on their activation.<sup>32</sup> The categories include inherently reactive, photo-activated, oxidatively activated, and reductively activated agents.

Although all of the categories of DNA cross-linking agents have been used in the treatment of cancer, the reductively activated agents show the most promise to complement radiation-based therapies. In radiation-based therapy the exposure of oxygenated tissues to ionizing radiation forms superoxide, which produces hydroxy radical.<sup>33</sup> The hydroxy radical species is responsible for damage to macromolecules of the cell, most notably DNA. Reaction with DNA affords a wide array of base oxidized nucleotides and leads also to indiscriminate strand scission of the phosphodiester backbone.<sup>24,34</sup> Unfortunately, the cells

of solid tumors exist in a state low in oxygen and the effectiveness of radiation based therapy is therefore limited. On the other hand, the presence of reductase enzymes coupled to the hypoxic environment of the tumor cells is well-suited for reductively activated DNA cross-linking agents. In the absence of  $O_2$ , the activated reduction product is long-lived enough to cause damage to macromolecules resulting in cytotoxicity.

Due to the four proposed alkylation sites on naphthyridinomycin (**7**) and its dependence on reducing conditions to alkylate DNA, it has potential to be a reductively activated DNA cross-linking agent. To investigate this possibility, DNA cross-linking studies were carried out with the pre-activated bioxalomycin  $\alpha_2$  (**2**), which has the same possible four alkylation sites as naphthyridinomycin (**7**).

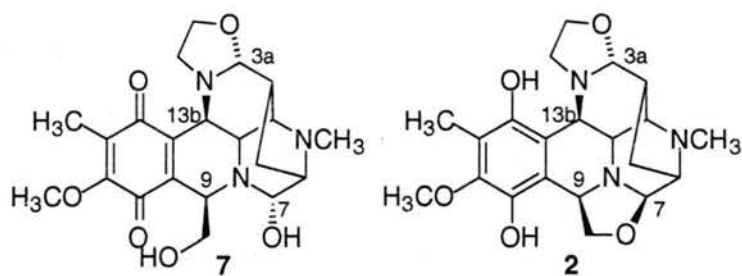


**Figure 11.** Postulated DNA alkylation sites on naphthyridinomycin and bioxalomycin  $\alpha_2$ .

### 3.2 DNA-Bioxalomycin $\alpha_2$ Interstrand Cross-Link Formation

The ability to mediate DNA alkylation by bioxalomycin  $\alpha_2$  (**2**) was assayed by DNA band shifts as described in Chapter 2. Incubating  $5'$ - $^{32}P$  labeled oligomer A of DNA template H with **2** at  $37^\circ C$  for 12 h resulted in band shifted products of retarded electrophilic mobilities characteristic of monoalkylated and interstrand cross-linked DNA (Figure 12, lane 2). The crude reaction was examined using denaturing gel electrophoresis (DPAGE), which separates the two DNA strands as they travel down the gel. Since the interstrand cross-linked DNA cannot separate, the mobility of the cross-linked product is much slower compared to the monoalkylated DNA. The doubling seen for the cross-link

product is presumed to be due to orientational isomerism of the drug with respect to the cross-linkable site.<sup>35</sup>

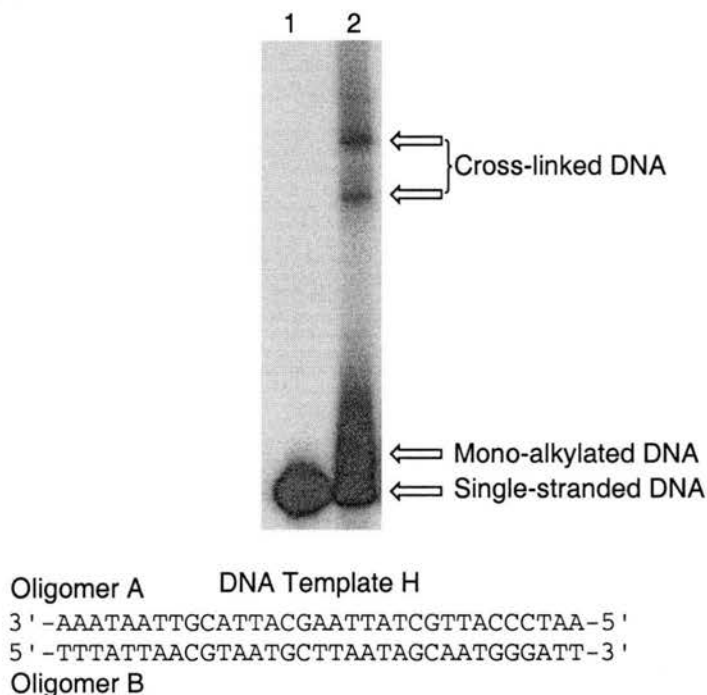


**Figure 12.** Reaction of DNA template H with bioxalomyacin  $\alpha_2$ .

The sequence specificity for the cross-link was obtained using the Fe(II)/EDTA digestion technique developed by Tullius and Dombroski<sup>36</sup> and extended by Hopkins.<sup>37</sup> In this technique the cross-linked product of 5'-<sup>32</sup>P labeled oligomer was isolated (Figure 13, A, lane 2 and Figure 13, B, lane 2) and subjected to Fe(II)/EDTA digestion, generating hydroxy radical, which cleaves the DNA sugar backbone non-selectively (Scheme 17 and 18, Chapter 2). On native DNA this produced an equimolar assortment of all fragment sizes up to and including the full length strand (Figure 13, A, lane 5 and Figure 13, B, lane 5). On the other hand, analogous treatment of the cross-linked product gave short fragments corresponding to cleavage at or to the radiolabeled side of the alkylated residue (Figure 13, A, lane 6 and Figure 13, B, lane 6). The observed cleavage patterns are consistent with the drug spanning from dG10 (oligomer A) to dG25 (oligomer B) demonstrating a 5'-CG-3' specificity.

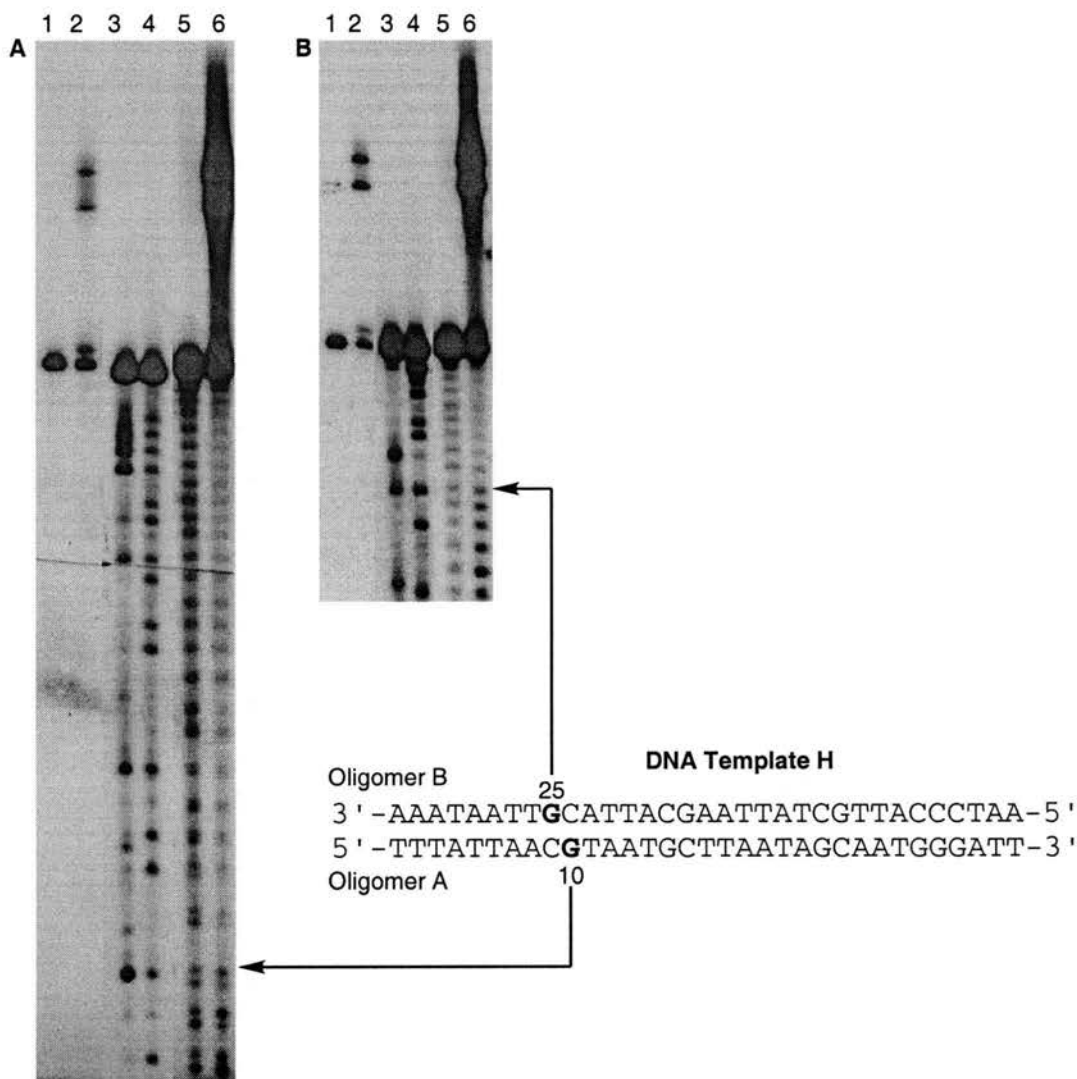


**Figure 13.** Autoradiograms A and B: Fe(II)/EDTA footprinting of cross-linked template H ( $^{32}\text{P}$ -labeled at the 5' terminus of oligo A and B, respectively). Lanes 1 and 2, standard DNA, cross-linked template H, lanes 3 and 4, Maxam Gilbert G, G+A respectively; lane 5, 1.5 mM Fe(II)/EDTA control; lane 6, cross-linked product after 1.5 mM Fe(II)/EDTA digestion.

Cross-linking studies with modified guanosine residues determined the nucleophilic moiety on the base responsible for alkylation. The most nucleophilic residue on guanosine is N-7, which is located in the major groove of DNA, due to electrostatic potential and accessibility values (Figure 14).<sup>38</sup> In the minor groove of DNA, alkylation of the 2-amino group of guanosine leads to DNA cross-linking such as that observed in the mitomycin family.<sup>39</sup> To determine the location on guanosine where the alkylation is occurring, reactions were conducted that contained bioxalomycin  $\alpha_2$  and DNA substituted with

modified guanosines that do not contain these nucleophilic residues. More specifically, substituting 7-deazaguanosine or inosine for guanosine can determine if bioxalomycin  $\alpha_2$  is alkylating at N-7 or the 2-amino group of guanosine, respectively.

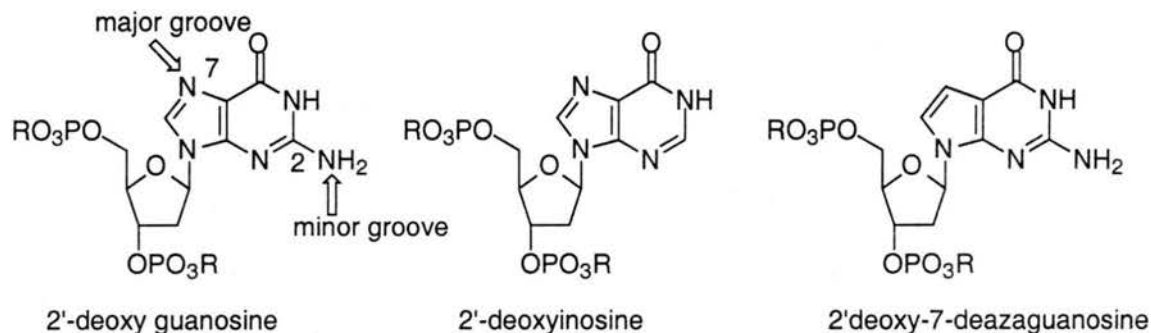


**Figure 14.** Structures of modified 2'-deoxyguanosine substrates.

Reaction of bioxalomycin  $\alpha_2$  with DNA template I resulted in two cross-linked products, one spanning dG25 (oligomer C) and dG10 (oligomer D), and the other between dG12 (oligomer C) and dG23 (oligomer D) (Figure 15, lane 2). Substituting a single 2'-deoxyinosine at the dG10 position of oligomer D gave a cross-linked band corresponding to the cross-link at dG12(C)-dG23(D) (Figure 15, lane 3). Incubation of the doubly 2'-deoxyinosine substituted duplex at dG10 and dG23 abolished cross-link formation (Figure 15, lane 4). This result implicates the alkylation events occur at the 2-amino group of guanosine in the minor groove of DNA. Additional evidence for this location of the alkylation was obtained by substituting 2'-deoxy-7-deazaguanosine at dG10 and dG23 of oligomer D. When bioxalomycin  $\alpha_2$  was allowed to react with the doubly 2'-deoxy-7-deazaguanosine-substituted substrate, cross-linked material was observed (Figure 15, lane 5) confirming that alkylation occurs at the exocyclic amine at C-2 of guanosine in the minor groove.

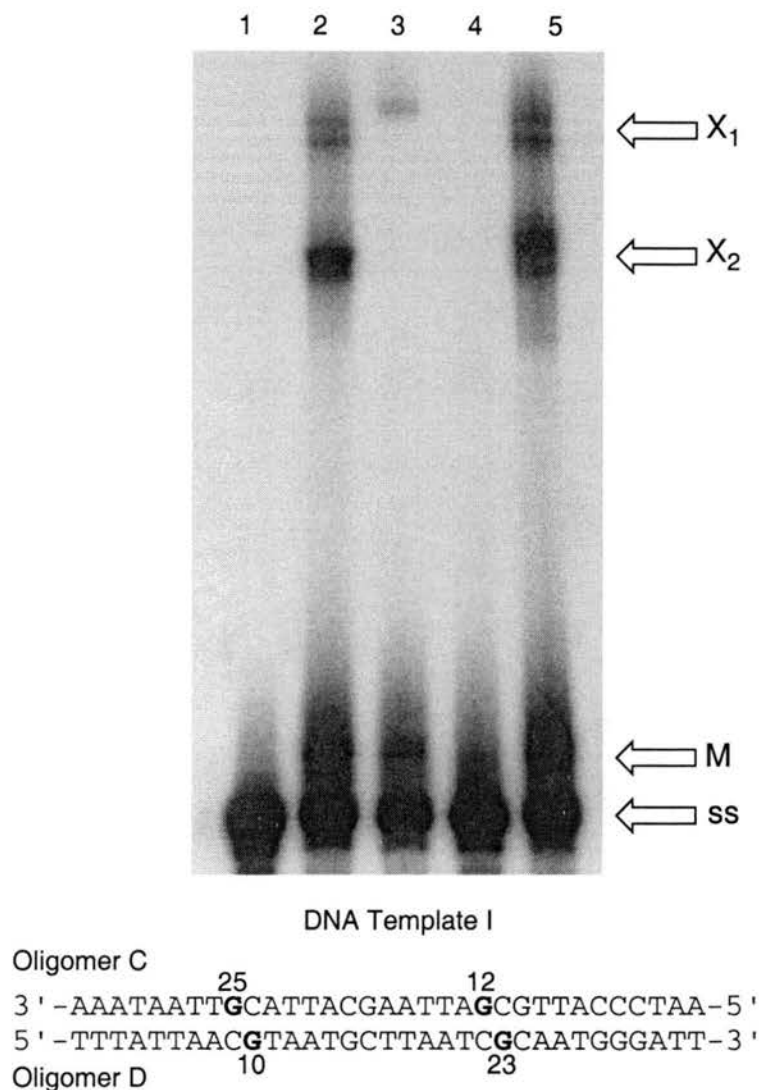
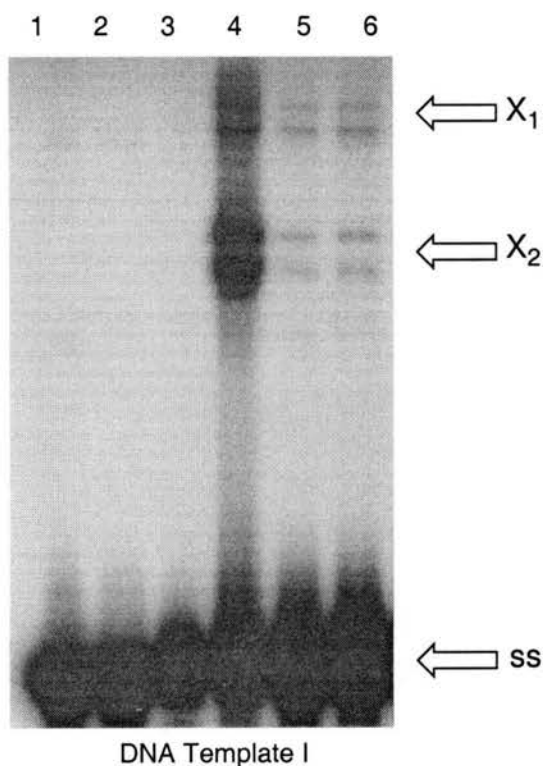
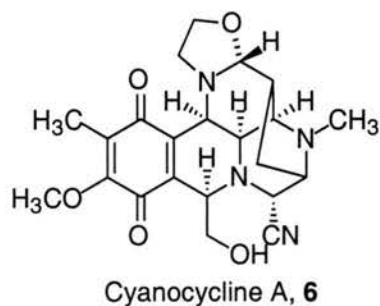


**Figure 15.** Bioxalomycin  $\alpha_2$  reactions with dG10/ dG23 substitutions in oligomer C. Lane 1 is native DNA template control. Lane 2 is cross-linked DNA product. Lane 3 is reaction of template 1 with bioxalomycin where inosine has been substituted at dG10(D). Lane 4 is reaction of template 1 with bioxalomycin where inosine has been substituted at dG10(D) and dG23(D). Lane 5 is reaction of template 1 with bioxalomycin where 2'-deoxy-deazaguanosine has been substituted at both dG10(D) and dG23(D). The cross-linked product at  $X_1$  is where the drug spans dG23(D) to dG12(C);  $X_2$  is where the drug spans dG10(D) to dG25(C); ss is single-stranded DNA; M is mono-alkylated DNA.

Since earlier molecular modeling suggested that the complete naphthyridinomycin molecule could not cross-link DNA,<sup>13b</sup> it was important to secure the molecular mass of the cross-linked DNA. The cross-link from the self complementary DNA substrate (Figure 16) was purified and the electrospray mass spectrum for the product was obtained. The





Oligomer C  
 25 12  
 3' - AAATAATTGCATTACGAATTAGCGTTACCCTAA - 5'  
 5' - TTTATTAACGTAATGCTTAATCGCAATGGGATT - 3'  
 Oligomer D  
 10 23

**Figure 18.** Cyanocycline A reactions with DNA template I. Lane 1 is native DNA template control. Lane 2 is native DNA with DTT (1.0 mM). Lane 3 is reaction of template I with cyanocycline A. Lane 4 is reaction of template I with bioxalomycin. Lane 4 and lane 6 is reaction of template I with cyanocycline A with DTT at 1.0 mM and 0.1 mM concentrations, respectively. The cross-linked product at X<sub>1</sub> is where the drug spans dG23(C) to dG12(D); X<sub>2</sub> is where the drug spans dG10(C) to dG25(D); ss is single-stranded DNA.

Cyanocycline A was found to cross-link DNA template I in low yield, but only in the presence of dithiothreitol (Figure 18). This experimental evidence lends further support for the importance of the reduction of the quinone to the hydroquinone in activating the electrophilic sites of this group of DNA cross-linking agents.

### 3.4 Conclusion

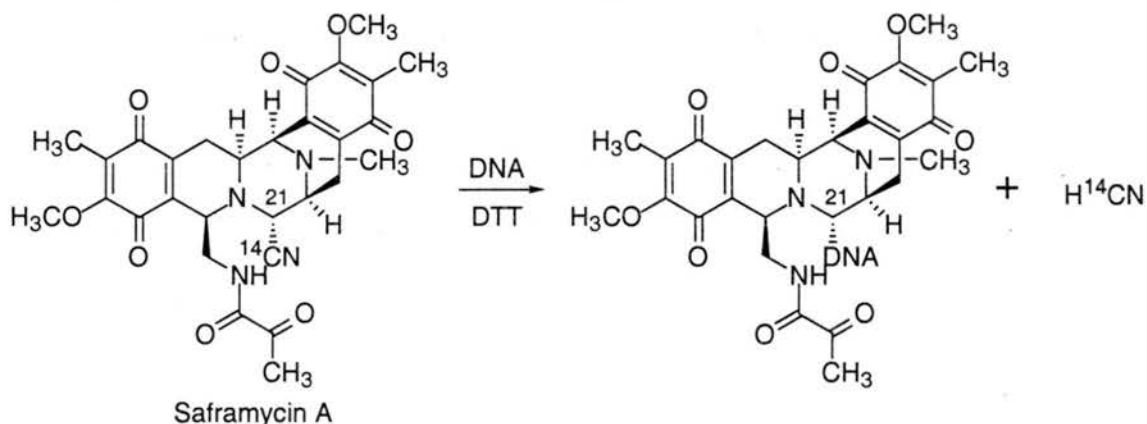
The experiments on the binding of bioxalomycin  $\alpha_2$  to DNA has demonstrated that the drug is capable of cross-linking DNA with 5'-CG-3' sequence specificity in the minor groove at the exocyclic amine at C-2 of guanosine. In addition, reductive activation of cyanocycline was found to be essential for the formation of cross-links for this drug. To further probe the mechanism of cross-linking, the points of attachment on bioxalomycin  $\alpha_2$  to guanosine should be identified.

Molecular modeling of the binding of bioxalomycin  $\alpha_2$  to a DNA tetramer, 5'-ACGT-3', was carried out to evaluate the four possible attachment sites of bioxalomycin  $\alpha_2$  (Appendix 4). Molecular mechanics were carried out using the cvff force-field in the molecular modeling package INSIGHT II v 2.3.5 (BIOSYM/Molecular Simulations, INC.). The drug was manually intercalated followed by 500 steps of energy minimization with the DNA backbone fixed between C-4' of the guanosine residues and C-3' of the cytosine residues. This constraint was released and the DNA-drug complex was further refined with 1000 steps of energy minimization using the conjugate gradient algorithm. The distances from the 2-amino group of guanosine to each potential electrophilic site of bioxalomycin were measured and are listed in Figure 19. The distances range from 3.60 to 4.73 Å and do not demonstrate any preference for a particular site on bioxalomycin  $\alpha_2$ . In addition from this molecular modeling, there is no obvious steric differences between the sites, which would favor any of them due to accessibility.

Site	Distance from 2-amino of guanosine (Å)
C-3a	3.71
C-7	4.73
C-9	3.60
C-13b	4.25

**Figure 19.** Distances from potential electrophilic sites of bioxalomycin  $\alpha_2$  to 2-amino group of guanosine measured after docking of drug in minor groove of DNA and subsequent minimization.

The potential of these sites being the attachment point to DNA can also be evaluated by examining previous experimental results. The case for C-7 of bioxalomycin  $\alpha_2$  is the strongest based on the work of Arai and co-workers on the alkylation of DNA by saframycin A.<sup>40</sup> When the cyano residue of saframycin was <sup>14</sup>C-labeled and incubated with DNA under reducing conditions, none of the radiation was observed in the resulting DNA-drug adduct (Scheme 33). From this result the authors concluded that the alkylation is occurring at C-21 of saframycin, which is analogous to C-7 of bioxalomycin  $\alpha_2$ .



**Scheme 33.** Alkylation of DNA induced by saframycin A under reducing conditions.

The crystal structure of the iminium ion at C-3a of cyanocycline was obtained by Nawata.<sup>41</sup> A solution of cyanocycline A in MeOH was neutralized with 0.1 M HBr, concentrated *in vacuo* and stored at -5 °C to give the corresponding crystals, whose

structure is shown in Figure 20. The crystal structure of the iminium ion lends support to nucleophilic attack at C-3a of bioxalomycin  $\alpha_2$ .

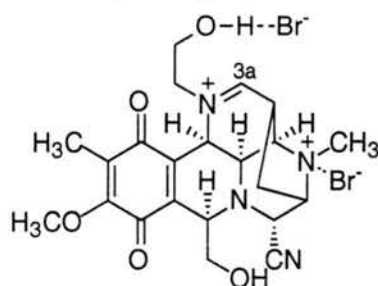
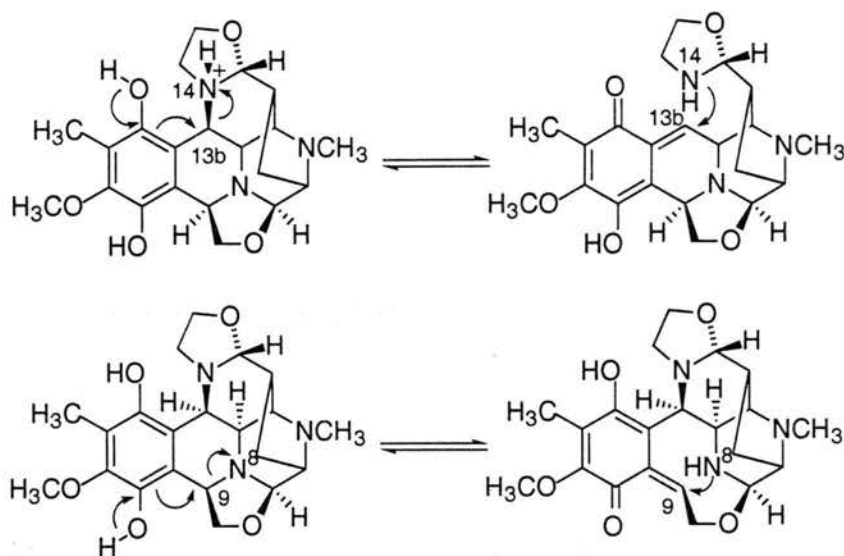


**Figure 20.** Structure of iminium ion obtained by X-ray crystallography of acidic solution of cyanocycline A.

Alkylation of DNA via a quinone methide to generate electrophilic sites at C-13b and/or C-9 is the final possibility. To generate a quinone methide from bioxalomycin  $\alpha_2$  it is necessary to have a leaving group at the benzylic position. In the case of alkylation at C-13b this is a possibility, since Remers found that N-14 of naphthyrdinomycin is protonated at pH 7 (Scheme 34).<sup>13b</sup> On the other hand, N-8 is not protonated at pH 7 and is thus not a good leaving group. The problem with the ortho quinone methide as the DNA alkylating agent is the facile intramolecular addition of the amine to the ortho quinone methide to regenerate bioxalomycin  $\alpha_2$  (Scheme 34). Due to this competing reaction, the alkylation of DNA though either ortho quinone methide seems less likely than nucleophilic attack of DNA at C-3a and C-7 of bioxalomycin  $\alpha_2$ .



**Scheme 34.** Generation of ortho quinone methide at C-13b and C-9.

The electrophilic sites of bioxalomycin  $\alpha_2$  could be unequivocally established by following a protocol that has been used to identify the sites of attack of other DNA cross-linking substances.<sup>42</sup> In these protocols the drug-DNA adduct is isolated and the DNA backbone digested enzymatically to give free nucleotides and the drug-DNA adduct, which was isolated by HPLC. The attachment points of the drug to the DNA were then assigned using spectroscopic measurements.

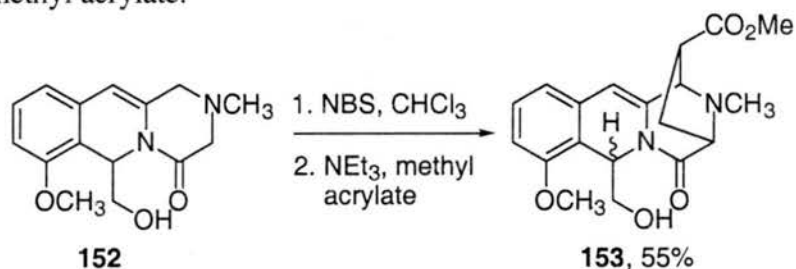
If this procedure is to be followed an ample supply of bioxalomycin  $\alpha_2$  is necessary. To provide this supply of bioxalomycin  $\alpha_2$ , a total synthesis of bioxalomycin  $\alpha_2$  has been initiated, and is discussed in Chapter 4.

## Chapter 4

### Synthetic Studies Towards Bioxalomycin $\alpha_2$

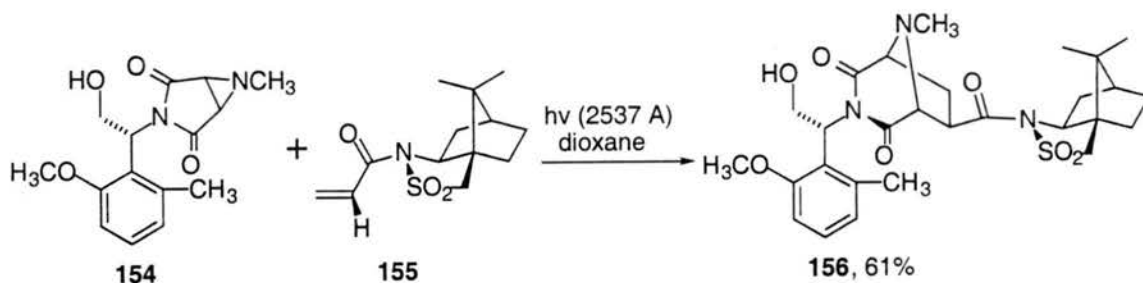
#### 4.1 Initial Strategy

The synthetic route towards bioxalomycin  $\alpha_2$  was based on the syntheses of ( $\pm$ )-quinocarcinamide by Flanagan and Williams,<sup>43</sup> and (-)-quinocarcin by Garner *et al.*<sup>44</sup> In these efforts, the key step to form the bridged piperazine ring is a [3 + 2] cycloaddition reaction between an azomethine ylide and an activated olefin (Schemes 40 and 41). In the Flanagan and Williams synthesis of ( $\pm$ )-quinocarcinamide, NBS oxidation of **152** followed by addition of NEt<sub>3</sub> formed the corresponding azomethine ylide, which was then trapped with methyl acrylate.



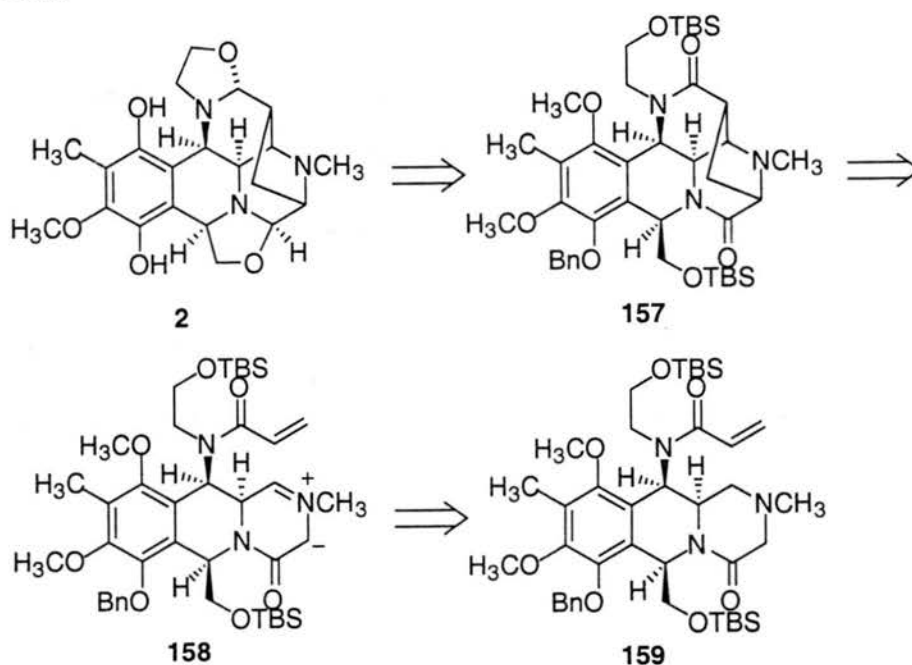
**Scheme 40.** Flanagan's [3 + 2] cycloaddition via azomethine ylide formation by NBS oxidation.

In the synthesis of (-)-quinocarcin by Garner, *et al.*, the azomethine ylide was generated by photo-decomposition of aziridine **154**. The azomethine ylide was then captured by Oppolzer's chiral acryloyl sultam to form **156** as the only stereoisomer in 61% yield.



**Scheme 41.** Garner's [3 + 2] cycloaddition step in his synthesis of (-)-quinocarcin.

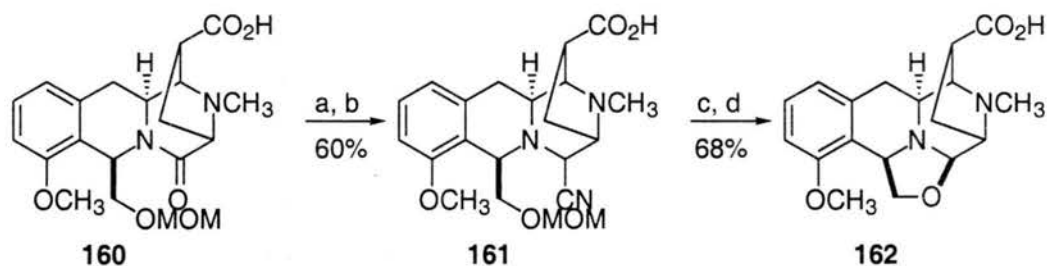
Taking the [3 + 2] cycloaddition strategy applied in these syntheses and placing the dipolarophile and the azomethine ylide in the same molecule resulted in the basic retrosynthesis of bioxalomycin  $\alpha_2$  outlined in Scheme 42. The key step is an intramolecular [3 + 2] cycloaddition between the azomethine ylide and the  $\alpha, \beta$ -unsaturated amide of **158**.



**Scheme 42.** Proposed [3 + 2] cycloaddition strategy to form main pentacyclic framework of bioxalomycin  $\alpha_2$ .

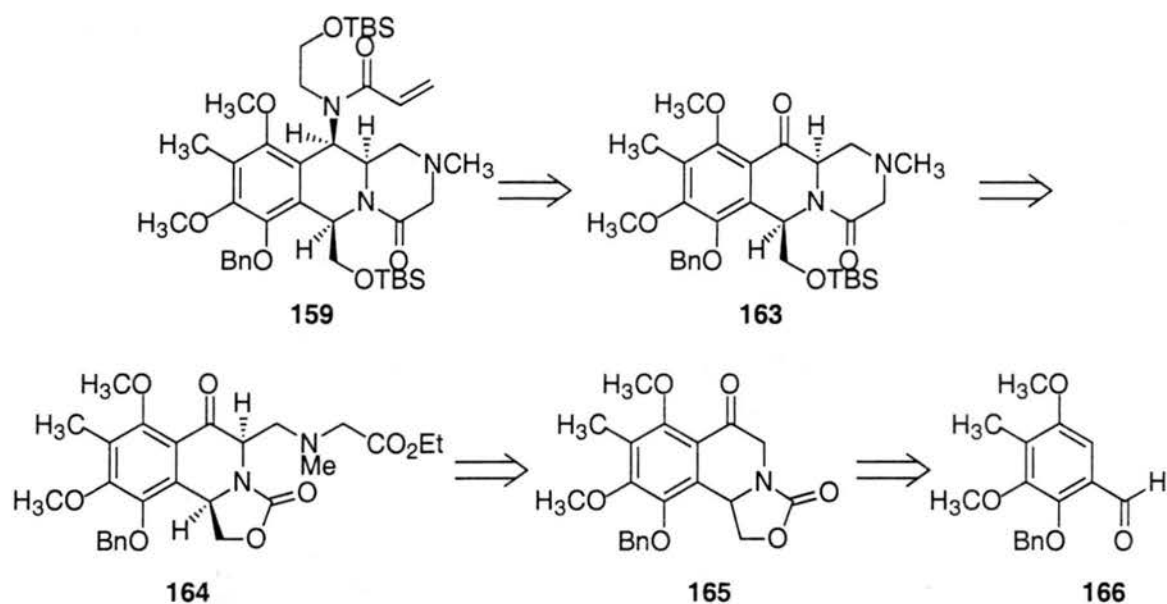
The generation of azomethine ylide **158** from lactam **159** might be accomplished using the same conditions (NBS, NEt<sub>3</sub>) described by Flanagan and Williams depicted in

Scheme 40. An alternate method to generate azomethine ylide **158** from **159** would be the base mediated decomposition of the N-oxide using the procedure described by Roussi.<sup>45</sup> Intramolecular capture of the azomethine ylide by the  $\alpha$ ,  $\beta$ -unsaturated amide moiety of **158** would form the pentacyclic core of bioxalomycin.



**Scheme 43.** Completion of (-)-quinocarcin by Garner. Key: (a) Li/NH<sub>3</sub>, THF, -33 °C; (b) NaCN, H<sub>2</sub>O; (c) MeSiCl, NaI, MeCN; (d) AgNO<sub>3</sub>, MeOH-H<sub>2</sub>O.

To finish the synthesis the oxazolidine rings must be constructed and the aromatic ring deprotected to the hydroquinone. A procedure outlined by Garner in his synthesis of quinocarcin could be used to form the oxazolidine rings (Scheme 43).<sup>42</sup> In this method, an aminonitrile is prepared by reduction first of the lactam to the carbinolamine and then displacement of the alcohol with NaCN. The oxazolidine rings were then closed by the addition of AgNO<sub>3</sub>. The formation of the hydroquinone could be accomplished by oxidizing to the quinone with DDQ, followed by reduction with activated zinc to the hydroquinone as outlined by Evans in his synthesis of (±)-cyanocycline (Chapter 1, Scheme 12).<sup>15b</sup>



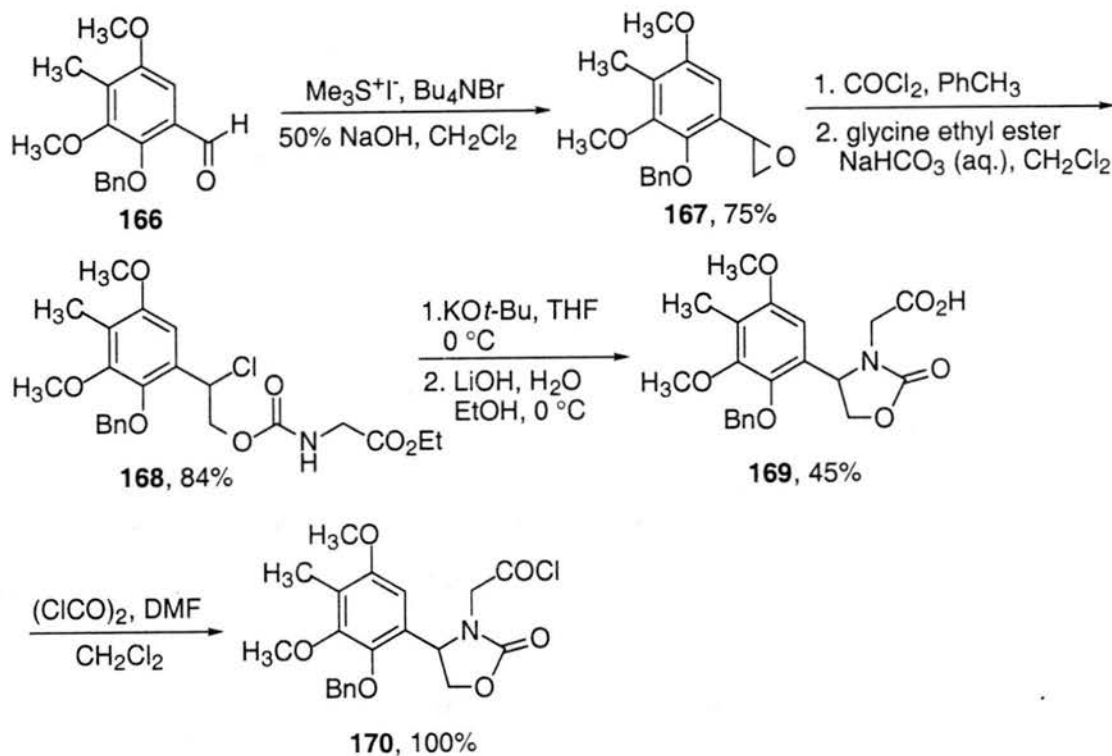
**Scheme 44.** Retrosynthetic analysis of azomethine ylide precursor **159**.

The construction of **159** would utilize chemistry already developed in the Williams group in the syntheses of quinuclidine analogs and quinuclidinamide (Scheme 44). The ketone functionality of **163** was envisioned to be used to construct the  $\alpha$ ,  $\beta$ -unsaturated amide of **162**. Under basic conditions, the oxazolidinone ring and the ester of **164** could be hydrolyzed in one step, resulting in the amino acid, which when coupled intramolecularly, would give **163**. Amino ester **164** could be prepared by alkylation of isoquinoline **165**  $\alpha$ - to the ketone. Isoquinoline **165** could be synthesized from aldehyde **166**.

#### 4.2 Synthesis of Isoquinoline 180

The first synthetic goal was the preparation of isoquinoline **165** from benzaldehyde **166**, which was prepared in 8 steps as previously described.<sup>14d,46</sup> Aldehyde **166** was converted to epoxide **167** using a sulfonium ylide (Scheme 45). Epoxide **167** was regioselectively opened with a 20% solution of phosgene in toluene to afford the chloroformate, which was acylated with glycine ethyl ester under Schotten-Baumen conditions to provide carbamate **168** in 84% yield. Deprotonation of the carbamate by

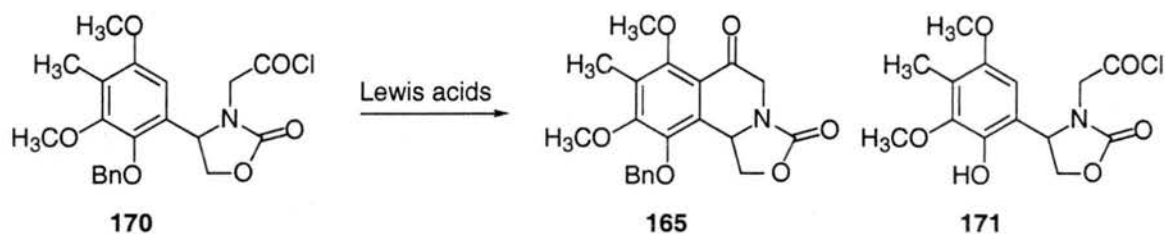
KOt-Bu followed by displacement of the chloride formed the oxazolidinone ring. Saponification of the ester under basic conditions afforded carboxylic acid **169** in 45% yield after recrystallization.



**Scheme 45.** Synthesis of Friedel-Crafts acylation precursor **170**.

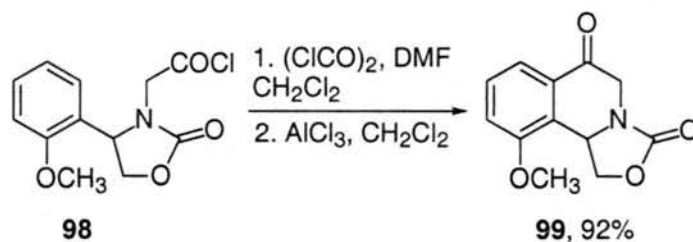
The preparation of acid chloride **170** was achieved quantitatively and cleanly as shown by <sup>1</sup>H-NMR spectroscopy (Scheme 45). After the addition of the  $\text{AlCl}_3$ ,  $\text{TiCl}_4$  or  $\text{AgOTf}_4$  to **170** to effect Friedel-Crafts ring closure only starting material was isolated (Table 1). More forcing conditions with  $\text{AlCl}_3$  resulted in debenzoylation to give phenol **171** as the major product.

**Table 1.** Friedel-Crafts acylation attempts of **170**.



Conditions	Product
$\text{AlCl}_3$ (4 eq.), $0^\circ\text{C}$	<b>170</b>
$\text{AlCl}_3$ (4 eq.), $25^\circ\text{C}$	<b>171</b>
$\text{TiCl}_4$ (1 eq.), $25^\circ\text{C}$	<b>170</b>
$\text{AgOTf}$ (4 eq.), $25^\circ\text{C}$	<b>170</b>

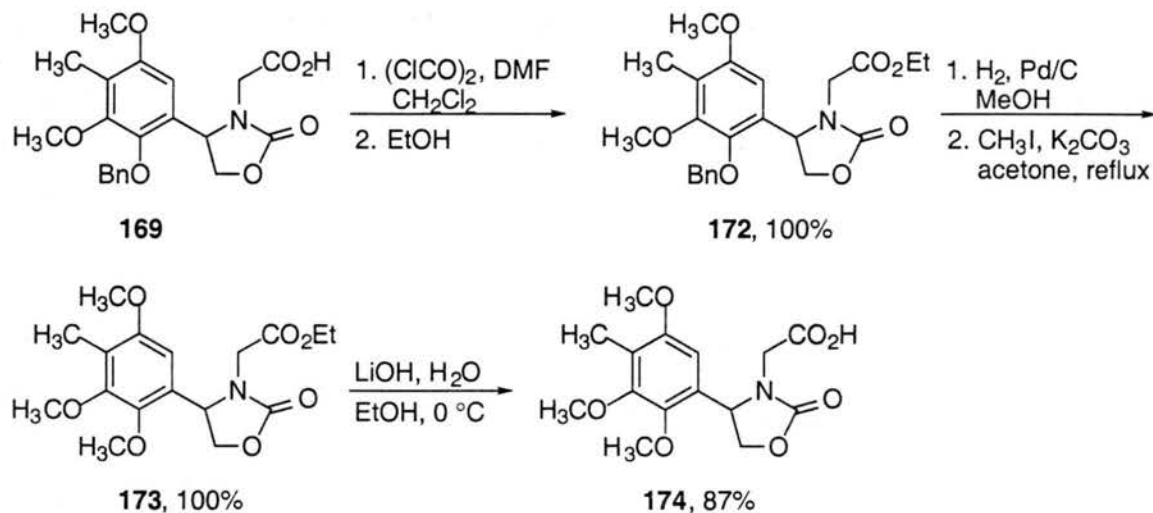
The failure of the Friedel-Crafts acylation was hard to rationalize since the reaction can be accomplished in good yield on a similar but less activated substrate (Scheme 46).<sup>25</sup> The lack of reactivity of **170** may be a steric consequence of the highly substituted aromatic ring. The benzyl substituent may block free rotation of the oxazolidinone ring and keep the reacting centers too far away from each other. If the group *ortho*- to the oxazolidinone ring were smaller, the oxazolidinone ring could then align itself in the proper position for the Friedel-Crafts acylation. To this end, Scheme 47 outlines the conversion of benzyl ether **169** to methyl ether **174**.



**Scheme 46.** Successful Friedel-Crafts acylation in the routes toward quinocarcin analogs.

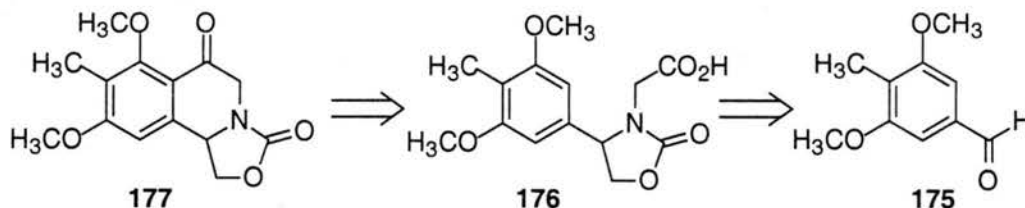
The carboxylic acid of **169** was esterified to afford **172**, which underwent hydrogenolysis of the benzyl group and protection of the phenol as the methyl ether to give

**173** in quantitative yield. Under basic conditions, the ester moiety of **173** was saponified to produce carboxylic acid **174** in 87% yield.



**Scheme 47.** Conversion of benzyl ether **169** to methyl ether **174**.

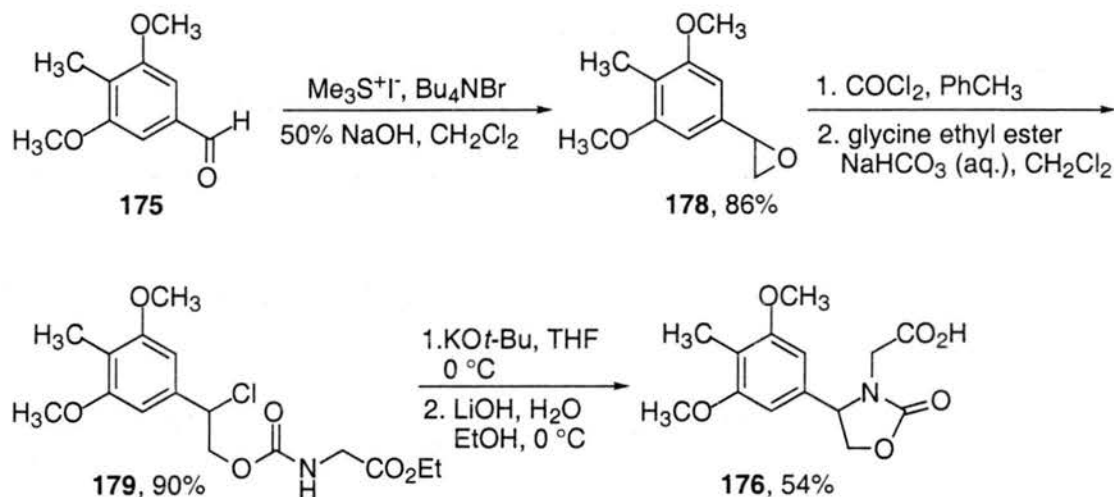
When the acid chloride of **174** was exposed to a variety of Friedel-Crafts conditions, only starting material was obtained. Apparently this conversion of the group ortho to the oxazolidinone had no positive effect on the Friedel-Crafts acylation. A new Friedel-Crafts precursor that has no substituent ortho to the oxazolidinone was considered next. The group *ortho*- to the oxazolidinone was removed in **176** resulting in a  $C_2$ -symmetric aryl moiety with two equivalent reaction centers on the ring (Scheme 48). In addition, the oxazolidinone should have free rotation since there are no ortho substituents.



**Scheme 48.** Retrosynthesis of isoquinoline **177**.

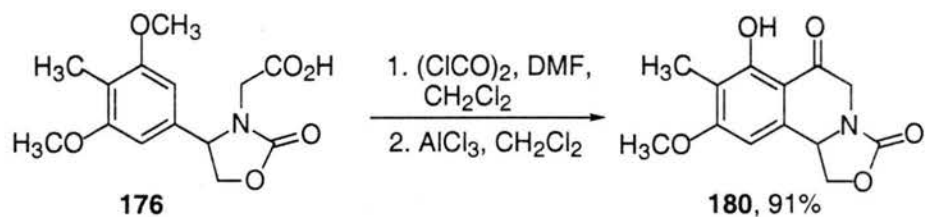
The synthesis began with 3,5-dimethoxy-4-methylbenzaldehyde (**175**), which was prepared from 3,4,5-trimethoxybenzaldehyde in 3 steps.<sup>47</sup> Aldehyde **175** was converted into oxazolidinone **176** using the same protocol as previously outlined (Scheme 49).

Reaction of aldehyde **175** with trimethylsulfonium iodide under phase transfer conditions afforded epoxide **178** in 86% yield. The epoxide was then opened with phosgene to give the chloroformate, which was stirred with glycine ethyl ester resulting in carbamate **179** in 90% yield. Oxazolidinone formation with  $\text{KO}t\text{-Bu}$ , followed by saponification of the ester with  $\text{LiOH}$  completed the synthesis of carboxylic acid **176** in 54% yield after recrystallization.



**Scheme 49.** Synthesis of carboxylic acid **176**.

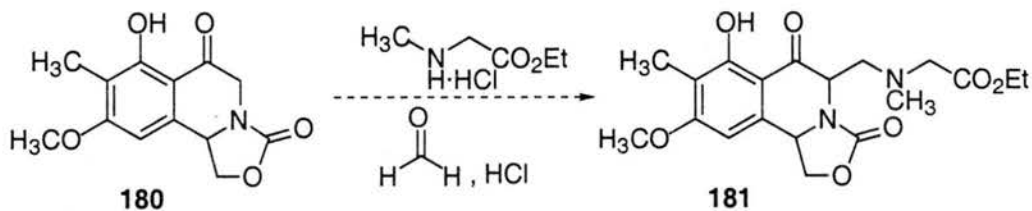
The acid chloride of **176** was prepared and when subjected to the standard Friedel-Crafts acylation conditions ( $\text{AlCl}_3$ ,  $\text{CH}_2\text{Cl}_2$ ), resulted in isoquinoline **180** in 91% yield (Scheme 50). In addition, under the Lewis acidic conditions one of the methoxy groups was demethylated. Based on literature precedent, the methyl ether *ortho*- to the ketone should be selectively removed due to coordination of the aluminum with the ketone.<sup>48</sup> In addition, the chemical shift of the phenol proton was independent of the concentration of the substrate indicative of an intramolecular hydrogen bond between the phenol and the ketone of **180**.



**Scheme 50.** Synthesis of isoquinoline **180**.

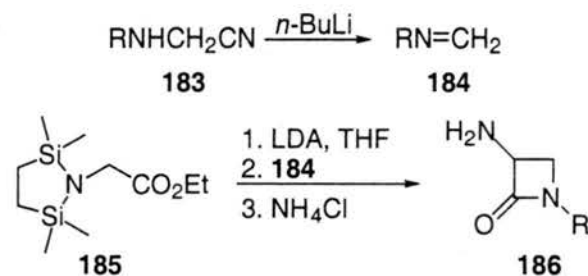
### 4.3 Mannich Reaction Attempts

The next step in the route was to attach an amino ester to **180**, and the most direct strategy was a Mannich reaction between **180** and sarcosine ethyl ester. The first attempts used the classical conditions for the Mannich reactions (Scheme 51).<sup>49</sup> Only starting material was isolated when the reaction was carried out with either formalin or paraformaldehyde as the formaldehyde equivalent in ethanol at reflux.



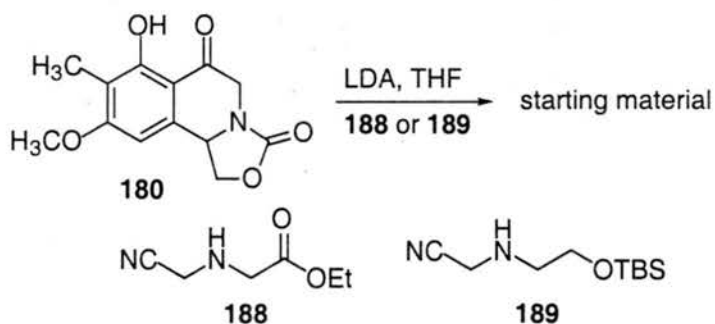
**Scheme 51.** Classical Mannich approach to **181**.

Due to the lack of reactivity of isoquinoline **180** to classical Mannich conditions, alternative protocols were explored. Overman has shown that formaldehyde imines can be formed from the reaction of secondary *N*-(cyanomethyl)amines with *n*-BuLi (Scheme 52).<sup>50</sup> In a subsequent publication,  $\beta$ -lactams were prepared by reacting the imines with ester enolates.<sup>51</sup> Though not discussed in the paper, the  $\beta$ -lactam ring could be a result of a stepwise addition of the ester enolate to the imine to produce the amine, which then attacks the carbonyl of the ester to form the four-membered ring. If this is indeed the case, the lithium enolate of **180** and an imine from a *N*-(cyanomethyl)amine could be generated and coupled in the same pot to form the simple Mannich reaction product.



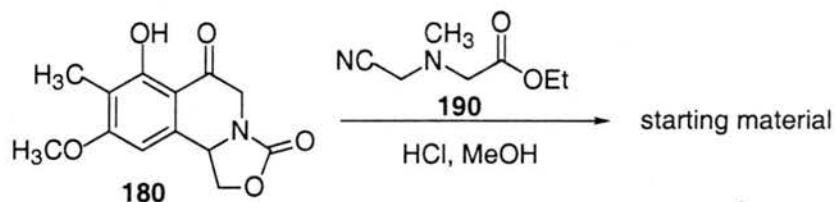
**Scheme 52.** Overman's preparation of  $\beta$ -lactams via formaldehyde imines.

Secondary *N*-(cyanomethyl)amine **188** was added to a solution of **180** and three equivalents of LDA, and stirred at room temperature (Scheme 53). After quenching with  $\text{NH}_4\text{Cl}$  only starting materials were isolated. Due to the acidic protons  $\alpha$  to the carbonyl in imine **188**, an alternative *N*-(cyanomethyl)amine, **189**, was prepared and subjected to the same reaction conditions. Again no reaction was observed and only starting material was isolated.



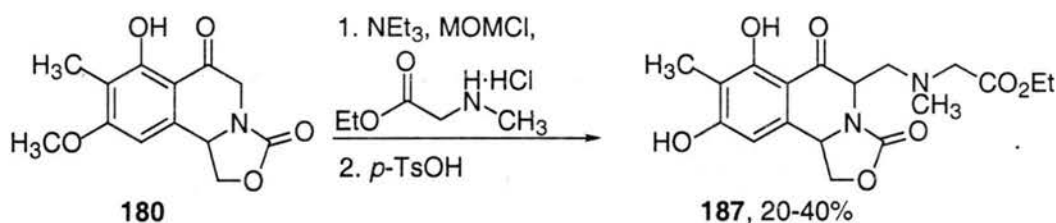
**Scheme 53.** Coupling of attempts of isoquinoline **180** to *N*-(cyanomethyl) amines **188** and **189** under basic conditions.

Tertiary *N*-(cyanomethyl) amines under acidic conditions are known to form an iminium ion, which can then undergo a Mannich reaction.<sup>52</sup> Unfortunately, when *N*-(cyanomethyl)amine **190** was stirred with **180** under acidic conditions, only starting material was recovered (Scheme 54).



**Scheme 54.** Coupling attempt of **180** with tertiary *N*-(cyanomethyl)amine **190** under acidic conditions.

Success with the Mannich reaction was accomplished following the methodology used to form an azomethine ylide from Williams' lactone.<sup>53</sup> Following this procedure the amine of sarcosine ethyl ester was alkylated with chloromethyl methyl ether in the first step (Scheme 55). The crude methoxymethyl adduct was then treated with *p*-toluenesulfonic acid to generate the iminium ion. In the presence of isoquinoline **180** this gave the demethylated product **187** in low to modest yields.



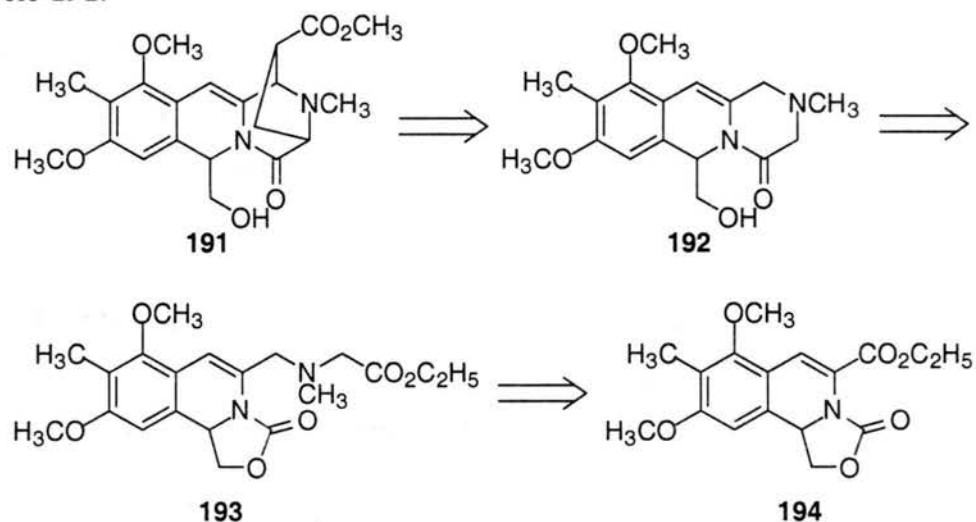
**Scheme 55.** Successful Mannich reaction to give **187**.

The yield of the Mannich reaction could not be increased above 40%, and the majority of the attempts at this reaction gave back only starting material. Due to the inconsistent results of the Mannich reaction, and interesting developments on other fronts, this route was no longer pursued.

#### 4.4 Aldol and $\beta$ -Lactam Routes

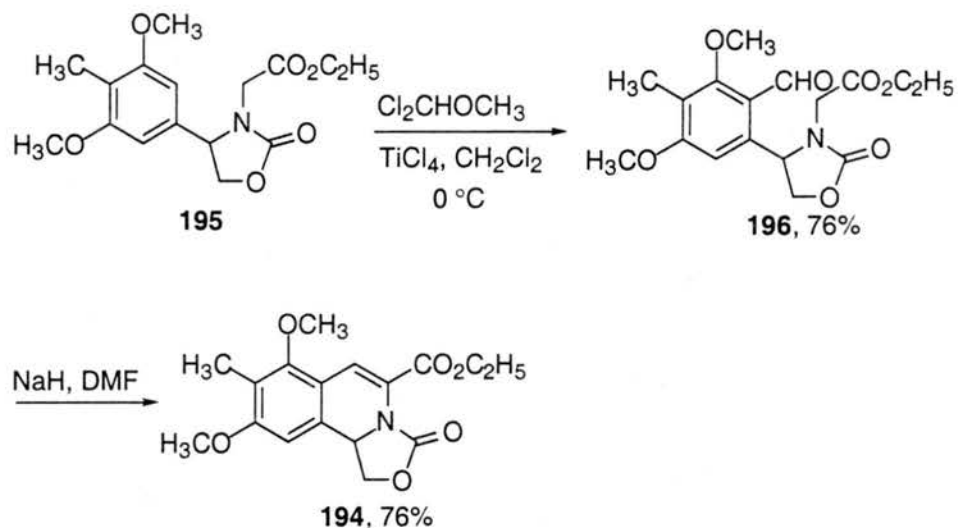
In addition to the Mannich attempts, a number of other strategies to functionalize the isoquinoline were explored. One of the desired intermediates was  $\alpha$ ,  $\beta$ -unsaturated ester **194** (Scheme 56). Ester **194** could be elaborated into amino ester **193** by reduction of the ester to the alcohol, transformation to the mesylate, and displacement of the mesylate with

sarcosine ethyl ester. Hydrolysis of the ester and oxazolidinone of **193** followed by an intramolecular peptide coupling would result in lactam **192**. The azomethine ylide could then be prepared using NBS and NEt<sub>3</sub> and, when captured by methyl acrylate, afford tetracycle **191**.



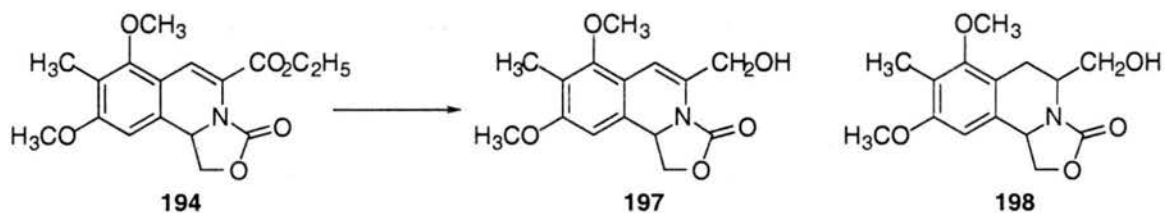
**Scheme 56.** Retrosynthetic analysis of tetracycle **191** from **194**.

The synthetic route to **194** that was developed did not involve isoquinoline **180**, but went through an intramolecular aldol reaction of aldehyde **196** (Scheme 57). Aldehyde **196** was prepared in good yield by the addition of Cl<sub>2</sub>CHOCH<sub>3</sub> to **195** in the presence of TiCl<sub>4</sub>. After screening a number of bases (LDA, LiN(SiCH<sub>3</sub>)<sub>2</sub>, NaOEt) to effect the intramolecular aldol reaction, sodium hydride was found to afford **194** in the highest yield.



**Scheme 57.** Intramolecular aldol reaction of **196** to afford **194**.

**Table 2.** 1, 2-Reduction attempts of  $\alpha$ ,  $\beta$ -unsaturated ester **194**.

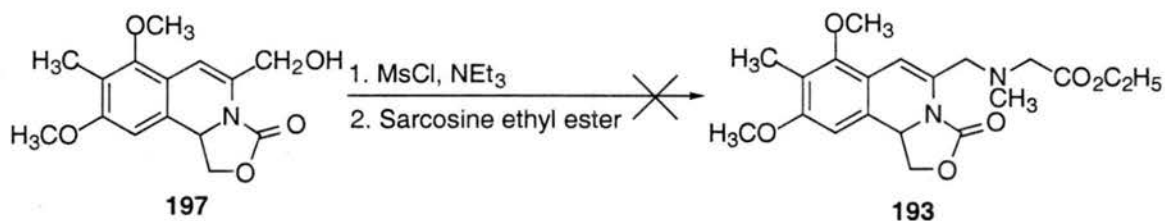


Conditions	Yield	Product
3 eq <i>n</i> -BuLi/DIBAL, -78 °C, 3 h	57%	<b>197, 194</b> (1:1)
4 eq <i>n</i> -BuLi/DIBAL, -78 °C, 3 h	100%	<b>197, 194*</b>
5 eq <i>n</i> -BuLi/DIBAL, -78 °C, 3 h	34%	<b>197*</b>
3 eq <i>n</i> -BuLi/DIBAL, -45 °C, 3 h	81%	<b>197, 194</b> (2:1)
3 eq <i>n</i> -BuLi/DIBAL, -10 °C, 30 min	84%	<b>197, 194</b> (3:1)
3 eq <i>n</i> -BuLi/DIBAL, RT, 30 min	27%	<b>197</b>
3 eq <i>n</i> -BuLi/DIBAL, RT, 3 h	55%	<b>197*</b>
6 eq LiBH <sub>4</sub> , MeOH, Et <sub>2</sub> O, reflux	53%	<b>197, 194</b> (1:1)
8 eq LiBH <sub>4</sub> , MeOH, Et <sub>2</sub> O, reflux	74%	<b>197, 194</b> (1:1)
3 eq LiBH <sub>4</sub> , MeOH, THF, RT	54%	<b>197, 198</b> (1:1)
2 eq LiBH <sub>4</sub> , CeCl <sub>2</sub> , MeOH, THF, RT	75%	<b>194</b>

\* is a mixture with an unidentifiable compound.

Unfortunately,  $\alpha$ ,  $\beta$ -unsaturated ester **194** could not be reduced cleanly nor completely (Table 2). The best yield, 27%, was achieved with three equivalents of an *n*-BuLi/DIBAL complex at room temperature.<sup>54</sup> Selective 1,2-reductions can also be realized with LiBH<sub>4</sub>,<sup>55</sup> but in the reduction of **194**, the desired allylic alcohol **197** was always accompanied by starting materials or undesired saturated alcohol **198**. The LiBH<sub>4</sub> reduction was also carried out in the presence of CeCl<sub>3</sub>,<sup>56</sup> but only starting materials were isolated.

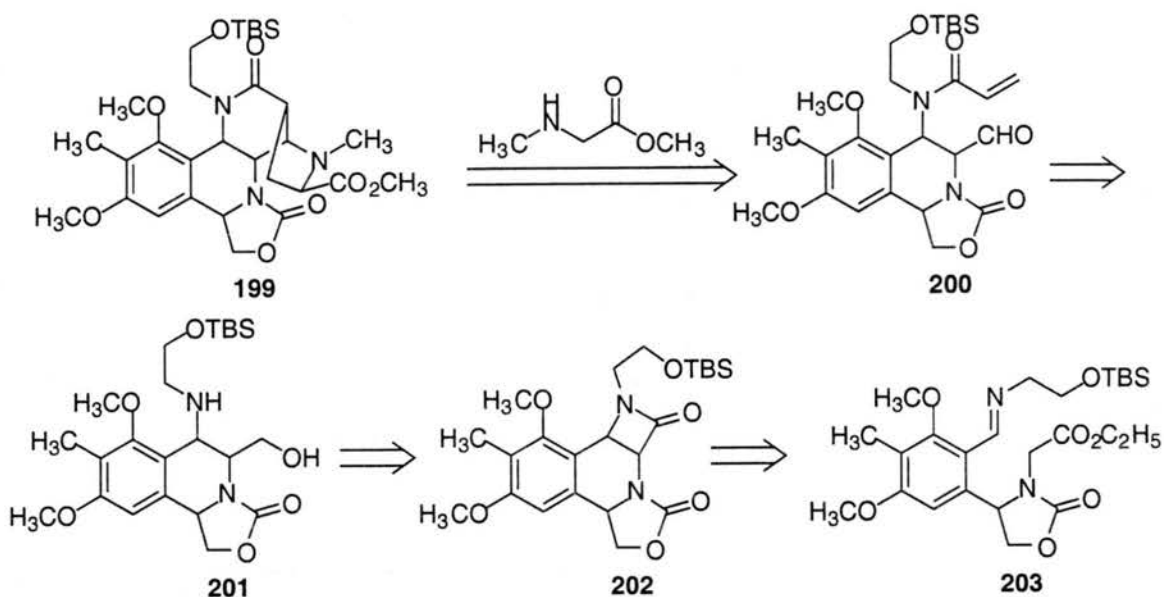
Although the reduction of ester **194** was never achieved in good yields, it did provide a satisfactory amount of allylic alcohol **197** to attempt the coupling reaction with sarcosine ethyl ester (Scheme 58). The mesylate of **197** was prepared and stirred with sarcosine ethyl ester in the presence of NEt<sub>3</sub>. The starting materials were completely consumed, but none of the desired coupling product was isolated.



**Scheme 58.** Coupling attempt of allylic alcohol **197** with sarcosine ethyl ester.

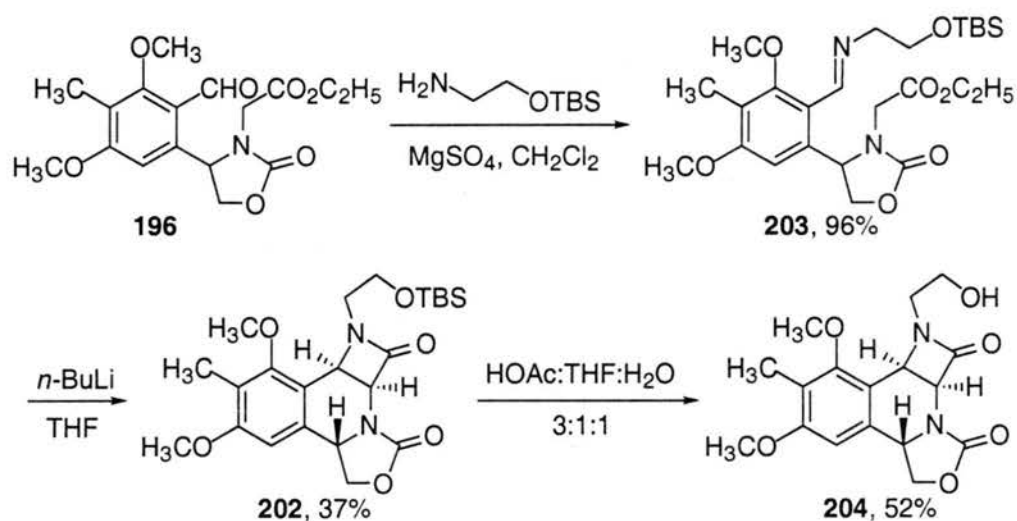
Although this route was abandoned, the successful intramolecular aldol condensation prompted an investigation of an intramolecular coupling between an imine and an ester. The condensation of an imine and an ester enolate is a popular method to prepare  $\beta$ -lactams.<sup>57</sup> Various enolates including zinc, aluminum, boron and lithium have been utilized in this transformation. An intramolecular condensation of imine **203** would prepare  $\beta$ -lactam **202** (Scheme 59). Reductive opening of the  $\beta$ -lactam would give amino alcohol **201**, whose amine could be acylated and alcohol oxidized to the aldehyde to afford **200**. Aldehydes can be condensed with amines under basic conditions to produce

azomethine ylides,<sup>58</sup> which in the case of **200** could react intramolecularly with the electron deficient olefin to give pentacyclic product **199**.



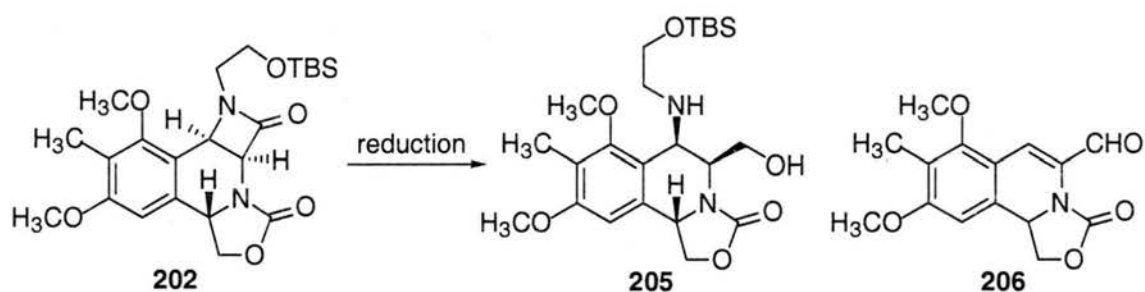
**Scheme 59.** Retrosynthetic analysis of pentacyclic lactam **199**.

Imine **203** was prepared by stirring aldehyde **196** with *O*-TBS protected ethanolamine and  $\text{MgSO}_4$  in  $\text{CH}_2\text{Cl}_2$  (Scheme 60). A number of bases (LDA,  $\text{LiN}(\text{SiCH}_3)_2$ ,  $\text{NaH}$ ) were examined to effect the condensation, but *n*-BuLi gave the cleanest reactions and most consistent yields of **202**. The reaction gave only one diastereomer whose relative stereochemistry was assigned by the X-ray crystal structure of free alcohol **204** (Appendix 2).



**Scheme 60.** Synthesis of  $\beta$ -lactam **202** via intramolecular condensation of an ester enolate with an imine.

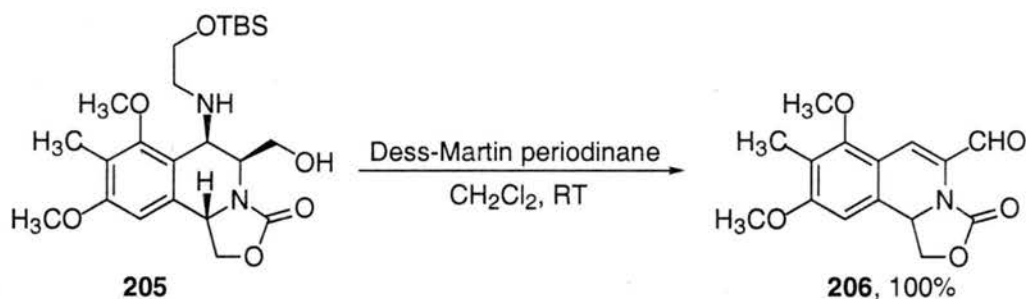
**Table 3.** Reduction attempts of  $\beta$ -lactam **202**.



Conditions	Product
2 eq Red-Al, THF, 0 °C	<b>202</b>
1 eq DIBAL, toluene, 0 °C	<b>202</b>
2 eq DIBAL, toluene, RT	<b>202</b>
4 eq LiAlH <sub>2</sub> (OEt) <sub>2</sub> , THF, 0 °C	decomp.
1 eq LiAlH <sub>2</sub> (OEt) <sub>2</sub> , THF, 0 °C	<b>202</b> , <b>206</b> (44%, 1:1)
1.5 eq LiAlH <sub>4</sub> , THF, 0 °C	<b>202</b>
2 eq LiAlH <sub>4</sub> , THF, RT	decomp.
10 eq BH <sub>3</sub> -THF, RT	<b>205</b> (27%)

The next step was the crucial reduction of the  $\beta$ -lactam functionality of **202**. A range of reducing conditions were investigated, and are shown in Table 3. All of the aluminum hydrides either gave recovered starting material back or decomposition of the starting material when the reaction was done under more forcing conditions. The exception is  $\text{LiAlH}_2(\text{OEt})_2$ ,<sup>59</sup> which reduced the lactam to  $\alpha,\beta$ -unsaturated aldehyde **206** via *in situ* elimination of the benzylic amine. Borane reduced  $\beta$ -lactams to the amino alcohol,<sup>60</sup> and when the reducing agent was switched to a  $\text{BH}_3$ -THF complex the reduction of **202** to amino alcohol **205** was accomplished in 27% yield.

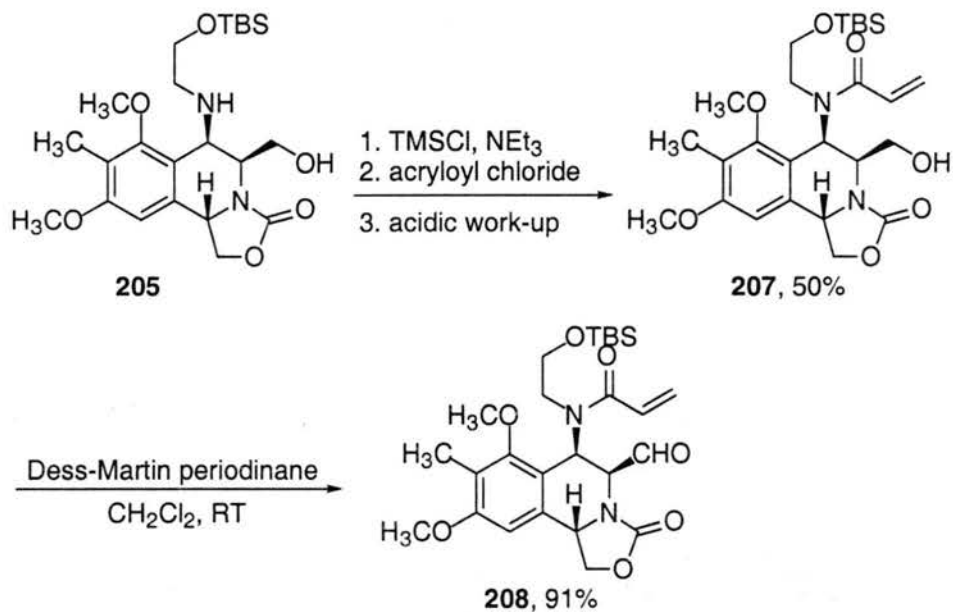
When alcohol **205** was subjected to Dess-Martin oxidation conditions only the eliminated product **206** was isolated (Scheme 61). An amine is a poor leaving group, yet this was the second time upon transformation to the aldehyde that the amino group was eliminated resulting in **206** (for another instance, see  $\text{LiAlH}_2(\text{OEt})_2$  reduction, Table 3). The amine may be coordinating to another species making it a better leaving group. In the case of the reduction with  $\text{LiAlH}_2(\text{OEt})_2$ , aluminum may be acting as the Lewis acid, while in the Dess-Martin oxidation the hypervalent iodide may be coordinating to the amine.



**Scheme 61.** Oxidation of **205** results in elimination to give aldehyde **206**.

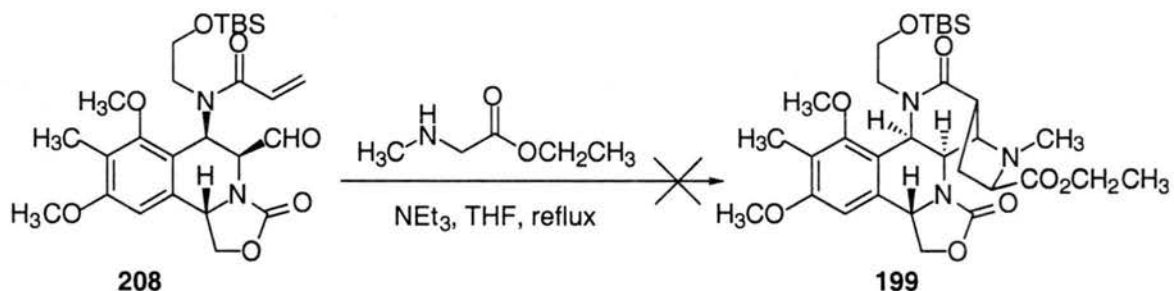
To preclude the coordination of the amine and subsequent elimination, the amine was first acylated with acryloyl chloride (Scheme 62). The acylation of the amine of **205** was cleanly accomplished by first protecting the primary alcohol of **205** as the TMS ether, then adding acryloyl chloride followed by an acidic workup to give **207**. The alcohol was

now easily oxidized using Dess-Martin periodinane to afford desired [3 + 2] cycloaddition precursor **208**.



**Scheme 62.** Preparation of [3 + 2] precursor **208**.

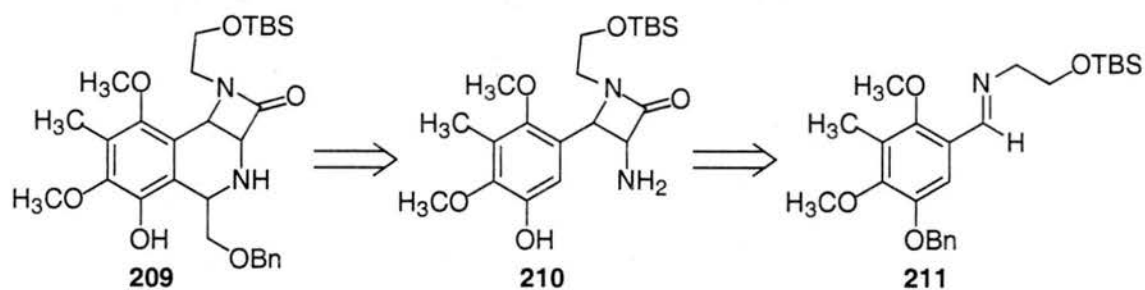
To prepare the azomethine ylide and effect the [3 + 2] cycloaddition, sarcosine ethyl ester and NEt<sub>3</sub> were added to **208** and the mixture was heated to reflux (Scheme 63).<sup>56,61</sup> The intramolecular [3 + 2] product **199** was not observed, instead the reaction cleanly afforded elimination product **206**. This elimination also occurred when **208** was refluxed in THF with only sarcosine ethyl ester or NEt<sub>3</sub>. In addition, if aldehyde **208** sat at 25 °C for a few days it completely eliminated to **206**. All of this evidence points towards a facile β-elimination problem with aldehyde **208**, which made the potential of this route limited.



**Scheme 63.** Intramolecular [3 + 2] cycloaddition attempt with sarcosine ethyl ester.

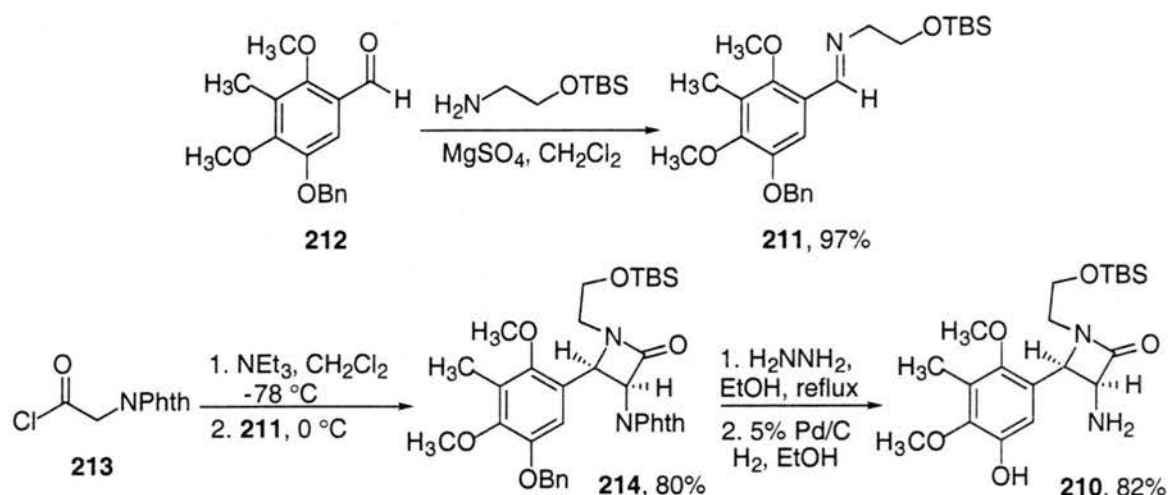
#### 4.5 Second Generation $\beta$ -Lactam Route

A new route was devised based on  $\beta$ -lactam **209**, whose structure contains some advantages over **205** (Scheme 64). The advantages include having the correct substitution of the aromatic ring and a free amine instead of a robust oxazolidinone ring. In addition, the previous synthesis of **205** had a number of low yielding steps, including the intramolecular condensation of the imine and ester enolate, which resulted in the wrong relative stereochemistry. In the new synthetic route, isoquinoline **209** could be prepared by a Pictet-Spengler condensation of benzyloxyacetaldehyde and **210**. The  $\beta$ -lactam ring of **210** was envisioned to come from a Staudinger reaction between a *N*-protected acid chloride and imine **211**.



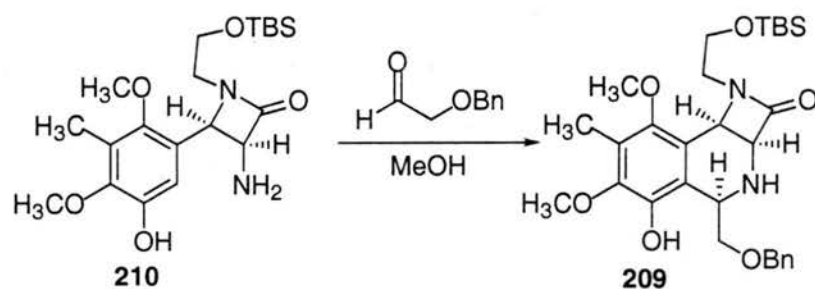
**Scheme 64.** Retrosynthesis of  $\beta$ -lactam **209**.

Aldehyde **212** was condensed with *O*-TBS protected ethanolamine and  $\text{MgSO}_4$  in  $\text{CH}_2\text{Cl}_2$  to afford imine **211** (Scheme 65). The ketene of phthalimidoacetyl chloride (**213**) was prepared by stirring **213** with  $\text{NEt}_3$  at  $-78\text{ }^\circ\text{C}$ . Then imine **211** was added and the reaction was warmed up to  $0\text{ }^\circ\text{C}$ , resulting in  $\beta$ -lactam **214** in 80% yield. The *syn*-stereochemistry was assigned by *nOe* experiments (Appendix 1). Hydrolysis of the phthalimide, followed by hydrogenolysis of the benzyl ether, afforded amino phenol **210**, which is the Pictet-Spengler precursor.



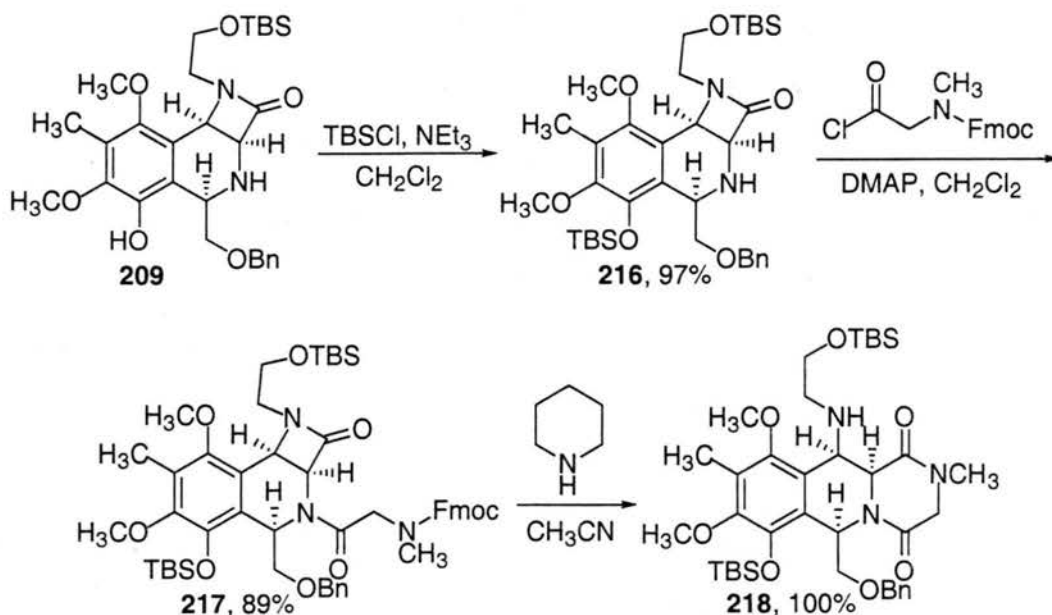
**Scheme 65.** Synthesis of Pictet-Spengler precursor **210**.

A number of reaction conditions were used to carry out the Pictet-Spengler reaction (Table 4). Benzyloxyacetaldehyde was prepared from glycerol in four steps following the procedure of Shiao.<sup>62</sup> The highest yield of the Pictet-Spengler reaction was obtained by heating the aldehyde with **210** at 50 °C in methanol. To achieve consistent yields of this reaction it was necessary to distill the aldehyde immediately before use. Pictet-Spengler reactions are often catalyzed by acid, but in this case the addition of acetic acid lowered the yield. The Pictet-Spengler reaction afforded only one diastereomer of **209**. Results of nOe experiments on later intermediates,  $\beta$ -lactam **235** and diketopiperazine **220** (see Appendix 1), were consistent with the all *cis* relationship of the three stereocenters.

**Table 4.** Pictet-Spengler attempts to form isoquinoline **209**.

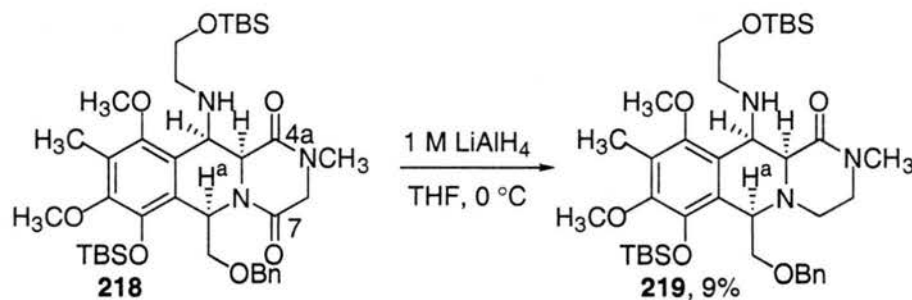
Eq. of aldehyde	acid (eq.)	Temp. (°C)	Product
1.0	---	25	<b>210</b>
1.2	---	50	<b>209</b> (86%)
1.5	---	65	<b>209</b> (19%)
5.0	---	65	Decomp.
1.2	AcOH (1.2)	25	<b>210</b> , <b>209</b> (27%, 1:1)
1.2	AcOH (1.2)	65	<b>209</b> (27%)
2.4	AcOH (1.2)	65	Decomp.

The phenol of **209** was then protected with TBSCl to afford **216**, which was coupled with the acid chloride of *N*-(Fmoc)-protected sarcosine in the presence of DMAP to give amide **217** (Scheme 66). Attempts at reductively opening the  $\beta$ -lactam ring of **217** were carried out using conditions similar to those before (Table 3). Under the reaction conditions examined, the  $\beta$ -lactam in **217** could not be reduced to the desired amino alcohol. When **217** was stirred with a 1 M  $\text{BH}_3$ -THF complex, which reduced **202** to amino alcohol **205**, only starting materials were observed. Using aluminum reducing agents ( $\text{LiAlH}_4$ , DIBAL, Red-Al) for the reduction resulted in cleavage of the amide bond to give **216**. As an alternative the amine of **217** was then deprotected with piperidine and the free amine attacked the  $\beta$ -lactam to afford diketopiperazine **218** in one step.



**Scheme 66.** Synthesis of diketopiperazine **218**.

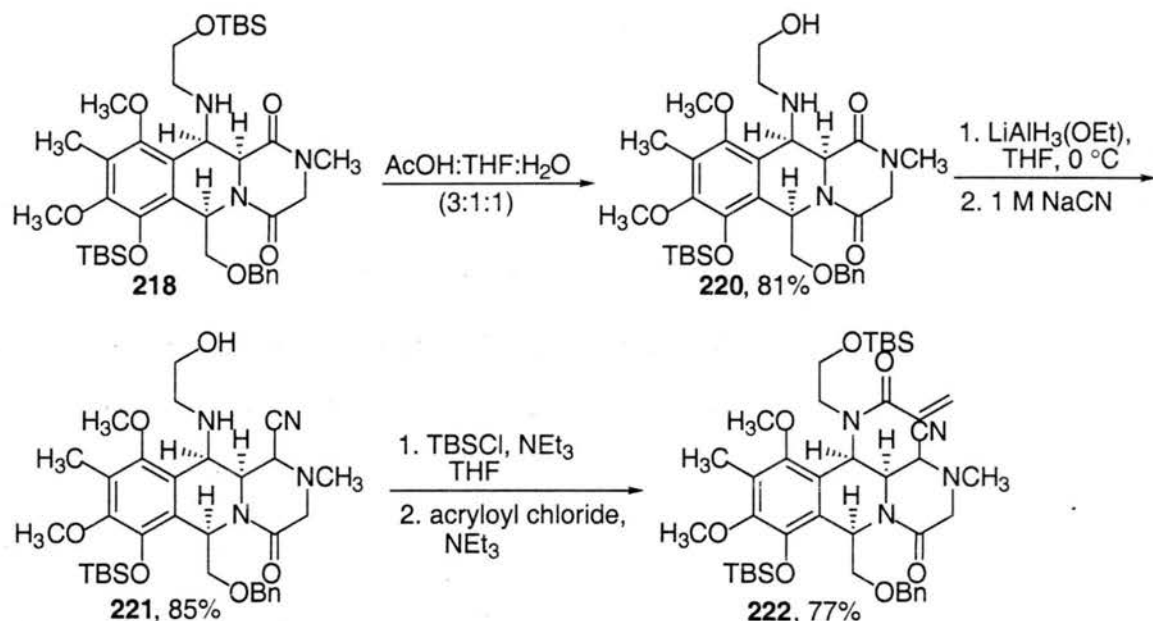
The next step was a regioselective reduction of the lactam carbonyl at C-4a over C-7 of **218** to the carbinolamine (Scheme 67). The regioselectivity of the reduction could perhaps be achieved by chelation of the reducing agent to the amine and the carbonyl at C-4a, activating the carbonyl towards reduction. When diketopiperazine **218** was exposed to  $\text{LiAlH}_4$  at  $0^\circ\text{C}$ , the undesired reduction product **219** was isolated. The regioselectivity of the reduction was assigned by the change of the chemical shift of  $\text{H}^a$ , which was at 6.2 ppm in **218** and moved upfield after the reduction.



**Scheme 67.** Reduction of **218** by  $\text{LiAlH}_4$ .

To increase the coordination of the aluminum and the ability to direct the reduction, the TBS ether of **218** was hydrolyzed under acidic conditions to afford amino alcohol **220**

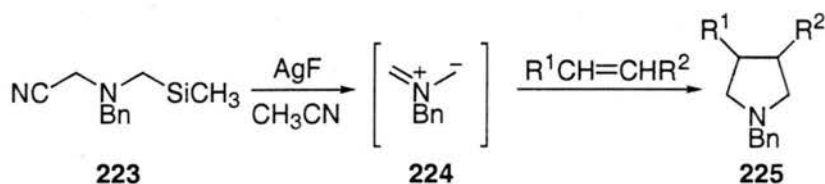
(Scheme 68). The reduction to the carbinolamine was accomplished at first with  $\text{LiAlH}_4$  in 54% yield and was later optimized to 85% yield using  $\text{LiAlH}_3(\text{OEt})$ . The unstable carbinolamine was never isolated. Instead the reaction was quenched with 1M NaCN, which resulted in aminonitrile **221** as one diastereomer (stereochemistry unassigned). To finish the synthesis of the [3 + 2] cycloaddition precursor, the alcohol was protected using TBSCl and the amine acylated with acryloyl chloride to afford **222**.



**Scheme 68.** Completion of the synthesis of [3 + 2] cycloaddition precursor **222**.

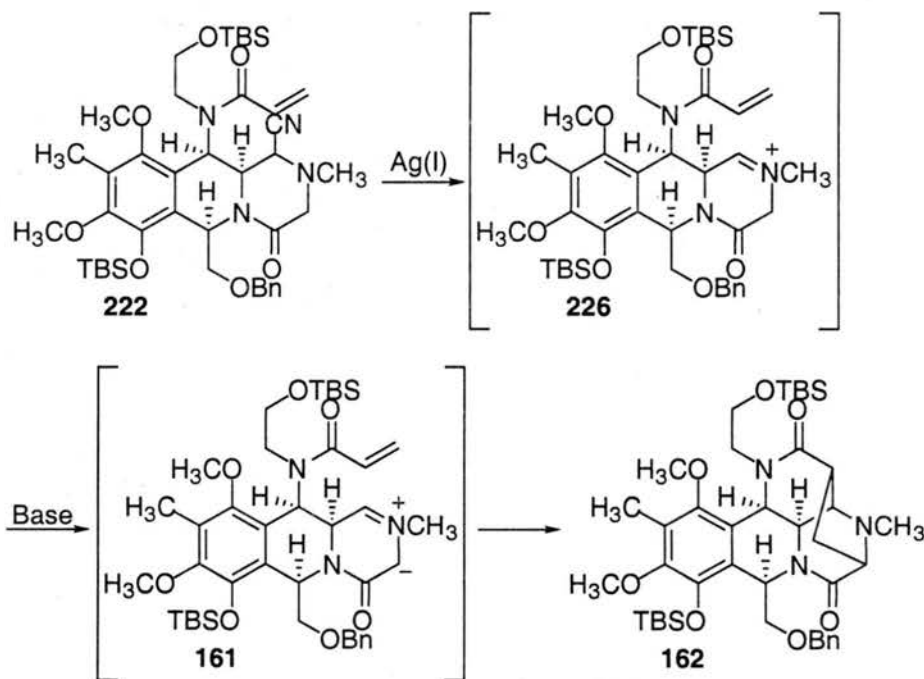
#### 4.6 Intramolecular [3 + 2] Cycloaddition Attempts

The generation of azomethine ylides from aminonitriles has been reported by Padwa and co-workers (Scheme 69).<sup>63</sup> In this strategy, addition of AgF to **223** formed the azomethine ylide, which was captured by a range of olefins resulting in substituted pyrrolidines.



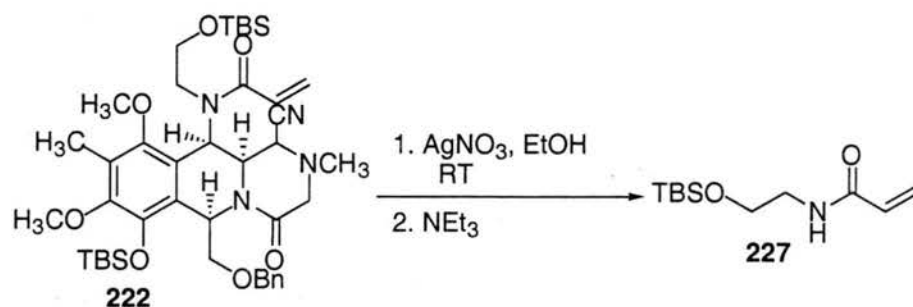
**Scheme 69.** Synthesis of pyrrolidines via azomethine ylide generation from  $\alpha$ -cyanoaminosilanes.

It was anticipated that this methodology could be extended to form an azomethine ylide in a stepwise fashion from **222** (Scheme 70). Aminonitriles have been used as iminium ion precursors, and the addition of a silver(I) salt to **222** could form iminium ion **226**.<sup>64</sup> Flanagan and Williams formed an azomethine ylide from a similar iminium ion with the addition of  $\text{NEt}_3$  (Chapter 4, Scheme 40). Thus it was believed that the addition of a base to iminium **226** would deprotonate the lactam to form intermediate **161**. Intramolecular capture of the azomethine ylide by the  $\alpha, \beta$ -unsaturated amide moiety would result in a bridged piperazine ring to give **162**.



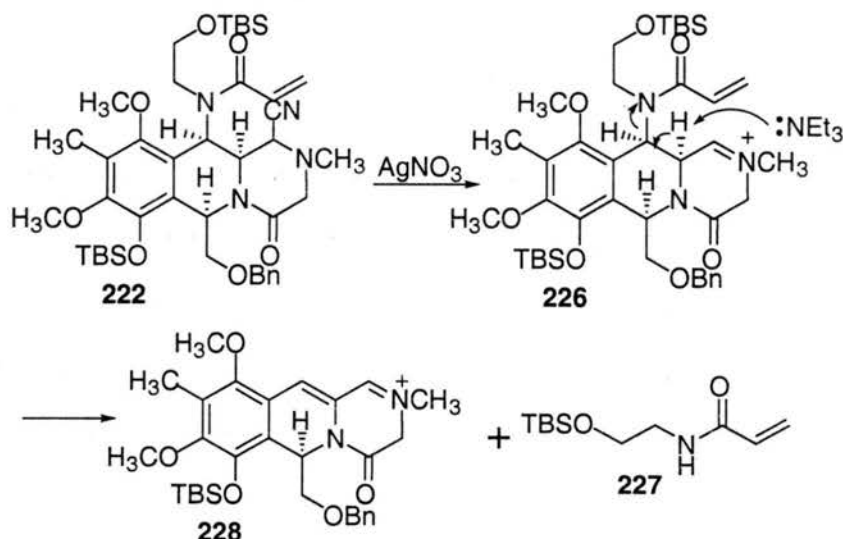
**Scheme 70.** Intramolecular [3 + 2] cycloaddition strategy to synthesize pentacyclic core of bioxalomycin  $\alpha_2$ .

Aminonitrile **222** was exposed to  $\text{AgNO}_3$ , forming a yellow solution with a precipitate (Scheme 71). After 30 minutes, the starting materials were consumed and  $\text{NEt}_3$  was added. Purification of the crude product mixture resulted in recovery of amide **227** and none of the desired product.



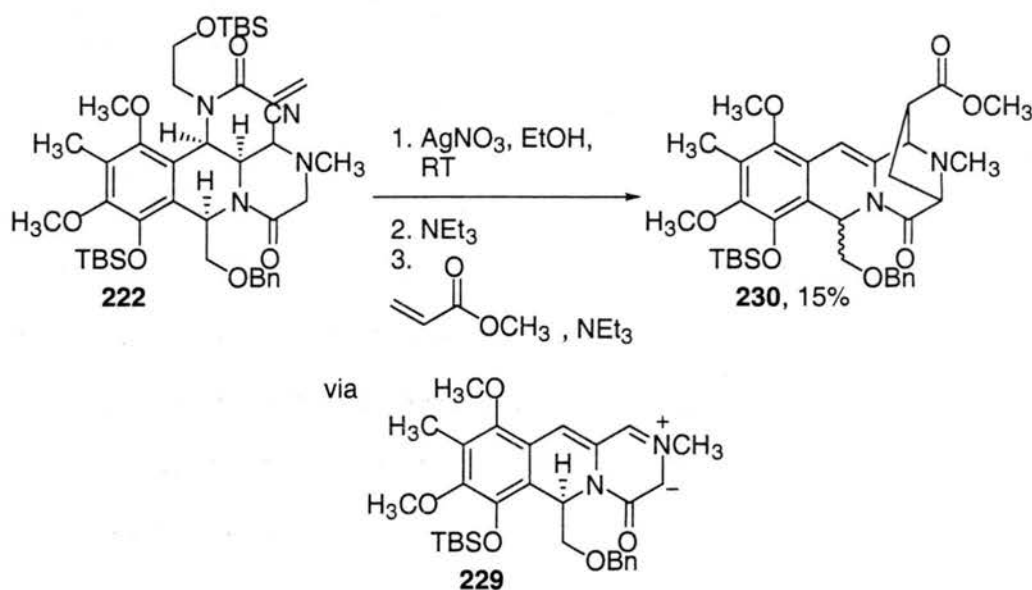
**Scheme 71.** Addition of  $\text{AgNO}_3$  and  $\text{NEt}_3$  to aminonitrile **222**.

Formation of amide **227** could be a result of deprotonation at the undesired position  $\alpha$  to the iminium ion and subsequent elimination of the amide side chain (Scheme 72). The elimination would generate iminium ion **228**, which is thermodynamically more stable than iminium ion **226** since it is conjugated to an electron-rich aromatic ring.



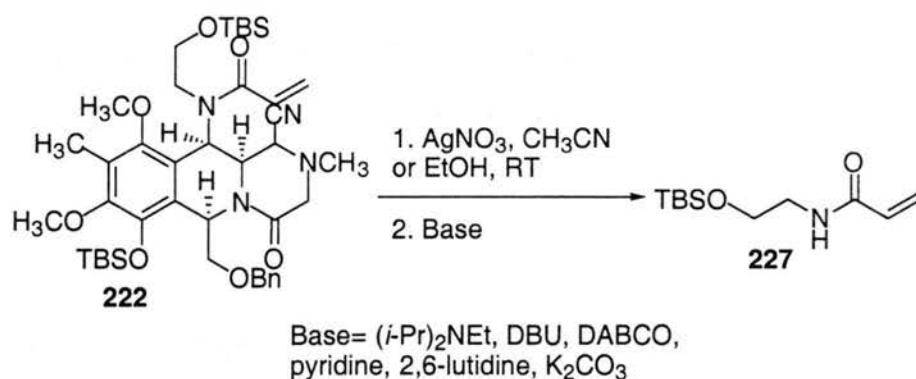
**Scheme 72.** Mechanism of elimination to form amide **227** and conjugated iminium ion **228**.

To probe for iminium ion **228**, a trapping experiment with methyl acrylate was devised (Scheme 73). In this experiment, after generation of **228** with  $\text{AgNO}_3$  and an equivalent of  $\text{NEt}_3$ , a second equivalent of  $\text{NEt}_3$  was added to form azomethine ylide **229**, which could then be captured by methyl acrylate. When the experiment was performed, the [3 + 2] product **230** was isolated as a 3:2 mixture of diastereomers.



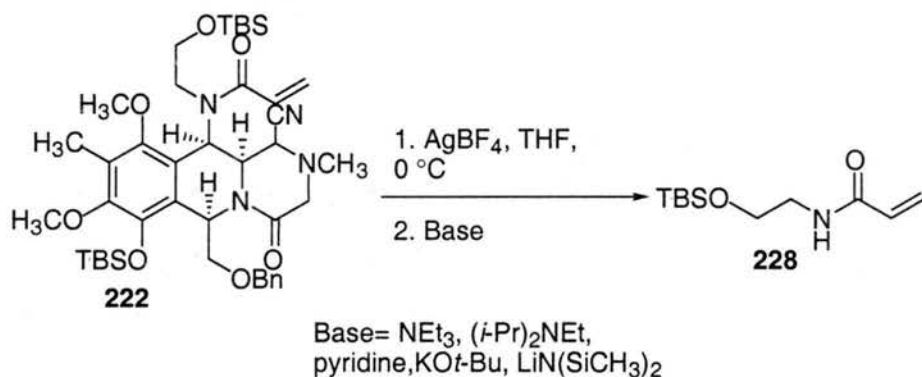
**Scheme 73.** Synthesis of tetracycle **230** via capture of azomethine ylide **229** by methyl acrylate.

Since the deprotonation that leads to elimination occurs at a tertiary center while the desired deprotonation to form azomethine ylide **161** is secondary, a number of bases were screened (Scheme 73). All of the bases led to elimination of amide **227**. The temperature and solvent were changed, but these variations did not result in any of the desired product. In addition, the elimination also occurred by letting aminonitrile **222** stir at room temperature in the presence of  $\text{AgNO}_3$  without any base.



**Scheme 74.** Attempts at [3 + 2] cycloaddition in the presence of AgNO<sub>3</sub>.

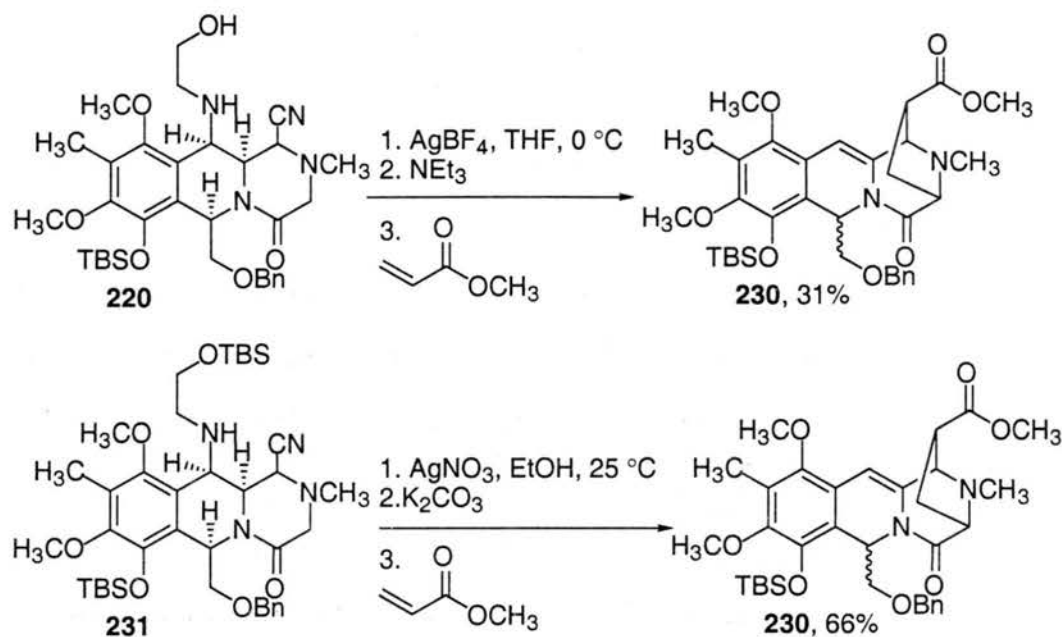
Due to the instability of iminium ion **226** at room temperature, the formation of **226** was also attempted at lower temperatures in ethanol and CH<sub>3</sub>CN. Unfortunately, complete iminium ion formation with AgNO<sub>3</sub> only occurred at room temperature in these solvents. Use of a different silver salt, AgBF<sub>4</sub> was then investigated. In THF at 0 °C, AgBF<sub>4</sub> catalyzed the decomposition of **222** to iminium ion **226**, but as before the addition of different bases led only to elimination (Scheme 75).



**Scheme 75.** Attempts at [3 + 2] cycloaddition in the presence of AgBF<sub>4</sub>.

To suppress elimination, the cycloaddition was also carried out on substrates that had an amine instead of an  $\alpha$ ,  $\beta$ -unsaturated amide at the benzylic position (Scheme 76). In these two examples the formation of the iminium ion of **220** or **231** also resulted in elimination. The addition of a second equivalent of base formed azomethine ylide **229**, which was trapped with methyl acrylate resulting in tetracycle **230**. Due to the  $\beta$ -

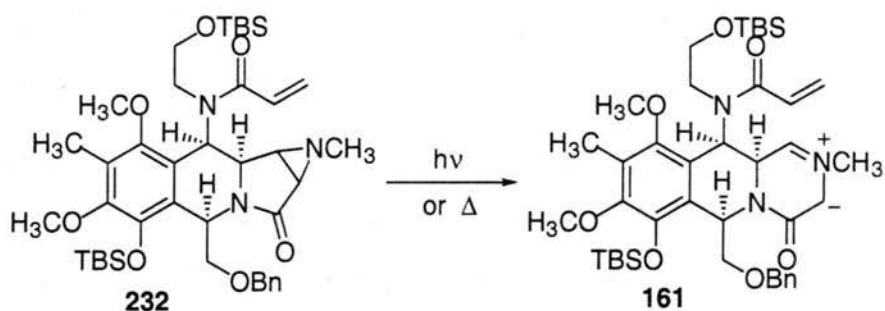
elimination with the stepwise generation of azomethine ylide **161** from the aminonitriles, other strategies to generate azomethine ylide **161** and construct the bridged piperazine were explored.



**Scheme 76.** Intermolecular [3 + 2] cycloadditions of **220** and **231**.

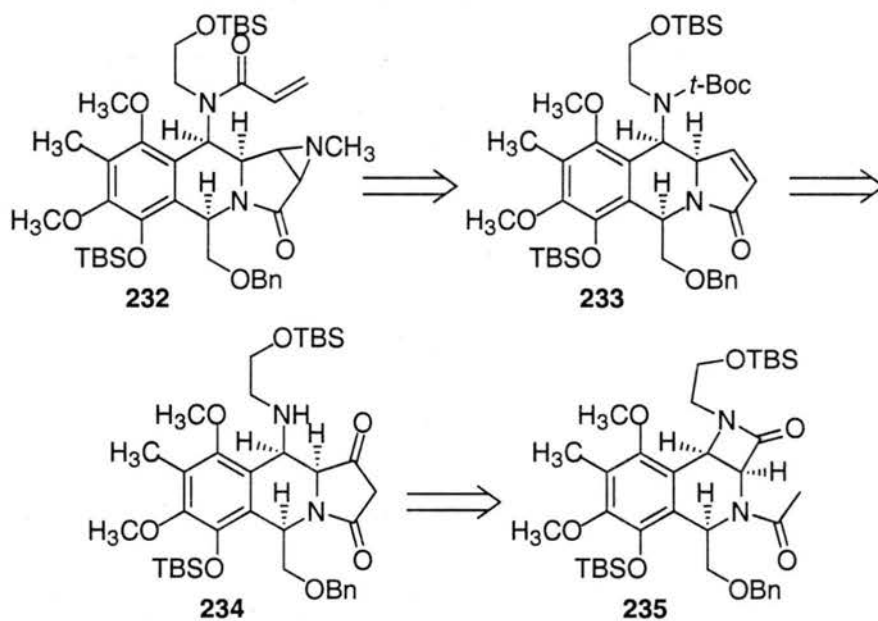
#### 4.7 Alternate Routes

A mild procedure to generate azomethine ylides is the photochemical or thermal decomposition of aziridines.<sup>65</sup> Two advantages of this approach are that the reaction is done under neutral conditions, and forms the azomethine ylide directly without formation of an iminium ion. The desired substrate for the intramolecular [3 + 2] reaction, aziridine **232**, is depicted in Scheme 77. After azomethine ylide **161** is generated it can react with the  $\alpha$ ,  $\beta$ -unsaturated amide moiety to afford the desired core structure of bioxalomycin  $\alpha_2$ .



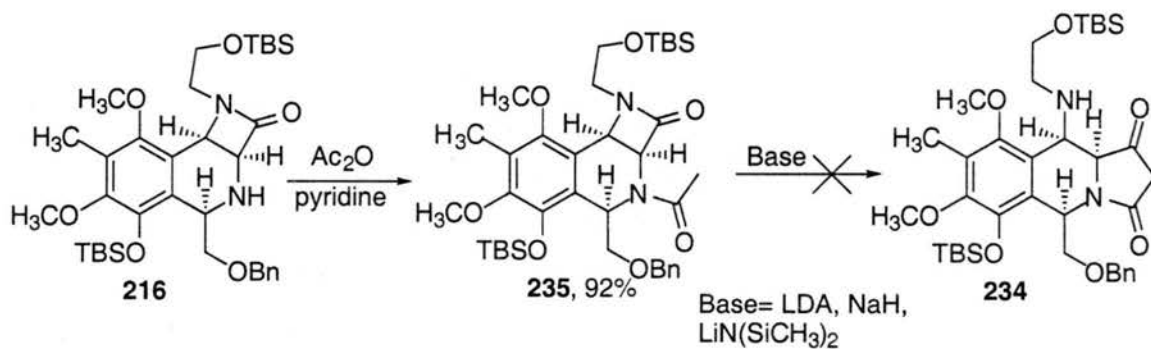
**Scheme 77.** Photochemical or thermal decomposition of aziridine **232** will result in desired azomethine ylide **161**.

The aziridine could be constructed from olefin **233**, which was envisioned to be synthesized from **235** using the procedure described by Murray (Scheme 78).<sup>66</sup> Following this protocol, the anion of the *N*-acyl moiety of **235** would be formed and opening of the  $\beta$ -lactam would afford **234**. It was envisioned that relief of the ring strain of the  $\beta$ -lactam would help push this reaction towards completion. The amine of **231** would then be protected, the ketone reduced, and the alcohol eliminated to afford **233**.<sup>64</sup> The aziridine of **232** could be prepared with the addition of methyl azide to the olefin to give the triazoline followed by photochemical extrusion of nitrogen as described by Garner.<sup>42</sup> Deprotection and acylation of the amine with acryloyl chloride would complete the synthesis of **232**.



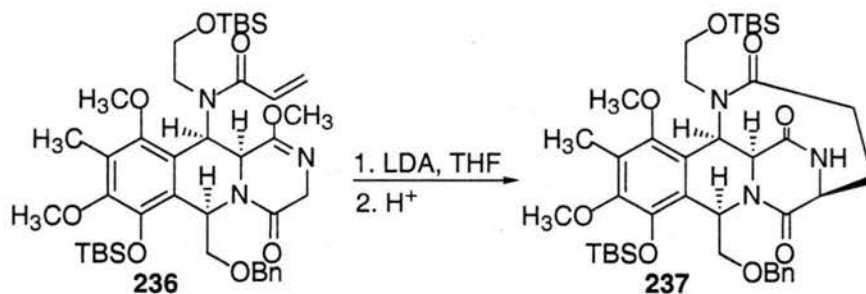
**Scheme 78.** Retrosynthetic analysis of aziridine **232**.

The synthesis of **232** starts with acylation of the amine of **216** with acetic anhydride to afford **235** (Scheme 79). The opening of the  $\beta$ -lactam of **235** was attempted using LDA and  $\text{LiN}(\text{SiCH}_3)_2$  in THF as described by Murray, but only starting material was recovered. Running the reaction with NaH in DMF cleanly deprotected the TBS group to give the free phenol. Due to the failure to open the  $\beta$ -lactam ring of **235**, this route was abandoned.



**Scheme 79.** Synthesis of **235** and subsequent base-catalyzed  $\beta$ -lactam opening attempts.

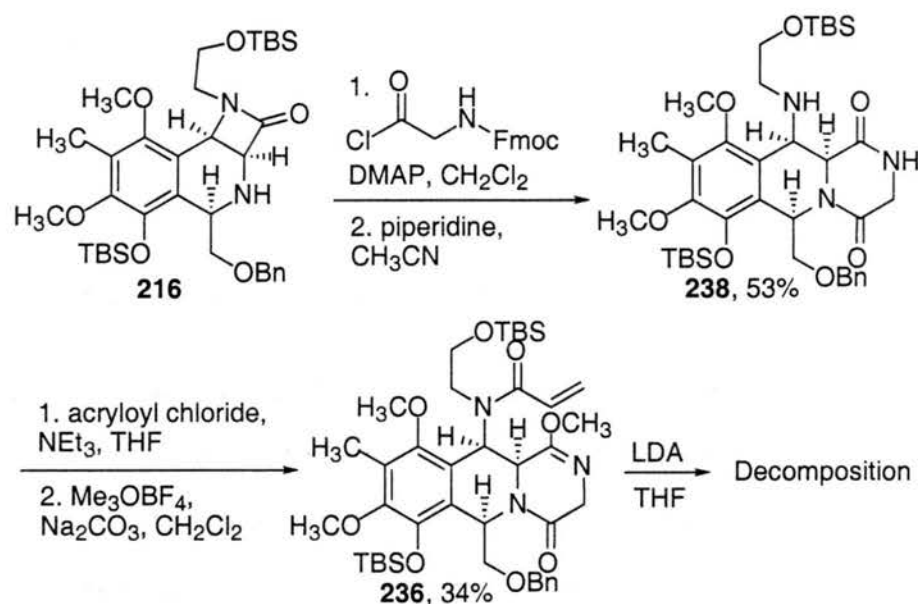
Another approach to the bridged piperazine ring is a stepwise strategy, in which the first step is an intermolecular Michael addition (Scheme 80). Fukuyama has shown that the lithium enolates of mono-lactim ethers of diketopiperazines can be generated and alkylated by alkyl halides.<sup>67</sup> The strategy was to extend this methodology by preparing the lithium enolate of **236** so that it can undergo an intramolecular Michael addition to afford **237**.



**Scheme 80.** Intramolecular Michael addition strategy to form **237**.

The synthesis of lactim ether **236** started with  $\beta$ -lactam **216**, which was acylated with the acid chloride of *N*-Fmoc glycine (Scheme 81). Stirring the protected amine in a

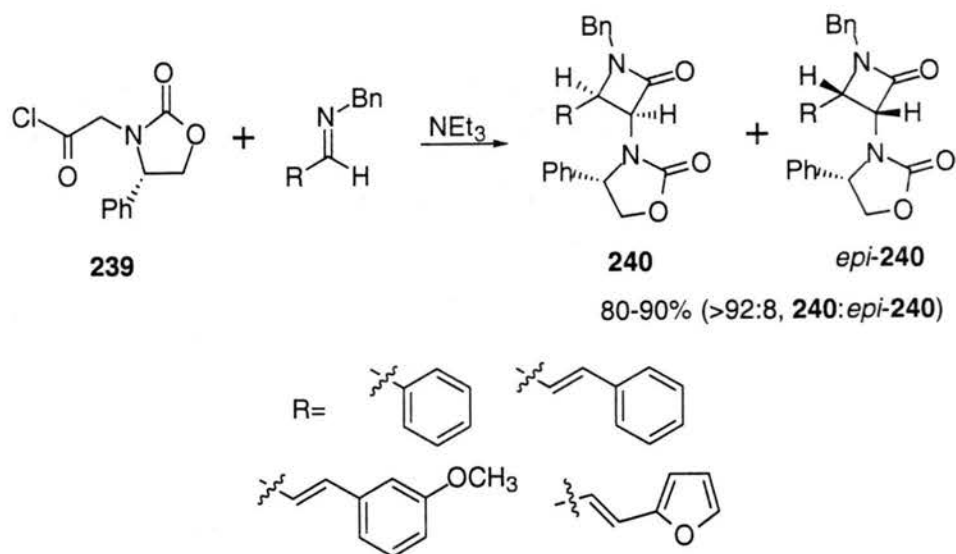
5% solution of piperidine in  $\text{CH}_3\text{CN}$  liberated the free amine, which opened the  $\beta$ -lactam to give diketopiperazine **238**. The amine was acylated with acryloyl chloride, and the lactim ether prepared by stirring the secondary lactam with  $\text{Me}_3\text{OBF}_4$  and  $\text{Na}_2\text{CO}_3$  to complete the synthesis of the intramolecular Michael precursor **236**. Unfortunately in the key Michael reaction, addition of LDA to **236** resulted in decomposition of the starting material.



**Scheme 81.** Synthesis of lactim ether **236** and attempted Michael addition.

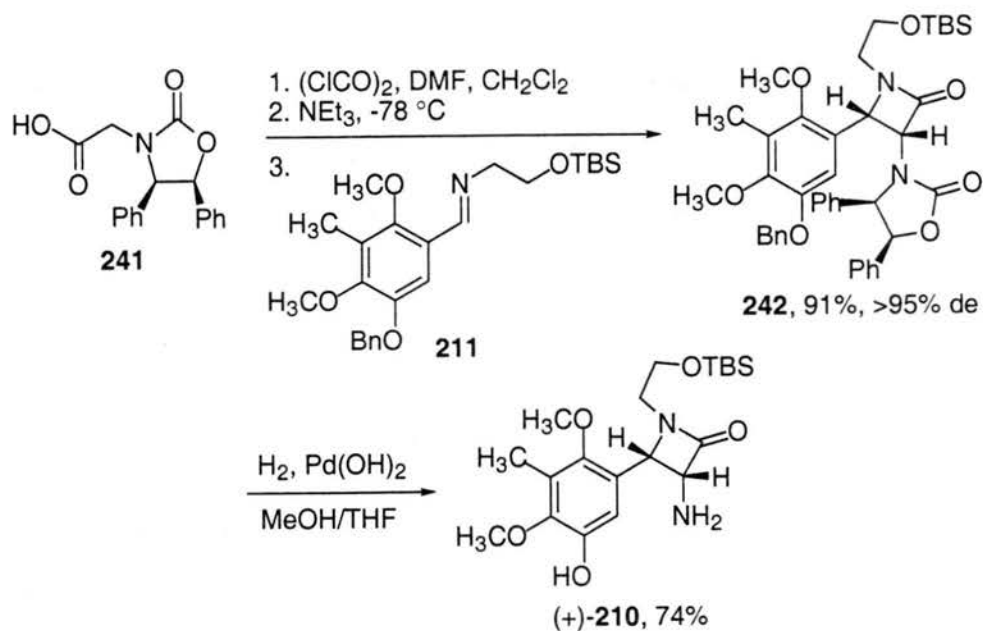
#### 4.8 Asymmetric Route

Evans has shown that the Staudinger reaction can be carried out asymmetrically using a chiral ketene (Scheme 82).<sup>68</sup> In this approach, the chiral monophenyl oxazolidinone of **239** was the nitrogen protecting group and controlled the stereoinduction.<sup>69</sup> Addition of  $\text{NEt}_3$  to **239** at  $-78^\circ\text{C}$  generated the ketene and addition of a number of imines resulted in the  $\beta$ -lactam. The yields for the asymmetric Staudinger reaction ranged from 80-90 % and the diastereomeric ratios of **240** and *epi*-**240** ranged from 92:8 to 97:3.



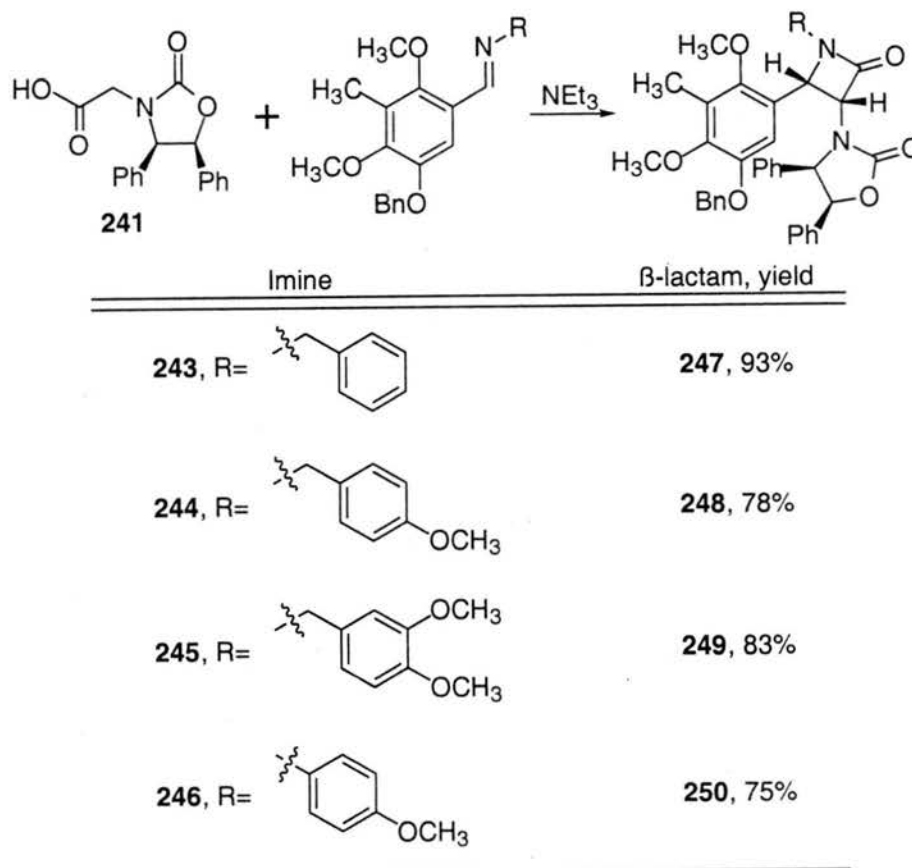
**Scheme 82.** Asymmetric Staudinger reaction developed by Evans.<sup>68</sup>

The asymmetric Staudinger reaction has also been carried out with diphenyl oxazolidinone auxiliary **241** (Scheme 83).<sup>70</sup> The Staudinger reaction between the ketene of **241** and **211** afforded  $\beta$ -lactam **242** in 91% yield as single diastereomer by <sup>1</sup>H-NMR spectroscopy. The absolute stereochemistry of the  $\beta$ -lactam methines have not been determined, but the stereochemistry shown in Scheme 83 is based on the stereochemical induction observed by Evans.<sup>68</sup> Hydrogenolysis of the oxazolidinone and benzyl ether was achieved in one step using Pd(OH)<sub>2</sub> to give (+)-**210** in 74% yield.



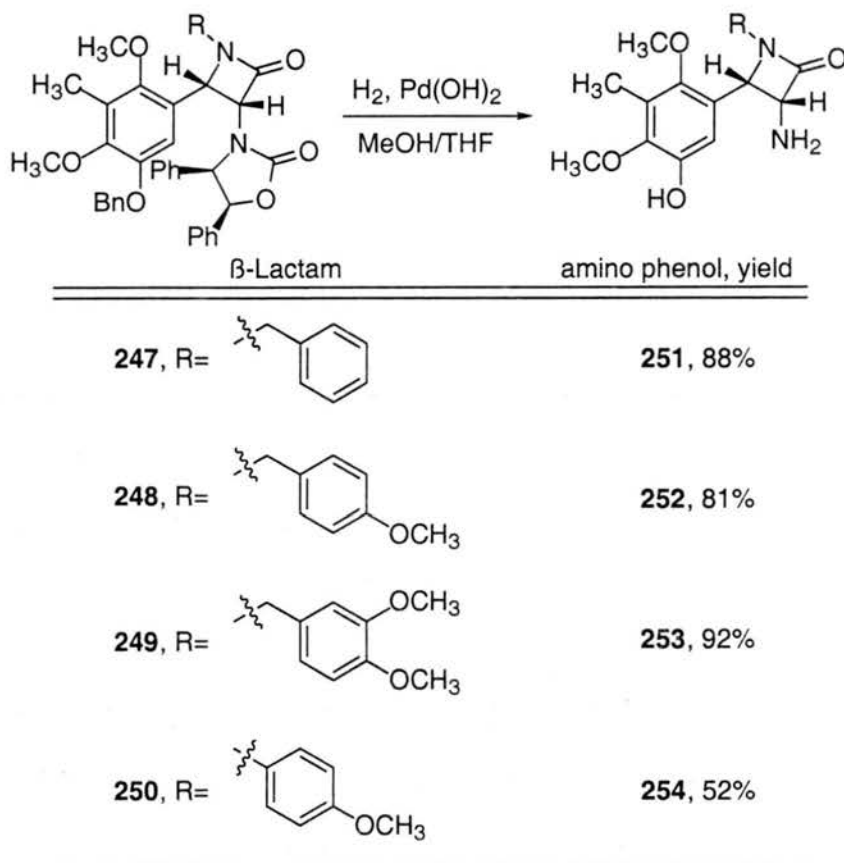
**Scheme 83.** Asymmetric preparation of amino phenol **210**.

**Table 5.** Asymmetric Staudinger reactions.



The asymmetric Staudinger reaction was carried out on a number of different imines (Table 5). All of the  $\beta$ -lactams were prepared as a single diastereomer as measured by  $^1\text{H-NMR}$  in good yield (75-93%). Deprotection of the benzyl ether and the oxazolidinone was accomplished as before using  $\text{Pd}(\text{OH})_2$  (Table 6). The hydrogenolysis conditions did not cleave any of the aromatic  $\beta$ -lactam protecting groups.

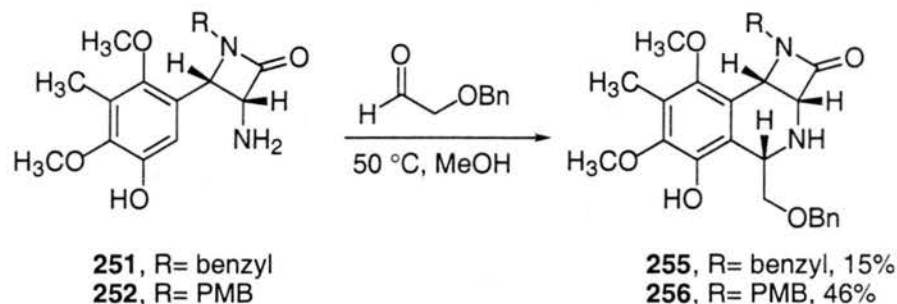
**Table 6.** Deprotection of benzyl ether and oxazolidinone.



The next step was the removal of the  $\beta$ -lactam protecting group. *p*-Methoxy phenyl groups have been used to protect the nitrogen of the  $\beta$ -lactam and are removed using ceric ammonium nitrate (CAN).<sup>71</sup> When **250** was exposed to CAN in  $\text{CH}_3\text{CN}/\text{H}_2\text{O}$ , this did not result in any of the deprotected  $\beta$ -lactam but only decomposition.

Pictet-Spengler reactions between benzyloxyacetaldehyde and amino phenol **251** and **249** were successful (Scheme 84). Deprotection of the *p*-methoxybenzyl (PMB)

group was unsuccessful using  $\text{CAN}^{72}$  or dissolving metal conditions. Benzyl protecting groups on  $\beta$ -lactams can be cleaved using  $\text{Li}/\text{NH}_3$ ,<sup>73</sup> but stirring **255** in dissolving metal conditions resulted in decomposition of starting material.



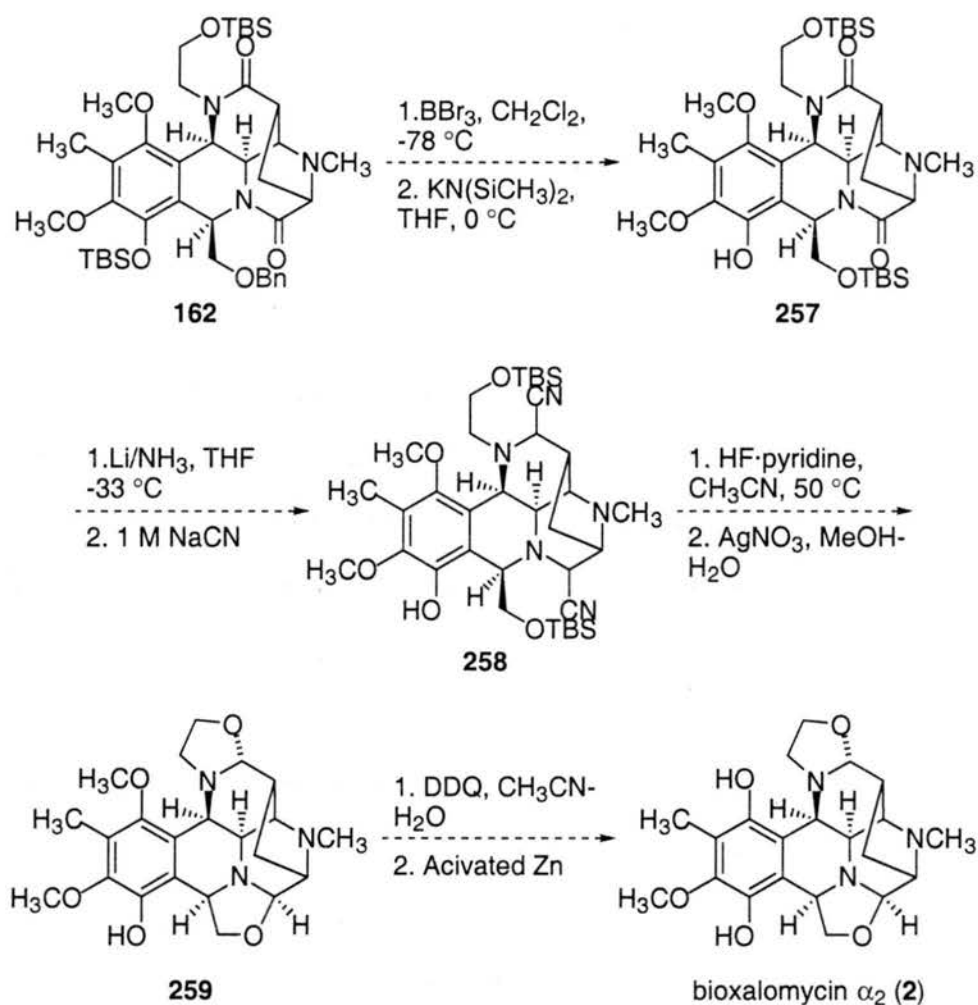
**Scheme 84.** Pictet-Spengler reactions.

#### 4.9 Conclusion

This chapter described the preparation of intramolecular [3 + 2] cycloaddition precursor **222** that could be used towards the synthesis of the bioxalomycin framework. Initial strategies towards **222** were based on earlier work in the Williams' group on the related substrate quinocarcin. These routes were unsuccessful, so a novel route was devised and completed. The synthesis had four key steps: 1) an intermolecular Staudinger reaction, that gave the required *syn* relationship at C-13b and C-13c; 2) a Pictet-Spengler reaction resulting in the desired relative stereochemistry at C-9; 3) an intramolecular transamidation to open a  $\beta$ -lactam ring; 4) a regioselective reduction of a diketopiperazine. The route can also be carried out asymmetrically via a Staudinger reaction whose ketene contains a chiral diphenyl oxazolidine auxiliary.

The stepwise generation of an azomethine ylide from aminonitrile **222** involved the formation of the iminium ion by exposure to a silver(I) salt followed by addition of a base. Unfortunately elimination of the  $\alpha$ ,  $\beta$ -unsaturated amide of **222** preceded azomethine ylide formation.

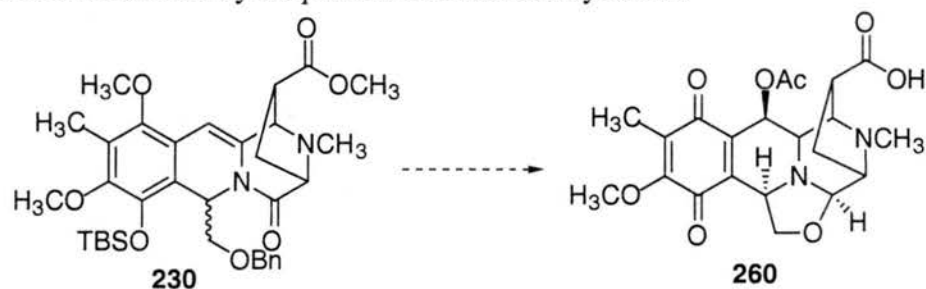
An approach through aziridine **232** to generate the azomethine ylide was investigated, but none of the desired aziridine was prepared. This strategy has the advantage of forming the azomethine ylide directly, which decreases the potential of elimination. A step-wise strategy to the bridged piperazine ring via an intramolecular Michael reaction was outlined. Although the required precursor, lactim ether **236**, was prepared, the intramolecular Michael reaction was unsuccessful.



**Scheme 75.** Proposed completion of synthesis of bioxalomycin  $\alpha_2$ .

If the intramolecular [3 + 2] cycloaddition could be accomplished and bis-amide **162** prepared it would take 8 steps to finish the synthesis of bioxalomycin  $\alpha_2$  (Scheme 75). The benzyl group could be removed using  $\text{BBr}_3$  as described by Fukuyama,<sup>15a</sup>

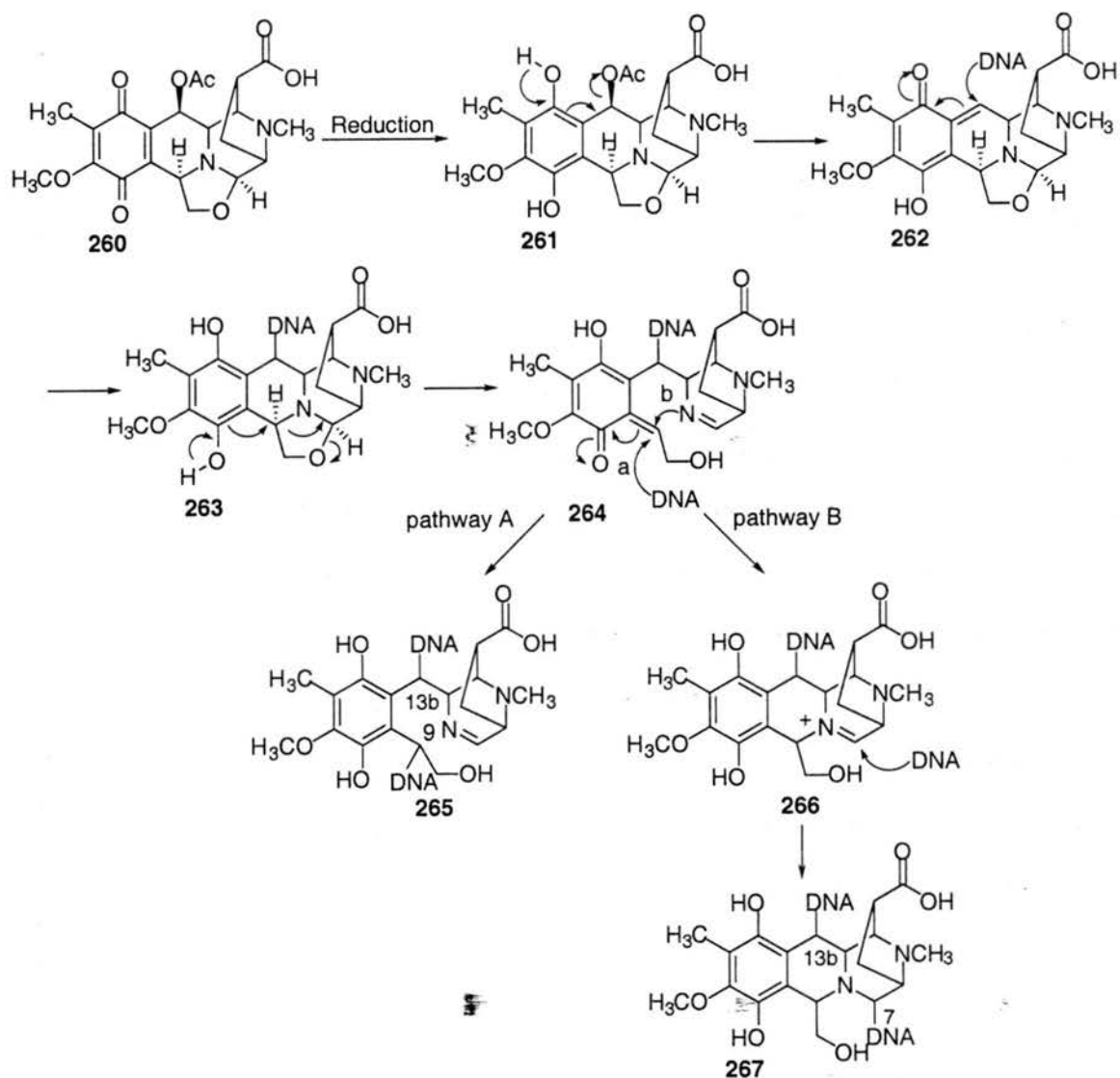
followed by a silyl migration using  $\text{LiN}(\text{SiCH}_3)_2$  to afford **257**.<sup>15b</sup> With the free phenol, **257** could be reduced using dissolving metal conditions to the bis-carbinolamine and then transformed to aminonitrile **258** using  $\text{NaCN}$ .<sup>15b,42</sup> The oxazolidine rings could then be closed by deprotection of the silyl groups followed by addition of  $\text{AgNO}_3$ .<sup>15b,42</sup> To finish the synthesis the aryl ring could be oxidized to the quinone with DDQ and then reduced with activated zinc to the hydroquinone as described by Evans.<sup>15b</sup>



**Scheme 76.** Potential reductively activated cross-linking agent **260**.

If bioxalomycin  $\alpha_2$  is not prepared using this route, the successful synthesis of **230** could prove to be useful as an entry into potential DNA cross-linking agents (Scheme 76). An example is quinone **260**, which contains an acetate at C-13b. The acetate could be attached via hydroboration of the olefin of **230**. The oxazolidine ring would then have to be closed, the methyl ester saponified, and the aromatic ring oxidized to the quinone to complete the synthesis of **260**.

The proposed mechanism of action of **260** is depicted in Scheme 77. After reduction to hydroquinone **261**, the acetate at could be displaced, forming ortho quinone methide **262**, which is susceptible to nucleophilic attack by DNA. The oxazolidine ring of **263** could then be opened to give another ortho-quinone methide, which could be attacked directly by DNA to give **265** (pathway A). On the other hand, the addition of the imine of **264** to the quinone methide would form iminium ion **266** (pathway B), which could then be attacked by DNA to afford **267**.



**Scheme 77.** Proposed mechanism of DNA cross-linking of **260**. Pathway A results in attack at C-13b and C-9, while pathway B results in attack at C-13b and C-7.

## References

1. *Structures of the Bioxalomycins and Their Relationship to Naphthyridinomycin*, Zaccardi, J.; Alluri, M.; Ashcroft, J.; Bernan, V.; Korshalla, J. D.; Morton, G. O.; Siegel, M.; Tsao, R.; Williams, D. R.; Maiese, W.; Ellestad, G. A., *J. Org. Chem.* (1994) **59**, 4045~4047.
2. *Naphthyridinomycin, a New Broad-Spectrum Antibiotic*, Kluepfel, D.; Baker, H. A.; Piattoni, G.; Sehal, S. N.; Sidorowicz, A.; Singh, K.; Vezina, C., *J. Antibiot.* (1975) **28**, 497~502.
3. *Cyanocycline A, a New Antibiotic.*, Hayashi, T.; Noto, T.; Nawata, Y.; Okazaki, H.; Sawada, M.; Ando, K., *J. Antibiot.* (1982) **35**, 771~777.
4. (a) *The Molecular Structure of Naphthyridinomycin- a Broad Spectrum Antibiotic*, Sygusch, J.; Brisse, F.; Hanessian, S., *Tetrahedron Lett.* (1974) 4021~4023. (b) *The Crystal and Molecular Structure of Naphthyridinomycin, C<sub>21</sub>H<sub>27</sub>N<sub>3</sub>O<sub>6</sub>, a Broad Spectrum Antibiotic*. Sygusch, J.; Brisse, F.; Hanessian, S., *Acta. Crysta.* (1976) **B32**, 1139~1142.
5. *Cyanonaphthyridinomycin: a Derivative of Naphthyridinomycin*, Zmijewski, M. J., Jr.; Goebel, M., *J. Antibiot.* (1982) **35**, 524~526.
6. *Mechanism of Action of Naphthyridinomycin on Escherichia coli*, Singh, K.; Sun, S.; Kluepfel, D., *Dev. Ind. Microbiol.* (1976) **17**, 209~221.
7. *Naphthyridinomycin, a DNA-Reactive Antibiotic*, Zmijewski, M. J., Jr.; Miller-Hatch, K.; Goebel, M., *Antimicrob. Agents Chemother.*, (1982) **21**, 787~793.
8. (a) *Inhibition of Nucleic Acid Biosynthesis in Prokaryotic and Eucaryotic Cells by Cyanocycline A*, Hayashi, T.; Okutomi, T.; Suzuki, S.; Okazaki, H., *J. Antibiot.* (1983) **36**, 1228~1235. (b) *Mechanistic Studies and Biological Activity of Bioxalomycin  $\alpha_2$ , a Novel Antibiotic Produced by Streptomyces viridostaticus subsp. "litoralis" LL-31F508*, Singh, M. P.; Peterson, P. J.; Jacobus, N. V.; Maiese, W. M.; Greenstein, M.; Steinberg, D. A., *Antimicrob. Agents and Chemother.* (1994) **38**, 1808~1812.
9. *The In Vitro Interaction of Naphthyridinomycin with Deoxynucleic Acids*, Zmijewski, M. J., Jr.; Miller-Hatch, K.; Mikolajczak, M., *Chem.-Biol. Interactions* (1985) **52**, 361~375.
10. *Molecular Mechanisms of Binding and Single Strand Scission of Deoxyribonucleic acid by the Antitumor Antibiotic Saframycin A*. Lown, J. W.; Joshua, A. V.; Lee, L. S., *Biochemistry* (1982) **21**, 419~428.
11. *Bioactivation as a Model for Drug Design Bioreductive Alkylation*, Moore, H. W., *Science* (1977) **197**, 527~532.

12. (a) *Potential Bioreductive Alkylating Agents. 2. Antitumor Effect and Biochemical Studies of Naphthoquinone Derivatives*, Lin, A. J.; Pardini, R. S.; Cosby, L. A.; Lillis, B. J.; Shansky, C. W.; Sartorelli, A. C., *J. Med. Chem.* (1973) **16**, 1268~1273. (b) *Potential Bioreductive Alkylating Agents. 3. Synthesis and Antineoplastic Activity of Acetoxymethyl and Corresponding Ethyl Carbamate Derivatives of Benzoquinones*, Lin, A. J.; Shansky, C. W.; Sartorelli, A. C., *J. Med. Chem.* (1974) **17**, 558~561. (c) *Potential Bioreductive Alkylating Agents. 4. Inhibition of Coenzyme Q Enzyme Systems by Lipoidal Benzoquinone and Naphthoquinone Derivatives*. A. J.; Pardini, R. S.; Cosby, L. A.; Lillis, B. J.; Sartorelli, A. C., *J. Med. Chem.* (1974) **17**, 668~672.
13. (a) *Naphthyridinomycin-DNA Adducts: a Molecular Modeling Study*, Cox, M. B.; Arjunan, P.; Arora, S. K., *J. Antibiot.* (1991) **44**, 885~894. (b) *Computer Simulation of the Binding of Naphthyridinomycin and Cyanocycline A to DNA*, Hill, G. C.; Wunz, T. P.; MacKenzie, N. E.; Gooley, P. R.; Remers, W. A., *J. Med. Chem.* (1991) **34**, 2079~2088.
14. (a) *Synthetic Approaches Toward Naphthyridinomycin, I. Stereoselective Synthesis of a Tetracyclic Intermediate*, Fukuyama, T.; Laird, A. A., *Tetrahedron Lett.* (1986) **27**, 6173~6176. (b) *The Total Synthesis of ( $\pm$ )-Naphthyridinomycin. I. Preparation of a Key Tetracyclic Lactam Intermediate*, Evans, D. A.; Biller, S. A., *Tetrahedron Lett.* (1985) **26**, 1907~1910. (c) *The Total Synthesis of ( $\pm$ )-Naphthyridinomycin. II. Construction of the Pentacyclic Carbon Skeleton*, Evans, D. A.; Biller, S. A., *Tetrahedron Lett.* (1985) **26**, 1911~1914. (d) *An Approach to the Synthesis of the Naphthyridinomycin Alkaloids: The Synthesis of Two Subunits*, Danishefsky, S.; O'Neill, B. T.; Taniyama, E.; Vaughn, K., *Tetrahedron Lett.* (1984) **25**, 4199~4202. (e) *A Mannich-Like Approach to Naphthyridinomycin*, Danishefsky, S.; O'Neill, B. T., *Tetrahedron Lett.* (1984) **25**, 4203~4206.
15. (a) *Stereocontrolled Total Synthesis of ( $\pm$ )-Cyanocycline A*, Fukuyama, T.; Li, L.; Laird, A. A.; Frank, R. K. *J. Am. Chem. Soc.* (1987) **109**, 1587~1589. (b) *Stereoselective Synthesis of ( $\pm$ )-Cyanocycline*, Evans, D. A.; Illig, C. R.; Saddler, J. C., *J. Am. Chem. Soc.* (1986) **108**, 2478~2479.
16. *Convenient Synthesis of Carboxylic Acid Anhydrides using N,N-Bis[2-oxo-3-oxazolidinyl]phosphorodiamidic Chloride*, Cabre-Castellvi, J.; Palomo-Coll, A.; Palomo-Coll, A. L., *Synthesis* (1981) 616~620.
17. *Stereochemistry of Carbohydrates*, Stoddart, J. F., Wiley; New York, (1971) Chapter 3, 67~87 and references cited therein.
18. *Stereocontrolled Total Synthesis of ( $\pm$ )-Saframycin B*, Fukuyama, T.; Sachelban, R. A., *J. Am. Chem. Soc.* (1982) **104**, 4957~4958.
19. *A Convenient Method for Constructing Oxazolidine and Thiazolidine Rings in C<sub>20</sub>-Diterpenoid Alkaloid Derivatives*, Pelletier, S.W.; Nowacki, J.; Mody, N. V., *Synth. Commun.* (1979) **9**, 201~206.
20. (a) *DC-52, a Novel Antitumor Antibiotic 1. Taxonomy, Fermentation, and Biological Activity*, Tomita, F.; Takahashi, K.; Shimizu, K.-I., *J. Antibiot.* (1983) **36**, 463~467. (b) *DC-52, a Novel Antitumor Antibiotic 2. Isolation, Physico-Chemical Characteristics and Structural Determination*, Takahashi, K.; Tomita, F., *J. Antibiot.* (1983) **36**, 468~470.

21. (a) *The Colony Inhibition of a New Chemotherapeutic Agent (KW2152) Against Human Lung Cancer Cell Lines*, Jett, J. R.; Saijo, N.; Hong, W.-S.; Sasaki, Y.; Takahashi, H.; Nakano, H.; Nakagawa, K.; Sakurai, M.; Suemase, K.; Teseda, M., *Investigational New Drugs* (1987) **5**, 155~159. (b) *Antitumor Activity of Quinocarmycin against Carcinoma of the Lung in Human Tumor Colongenic Assay*, Chiang, C.D.; Kanzawa, F.; Matsushima, Y.; Nakano, H.; Nakagawa, K.; Takahashi, H.; Tereda, M.; Morinaga, S.; Tsuchiya, R.; Sasaki, Y.; Saijo, N., *J. Pharmacobio-Dyn.* (1987) **10**, 431~435. (c) *Antitumor Activity of a Novel Antitumor Antibiotic, Quinocarmycin Citrate (KW2152)*, Fujimoto, K.; Oka, T.; Morimoto, M., *Cancer Research* (1987) **47**, 1516~1522.
22. *Cannizzaro-Based O<sub>2</sub>-Dependent Cleavage of DNA by Quinocarcin*, Williams, R. M.; Glinka, T.; Flanagan, M. E.; Gallegos, R.; Coffman, H.; Pei, D., *J. Am. Chem. Soc.* (1992) **114**, 733-740.
23. (a) *Iron-Catalyzed Hydroxyl Radical Formation*, Graf, E.; Mahoney, J. R.; Bryant, R. G.; Eaton, J. W., *J. Biol. Chem.* (1984) **259**, 3620~3624. (b) *Phytic Acid*, Graf, E.; Empson, K. L.; Eaton, J. W., *J. Biol. Chem.* (1987) **262**, 11647~1650. (c) *Microsomal Lipid Peroxidation: Mechanisms of Initiation*, Urisini, F.; Mariorino, M.; Hochstein, P.; Erstner, L., *Free Radical Biol. and Med.* (1989) **6**, 31~36. (d) *The Deoxyribose Method: A simple "Test-Tube" Assay for Determination of Rate Constants for Reactions of Hydroxyl Radical*, Halliwell, B.; Gutteridge, J. M. C.; Aruoma, O. I., *Analytical Biochem.* (1987) **165**, 215~219. (e) *Fenton's Reagent Revisited*, Walling, C., *Acc. Chem. Res.* (1975) **8**, 125~131. (f) *On the Participation of Higher Oxidation States of Iron and Copper in Fenton Reactions*, Sutton, H. C.; Winterbourn, C. C., *Free Radical Biol. and Med.* (1989) **6**, 53~60. (g) *Role of Superoxide in Deoxyribonucleic Acid Strand Scission*, Lesko, S. A.; Lortentzen, R. J.; Ts'o, P. O. P., *Biochemistry* (1980) **19**, 3023~3028. (h) *Role of Iron in Adriamycin Biochemistry*, Myers, C.; Gianni, L.; Zweier, J.; Muindi, J.; Sinha, B. K.; Eliot, H., *Federation Proc.* (1986) **45**, 2792~2797.
24. *Mechanisms of Bleomycin-Induced DNA Degradation*, Stubbe, J.; Kozarich, J. W., *Chem. Rev.* (1987) **87**, 1107~1136.
25. *Synthesis, Conformation, Crystal Structures and DNA Cleavage Abilities of Tetracyclic Analogs of Quinocarcin*, Williams, R. M.; Glinka, T.; Gallegos, R.; Ehrlich, P. P.; Flanagan, M. E.; Coffman, H.; Park, G., *Tetrahedron* (1991) **47**, 2629~2642.
26. *The Total Synthesis of Distamycin A*, Bailer, M.; Yagen, B.; Mechoulam, R., *Tetrahedron* (1978) **34**, 2389~2391.
27. *Netropsin and Spemine Conjugates of a Water-Soluble Quinocarcin Analog: Analysis of Sequence -Specific DNA Intercations*. Flanagan, M. E.; Rollins, S. B.; Williams, R. M., *Chem. & Biol.* (1995) **2**, 147~156.
28. *Computer Simulation of the Binding of Quinocarcin to DNA Prediction of Mode of Action and Absolute Configuration*, Hill, G. C.; Wunz, T. P.; Remers, W. A., *J. Computer-Aided Mol. Design* (1988) **2**, 91~106.
29. *Efficient Synthesis of Oligo-N-Methylpyrrolecarboxamides and Related Compounds*, Nishiwaki, E.; Tanaka, S.; Lee, H.; Shibuya, M., *Heterocycles* (1988) **27**, 1945~1952.
30. (a) *Generation of Superoxide Free Radical During the Autoxidation of Thiols*, Misra, H. P., *J. Biol. Chem.* (1974) **249**, 2151~2155. (b) *Superoxide Dismutase: Improved*

---

*Assays and an Assay Applicable to Acrylamide Gels*, Beauchamp, C.; Fidovich, I., *Anal. Biochem.* (1971) **44**, 276~287. (c) *Syntheses of Some p-Nitrophenyl Substituted Tetrazolium Salts as Electron Acceptors for the Demonstration of Dehydrogenases*, Tsou, K. C.; Cheng, C. S.; Nachlas, M. M.; Seligman, A. M. *J. Am. Chem. Soc.* (1956) 6139~6144.

31. *Synthesis and Biological Evaluation of Quinocarcin Derivatives*, Saito, H.; Kobayashi, S.; Uosaki, Y.; Sato, A.; Fujimoto, K.; Miyoshi, K.; Ashizawa, T.; Morimoto, M.; Hirata, T., *Chem. Pharm. Bull.* (1990) **38**, 1278~1285.

32. For a comprehensive review see: *DNA Cross-Linking Agents as Antitumor Drugs*, Rajsiki, S. R.; Williams, R. M., *Chem. Rev.* (1998) **98**, 2723~2795.

33. (a) *Single- and Double-Strand Break Formation in DNA Irradiated in Aqueous Solution: Dependence on Dose and OH Radical Scavenger Concentration*, Siddiqi, M. A.; Bothe, E., *Rad. Res.* (1987) **112**, 449~463. (b) *Effects of Ionizing Radiation on Deoxyribonucleic Acid and Related Systems. Part I. The Role of Oxygen*, Boon, P. J.; Cullis, P. M.; Symons, M. C. R.; Wren, B. W., *J. Chem. Soc. Perkin Trans. II* (1984) 1393~1399.

34. Box, H. C.; Schroder, E. A.; Budzinski, E. E. *Radiation Damage in DNA: Structure/Function Relationships at Early Times*, Fuciarelli, A. F.; Zimbrick, J. D.; Eds. Battelle Press; Columbus, OH, 1995; pp 295~280.

35. *FR900482, A Close Cousin of Mitomycin C that Exploits Mitosene-Based DNA Cross-Linking*, Williams, R. M.; Rajsiki, S. R.; Rollins, S. B., *Chem. Biol.* (1997) **4**, 127~137.

36. *Hydroxyl Radical "Footprinting"; High-Resolution Information About DNA-Protein Contacts and Application to  $\lambda$  Repressor and Cro Protein*, Tullius, T. D.; Dombroski, B. A., *Proc. Natl. Acad. Sci. U.S.A.* (1986) **83**, 5469~5473.

37. *Determination at Single-Nucleotide Resolution of the Sequence Specificity of DNA Interstrand Cross-Linking Agents in DNA Fragments*, Weidner, M. F.; Millard, J. T.; Hopkins, P. B., *J. Am. Chem. Soc.* (1989) **111**, 9270~9272.

38. *Two Aspects of DNA Polymorphism and Microheterogeneity: Molecular Electrostatic Potential and Steric Accessibility*, Pullman, B.; Lavery, R.; Pullman A., *Eur. J. Biochem.* (1982) **124**, 229~238.

39. For a review see: *Mitomycin C: Small, Fast, and Deadly (But Very Selective)*, Tomasz, M., *Chem. & Biol.* (1995) **2**, 575~579.

40. *Binding of Saframycin A, a Heterocyclic Quinone Anti-tumor Antibiotic to DNA as Revealed by the Use of the Antibiotic Labeled with [<sup>14</sup>C]Tyrosine or [<sup>14</sup>C]Cyanide*. Ishiguro, K.; Takahashi, K.; Yazawa, K.; Sakiyama, S.; Arai, T., *J. Biol. Chem.* (1981) **256**, 2162~2167.

41. *X-Ray Crystallographic Determination of the Molecular Structures of the Antibiotic Cyanocycline A and Related Compounds*, Hayashi, T.; Nawata, Y., *J. Chem. Soc. Perkin Trans. II* (1983) 335~343.

42. (a) *Isolation and Structure of a Covalent Cross-Link Adduct Between Mitomycin C and DNA*, Tomasz, M.; Lipman, R.; Chowdary, D.; Pawlak, J.; Verdine, G. L.; Nakanishi, K., *Science* (1987) **235**, 1204~1208. (b) *DNA Interstrand Cross-Linking by Formaldehyde: Nucleotide Sequence Preference and Covalent Structure of the Predominant Cross-Link Formed in Synthetic Oligonucleotides*, Huang, H.; Hopkins, P. B., *J. Am. Chem. Soc.* (1993) **115**, 9402~9408. (c) *Covalent Structure of the DNA-DNA Interstrand Cross-Link Formed by Reductively Activated FR66979 in Synthetic DNA Duplexes*, Huang, H.; Pratum, T. K.; Hopkins, P. B., *J. Am. Chem. Soc.* (1994) **116**, 2703~2709.
43. *Synthetic Studies on Quinocarcin: Total Synthesis of ( $\pm$ )-Quinocarcinamide via Dipole Cycloaddition of an Azomethine Ylide Generation by NBS Oxidation*, Flanagan, M. E.; Williams, R. M., *J. Org. Chem.* (1995) **60**, 6791~6797.
44. *The Asymmetric Synthesis of (-)-Quinocarcin via a 1,3-Dipolar Cycloaddition Strategy*. Garner, P.; Ho, W. B.; Shin, H., *J. Am. Chem. Soc.* (1993) **115**, 10742~10753.
45. (a) *Trimethylamine N-Oxide as a Precursor of Azomethine Ylides*, Beugelmans, R.; Negron, G.; Roussi, G., *J. Chem. Soc., Chem. Commun.* (1983) 31~32. (b) *A New Route to Hexahydropyrrolizines Derivatives Via Nonstabilized Ylide Generated From N-Methylpyrrolidine N-Oxide*, Chastanet, J.; Roussi, G., *Heterocycles* (1985) **23**, 653~657. (c) *N-Methylpiperidine N-Oxide as a Source of Nonstabilized Ylide: A New and Efficient Route to Octahydroindolizine Derivatives*, Chastanet, J.; Roussi, G., *J. Org. Chem.* (1985) **50**, 2910~2914.
46. *Synthetic Studies for Mitomycins. I. Total Synthesis of Deiminomitomycin A*, Wakatsubo, F.; Coluzza, D. E.; Kishi, Y., *J. Am. Chem. Soc.* (1977) **99**, 4835~4836. Benzaldehyde **166** was prepared from 2, 6-dimethoxytoluene by the following sequence of steps: 1)  $\text{Cl}_2\text{CHOCH}_3$ ,  $\text{TiCl}_4$ ,  $\text{CH}_2\text{Cl}_2$ , 0 °C. 2) MCPBA,  $\text{CH}_2\text{Cl}_2$ , 0 °C. 3)  $\text{NaOCH}_3$ ,  $\text{CH}_3\text{OH}$ , 0 °C. 4) allyl bromide,  $\text{K}_2\text{CO}_3$ , acetone, reflux. 5) *N,N*-dimethylaniline, 190 °C. 6)  $\text{NaH}$ ,  $\text{BnBr}$ , DMF. 7)  $\text{PdCl}_2(\text{CH}_3\text{CN})_2$ ,  $\text{CH}_2\text{Cl}_2$ , reflux. 8)  $\text{O}_3$ ,  $\text{MeOH}$ , -78 °C, sudan red-7B indicator.
47. *Regioselective Reductive Alkylation of 3,4,5-Trimethoxybenzaldehyde Dimethylacetal: A New Synthesis of 4-Alkyl-3,5-dimethoxybenzaldehydes and 2,5-Dialkyl-1,3-dimethoxybenzenes*, Azzena, U.; Cossu, S.; Denurra, T.; Melloni, G.; Piroddi, A. M., *Synthesis* (1990) 313~314.
48. *Synthesis of Ansamycins: An Approach to the Naphthoquinone Portion of the Riframycins and Streptovaricins*, Parker, K. A.; Petraitis, J. J., *Tetrahedron Lett.* (1981) **22**, 397~400.
49. *Advances in the Chemistry of Mannich Bases*, Tramontini, M., *Synthesis* (1973) 703~775.
50. *A Convenient Synthesis of Unsymmetrical Secondary Amines. In situ Formation of Unstable Formaldehyde Imines*, Overman, L. E.; Burk, R. M., *Tetrahedron Lett.* (1984) **25**, 1635~1638.
51. *A Convenient Synthesis of 4-Unsubstituted  $\beta$ -Lactams*, Overman, L. E.; Osawa, T., *J. Am. Chem. Soc.* (1985) **107**, 1698~1701.

- 
52. 2-Cyano  $\Delta^3$  Piperidines XI: Biomimetic Synthesis of the Ladybug Alkaloids of the Adaline Series, Medina, D. H. G.; Grierson, D. S.; Husson, H.-P., *Tetrahedron Lett.* (1983) **24**, 2099~2102.
53. Asymmetric [1,3]- Dipolar Cycloaddition Reactions: Synthesis of Highly Substituted Proline Derivatives, Williams, R. M.; Zhai, W.; Aldous, D. J.; Aldous, S. C., *J. Org. Chem.* (1992) **57**, 6528~6532.
54. Ate Complex from Diisobutylaluminum Hydride and n-Butyllithium as a Powerful and Selective Reducing Agent for the Reduction of a Selected Organic Compounds Containing Various Functional Groups, Kim, S.; Ahn, K. H., *J. Org. Chem.* (1984) **49**, 1717~1724.
55. Mixed Solvents Containing Methanol as Useful Reaction Media for Unique Chemoselective Reductions with Lithium Borohydride, Soai, K.; Ookawa, A., *J. Org. Chem.* (1986) **51**, 4000~4005.
56. Lathanides in Organic Chemistry. 1. Selective 1,2-Reductions of Conjugated Ketones, Luche, J.-L., *J. Am. Chem. Soc.* (1978) **100**, 2226~2227.
57. For a review see: *The Ester Enolate-Imine Condensation Route to  $\beta$ -Lactams*, Hart, D. J.; Ha, D.-C., *Chem. Rev.* (1989) **89**, 1447~1465.
58. Intramolecular [3 + 2] Cycloaddition Routes to Carbon-Bridged Dibenzocycloheptanes and Dibenzazepines, Confalone, P. N.; Huie, E. M., *J. Org. Chem.* (1983) **48**, 2994~2997.
59. Selective Reductions. V. The Partial Reduction of Tertiary Amides by Lithium Di- and Triethoxyaluminumhydrides- a New Aldehyde Synthesis via the Dimethylamides. Brown, H. C.; Tsukamoto, A., *J. Am. Chem. Soc.* (1964) **86**, 1089~1095.
60. On the Reduction of  $\beta$ -Lactams with Diborane, Sammes, P. G.; Smith, S., *J. Chem. Soc., Chem. Comm.* (1982) 1143~1144.
61. *Synthesis and Biomechanistic Studies of Quinocarcin and Structural Analogs*, Flanagan, M. E., Ph.D. Thesis, Colorado State University, Ft. Collins, Colorado, Spring 1995.
62. A Convenient Synthesis of Protected  $\alpha$ -Hydroxyacetaldehydes, Shiao, M.-J.; Yang, C.-Y.; Lee, S.-H.; Wu, T.-C., *Syn. Comm.* (1988) **18**, 359~366.
63. Synthesis of Pyrrolidines Using an  $\alpha$ -Cyanoaminosilane as an Azomethine Equivalent, Padwa, A.; Chen, Y.-T., *Tetrahedron Lett.* (1983) **24**, 3447~3450.
64. The Cyanomethyl Group for Nitrogen Protection and Iminium Generation in ring-Enlarging Pyrrolidine Annulations. A Short Synthesis of the Amaryllidaceae Alkaloid d,l-Crinine, Overman, L. E.; Jacobsen, E. J., *Tetrahedron Lett.* (1982) **23**, 2741~2744.
65. For some examples see: a) *Intermolecular and Intramolecular Azomethine Ylide [3 + 2] dipolar Cycloadditions for the Synthesis of Highly Functionalized Pyrroles and Pyrrolidines*, DeShong, P.; Kell, D. A.; Sidler, D. R., *J. Org. Chem.* (1985) **50**,

- 2309~2315. b) *Complex Pyrrolidines via a Tandem Michael Reaction/ 1,3-Dipolar Cycloaddition Sequence. A Novel Method for the Generation of Unsymmetrical Azomethine Ylides*, Garner, P.; Arya, F.; Ho, W.-B., *J. Org. Chem.* (1990) **55**, 412~414. c) *Intramolecular 1,3-Dipolar Cycloaddition of Stabilized Azomethine Ylides to Unactivated Dipolarophiles*, Henke, B. R.; Kouklis, A. J.; Heathcock, C. H., *J. Org. Chem.* (1992) **57**, 7056~7066.
66. *An Efficient Route to the Pyrrolizidine Ring System via an N-Acyl Anion Cyclisation Process*, Murray, A.; Proctor, G. R.; Murray, J. P., *Tetrahedron*, (1996) **52**, 3757~3766.
67. *Synthesis of Unsymmetrically Substituted 2,5-Piperazinediones: Regioselective Alkylation of Piperazinedione Derivatives*, Fukuyama, T.; Frank, R. K.; Laird, A. A., *Tetrahedron Lett.*, (1985) **26**, 2955~2958.
68. *The Asymmetric Synthesis of  $\beta$ -Lactam Antibiotics-I. Application of Chiral Oxazolidinones in the Staudinger Reaction*, Evans, D. A.; Sjogren, E. B., *Tetrahedron Lett.* (1985) **26**, 3783~3786.
69. *Chiral Control in the Staudinger Reaction between Ketenes and Imines. A Theoretical SCF-MO Study on Asymmetric Torquoselectivity*, Cossio, F. P.; Arrieta, A.; Lecea, B.; Ugalde, J. M., *J. Am. Chem. Soc.* (1994) **116**, 2085~2093.
70. (a) *A Contribution to the Asymmetric Synthesis of 3-Amino  $\beta$ -Lactams: The Diastereoselective [2+2] Cycloaddition Reaction of Chiral Aminoketene Equivalents with Enolizable Aldehyde-Derived Imines*, Palomo, C.; Aizpurua, J. M.; Legido, M.; Mielgo, A.; Galarza, R., *Chem.-Eur. J.* (1997) **3**, 1432~1441. (b) *Application of erythro-2-Amino-1,2-diphenylethanol as a Highly Efficient Chiral Auxillary. Highly Stereoselective Staudinger-Type  $\beta$ -Lactam Synthesis Using a 2-Chloro-1-methylpyridinium Salt as the Dehydrating Agent*, Matsui, S.; Hashimoto, Y.; Saigo, K., *Synthesis* (1998) **8**, 1161~1166.
71. *Oxidative N-Dearylation of 2-Azetidinones. p-Anisidine as a Source of Azetidinone Nitrogen*, Kronenthal, D. R.; Han, C. Y.; Taylor, M. K., *J. Org. Chem.* (1982) **47**, 2765~2768.
72. *Oxidative Removal of N-(4-Methoxybenzyl) Group on 2,5-Piperazinediones with Cerium(IV) Diammonium Nitrate*, Yamaura, M.; Suzuki, T.; Hashimoto, H.; Yoshimura, J.; Okamoto, T.; Shin, C., *Bull. Chem. Soc. Jpn.*, (1985) **58**, 1413~1420.
73. *Synthesis and X-ray Crystal Structure Determination of 1,3-Bridged  $\beta$ -Lactams: Novel Anti-Bredt  $\beta$ -Lactams*, Williams, R. M.; Lee, B. H.; Miller, M. M.; Anderson, O. P., *J. Am. Chem. Soc.* (1989) **111**, 1073~1081.

## Experimental Section

### 5.1 General Procedures.

Bioxalomycin  $\alpha_2$  was kindly supplied by the American Cyanamid Company, Pearl River, New York. Cyanocycline A was kindly provided by Professor Steve Gould (Oregon State University). All drug concentrations were made up to 54 mM in water immediately prior to use. Deoxyoligonucleotides ("oligos") were synthesized on the Applied Biosystems 380B DNA synthesizer using standard phosphoramidite chemistry (reagents and phosphoramidites from GLEN Research). Deoxyoligonucleotides were deprotected by heating 15 h at 55 °C in  $\text{NH}_4\text{OH}$ , followed by filtering of the CPG resin and concentration of supernatant *in vacuo*. All oligos were purified by 20% denaturing polyacrylamide gel electrophoresis (DPAGE). Oligos of interest were 5'-end-labeled with  $[\gamma\text{-}^{32}\text{P}]\text{ATP}$  and T4 polynucleotide kinase (New England Biolabs). Labeled oligos were then hybridized to their corresponding blunt-ended complements in 20 mM phosphate buffer (pH= 8) by heating the equimolar mixture of oligos to 80 °C for 15 min, and cooling to RT over 2 h.  $\text{FeSO}_4$  (from Mallinckrodt) solutions were made up to 4 mM using 4 mM EDTA 5 min before use. Gel-loading buffer contained 0.03% bromophenol blue and 0.03% xylene cyanole in formamide. Dimethyl sulfate and formic acid (88%) for Maxam-Gilbert sequence reactions were obtained from Mallinckrodt. Centrex MF 0.45  $\mu\text{M}$  cellulose acetate spin filters were obtained from Schleicher & Schuell. Samples were counted on a Packard 1500 Tri-Carb liquid scintillation analyzer.

Unless otherwise noted, materials were obtained from commercially available sources and used without further purification. Diethyl ether and THF were distilled from sodium benzophenone ketyl under a nitrogen atmosphere. Methylene chloride and triethylamine were distilled under a nitrogen atmosphere from calcium hydride. Dimethyl formamide was dried over 4A molecular sieves. The molecular sieves were activated by heating at 150 °C at 1 mm Hg for 3 h in a vacuum oven.

All reactions involving hygroscopic substances were conducted with flame or oven dried glassware under an inert atmosphere (Ar) dried by passage of atmospheric gases through a column packed with CaSO<sub>4</sub>.

Chromatographic separations were performed with EM Science TLC plates (silica gel 60, F254, 20 x 20 cm x 250 μm) or with EM Science 230-400 mesh silica gel under positive air pressure. Reactions and chromatographic fractions were monitored and analyzed with EM Science TLC plates. Visualization on TLC were achieved with ultraviolet light and heating of TLC plates submerged in a 5% solution of phosphomolybdic acid in 95% ethanol (PMB) or 2,4-dinitrophenylhydrazine in 2 M HCl (DNP) or *p*-anisaldehyde in 95% ethanol or Dragendorff solution.

Melting points were determined in open capillary tubes with a Mel-Temp apparatus and are uncorrected.

Infrared spectra were recorded on a Perkin-Elmer 1600 series FTIR as thin films from methylene chloride and are reported as  $\lambda_{\text{max}}$  in wavenumbers (cm<sup>-1</sup>).

Elemental analyses were performed by M-H-W Laboratories, Phoenix, AZ, and are accurate to within ±0.4% of the calculated values. Mass spectra were obtained on a 1992 Fisons VG Autospec at the Chemistry Department at Colorado State University.

Nuclear magnetic resonance (NMR) spectra were acquired using a Bruker AC-300, Varian 300 or 400 spectrometer. NMR chemical shifts are given in parts per million (ppm) relative to internal CHCl<sub>3</sub>, DMSO, or methanol. Proton (<sup>1</sup>H) NMR are tabulated in the following order: multiplicity (s, singlet; d, doublet; t, triplet; q, quartet; and m, multiplet),

coupling constant in hertz, and number of protons. When appropriate, the multiplicity of a signal is denoted as "br" to indicate that the signal was broad.

**Drug-DNA Cross-link Formation.** To 10  $\mu\text{L}$  of a 180  $\mu\text{M}$  (in duplex) stock solution (in phosphate buffer (pH=8)) of 5'- $^{32}\text{P}$  end-labeled DNA was added 11  $\mu\text{L}$  of 80 mM phosphate buffer (pH= 8), 23  $\mu\text{L}$  of  $\text{H}_2\text{O}$ , and 10  $\mu\text{L}$  of drug stock solution to yield a drug concentration of 10 mM. Reactions were incubated at 37  $^\circ\text{C}$  for 12 h. The oligos were then ethanol-precipitated, dried *in vacuo* and resuspended in 10  $\mu\text{L}$  of water and 30  $\mu\text{L}$  DPAGE loading dye. Reactions were loaded onto a 20% denaturing gel, electrophoresis was carried out for 5 h at 2000 V, and the bands visualized by autoradiography. Cross-linked product bands were excised from the gel, crushed and eluted out of the gel for 15 min at RT in 500 mM  $\text{NH}_4\text{OAc}$ , 1 mM EDTA buffer. The gel was then filtered off with a Centrex 0.45  $\mu\text{m}$  centrifugation filter and the supernatant volume decreased by *n*-BuOH extraction to 200  $\mu\text{L}$ . The DNA isolated was ethanol-precipitated and dried *in vacuo*. Each alkylation product was resuspended with 20  $\mu\text{L}$  of distilled de-ionized water.

**Footprinting reactions.** From each deoxyoligonucleotide solution, a 7.5  $\mu\text{L}$  aliquot was removed for use in the footprinting reaction. To this aliquot 7.5  $\mu\text{L}$  of 80 mM phosphate buffer (pH 8) and 10  $\mu\text{L}$  4 mM  $\text{FeSO}_4$ -EDTA solution to afford reactions 1.6 mM in Fe(II)-EDTA. Footprinting reactions were then incubated at 37  $^\circ\text{C}$  for 3 h, after which time, the samples were ethanol precipitated and dried *in vacuo*. Dried pellets were counted by liquid scintillation (LSC). Samples were loaded such that the standard duplex and cross-linked product lanes contained 1000 counts, Fe(II)-EDTA lanes contained 25,000 counts (for Fe(II)-EDTA standard and native duplex after cross-linking and Fe(II)-EDTA digestion). The G and G+A Maxim-Gilbert sequencing lanes were loaded 5,000 and 7,500 counts, respectively. Electrophoresis was carried out at 1500 V for 5 h followed by autoradiography at -80  $^\circ\text{C}$  for 24 h.

### **Preparation of Bioxalomycin $\alpha_2$ Cross-linked DNA for Mass Spectrometry.**

To 95  $\mu\text{L}$  of a 6.3 mM (in duplex) solution of duplex in  $\text{H}_2\text{O}$  was added 30  $\mu\text{L}$  of 80 mM phosphate buffer (pH 8) and 28  $\mu\text{L}$  of bioxalomycin  $\alpha_2$  (54 mM). The reaction was incubated overnight at 37  $^\circ\text{C}$  and then ethanol-precipitated. The pellet was resuspended in 100  $\mu\text{L}$  of  $\text{H}_2\text{O}$  and 200  $\mu\text{L}$  of DPAGE dye and loaded onto a 20% preparative DPAGE gel. The electrophoresis was carried out at 1000 V for 5 h to give a clean separation of the cross-linked material. The cross-linked product band was visualized by hand-held UV and cut out of the gel. The bands were crushed and soaked with shaking in 500 mM  $\text{NH}_4\text{OAc}$ , 1 mM EDTA buffer for 15 min at RT and then the gel filtered off and the volume of the supernatant reduced and ethanol-precipitated. The pellet was resuspended in 150  $\mu\text{L}$   $\text{H}_2\text{O}$  and to the solution was added 50  $\mu\text{L}$   $\text{NH}_4\text{OAc}$  (5 M, pH 5.2). The sample was allowed to stand at RT for 10 min and was then ethanol-precipitated with 600  $\mu\text{L}$  of EtOH and dried *in vacuo*.

## 5.2 Preparation of Compounds



### 3-Carbethoxy-(2,2'-carbonyl)-3-hydroxymethyl-8-methoxydihydroisoquinoline (113).

DMF (1.06 mL, 13.6 mmol) followed by oxalyl chloride (1.33 mL, 20.5 mmol) was added to a solution of **100** (4.19 g, 13.6 mmol) in 50 mL of  $\text{CH}_2\text{Cl}_2$  at RT. After 30 min the solvent was stripped off and the residue dissolved in  $\text{NEt}_3$  (30 mL) and heated at reflux for 2 h. After cooling to RT the reaction was diluted with  $\text{Et}_2\text{O}$ , washed with water, and dried over  $\text{MgSO}_4$  to give 3.70 g (94%) of **113**. m.p.= 117-119 °C (recryst.  $\text{Et}_2\text{O}$ ). TLC (1/1 EtOAc/Hex)  $R_f = 0.26$  (UV and PMA).  $^1\text{H-NMR}$  (300 MHz) ( $\text{CDCl}_3$ )  $\delta$  1.32 (t,  $J = 7.2$  Hz, 3H); 3.80 (s, 3H); 4.32 (dq,  $J = 2.5, 7.2$  Hz, 2H); 4.59 (dd,  $J = 8.4, 9.3$  Hz, 1H); 5.01 (dd,  $J = 8.7, 9.3$  Hz, 1H); 5.29 (dd,  $J = 8.4, 8.7$  Hz, 1H); 6.86 (dd,  $J = 7.8, 8.7$  Hz, 2H); 6.90 (s, 1H); 7.25 (dd,  $J = 7.4, 8.7$  Hz, 1H).  $^{13}\text{C-NMR}$  (75 MHz) ( $\text{CDCl}_3$ )  $\delta$  14.2, 53.5, 55.7, 61.8, 70.7, 112.6, 120.6, 122.1, 123.0, 127.5, 129.7, 130.3, 155.3, 155.6, 162.6. IR (NaCl, neat) 2981, 2360, 2343, 1767, 1724, 1635, 1575, 1476, 1405, 1306, 1263, 1213, 1092  $\text{cm}^{-1}$ . Anal. Calcd for  $\text{C}_{15}\text{H}_{15}\text{NO}_5$ : C, 62.28; H, 5.23; N, 4.84. Found: C, 62.18; H, 5.40; N, 4.89.

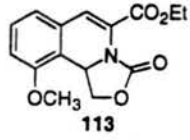
Filename: FEB09-1485.D05

0.571 0.485  
1.2

0.531 0.574 0.554 1.1

1.72

1.63



0 95 90 85 80 75 70 65 60 55 50 PPM 45 40 35 30 25 20 15 10 0.5 0

PPM

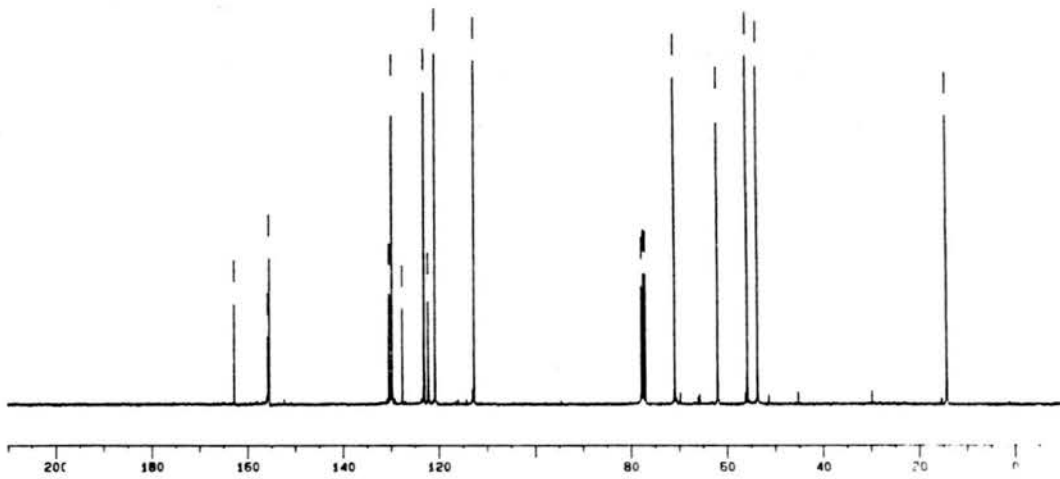
162.828  
158.271  
157.271

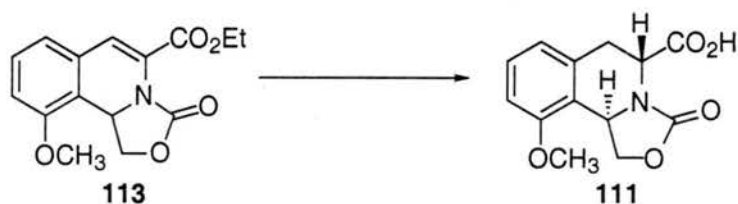
130.292  
127.502  
126.491  
125.481  
112.373

BH-485

77.827  
77.000  
76.212  
61.288  
55.493  
55.211

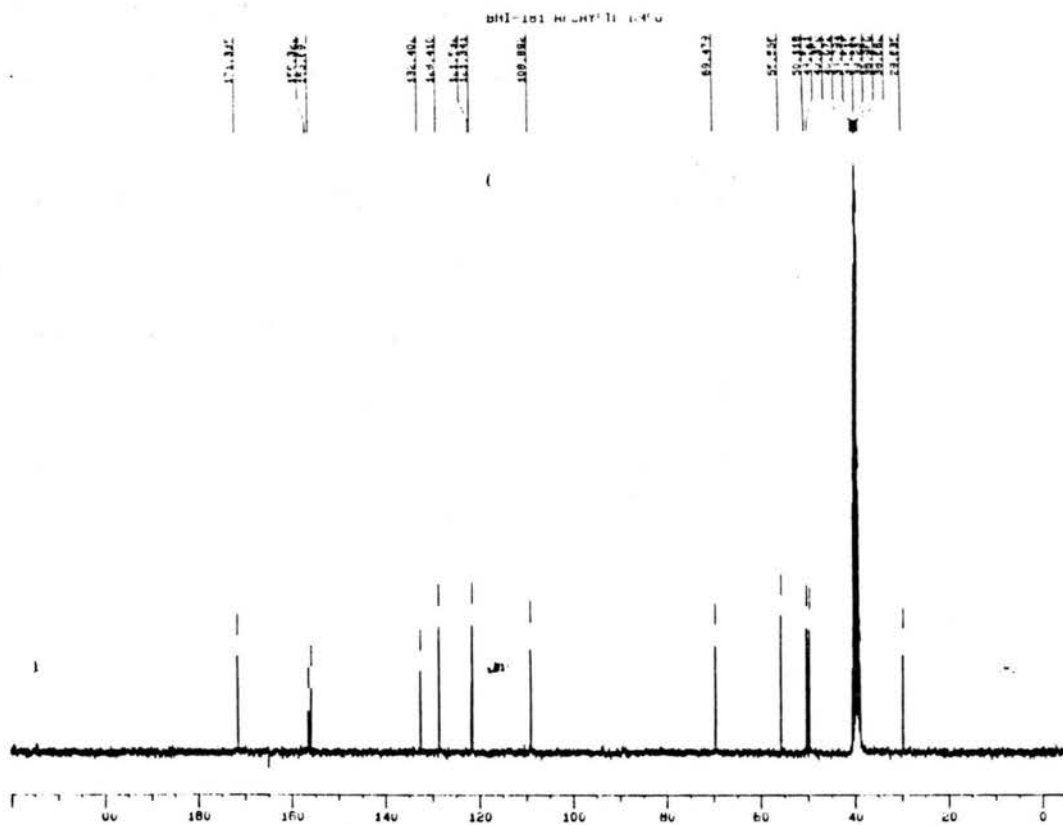
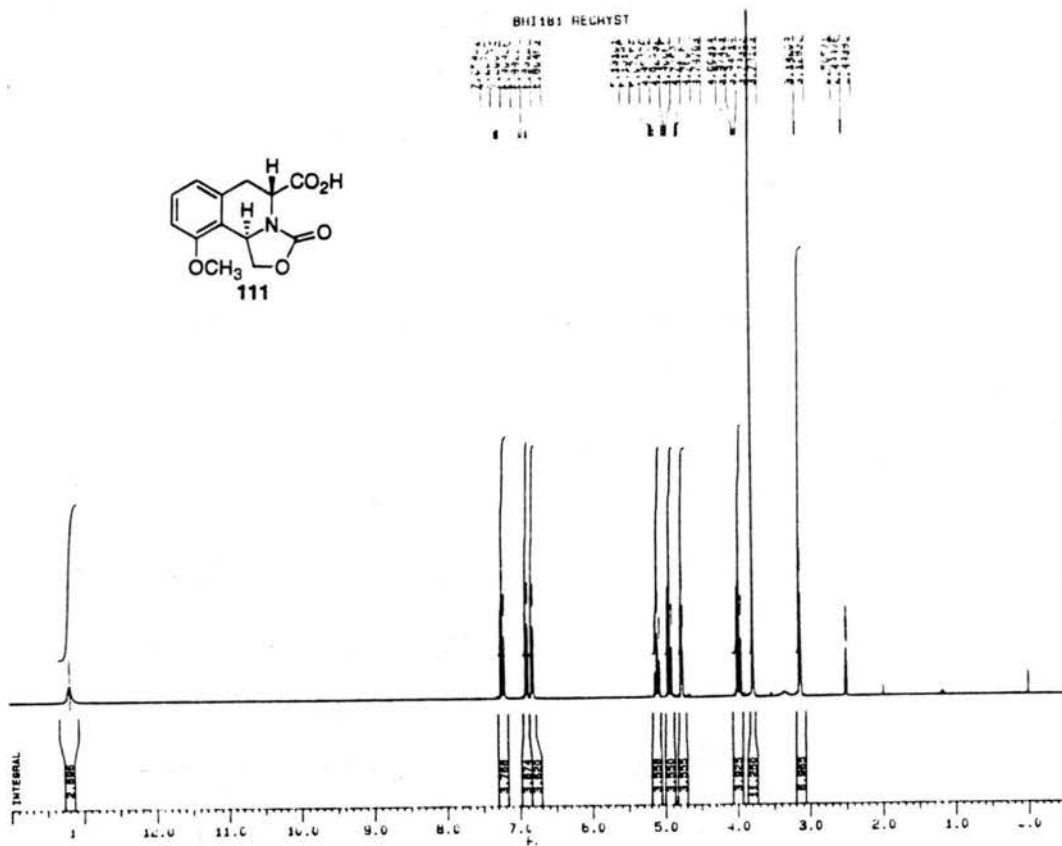
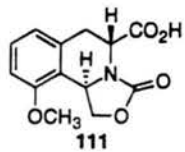
15.228

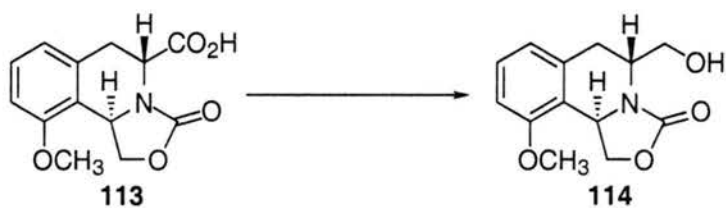




**1-Carboxyl-(2,2'-carbonyl)-3-hydroxymethyl-8-methoxytetrahydroisoquinoline (111).**

Ester **113** (5.65g, 19.5 mmol) was dissolved in 325 mL of EtOH and 5% Pd/C (10.4 g, 4.9 mmol) was added. Hydrogen was bubbled through the solution for 5 min and the reaction was allowed to stir under an atmosphere of H<sub>2</sub> overnight. Argon gas was bubbled through the reaction and it was filtered through a pad of celite to give the saturated ethyl ester as a mixture of diastereomers (4.46 g, 78%). To a stirred solution of the ethyl ester (2.25 g, 8.12 mmol) in 100 mL of EtOH and 40 mL of H<sub>2</sub>O at 0 °C was added LiOH·H<sub>2</sub>O (511 mg, 12.2 mmol). After 3 h at 0 °C the volume of the reaction was reduced by half and acidified with 1M HCl. The reaction was extracted with ethyl acetate, dried over NaSO<sub>4</sub> and concentrated to afford acid **111** (92% yield). The acid was purified for analytical sample by recrystallization. m.p.= 230-232 °C (recryst. EtOAc-EtOH). <sup>1</sup>H-NMR (300 MHz) (DMSO-d<sub>6</sub>) δ 3.14 (d, J= 4.1 Hz, 2H); 3.78 (s, 3H); 3.97 (t, J= 8.7 Hz, 1H); 4.76 (dd, J= 4.1, 4.6 Hz, 1H); 4.93 (t, J= 8.6 Hz, 1H); 5.10 (t, J= 8.8 Hz, 1H); 6.83 (d, J= 7.7 Hz, 1H); 6.99 (d, J= 8.2 Hz, 1H); 7.23 (dd, J= 8.1, 7.9 Hz, 1H); 13.20 (bs, 1H). <sup>13</sup>C-NMR (75 MHz) (DMSO-d<sub>6</sub>) δ 29.6, 49.5, 50.1, 55.6, 69.5, 108.9, 121.3, 121.5, 128.4, 132.4, 155.7, 156.3, 171.3. Anal. Calcd for C<sub>13</sub>H<sub>13</sub>NO<sub>5</sub>: C, 59.31; H, 4.98; N, 5.32. Found: C, 59.81; H, 5.12; N, 5.31.

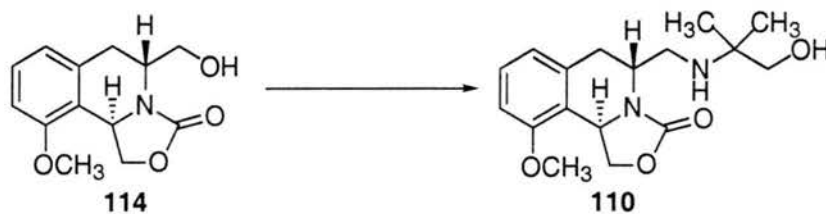




***trans*-1-Hydroxymethyl-(2,2'-carbonyl)-3-hydroxymethyl-8-methoxy tetrahydroisoquinoline (114).**

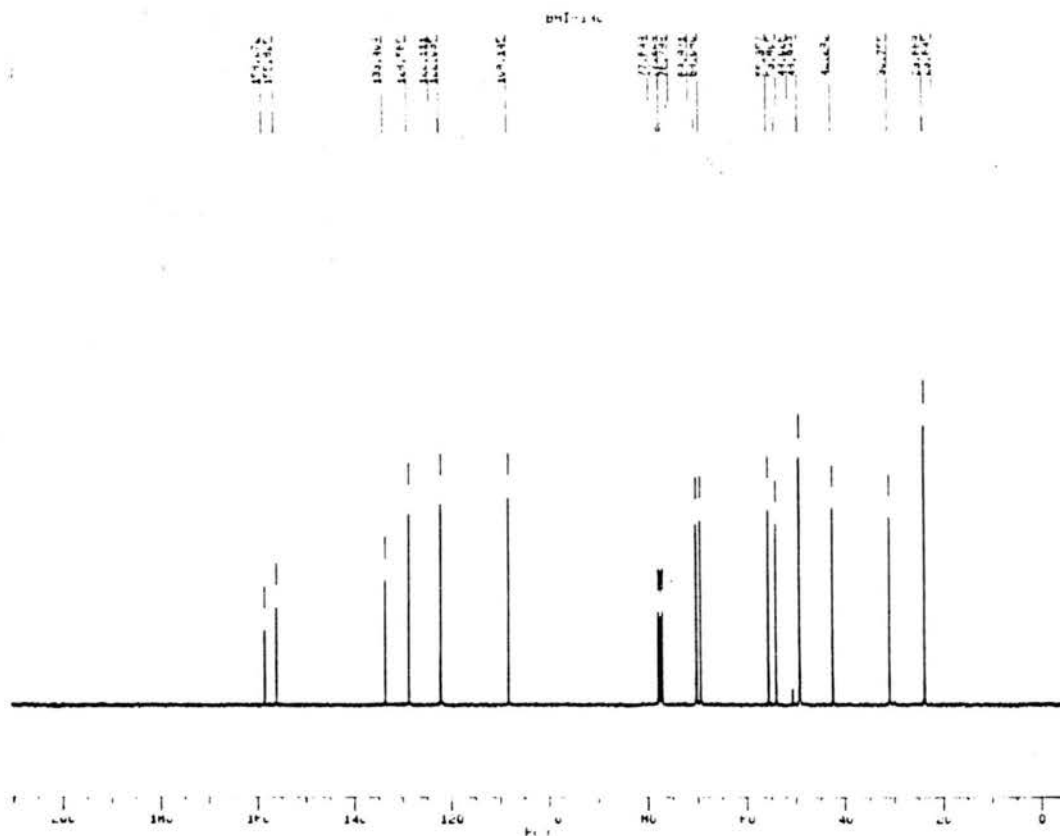
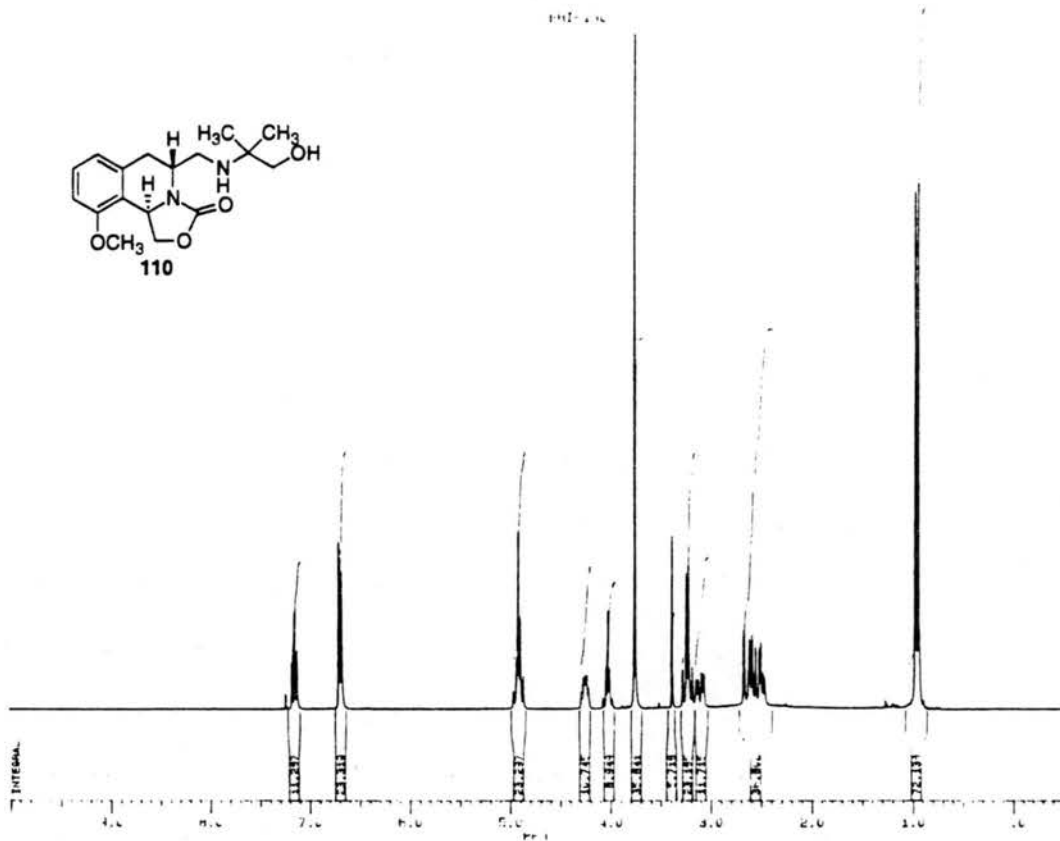
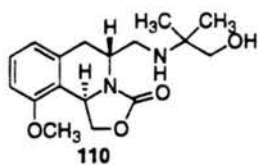
To a solution of acid **113** (3.31 g, 12.57 mmol) in 200 mL of CH<sub>2</sub>Cl<sub>2</sub> was added oxalyl chloride (1.40 mL, 22.00 mmol) and a drop of DMF. After 2 h the solvent was stripped off. The acid chloride was dissolved in 150 mL of CH<sub>2</sub>Cl<sub>2</sub> and cooled to -78 °C. A slurry of NaBH<sub>4</sub> (2.38 g, 62.85 mmol) in 75 mL of EtOH was made, cooled to 0 °C, and added to the reaction. The cooling bath was removed and the reaction was allowed to warm up to RT. After 2 hours the reaction was quenched by careful addition of 1M HCl at 0 °C. The reaction was washed with CH<sub>2</sub>Cl<sub>2</sub> and the organic phase dried over MgSO<sub>4</sub> and concentrated. The crude was purified with column chromatography (SiO<sub>2</sub>, 3/1 EtOAc/Hex) giving 3.10 g (98%) of **114** as yellow plates. m.p.= 108-110 °C (recryst. EtOAc). TLC (3/1 EtOAc/Hex) R<sub>f</sub> = 0.18 (UV). <sup>1</sup>H-NMR (300 MHz) (CDCl<sub>3</sub>) δ 2.24 (t, J= 6.1, 1H, D<sub>2</sub>O exch.); 2.69 (d, J= 16.9, 1H); 3.13 (dd, J= 7.0, 16.8 Hz, 1H); 3.59-3.64 (m, 2H); 3.78 (s, 3H); 4.08 (t, J= 8.3 Hz, 1H); 4.36 (dd, J=7.0, 14.1, 1H); 4.92 (dd, J= 8.5, 8.7 Hz, 1H); 5.02 (dt, J= 8.3, 8.5 Hz, 1H); 6.73 (dd, J= 6.0, 8.0 Hz, 2H); 7.20 (t, J= 8.0 Hz, 1H). <sup>13</sup>C-NMR (75 MHz) (CDCl<sub>3</sub>) δ 28.8, 49.5, 50.0, 55.5, 61.7, 70.2, 108.3, 122.2, 128.7, 133.4, 156.0, 158.4, 169.6. IR (NaCl, neat) 3421, 2942, 1737, 1586, 1473, 1257, 1094 cm<sup>-1</sup>. Anal. Calcd for C<sub>13</sub>H<sub>17</sub>NO<sub>4</sub>: C, 62.64; H, 6.07; N, 5.62. Found: C, 62.49; H, 5.94; N, 5.66.

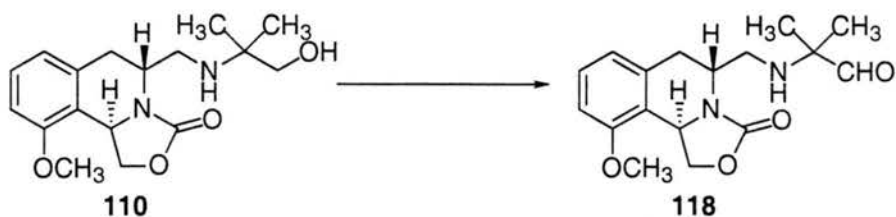




***trans*-1-Hydroxymethyl-(2,2'-carbonyl)-3-(*N*-2,2-dimethylethoxy)-aminomethyl-8-methoxytetrahydroisoquinoline (110).**

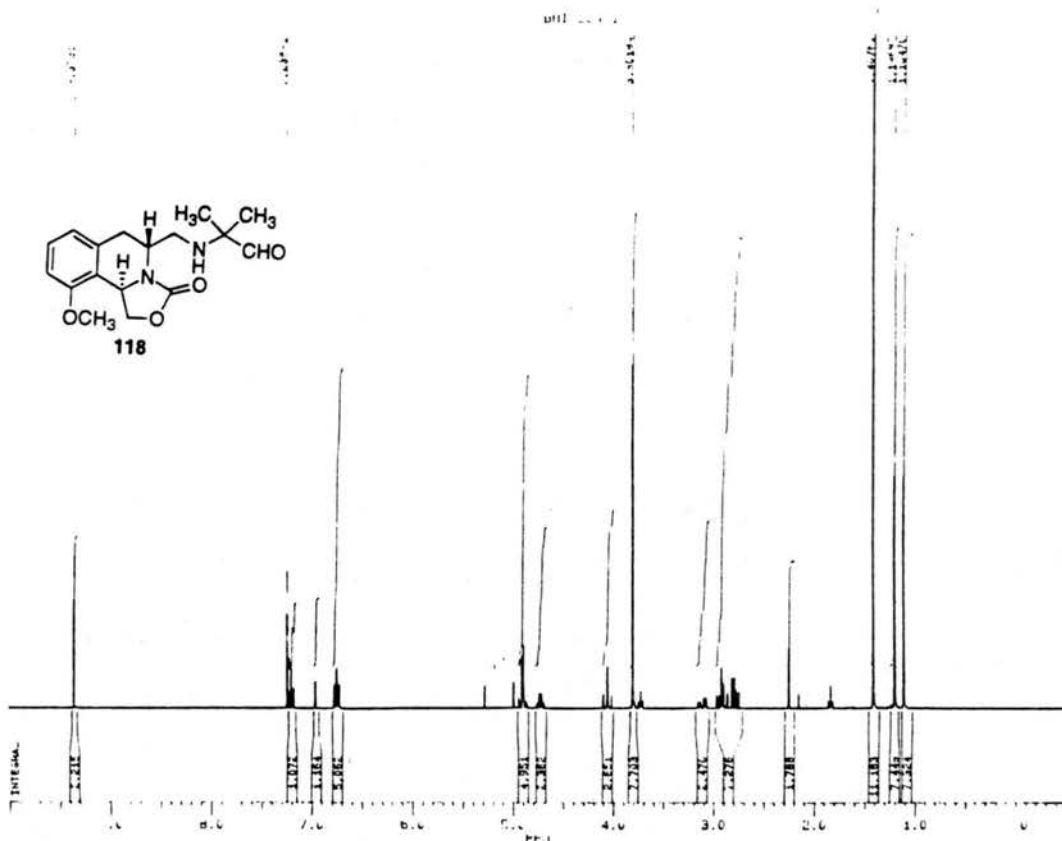
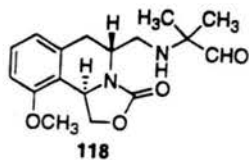
Methanesulfonyl chloride (116  $\mu$ L, 1.5 mmol) and  $\text{NEt}_3$  (348  $\mu$ L, 2.5 mmol) were added to a solution of alcohol **114** (250 mg, 1 mmol) in 2 mL of  $\text{CH}_2\text{Cl}_2$  at 0  $^\circ\text{C}$ . After 2 h the reaction was run through a short plug of silica with 10/1  $\text{CH}_2\text{Cl}_2/\text{MeOH}$  as the eluent. The mesylate was redissolved in 3 mL of  $\text{CHCl}_3$  and 2-amino-2-methyl-1-propanol (0.95 mL, 10 mmol) was added. The reaction was allowed to reflux for 2 days. It was diluted with  $\text{CH}_2\text{Cl}_2$ , washed with  $\text{NaHCO}_3$  (sat.), dried over  $\text{MgSO}_4$  and concentrated. The crude product was purified by column chromatography ( $\text{SiO}_2$ , 10/1  $\text{CH}_2\text{Cl}_2/\text{MeOH}$ ) affording **110** (236 mg, 70%) as slightly yellow plates. TLC (10/1  $\text{CH}_2\text{Cl}_2/\text{MeOH}$ )  $R_f = 0.28$  (UV and dragendorff). m.p. = 111-115  $^\circ\text{C}$  (recryst. MeOH).  $^1\text{H-NMR}$  (300 MHz) ( $\text{CDCl}_3$ )  $\delta$  0.94 (s, 3H); 0.97 (s, 3H); 2.50 (br s, 1H); 2.51 (dd,  $J = 5.3, 11.7$  Hz, 1H); 2.56-2.67 (m, 2H); 3.11 (dd,  $J = 6.8, 16.7$  Hz, 1H); 3.24 (dd,  $J = 10.8, 17.9$  Hz, 2H); 3.39 (s, 1H,  $\text{D}_2\text{O}$  exch.); 3.76 (s, 3H); 4.02 (t,  $J = 5.7$ , 1H); 4.22-4.29 (m, 1H); 4.87-4.97 (m, 2H); 6.69 (d,  $J = 8.0$  Hz, 2H); 7.15 (t,  $J = 8.0$  Hz, 1H).  $^{13}\text{C-NMR}$  (75 MHz) ( $\text{CDCl}_3$ )  $\delta$  23.6, 23.7, 30.8, 42.3, 49.0, 49.0, 53.8, 55.4, 69.1, 70.0, 108.1, 122.0, 122.1, 128.6, 133.4, 155.8, 158.3. IR (NaCl, neat) 3441, 2964, 1748, 1586, 1472, 1258, 1094  $\text{cm}^{-1}$ . Anal. Calcd for  $\text{C}_{17}\text{H}_{24}\text{N}_2\text{O}_4$ : C, 63.73; H, 7.55; N, 8.74. Found: C, 63.53; H, 7.46; N, 8.66.

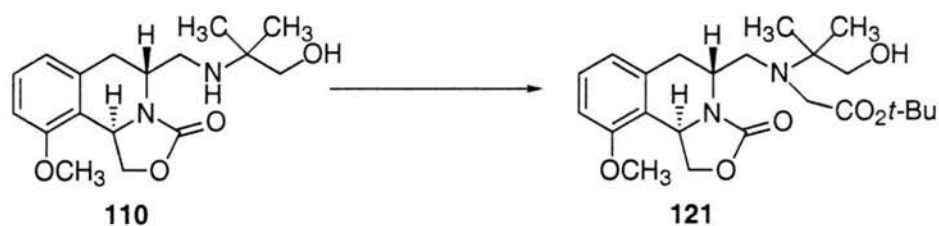




***trans*-1-Hydroxymethyl-(2,2'-carbonyl)-3-(*N*-2,2-dimethylformyl)-aminomethyl-8-methoxytetrahydroisoquinoline (118).**

Amino alcohol **110** (25 mg, 0.074 mmol) was dissolved in 5 mL of dry ether and through this solution was bubbled dry HCl precipitating the HCl salt. The mixture was then concentrated to a dry solid and the material redissolved in 2 mL of CH<sub>2</sub>Cl<sub>2</sub>. To the solution of the HCl salt was added Dess-Martin periodinane (60.1 mg, 0.14 mmol) at RT. The reaction stirred for 2 h at RT after which a solution of 0.2 mL of NaHCO<sub>3</sub> (1 M) with sodium thiosulfate (31 mg) dissolved in it was added. The quenched reaction was allowed to stir for 30 min and was then extracted with CH<sub>2</sub>Cl<sub>2</sub>. The organic phase was dried over MgSO<sub>4</sub> and concentrated to yield **118** (14 mg, 57%) as a clear oil. TLC (3/1 EtOAc/Hex) R<sub>f</sub> = 0.58 (UV and DNP). <sup>1</sup>H-NMR (300 MHz) (CDCl<sub>3</sub>) δ 1.10 (s, 3H); 1.20 (s, 3H); 2.78 (dd, J= 7.8, 13.5 Hz, 1H); 2.89 (d, J= 17.6 Hz, 1H); 2.93 (dd, J= 6.8, 13.5 Hz, 1H); 3.11 (dd, J= 6.8, 16.9 Hz, 1H); 3.80 (s, 3H); 4.05 (dd, J= 12.2, 12.7 Hz, 1H); 4.72 (dd, J= 6.8, 13.5 Hz, 1H); 4.90 (dd, J= 8.9, 12.8 Hz, 2H); 6.75 (t, J= 8.0 Hz, 2H); 7.20 (t, J= 8.0 Hz, 1H); 9.35 (s, 1H).





***trans*-1-Hydroxymethyl-(2,2'-carbonyl)-3-(*N*-2,2-dimethylethoxy-*N*-*t*-butyl-carboxymethyl)-aminomethyl-8-methoxytetrahydroisoquinoline (121).**

To a solution of **110** (183 mg, 0.54 mmol) in 4 mL of DMF was added NaHCO<sub>3</sub> (454 mg, 5.4 mmol), NaI (809 mg, 5.4 mmol) and *t*-butyl bromoacetate (0.88 mL, 5.4 mmol) at RT. After 12 h the reaction was diluted with CH<sub>2</sub>Cl<sub>2</sub> and washed with water. The layers were separated and the organic layer dried over MgSO<sub>4</sub>. Column chromatography (3/1 EtOAc/ Hex) gave **121** (195 mg, 83%) as a yellow solid. TLC (3/1 EtOAc/ Hex) R<sub>f</sub> = 0.50 (UV and dragendorff). m.p= 152-154 °C (recryst. EtOAc). <sup>1</sup>H-NMR (300 MHz) (CDCl<sub>3</sub>) δ 0.91 (s, 3H); 0.92 (s, 3H); 1.46 (s, 9H); 2.61 (dd, J= 6.9, 13.0 Hz, 1H); 2.76 (dd, J= 8.5, 13.0 Hz, 1H); 2.99 (d, J= 3.5 Hz, 2H); 3.05 (1/2 ABq, J= 11.6 Hz, 1H); 3.20 (1/2 ABq, J= 11.6 Hz, 1H); 3.27 (1/2 ABq, J= 18.1 Hz, 1H); 3.45 (1/2 ABq, J= 18.1 Hz, 1H); 3.73 (br s, 1H, D<sub>2</sub>O exch.); 3.80 (s, 3H); 4.04 (dd, J= 8.0, 9.0 Hz, 1H); 4.22 (m, 1H); 4.88 (dd, J= 8.0, 9.0 Hz, 1H); 4.98 (dd, J= 8.0, 9.0 Hz, 1H); 6.72 (d, J= 8.0 Hz, 1H); 6.78 (d, J= 8.0 Hz, 1H); 7.19 (t, J= 8.0 Hz, 1H). <sup>13</sup>C-NMR (75 MHz) (CDCl<sub>3</sub>) δ 21.1, 23.1, 28.2, 29.4, 47.5, 49.5, 49.6, 51.7, 55.5, 59.0, 69.1, 70.1, 82.0, 108.2, 122.0, 122.7, 128.8, 133.6, 155.9, 157.9, 173.7. IR (NaCl, neat) 3466, 2976, 1755, 1587, 1473, 1258, 1152 cm<sup>-1</sup>. Anal. Calcd for C<sub>23</sub>H<sub>34</sub>N<sub>2</sub>O<sub>6</sub>: C, 63.58; H, 7.93; N, 6.45. Found: C, 63.71; H, 7.93; N, 6.22.

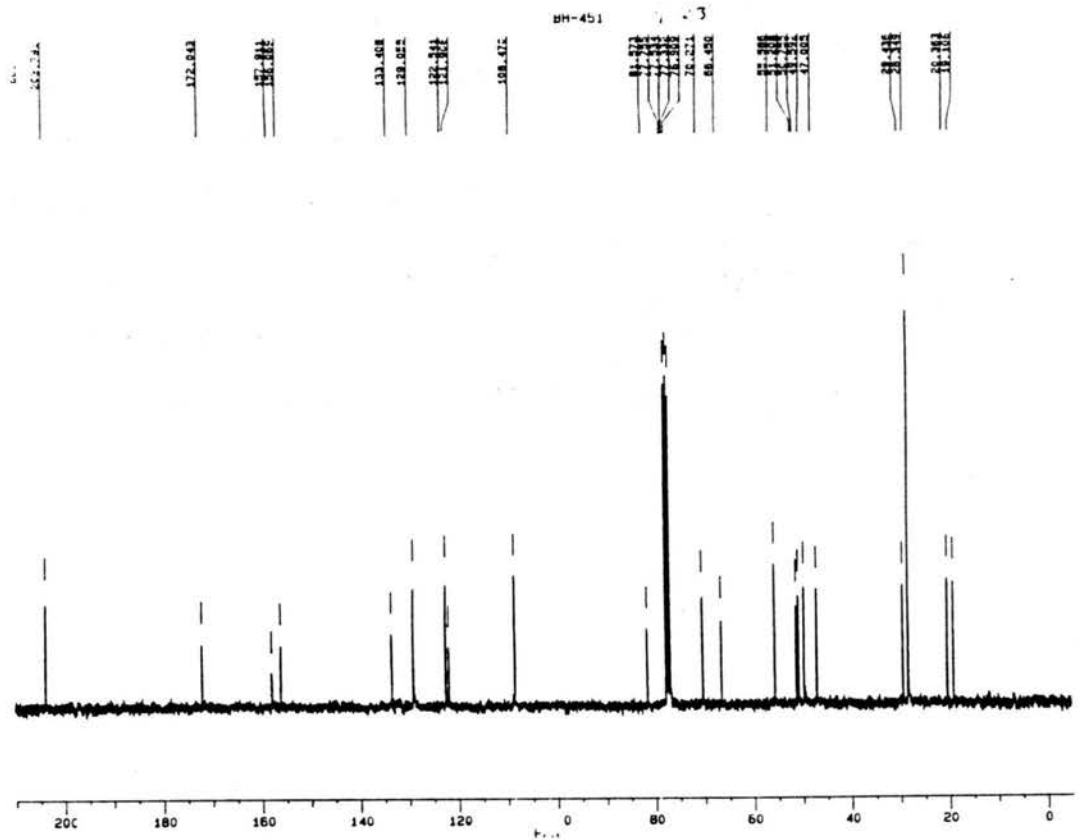
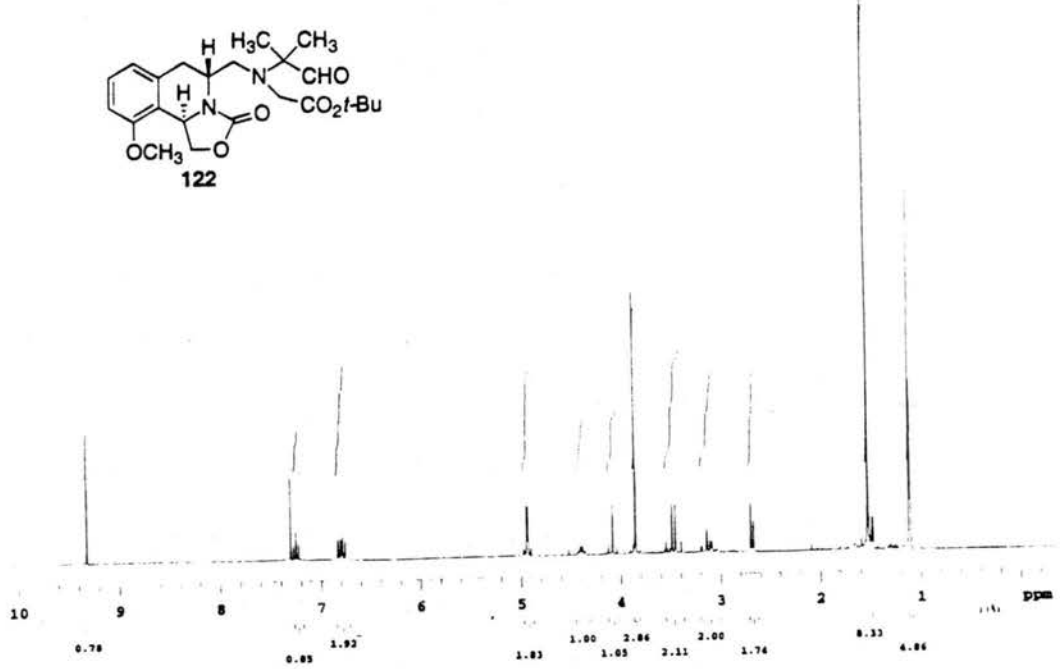
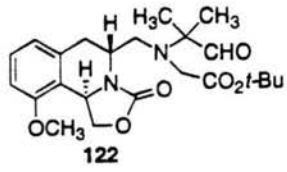


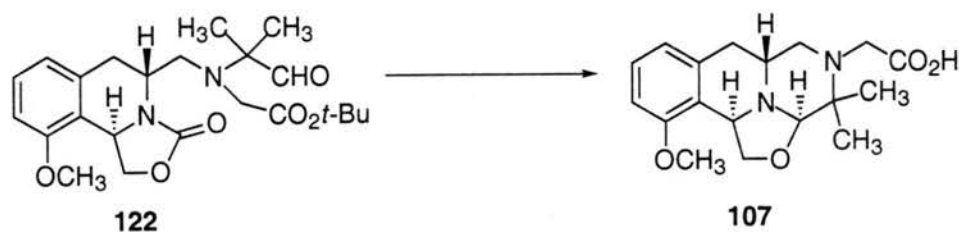


***trans*-1-Hydroxymethyl-(2,2'-carbonyl)-3-(*N*-2,2-dimethyl-2-*N*-*t*-butyl-carboxymethyl)-aminomethyl-8-methoxytetrahydroisoquinoline (122).**

Dess-Martin periodinane (48 mg, 0.11 mmol) was added to **121** (32 mg, 0.076 mmol) in 1 mL of CH<sub>2</sub>Cl<sub>2</sub>. The reaction stirred for 30 min at RT after which a solution of 1 mL of NaHCO<sub>3</sub> (1 M) with sodium thiosulfate (273 mg) dissolved in it was added. The quenched reaction was allowed to stir for 30 min and was extracted with CH<sub>2</sub>Cl<sub>2</sub>. The organic phase was dried over MgSO<sub>4</sub> and concentrated to yield **122** (30 mg, 90%) as a yellow oil. TLC (3/1 EtOAc/ Hex) R<sub>f</sub> = 0.65 (UV and dragendorff). <sup>1</sup>H-NMR (300 MHz) (CDCl<sub>3</sub>) δ 1.03 (s, 3H); 1.04 (s, 3H); 1.45 (s, 9H); 2.61 (d, J = 7.5 Hz, 2H); 3.05 (m, 2H); 3.37 (1/2 ABq, J = 17.7 Hz, 1H); 3.44 (1/2 ABq, J = 18.0 Hz, 1H); 3.78 (s, 3H); 4.01 (t, J = 12.0 Hz, 1H); 4.33 (dd, J = 7.0, 16.0 Hz, 1H); 4.87 (dd, J = 9.0, 12.0 Hz, 2H); 6.71 (d, J = 7.0 Hz, 1H); 6.75 (d, J = 8.0 Hz, 1H), 7.18 (t, J = 8.0 Hz, 1H); 9.26 (s, 1H). <sup>13</sup>C-NMR (75 MHz) (CDCl<sub>3</sub>) δ 19.0, 20.3, 28.2, 29.3, 46.9, 49.5, 50.9, 51.1, 55.5, 66.4, 70.2, 81.5, 108.4, 121.8, 122.4, 129.0, 132.9, 156.0, 158.0, 171.9, 203.7. IR (NaCl, neat) 2977, 1755, 1587, 1473, 1393, 1368, 1258, 1155, 1096 cm<sup>-1</sup>. HRMS (FAB) calcd for C<sub>23</sub>H<sub>33</sub>N<sub>2</sub>O<sub>6</sub> (M+H) 433.2339; found 433.2345.

BH199073-5





**4 $\alpha$ ,6 $\alpha$ ,11 $\alpha$  $\beta$ -2-Aza-2-carboxyacetyl-1,3,4,6,11 $\alpha$ -hexahydro-7-methoxy-5,4-oxazolo-3,3-dimethyl-2*H*-benzo[*b*]quinolizine (107).**

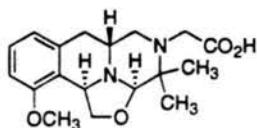
To a solution of **122** (120 mg, 0.27 mmol) in 17 mL of EtOH was added 1.66 mL of 2 M LiOH. This solution was degassed by bubbling through nitrogen and heated at reflux for 24 h. After cooling to RT, the reaction was concentrated and chromatographed (10/1 CH<sub>2</sub>Cl<sub>2</sub>/ MeOH) to give 60 mg (67%) of **107** as a yellow foam. TLC (10/1 CH<sub>2</sub>Cl<sub>2</sub>/ MeOH) R<sub>f</sub> = 0.20 (UV and Dragendorff). <sup>1</sup>H-NMR (300 MHz) (MeOH-d<sub>4</sub>)  $\delta$  1.55 (s, 3H); 1.59 (s, 3H); 2.73 (m, 2H); 3.16 (m, 1H); 3.46 (m, 2H); 3.50 (1/2 ABq, J= 16.0 Hz, 1H); 3.62 (dd, J= 8.0, 9.0 Hz, 1H); 3.82 (s, 3H); 3.91 (1/2 ABq, J=16.0 Hz, 1H); 4.26 (dd, J= 8.0, 9.0 Hz, 1H); 4.47 (s, 1H); 4.54 (t, J= 9.0 Hz, 1H); 6.78 (d, J= 8.0 Hz, 1H); 6.83 (d, J= 8.0 Hz, 1H); 7.19 (t, J= 8.0 Hz, 1H). <sup>13</sup>C-NMR (75 MHz) (MeOH-d<sub>4</sub>)  $\delta$  170.3, 158.2, 135.5, 129.2, 123.9, 121.9, 109.3, 96.5, 69.6, 62.5, 60.7, 56.1, 54.3, 53.8, 32.9, 22.5, 20.2. IR (NaCl, neat) 3381, 2953, 1651, 1472, 1383, 1340, 1261 cm<sup>-1</sup>. HRMS (FAB) calcd for C<sub>18</sub>H<sub>25</sub>N<sub>2</sub>O<sub>4</sub> (M+H) 333.1814; found 333.1816.

0.254 0.710

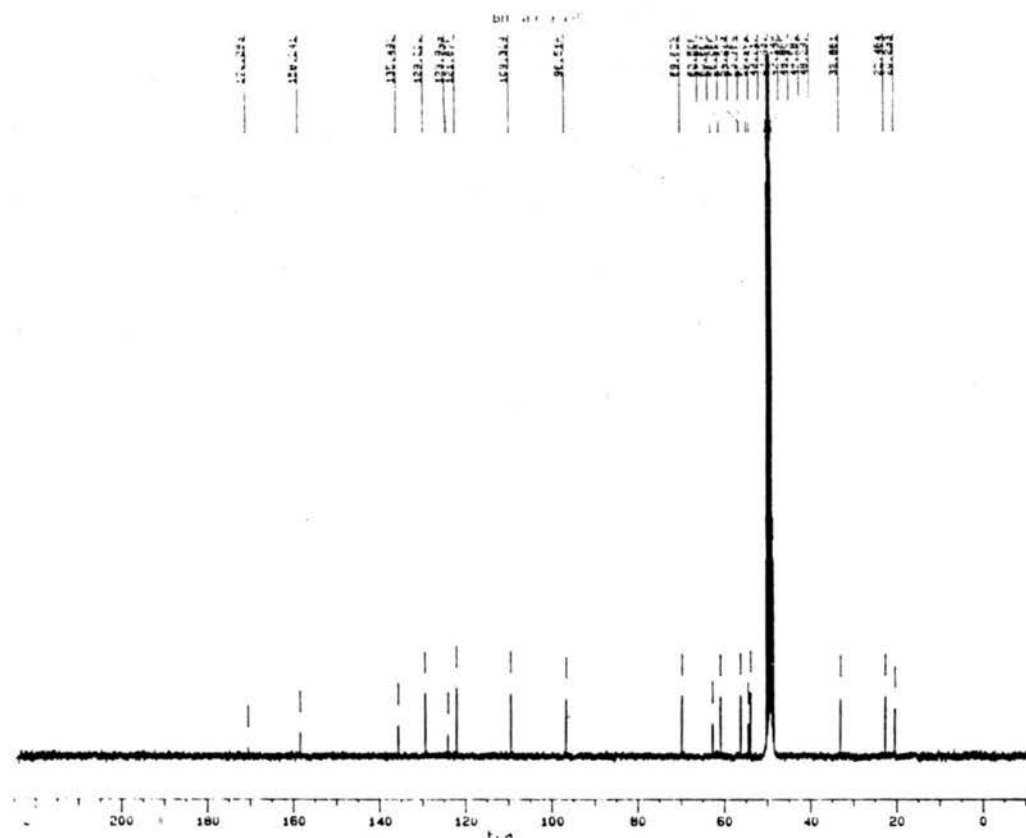
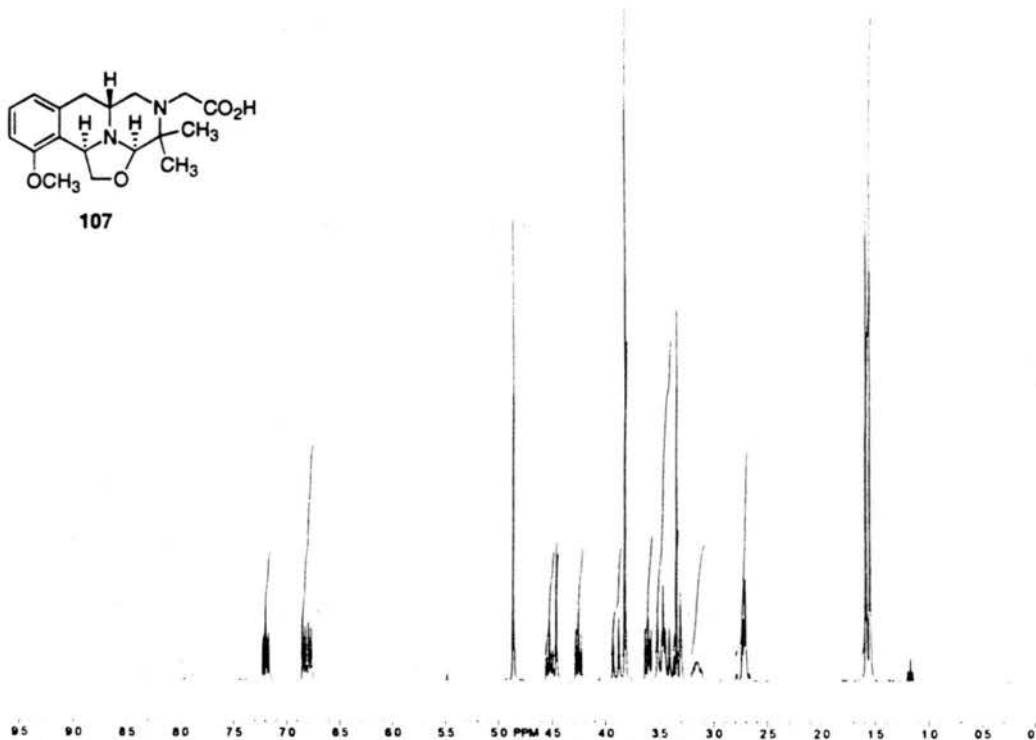
0.352 0.361 0.375 0.404 0.418

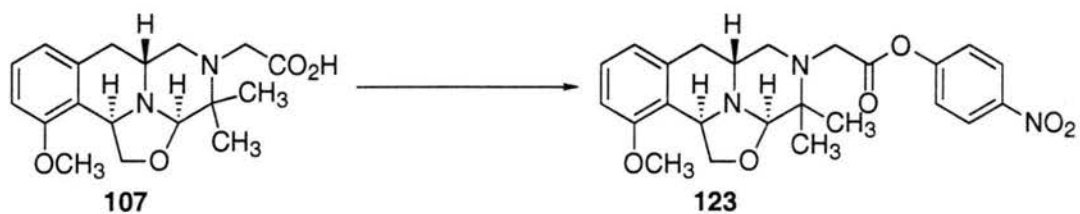
0.354 1.06 1.06 0.364 0.722

2.13



107

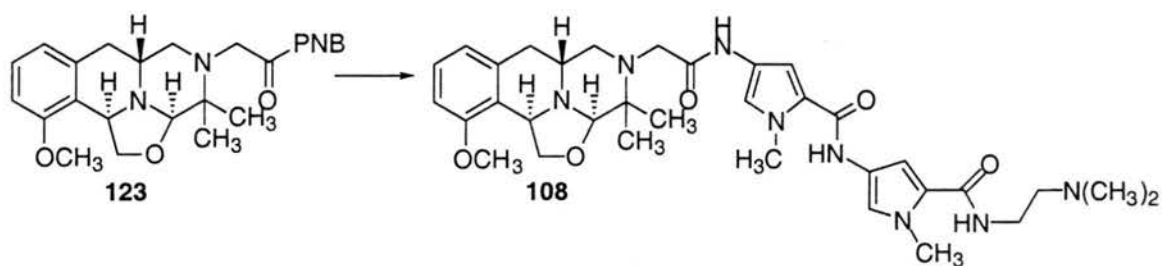




**4 $\alpha$ ,6 $\alpha$ ,11 $\alpha$  $\beta$ -2-Aza-3,3-dimethyl-1,3,4,6,11a-hexahydro-2-(4-nitrophenoxyacetyl)-7-methoxy-5,4-oxazolo-2H-benzo[*b*]quinolizine (123).**

To a stirred mixture of **107** (12.0 mg, 0.036 mmol) and *p*-nitrophenol (5.5 mg, 0.040 mmol) in 2 mL of CH<sub>2</sub>Cl<sub>2</sub> and cooled to 0 °C was added 1,3-dicyclohexylcarbodiimide (8.2 mg, 0.040 mmol). The reaction stirred at 0 °C for 1 h, and was then warmed to RT and stirred for an additional 15 h. The reaction mixture was then concentrated under reduced pressure and purified by PTLC (10/1 CH<sub>2</sub>Cl<sub>2</sub>/MeOH) to afford 8.5 mg (52%) of *p*-nitrophenylester **123** as a yellow oil. TLC (10/1 CH<sub>2</sub>Cl<sub>2</sub>/MeOH) R<sub>f</sub> = 0.76 (UV and dragendorff). <sup>1</sup>H-NMR (300 MHz) (CDCl<sub>3</sub>)  $\delta$  1.28 (s, 3H); 1.40 (s, 3H); 2.57 (dd, J= 2.7, 15.6 Hz, 1H); 2.71 (dd, J= 11.1, 15.6 Hz, 1H); 2.89-2.92 (m, 2H); 3.01-3.08 (m, 1H); 3.51 (1/2 ABq, J= 17.1 Hz, 1H); 3.60 (dd, J= 7.8, 8.7 Hz, 1H); 3.78 (s, 3H); 3.84 (1/2 ABq, J= 17.1 Hz, 1H); 4.15-4.20 (m, 2H); 4.44 (t, J= 8.7 Hz, 1H); 6.67 (d, J= 8.1 Hz, 1H); 6.72 (d, J= 7.5 Hz, 1H); 7.12 (dd, J= 7.5, 8.1 Hz, 1H); 7.28 (d, J= 9.0 Hz, 2H); 8.25 (d, J= 9.0 Hz, 2H). <sup>13</sup>C-NMR (75 MHz) (CDCl<sub>3</sub>)  $\delta$  169.5, 156.7, 155.2, 145.3, 135.4, 127.3, 125.2, 123.5, 122.3, 120.7, 107.4, 97.6, 67.7, 59.4, 55.3, 55.2, 51.9, 51.7, 48.5, 32.8, 25.1, 19.3. IR (NaCl, neat) 2936, 1781, 1590, 1523, 1472, 1346, 1261, 1207, 1105, 1012, 914, 864 cm<sup>-1</sup>.



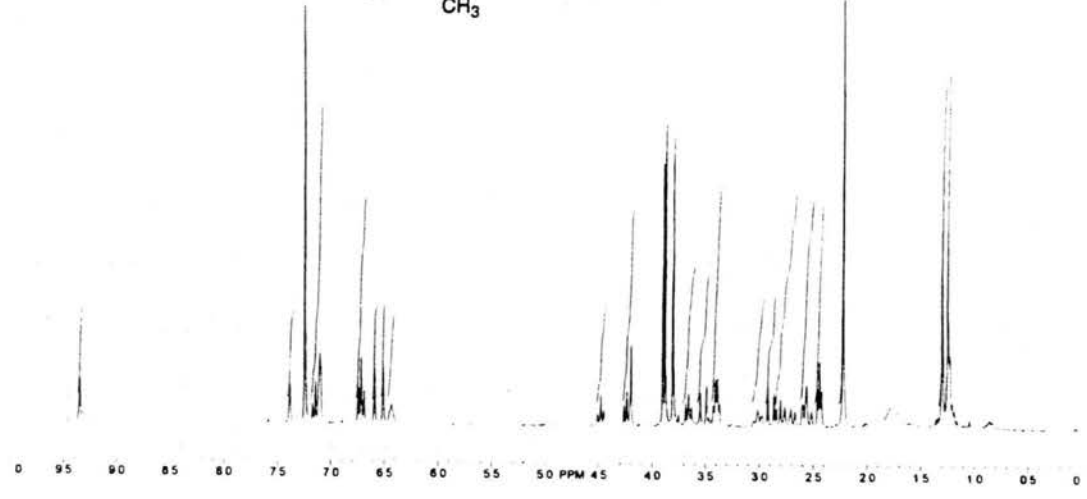
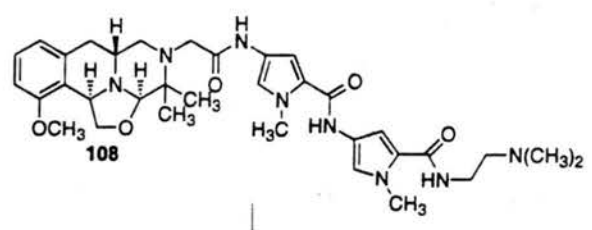


### Netropsin conjugate (**123**)

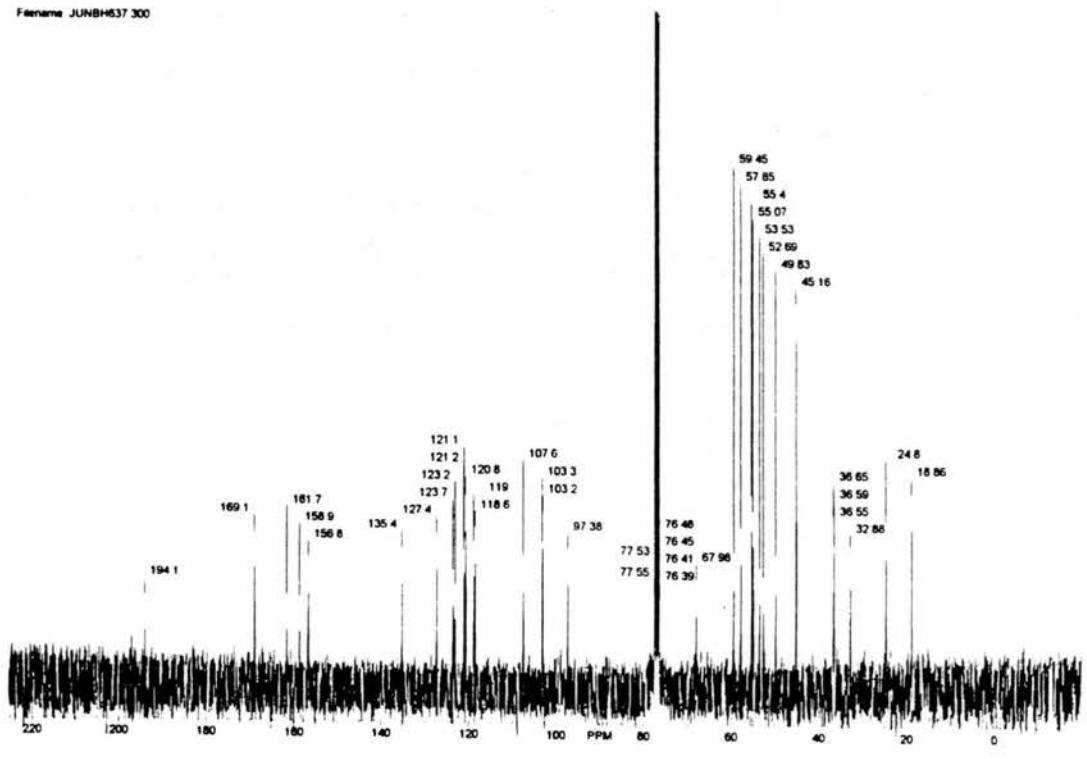
To a stirred solution of **106** (10.2 mg, 0.028 mmol) in 0.5 mL of DMF and degassed with argon was added 5% Pd/C (6 mg, 0.0028 mmol) and the resulting mixture saturated with hydrogen. The mixture was then stirred at RT under 1 atm of hydrogen for 24 h. The reaction mixture was then filtered through celite into a solution of **123** (8.5 mg, 0.029 mmol) dissolved in 0.5 mL of DMF. To the reaction was added NEt<sub>3</sub> (12 μl, 0.087 mmol) and the resulting solution stirred at RT for 7 h. The reaction mixture was then concentrated and the crude product purified by PTLC (3% conc. NH<sub>4</sub>OH in methanol) to give 5.6 mg (31%) of netropsin conjugate **108** as a yellow oil. TLC (3% NH<sub>4</sub>OH in MeOH) R<sub>f</sub> = 0.59 (UV and Dragendorff). <sup>1</sup>H-NMR (300 MHz) (CDCl<sub>3</sub>) δ 1.25 (s, 3H); 1.30 (s, 3H); 2.23 (s, 6H); 2.44 (t, J = 5.7 Hz, 2H); 2.52-2.61 (m, 2H); 2.67-2.72 (m, 1H); 2.81 (t, J = 11.3 Hz, 1H); 2.89 (d, J = 17.4 Hz, 1H); 2.98-3.05 (m, 1H); 3.40 (q, J = 5.7 Hz, 2H); 3.52 (d, J = 17.4 Hz, 1H); 3.66 (dd, J = 7.8, 8.4 Hz, 1H); 3.80 (s, 3H); 3.88 (s, 3H); 3.90 (s, 3H); 4.20 (s, 1H); 4.24 (dd, J = 7.8, 8.4 Hz, 1H); 4.48 (t, J = 8.7 Hz, 1H); 6.43 (m, 1H); 6.51 (d, J = 1.8 Hz, 1H); 6.59 (d, J = 1.8 Hz, 1H); 6.71 (dd, J = 7.8, 8.4 Hz, 2H); 7.09 (d, J = 1.8 Hz, 1H); 7.10 (d, J = 1.8 Hz, 1H); 7.14 (dd, J = 7.8, 8.4 Hz, 1H); 7.38 (br s, 1H); 9.34 (br s, 1H). <sup>13</sup>C-NMR (75 MHz) (CDCl<sub>3</sub>) δ 169.1, 161.7, 158.9, 156.7, 135.3, 127.4, 123.6, 123.1, 121.2, 121.1, 120.7, 118.9, 118.6, 107.6, 103.3, 103.2, 97.4, 77.2, 68.0, 59.4, 57.9, 55.4, 55.0, 53.5, 52.7, 49.8, 45.1, 36.6, 36.5, 32.8, 24.8, 18.8. IR (NaCl, neat) 3293, 2935, 2845, 2775, 1654, 2586, 1541,

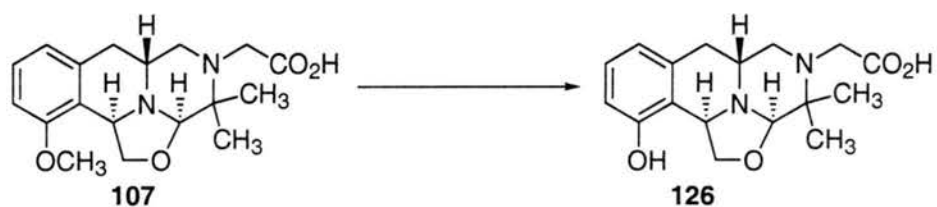
1467, 1437, 1402, 1261, 1203, 1163, 1063  $\text{cm}^{-1}$ . HRMS (FAB) calcd for  $\text{C}_{34}\text{H}_{47}\text{N}_8\text{O}_5$   
(M+H) 647.3669; found 647.3677.

0.14, 0.32, 1.59, 0.485, 0.18344, 0.151, 0.8665, 0.205, 0.1660, 0.335, 0.327, 0.311, 0.438, 2.160, 3.46, 0.166, 0.326, 0.943, 0.509, 0.545



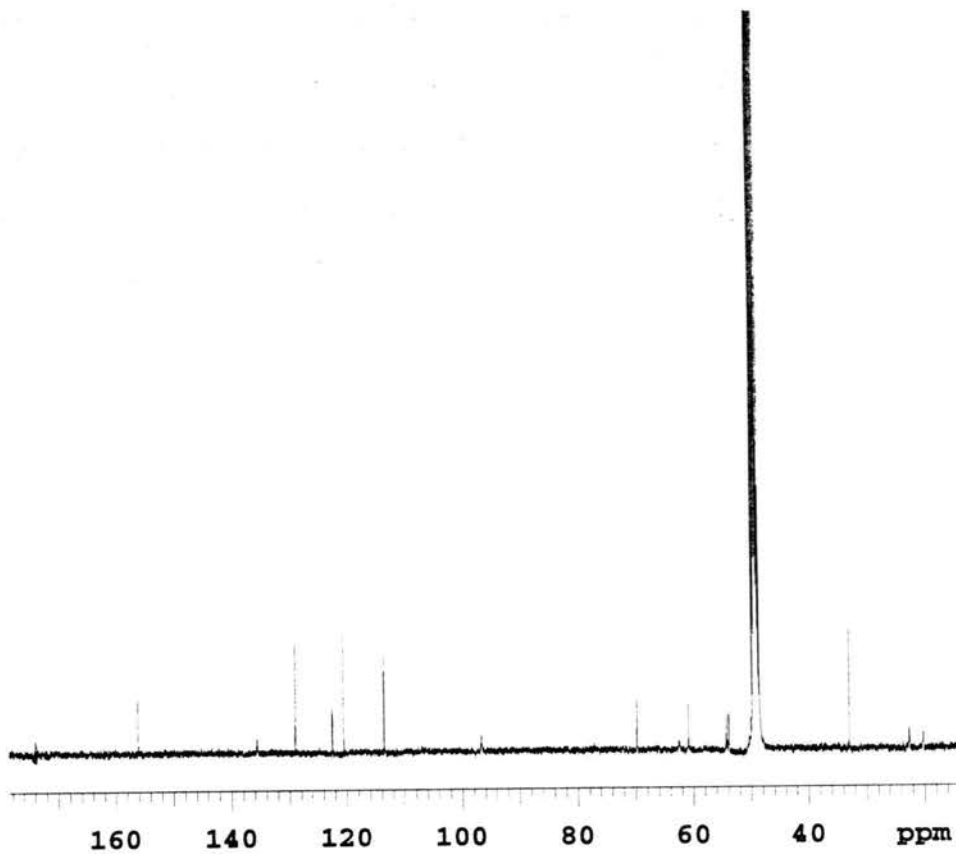
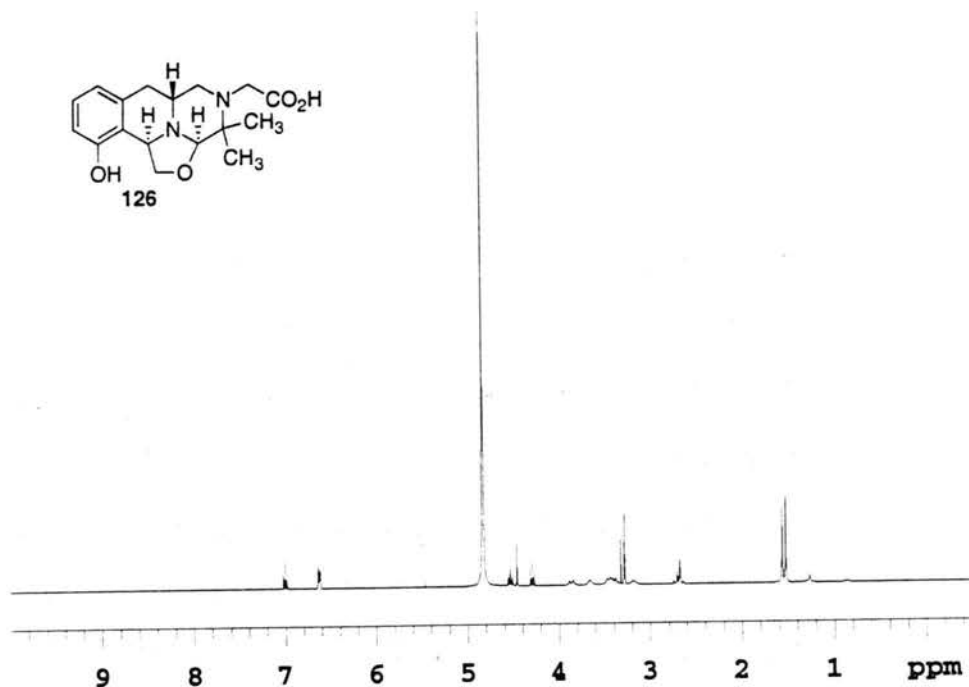
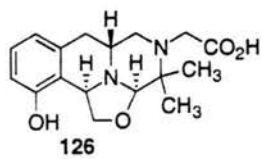
Filename JUNBH537.300

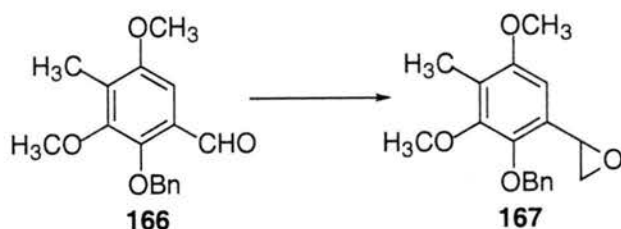




**4 $\alpha$ ,6 $\alpha$ ,11 $\beta$ -2-Aza-2-carboxyacetyl-1,3,4,6,11a-hexahydro-7-hydroxy-5,4-oxazolo-3,3-dimethyl-2H-benzo[*b*]quinolizine (126)**

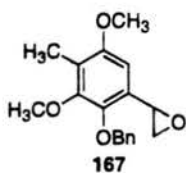
To a solution of **107** (10 mg, 0.030 mmol) in 0.5 mL of CH<sub>2</sub>Cl<sub>2</sub> in a oven-dried three-neck flask fitted with a septum, argon line, and drying tube containing CaCl<sub>2</sub> was added BBr<sub>3</sub> (1.0 M soln., 180  $\mu$ L, 0.18 mmol) at -78  $^{\circ}$ C. The reaction was then allowed to warm up to RT and stir overnight. The reaction was quenched with water and extracted with CH<sub>2</sub>Cl<sub>2</sub>. After concentration the residue was chromatographed (PTLC, 10/1 CH<sub>2</sub>Cl<sub>2</sub>/MeOH) to give 3.3 mg of **107** (33%) and 4.5 mg of phenol analog **126** (47%) as a clear oil. TLC (10/1 CH<sub>2</sub>Cl<sub>2</sub>/MeOH) R<sub>f</sub> = 0.07 (UV and PMA). <sup>1</sup>H-NMR (300 MHz) (MeOH-d<sub>4</sub>)  $\delta$  1.55 (s, 3H); 1.59 (s, 3H); 2.69-2.73 (m, 2H); 3.14-3.24 (m, 1H); 3.35 (s, 1H); 3.40-3.52 (m, 2H); 3.64-3.73 (m, 1H); 3.85-3.94 (m, 1H); 4.32 (t, J= 8.4 Hz, 1H); 4.49 (s, 1H); 4.56 (t, J= 8.4 Hz, 1H); 6.65 (dd, J= 2.7, 7.8 Hz, 2H); 7.03 (t, J= 7.8 Hz, 1H). <sup>13</sup>C-NMR (100 MHz) (MeOH-d<sub>4</sub>)  $\delta$  174.0, 156.1, 135.5, 128.9, 122.5, 120.5, 113.5, 96.6, 69.8, 62.4, 60.9, 54.3, 53.9, 32.9, 22.6, 20.1. IR (NaCl, neat) 3409, 2926, 1640, 1466, 1380, 1277, 1160, 1123 cm<sup>-1</sup>. HRMS (FAB) calcd for C<sub>17</sub>H<sub>23</sub>N<sub>2</sub>O<sub>4</sub> (M+H) 319.1658; found 319.1655.





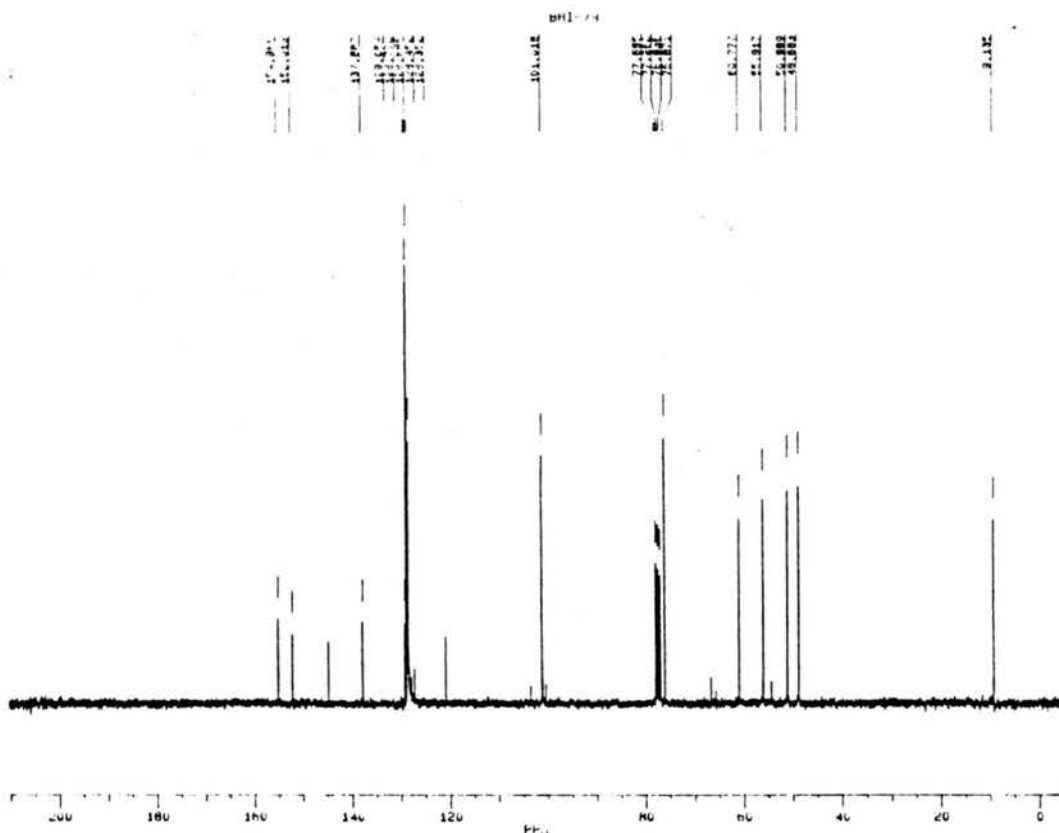
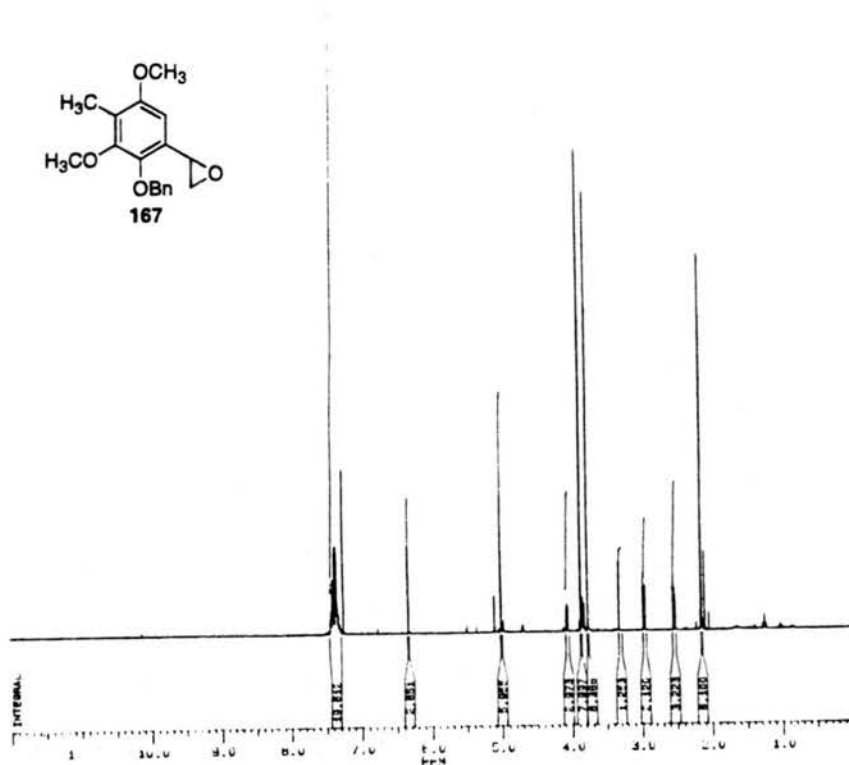
**(2-benzyloxy-3,5-methoxy-4-methylphenyl)oxirane (167)**

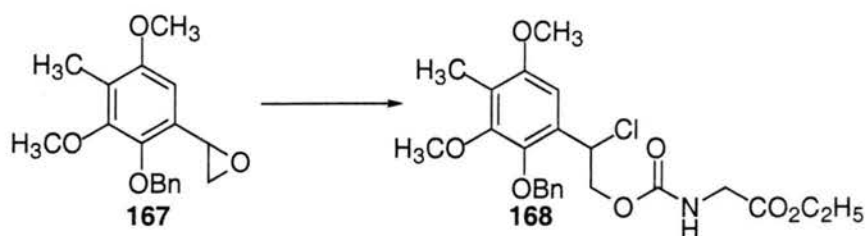
To a solution of aldehyde **166** (7.0 g, 24.5 mmol) in  $\text{CH}_2\text{Cl}_2$  (80 mL) was added trimethylsulfonium iodide (6.0 g, 29.4 mmol), tetrabutylammonium iodide (90 mg, 0.24 mmol) and 50% NaOH (55 mL). The reaction was allowed to stir at RT for 2 days. The reaction was then diluted with  $\text{H}_2\text{O}$ , the layers separated, and the organic phase washed with NaCl (sat.) and dried over  $\text{Na}_2\text{SO}_4$ . The crude reaction was concentrated and Kugelrohr distilled to give 5.55 g (75% yield) of **167** as a slightly yellow oil. TLC (3/1 Hex/ EtOAc)  $R_f = 0.41$  (UV).  $^1\text{H-NMR}$  (300 MHz) ( $\text{CDCl}_3$ )  $\delta$  2.10 (s, 3H); 2.52 (dd,  $J = 5.7, 2.6$  Hz, 1H); 2.95 (dd,  $J = 4.1, 5.7$  Hz, 1H); 3.77 (s, 3H); 3.88 (s, 3H); 4.05 (dd,  $J = 2.6, 4.1$  Hz, 1H); 5.02 (s, 2H); 6.39 (s, 1H); 7.39 (m, 5H).  $^{13}\text{C-NMR}$  (75 MHz) ( $\text{CDCl}_3$ )  $\delta$  154.9, 151.9, 144.6, 137.6, 129.0, 128.7, 128.6, 128.4, 128.3, 120.7, 101.0, 75.8, 60.7, 55.9, 50.9, 48.6, 9.1. HRMS (FAB) calcd for  $\text{C}_{18}\text{H}_{21}\text{O}_4$  (M+H) 301.1440; found 301.1432.



BRUKER

A1000417.01.1  
 DATE 1-8-94  
 SF 300.133  
 CY 210.0  
 C1 477.645  
 S1 32768  
 TL 32768  
 SW 5000.000  
 HZ/PT .300  
 MW 3.0  
 MD 4.0  
 AU 3.277  
 HG 30  
 HD 16  
 TE 297  
 FW 6306  
 GC 4395.480  
 DP 63L PU  
 LB -.150  
 NB .150  
 CX 20.00  
 CY 0.0  
 F1 12.001F  
 F2 .040F  
 HZ/CM 180.084  
 PPM/CM .600  
 SH 3373.64

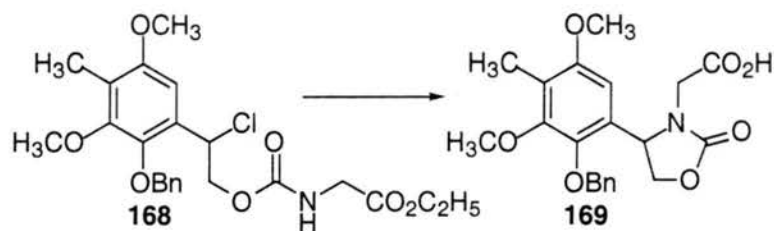




**O-2-Chloro-2-(2'-benzyloxy-3',5'-methoxy-4'-methyl)phenyl-N-ethoxyacetyl carbamate (168)**

To a solution of epoxide **167** (5.55 g, 18.5 mmol) in 25 mL of toluene was added phosgene (20%, 1.93 M in toluene, 100 mL, 193 mmol) at RT and sealed in a flask and stirred at RT for 60 h. The excess phosgene was then removed by bubbling nitrogen into the reaction and through a NaOH scrubber for 2 h. The reaction was then concentrated under reduced pressure producing the chloroformate as an oil. The chloroformate was redissolved in 65 mL of  $\text{CH}_2\text{Cl}_2$  and a solution of  $\text{NaHCO}_3$  (sat., 65 mL) added followed by a solution of glycine ethyl ester hydrochloride (2.58 g, 18.5 mmol) in a small amount of water. The resulting two phase reaction was stirred vigorously at RT for 20 min, at which time the layers were separated and the organic layer washed with water, dried over  $\text{Na}_2\text{SO}_4$  and concentrated to give 7.65 g (84%) of **168** as a yellow oil. TLC (3/1 Hex/ EtOAc)  $R_f = 0.31$  (UV and PMA).  $^1\text{H-NMR}$  (300 MHz) ( $\text{CDCl}_3$ )  $\delta$  1.23 (t,  $J = 7.0$  Hz, 3H); 2.18 (s, 3H); 3.82 (s, 3H); 3.89 (s, 3H); 3.93 (dd,  $J = 2.2, 5.5$  Hz, 2H); 4.19 (q,  $J = 7.0$  Hz, 2H); 4.50 (dd,  $J = 8.4, 11.7$  Hz, 1H); 5.02 (s, 2H); 5.26 (br s, 1H,  $\text{D}_2\text{O}$  exch.); 5.39-5.45 (m, 1H); 5.48 (dd,  $J = 5.5, 8.4$  Hz, 1H); 6.67 (s, 1H); 7.40 (m, 5H).  $^{13}\text{C-NMR}$  (75 MHz) ( $\text{CDCl}_3$ )  $\delta$  170.0, 167.8, 155.8, 154.9, 152.2, 143.3, 137.5, 128.8, 122.5, 104.3, 75.8, 68.2, 67.3, 61.7, 60.7, 59.2, 56.0, 54.4, 43.0, 14.3, 9.2. IR (NaCl, neat) 3361, 2940, 1730, 1460, 1410, 1203, 1131, 1025  $\text{cm}^{-1}$ .

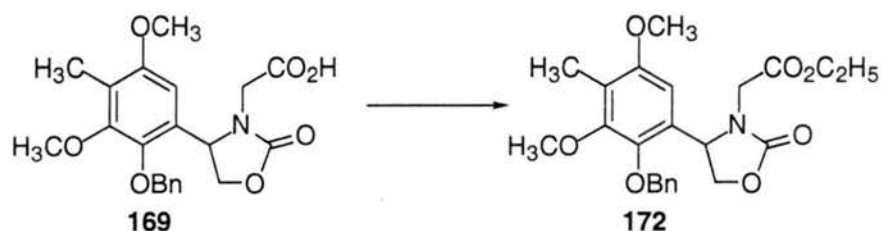




**1-(Carboxy)methyl-5-(2'-benzyloxy-3',5'-methoxy-4'-methyl)phenyloxazolidin-2-one (169).**

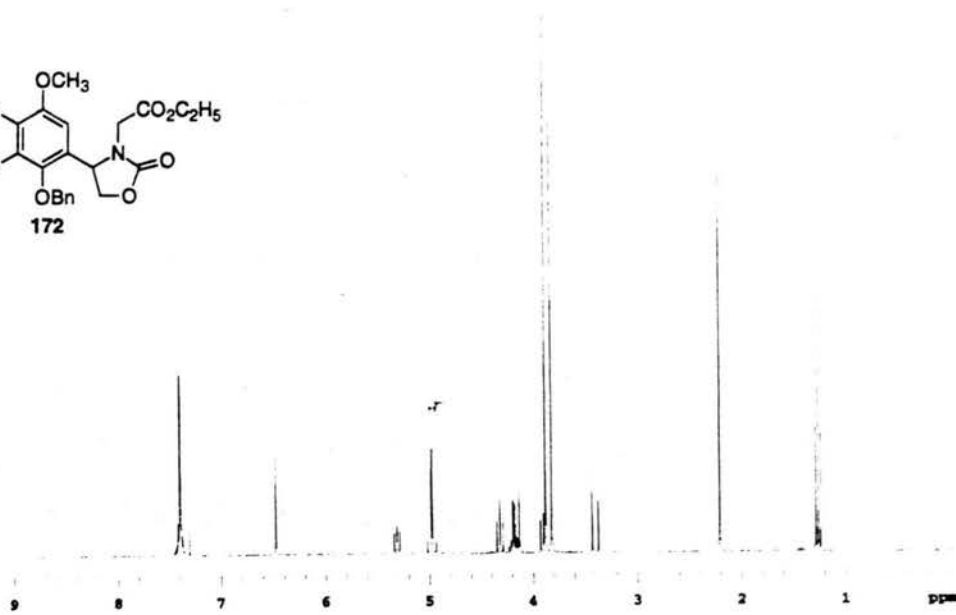
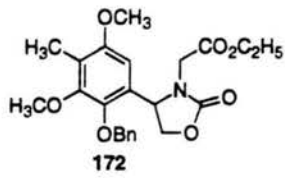
To a solution of **168** (7.65 g, 16.4 mmol) in THF (50 mL) cooled to 0 °C, was added slowly a solution of KO<sup>t</sup>-Bu (2.21 g, 18.1 mmol) in THF (25 mL) with stirring. After 30 min the reaction mixture was diluted with water, slightly acidified with dilute HCl and extracted with CH<sub>2</sub>Cl<sub>2</sub>. The organic extract was dried over NaSO<sub>4</sub>, filtered and concentrated to give 6.92 g of an orange oil. The oil was redissolved in 50 mL of EtOH and LiOH·H<sub>2</sub>O (897 mg, 21.4 mmol) was added in 25 mL of H<sub>2</sub>O at 0 °C. The reaction stirred for 30 min and then the volume reduced by half by reduced pressure. The reaction was diluted with water and acidified with HCl (1 M) and extracted with EtOAc. The organic layer was dried over NaSO<sub>4</sub>, filtered and concentrated to give 6.15 g (93 %) of carboxylic acid **169**. The crude product was purified by recrystallization from EtOAc-Hex to yield 3.17 g (45%) of **169** as a white solid. m.p.= 154-156 °C (EtOAc-Hex). <sup>1</sup>H-NMR (300 MHz) (CDCl<sub>3</sub>) δ 2.15 (s, 3H); 3.36 (d, J= 18.0 Hz, 1H); 3.75 (s, 3H); 3.81 (dd, J= 8.0, 9.0 Hz, 1H); 3.82 (s, 3H); 4.07 (d, J= 18.0 Hz, 1H); 4.18 (t, J= 9.0 Hz, 1H); 4.93 (1/2 ABq, J= 11.0 Hz, 1H); 5.00 (1/2 ABq, J= 11.0 Hz, 1H); 5.14 (dd, J= 9.0, 8.0 Hz, 1H); 6.39 (s, 1H); 7.30 (m, 5H); 8.33 (br s, 1H). <sup>13</sup>C-NMR (75 MHz) (CDCl<sub>3</sub>) δ 173.0, 159.2, 155.4, 152.4, 143.8, 136.8, 129.2, 128.9, 128.8, 127.7, 122.5, 102.4, 75.5, 69.9, 60.7, 56.1, 54.3, 43.5, 9.2. IR (NaCl, neat) 3361, 2940, 1730, 1460, 1410, 1203, 1131, 1025 cm<sup>-1</sup>.



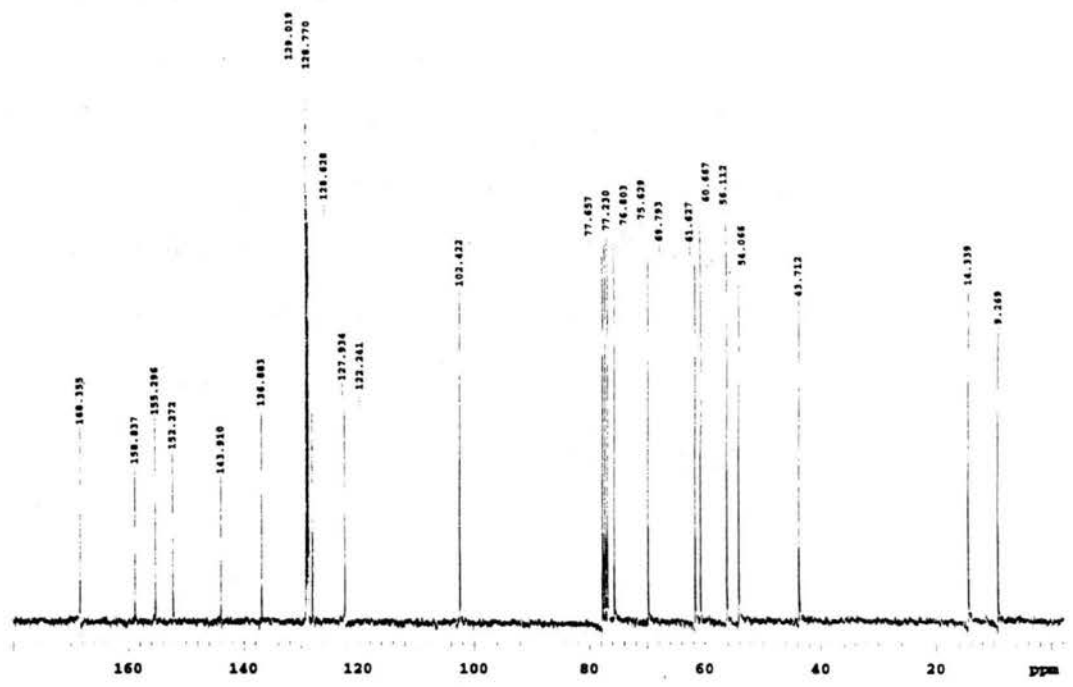


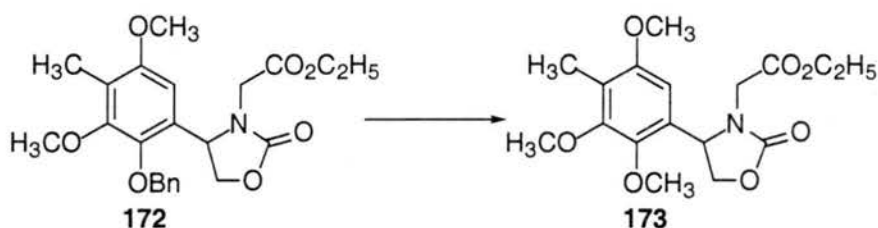
**1-(Carboethoxy)methyl-5-(2'-benzyloxy-3',5'-methoxy-4'-methyl)phenyloxazolidin-2-one (172).**

Oxalyl chloride (57  $\mu$ L, 0.87 mmol) and a drop of DMF were added to a solution of **169** (200 mg, 0.49 mmol) in 5 mL of  $\text{CH}_2\text{Cl}_2$ . After 15 min the reaction was quenched with the addition of EtOH (5 mL). Evaporation of the solvent afforded 219 mg (100%) of **172** as a clear oil. TLC (3/1 Hex/ EtOAc)  $R_f = 0.91$  (UV and PMA).  $^1\text{H-NMR}$  (300 MHz) ( $\text{CDCl}_3$ )  $\delta$  1.26 (t,  $J = 7.2$  Hz, 3H); 2.21 (s, 3H); 3.40 (d,  $J = 17.9$  Hz, 1H); 3.83 (s, 3H); 3.89 (s, 3H); 3.90 (dd,  $J = 7.3, 8.4$  Hz, 1H); 4.14-4.23 (m, 3H); 4.33 (t,  $J = 8.4$  Hz, 1H); 4.96 (d,  $J = 11.0$  Hz, 1H); 5.00 (d,  $J = 11.0$  Hz, 1H); 5.32 (dd,  $J = 7.3, 8.4$  Hz, 1H); 6.48 (s, 1H); 7.40-7.42 (m, 5H).  $^{13}\text{C-NMR}$  (75 MHz) ( $\text{CDCl}_3$ )  $\delta$  168.5, 159.01, 155.5, 152.5, 144.1, 137.1, 129.2, 128.9, 128.8, 128.1, 122.4, 102.6, 75.7, 69.9, 61.7, 60.7, 56.2, 54.1, 43.8, 14.3. IR (NaCl, neat) 2934, 1766, 1462, 1414, 1207, 1130, 1084, 1026  $\text{cm}^{-1}$ .



13C OBSERVE

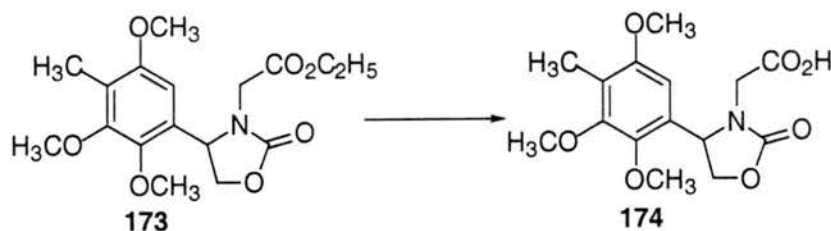




**1-(Carboethoxy)methyl-5-(2',3',5'-methoxy-4'-methyl)phenyl  
oxazolidin-2-one (173).**

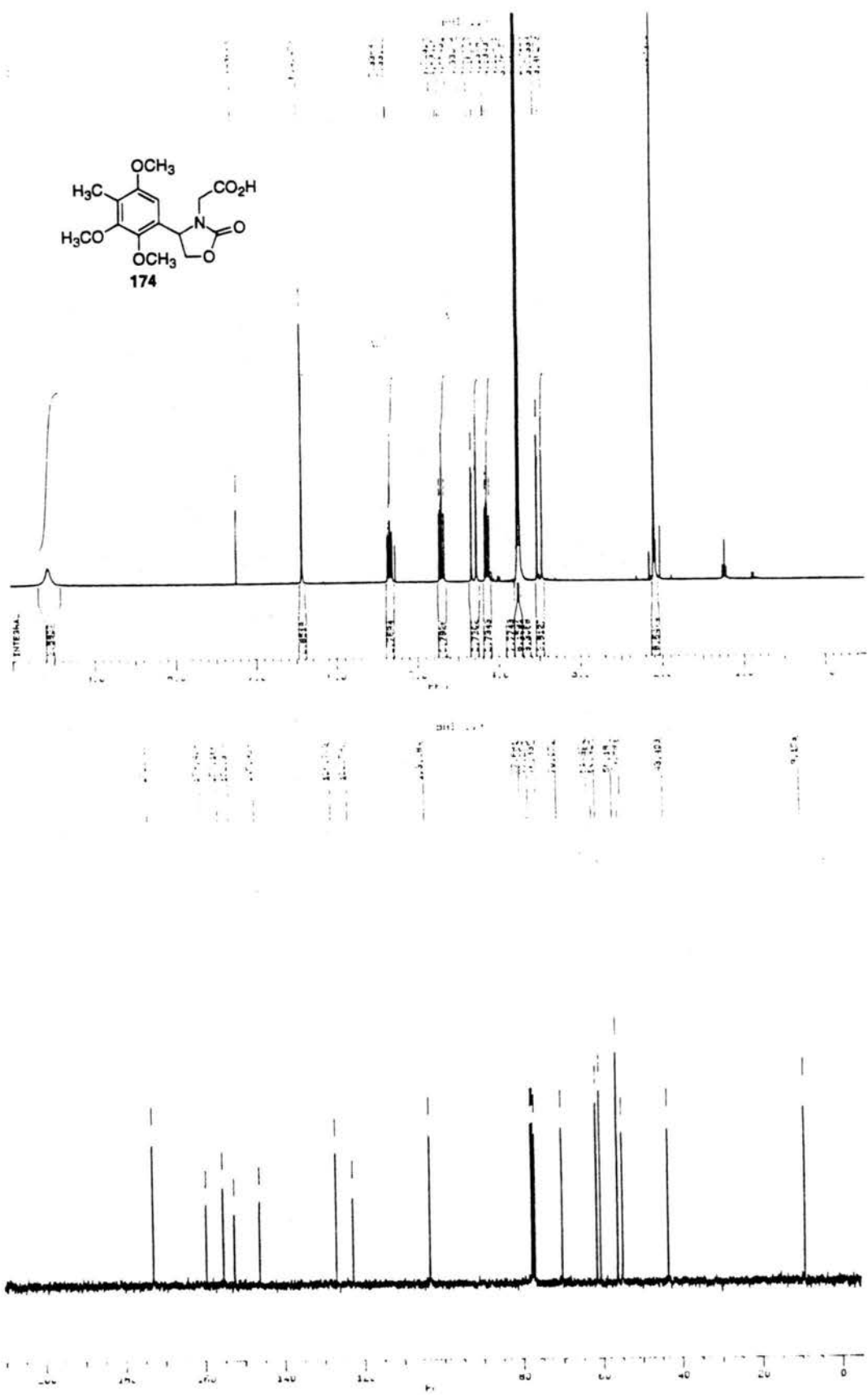
A solution of **172** (219 mg, 0.51 mmol) in 8 mL of MeOH was purged with argon for 10 min and sealed. Next Pd/C (5%, 46 mg) was added and a small balloon of H<sub>2</sub> was introduced into the solution through a pipette. The flask was sealed with a septum and a balloon of H<sub>2</sub> was fitted on top via a syringe. The reaction stirred overnight at RT after which argon was bubbled through the solution for 5 min. The methanol was stripped off and EtOAc was used to wash the residue through a short plug of celite to yield the phenol (166 mg, 100%) as a clear oil. The resulting phenol (53.7 mg, 0.16 mmol) was put into solution with 3 mL of acetone. K<sub>2</sub>CO<sub>3</sub> (109.5 mg, 0.16 mmol) and iodomethane (100  $\mu$ L, 1.60 mmol) were added and the reaction was refluxed. After 3 h the reaction was allowed to cool to RT and then filtered through a glass frit to give 187 mg (100%) of **173** as a clear oil. TLC (3/1 EtOAc/Hex) R<sub>f</sub> = 0.51 (UV and PMA). <sup>1</sup>H-NMR (300 MHz) (CDCl<sub>3</sub>)  $\delta$  1.30 (t, J= 7.2 Hz, 3H); 2.16 (s, 3H); 3.49 (d, J= 18.0 Hz, 1H); 3.80 (s, 3H); 3.82 (s, 3H); 3.84 (s, 3H); 4.17 (dd, J= 7.5, 8.7 Hz, 1H); 4.20-4.25 (m, 2H); 4.34 (d, J= 18.0 Hz, 1H); 4.76 (t, J= 8.7 Hz, 1H); 5.43 (dd, J= 7.5, 8.7 Hz, 1H); 6.48 (s, 1H). <sup>13</sup>C-NMR (75 MHz) (CDCl<sub>3</sub>)  $\delta$  168.5, 158.8, 155.0, 152.3, 145.9, 127.1, 122.2, 103.0, 69.7, 61.5, 61.2, 60.3, 56.1, 54.4, 43.6, 14.2, 9.0. IR (NaCl, neat) 2929, 1765, 1464, 1411, 1205, 1138, 1088, 1030 cm<sup>-1</sup>.

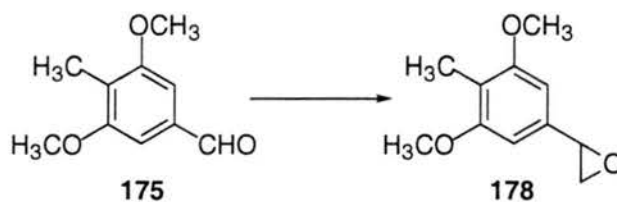




**1-(Carboxy)methyl-5-(2',3',5'-methoxy-4'-methyl)phenyl  
oxazolidin-2-one (174).**

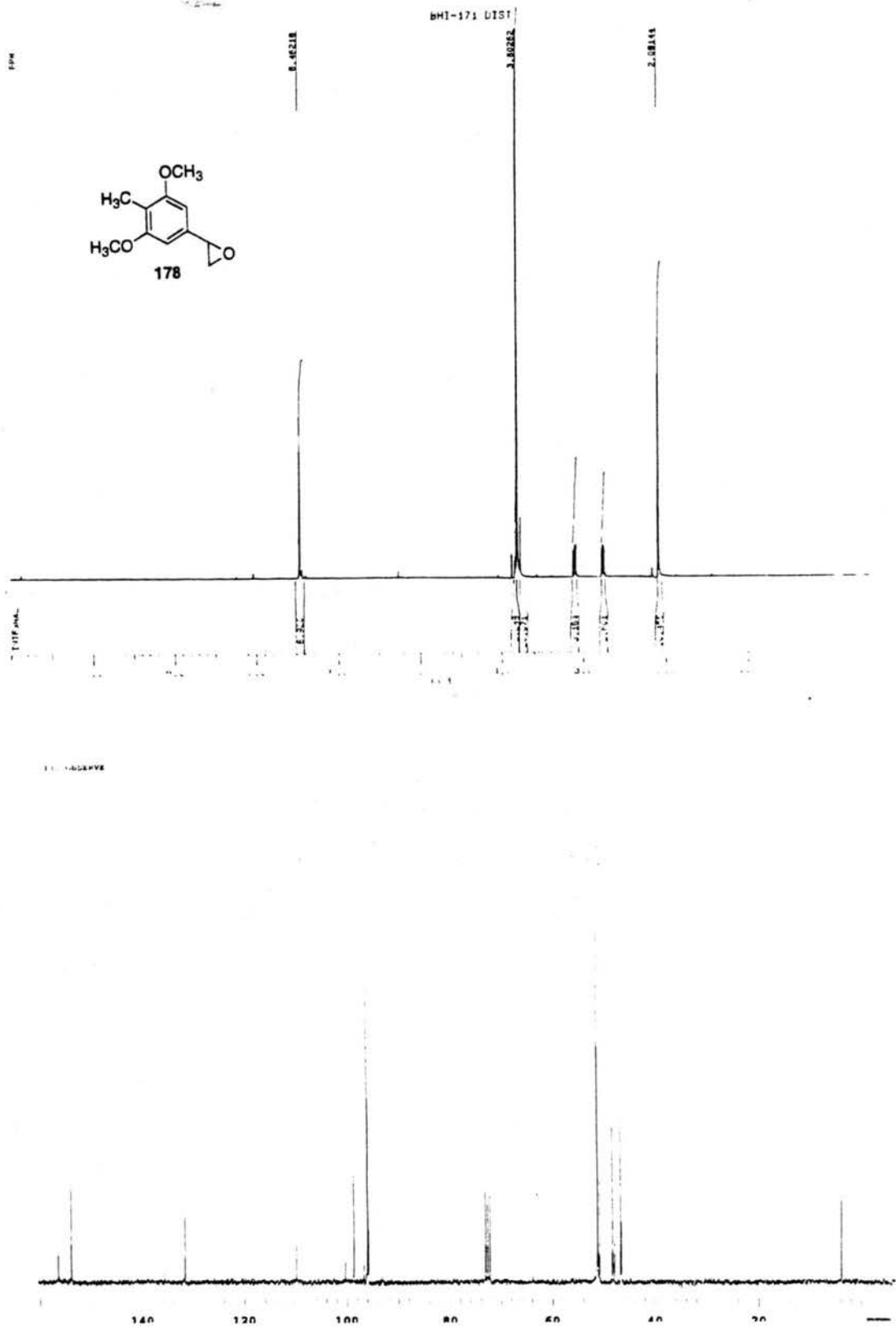
To a solution of **173** (103 mg, 0.29 mmol) in 2 mL of EtOH was added LiOH·H<sub>2</sub>O (16 mg, 0.38 mmol) in water (1 mL) at 0 °C. After 30 min the reaction mixture was concentrated under pressure to half of its volume, diluted with H<sub>2</sub>O, acidified and extracted with ethyl acetate. The extract was dried over MgSO<sub>4</sub>, filtered and concentrated to give 94 mg (87%) of **174** as a yellow solid. m.p.= 134-136 °C (recryst. EtOAc). <sup>1</sup>H-NMR (300 MHz) (CDCl<sub>3</sub>) δ 2.10 (s, 3H); 3.49 (d, J= 18.3 Hz, 1H); 3.74 (s, 3H); 3.760 (s, 3H); 3.767 (s, 3H); 4.14 (dd, J= 7.5, 9.0 Hz, 1H); 4.31 (d, J= 18.3 Hz, 1H); 4.70 (t, J= 9.0 Hz, 1H); 5.33 (dd, J= 7.5, 9.0 Hz, 1H); 6.42 (s, 1H); 9.60 (br s, 1H, D<sub>2</sub>O exch.). <sup>13</sup>C-NMR (75 MHz) (CDCl<sub>3</sub>) δ 172.7, 159.4, 155.2, 152.4, 145.9, 126.8, 122.6, 103.3, 701.1, 61.4, 56.2, 54.9, 43.4, 9.2. IR (NaCl, neat) 3257, 2935, 1746, 1463, 1409, 1227, 1190, 1130 cm<sup>-1</sup>.

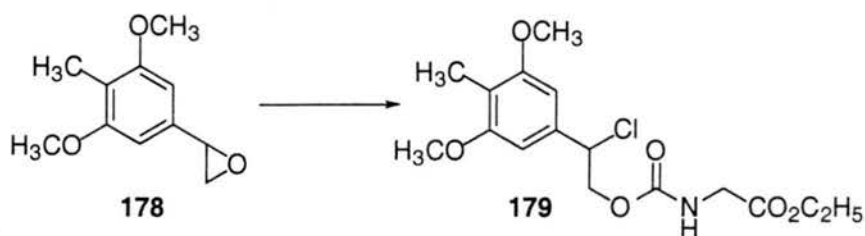




**(3,5-Methoxy-4-methyl)oxirane (178).**

To a solution of aldehyde **175** (6.8 g, 37.9 mmol) in  $\text{CH}_2\text{Cl}_2$  (115 mL) was added trimethylsulfonium iodide (9.3 g, 45.5 mmol), tetrabutylammonium iodide (140 mg, 0.38 mmol) and 50% NaOH (75 mL). The reaction was allowed to stir at RT for 2 days. The reaction was then diluted with  $\text{H}_2\text{O}$ , the layers separated, and the organic phase washed with NaCl (sat.) and dried over  $\text{Na}_2\text{SO}_4$ . The crude reaction was concentrated and Kugelrohr distilled to give 6.33 g (86% yield) of **178** as a yellow oil. TLC (3/1 Hex/EtOAc)  $R_f = 0.40$  (UV and PMA).  $^1\text{H-NMR}$  (300 MHz) ( $\text{CDCl}_3$ )  $\delta$  2.08 (s, 3H); 2.76 (dd,  $J = 2.6, 5.6$  Hz, 1H); 3.10 (dd,  $J = 4.1, 5.6$  Hz, 1H); 3.80 (s, 6H); 3.83 (dd,  $J = 2.6, 4.1$  Hz, 1H); 6.46 (s, 2H).  $^{13}\text{C-NMR}$  (75 MHz) ( $\text{CDCl}_3$ )  $\delta$  158.5, 136.2, 103.3, 100.6, 55.9, 53.0, 51.4, 8.40. IR (NaCl, neat) 2940, 1594, 1461, 1470, 1384, 1236, 1142, 832  $\text{cm}^{-1}$ . HRMS (FAB) calcd for  $\text{C}_{11}\text{H}_{15}\text{O}_3$  (M+H) 195.1021; found 195.1016.

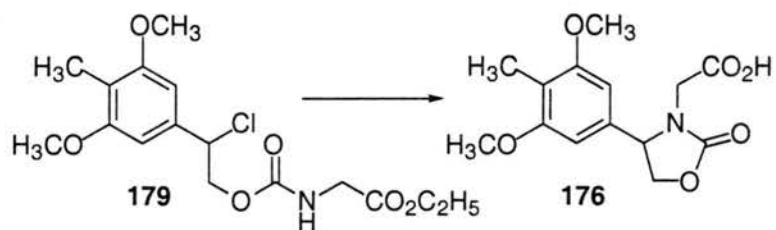




**O-2-Chloro-2-(3',5'-methoxy-4'-methyl)phenyl-N-ethoxyacetyl carbamate (179).**

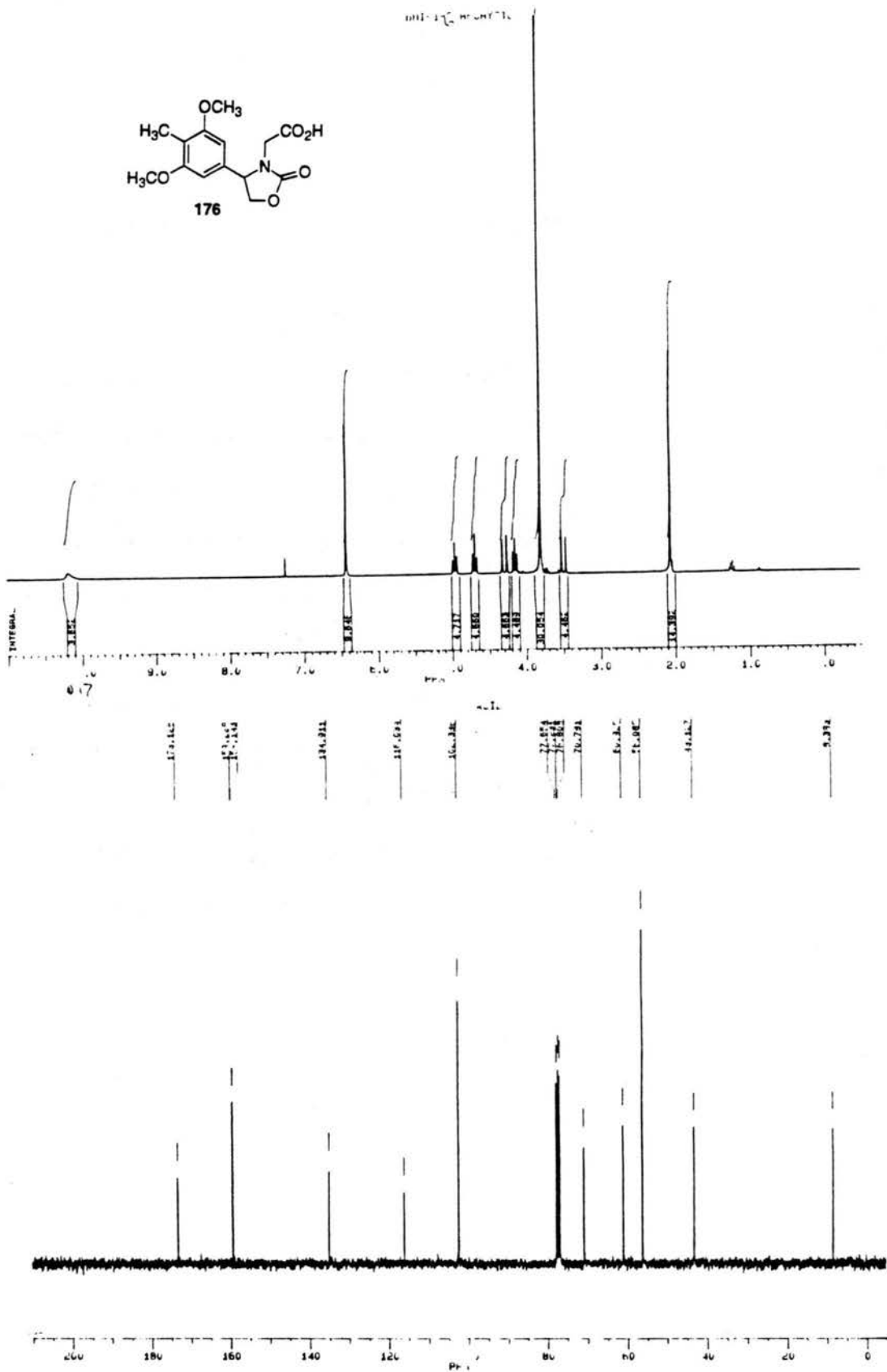
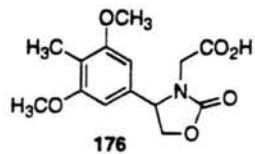
To a solution of epoxide **178** (8.31 g, 42.8 mmol) in 100 mL of toluene was added phosgene (20%, 1.93 M in toluene, 100 mL, 193 mmol) at RT and sealed in a flask and stirred at RT for 1 week. The excess phosgene was then removed by bubbling nitrogen into the reaction and through a NaOH scrubber for 2 h. The reaction was then concentrated under reduced pressure producing the chloroformate as an oil. The material was redissolved in 150 mL of  $\text{CH}_2\text{Cl}_2$  and a solution of  $\text{NaHCO}_3$  (sat., 150 mL) was added followed by a solution of glycine ethyl ester hydrochloride (5.97 g, 42.8 mmol) in a small amount of water. The resulting two phase reaction was stirred vigorously at RT for 20 min, at which time the layers were separated and the organic layer washed with water, dried over  $\text{Na}_2\text{SO}_4$  and concentrated to give 13.91 g (90%) of **179** as a yellow oil. TLC (3/1 Hex/EtOAc)  $R_f = 0.19$  (UV and PMA).  $^1\text{H-NMR}$  (300 MHz) ( $\text{CDCl}_3$ )  $\delta$  1.26 (t,  $J = 7.2$  Hz, 3H); 2.05 (s, 3H); 3.81 (s, 6H); 3.92 (d,  $J = 5.4$  Hz, 2H); 4.20 (q,  $J = 7.2$  Hz, 2H); 4.43 (d,  $J = 5.4$  Hz, 1H); 4.45 (d,  $J = 7.2$  Hz, 1H); 5.02 (t,  $J = 7.2$  Hz, 1H); 5.33 (br t,  $J = 5.4$  Hz, 1H  $\text{D}_2\text{O}$  exch.); 6.55 (s, 2H).  $^{13}\text{C-NMR}$  (75 MHz) ( $\text{CDCl}_3$ )  $\delta$  169.8, 158.4, 155.8, 135.9, 115.4, 102.8, 68.8, 61.7, 60.9, 55.9, 42.9, 14.3, 8.4. IR (NaCl, neat) 3357, 2943, 1729, 1592, 1529, 1461, 1419, 1204, 1141, 1055, 1026  $\text{cm}^{-1}$ .

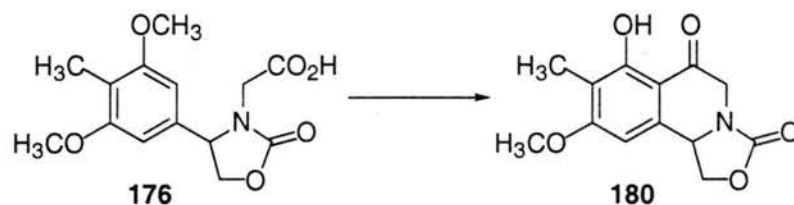




**1-(Carboxy)methyl-5-(3',5'-methoxy-4'-methyl)phenyloxazolidin-2-one (176).**

To a solution of **179** (49.35 g, 137.2 mmol) in THF (350 mL) cooled to 0 °C, a solution of KO<sup>t</sup>-Bu (16.9 g, 150.9 mmol) in THF (100 mL) was added slowly with stirring. After 30 min the reaction mixture was diluted with water, slightly acidified with dilute HCl and extracted with CH<sub>2</sub>Cl<sub>2</sub>. The organic extract was dried over NaSO<sub>4</sub>, filtered and concentrated to give 40.56 g of an oil. The oil was redissolved in 400 mL of EtOH and LiOH·H<sub>2</sub>O (7.48 mg, 178.3 mmol) was added in 100 mL of H<sub>2</sub>O at 0 °C. The reaction stirred for 30 min and then the volume reduced by half by reduced pressure. The reaction was diluted with water and acidified with HCl (1 M) and extracted with EtOAc. The organic layer was dried over NaSO<sub>4</sub>, filtered and concentrated to give 38.0 g (94%) of carboxylic acid **176**. The crude product was purified by recrystallization from EtOAc-Hex to give 19.65 g (49%) of **176** as white plates. m.p.= 181-184 °C (recrys. EtOAc-Hex) <sup>1</sup>H-NMR (300 MHz) (CDCl<sub>3</sub>) δ 2.05 (s, 3H); 3.49 (1/2 ABq, J= 18.3 Hz, 1H); 3.80 (s, 6H); 4.14 (t, J= 8.6 Hz, 1H); 4.29 (1/2 ABq, J= 18.3 Hz, 1H); 4.69 (t, J= 8.6 Hz, 1H); 4.96 (t, J= 8.6 Hz, 1H); 6.42 (s, 2H); 10.17 (br s, 1 H, D<sub>2</sub>O exch.). <sup>13</sup>C-NMR (75 MHz) (CDCl<sub>3</sub>) δ 173.1, 159.2, 159.1, 134.9, 116.0, 102.3, 70.8, 60.9, 56.1, 43.1, 8.4. HRMS (FAB) calcd for C<sub>14</sub>H<sub>17</sub>NO<sub>6</sub> (M+) 295.1056; found 295.1053.

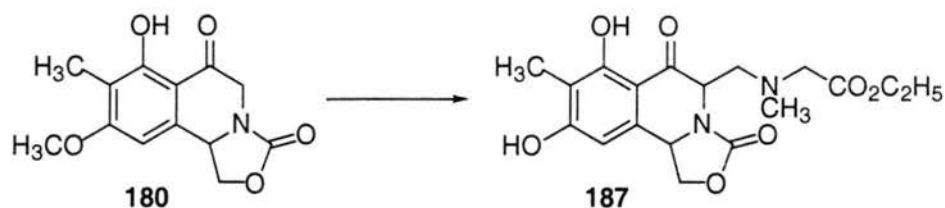




**2,2'-carbonyl-4-keto-9,11-methoxy-10-methyltetrahydroisoquinoline (180).**

To a solution of **176** (100 mg, 0.34 mmol) and 1 drop of DMF in 2 mL of  $\text{CH}_2\text{Cl}_2$  was added oxalyl chloride (39  $\mu\text{L}$ , 0.59 mmol) at RT. The reaction stirred for 1 h and was then concentrated. The yellow residue was dissolved in 2 mL of  $\text{CH}_2\text{Cl}_2$  and  $\text{AlCl}_3$  (181 mg, 1.36 mmol) was added at RT. The reaction stirred for 7 h and was then quenched by  $\text{H}_2\text{O}$ . The crude product was purified by chromatography (3/1 EtOAc/Hex) to yield 82 mg (92%) of **180** as a yellow foam. TLC (3/1 Hex/EtOAc)  $R_f = 0.22$  (UV and PMA).  $^1\text{H-NMR}$  (300 MHz) ( $\text{CDCl}_3$ )  $\delta$  2.03 (s, 3H); 3.89 (s, 3H); 3.95 (1/2 ABq,  $J = 18.6$  Hz, 1H); 4.45 (dd,  $J = 5.7, 8.5$  Hz, 1H); 4.63 (1/2 ABq,  $J = 18.6$  Hz, 1H); 4.85 (t,  $J = 8.5$  Hz, 1H); 5.08 (dd,  $J = 5.7, 8.5$  Hz, 1H); 6.12 (s, 1H); 12.33 (s, 1H,  $\text{D}_2\text{O}$  exch.)  $^{13}\text{C-NMR}$  (75 MHz) ( $\text{CDCl}_3$ )  $\delta$  195.2, 164.7, 162.7, 156.8, 140.6, 113.7, 109.2, 97.9, 68.6, 56.2, 53.3, 48.6, 7.5. IR (NaCl, neat) 2926, 1756, 1626, 1420, 1793, 1227, 1121  $\text{cm}^{-1}$ . HRMS (FAB) calcd for  $\text{C}_{13}\text{H}_{14}\text{NO}_5$  ( $\text{M}+\text{H}$ ) 264.0872; found 264.0880.

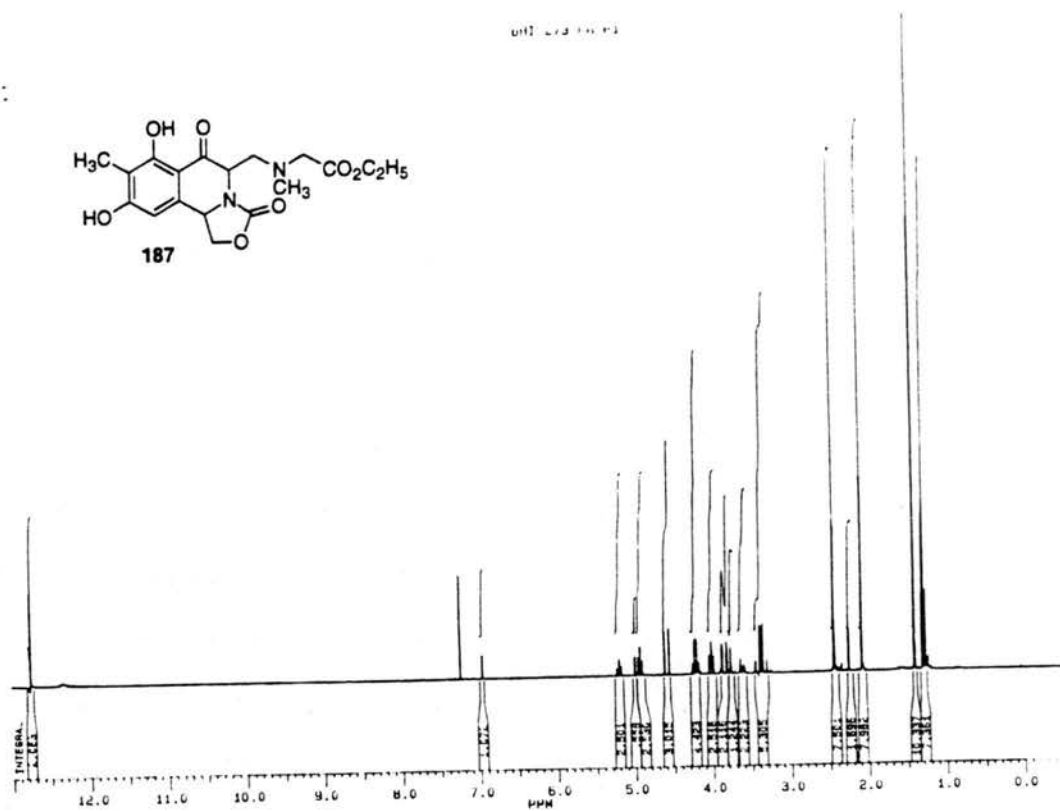
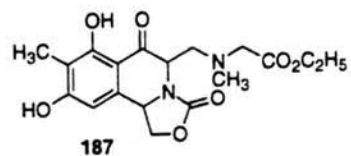


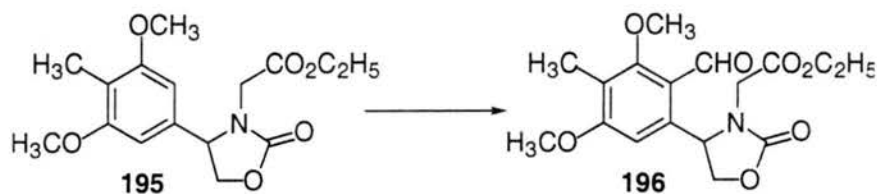


**2,2'-carbonyl-3-(*N*-methyl-*N*-2-carboethoxy)aminomethyl-4-keto-9,11-methoxy-10-methyltetrahydroisoquinoline (187).**

Chloromethyl methyl ether (40  $\mu$ L, 0.53 mmol) and  $\text{NEt}_3$  (135  $\mu$ L, 0.97 mmol) were added to sarcosine ethyl ester·HCl (68 mg, 0.44 mmol) in 2 mL of  $\text{CH}_2\text{Cl}_2$  at RT, forming a white precipitate ( $\text{NH}_4\text{Cl}$ ). After 1 h, *p*-TsOH (21 mg, 0.11 mmol) was added, followed by **180** (30 mg, 0.11 mmol). The reaction stirred for 3 days at RT and was then concentrated. The crude product was purified by column chromatography (3/1 EtOAc/Hex) to yield 17 mg (40%) of **187** as a yellow oil. TLC (3/1 Hex/EtOAc)  $R_f = 0.34$  (UV and PMA).  $^1\text{H-NMR}$  (300 MHz) ( $\text{CDCl}_3$ )  $\delta$  1.28 (t,  $J = 7.2$  Hz, 3H); 2.10 (s, 3H); 2.49 (s, 3H); 3.32 (d,  $J = 17.0$  Hz, 1H); 3.41 (d,  $J = 17.0$  Hz, 1H); 3.59-3.63 (m, 1H); 3.84 (d,  $J = 17.8$  Hz, 1H); 3.85 (d,  $J = 17.8$  Hz, 1H); 4.01 (t,  $J = 8.1$  Hz, 1H); 4.21 (dq,  $J = 1.5, 7.2$  Hz, 2H); 4.58 (d,  $J = 17.8$  Hz, 1H); 4.92 (t,  $J = 8.5$  Hz, 1H); 5.20 (t,  $J = 8.2$  Hz, 1H); 6.98 (s, 1H); 12.77 (s, 1H,  $\text{D}_2\text{O}$  exch.).

011-23-10-13





**1-(Carboethoxy)methyl-5-(2'-formyl-3',5'-methoxy-4'-methyl)phenyloxazolidin-2-one (196).**

To a solution of ethyl ester **195** (100 mg, 0.34 mmol) and  $\text{Cl}_2\text{CHOCH}_3$  (82  $\mu\text{L}$ , 1.02 mmol) in 5 mL of  $\text{CH}_2\text{Cl}_2$  at 0 °C was added  $\text{TiCl}_4$  (149  $\mu\text{L}$ , 1.35 mmol). After 45 min the reaction was poured over ice. The layers were separated and the aqueous layer extracted with  $\text{CH}_2\text{Cl}_2$ . The combined organic extracts were dried over  $\text{MgSO}_4$  and concentrated to give 101 mg (85%) of a white foam which turned black upon standing. The crude product was purified by pushing it through a short plug of silica gel with EtOAc to give 91 mg (76%) of **196** as a white foam. The excess titanium could also be removed by filtering the crude product through a plug of florisil. TLC (3/1 EtOAc/Hex)  $R_f = 0.47$  (UV and PMA).  $^1\text{H-NMR}$  (300 MHz) ( $\text{CDCl}_3$ )  $\delta$  1.21 (t,  $J = 7.2$  Hz, 3H); 2.11 (s, 3H); 3.54 (1/2 ABq,  $J = 17.7$  Hz, 1H); 3.79 (s, 3H); 3.87 (s, 3H); 3.85-3.95 (m, 1H); 4.10-4.18 (m, 2H); 4.28 (1/2 ABq,  $J = 17.7$  Hz, 1H); 4.95 (t,  $J = 9.0$  Hz, 1H); 5.64 (dd,  $J = 5.7, 9.3$  Hz, 1H); 6.73 (s, 1H); 10.26 (s, 1H).  $^{13}\text{C-NMR}$  (75 MHz) ( $\text{CDCl}_3$ )  $\delta$  8.7, 14.2, 44.6, 56.3, 57.1, 61.8, 63.4, 70.4, 103.4, 120.3, 120.5, 140.5, 159.5, 164.1, 165.0, 168.2, 191.0. IR (NaCl, neat) 2944, 1764, 1674, 1596, 1568, 1423, 1379, 1295, 1128, 1211, 1026  $\text{cm}^{-1}$ .

0.410

0.437

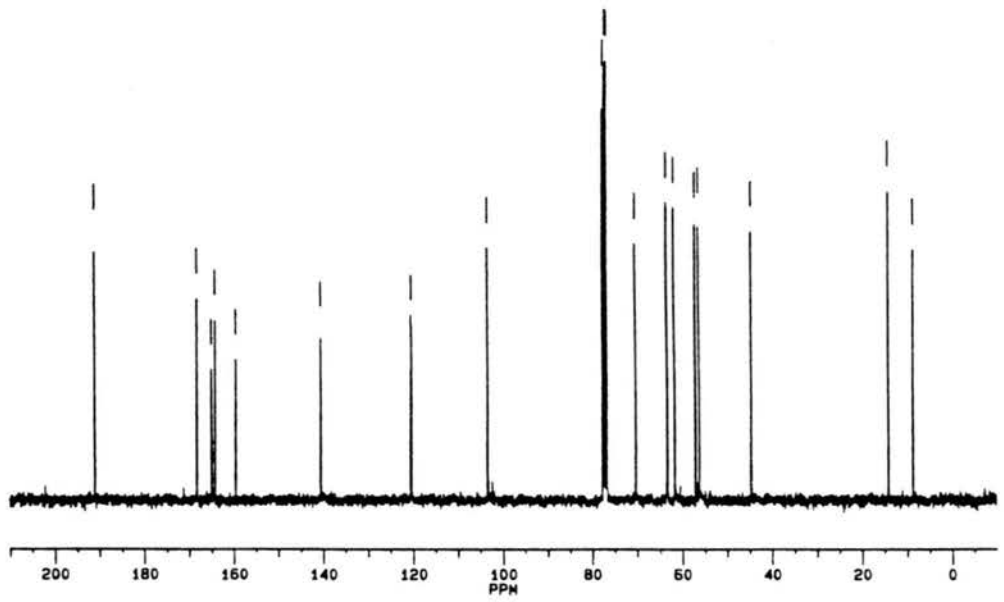
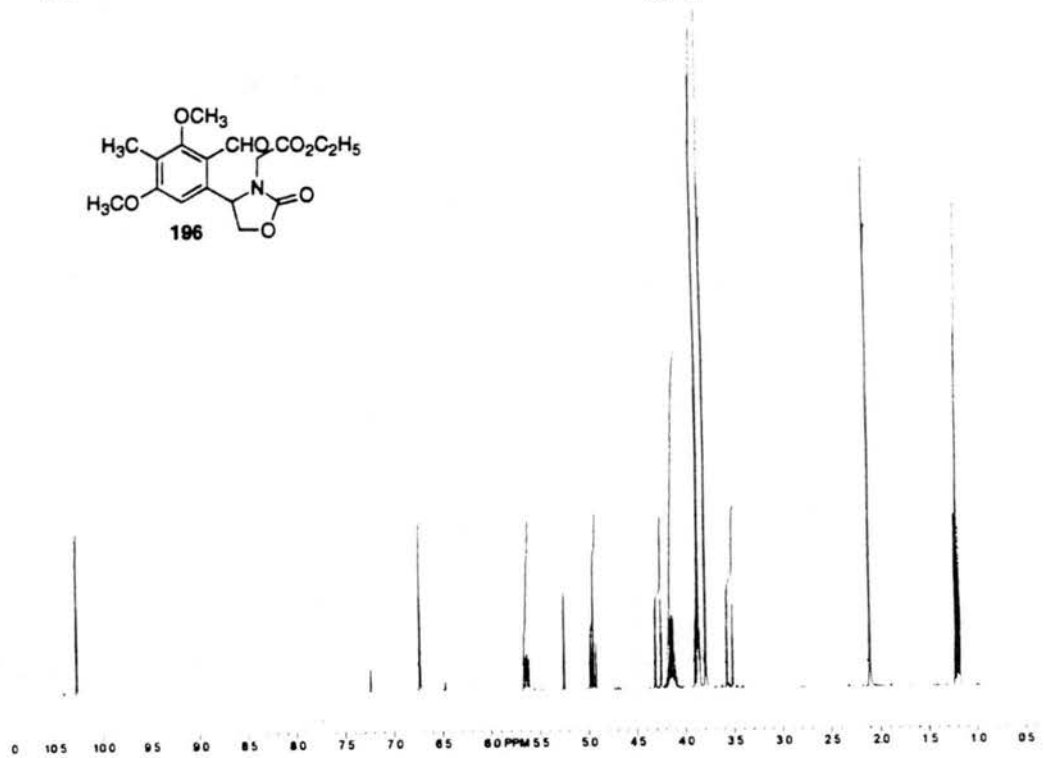
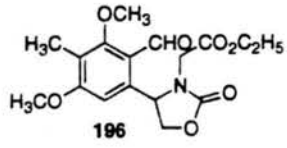
0.436

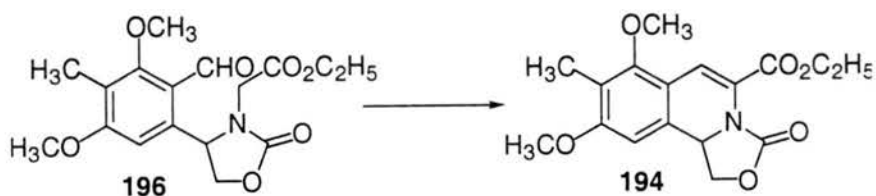
0.453

0.451 1.92 0.471  
0.936 1.37

1.33

1.42

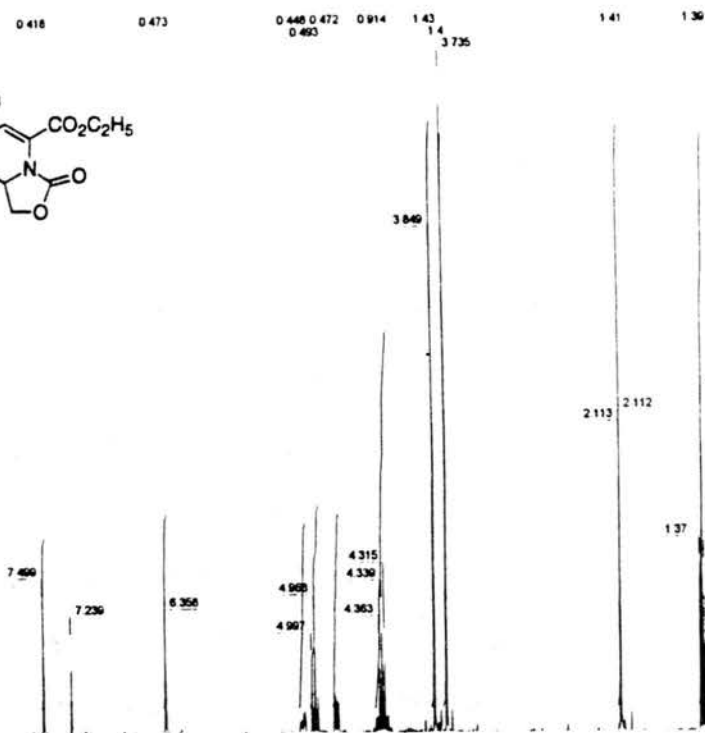
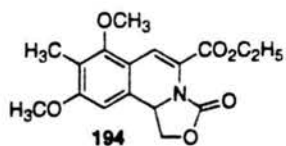




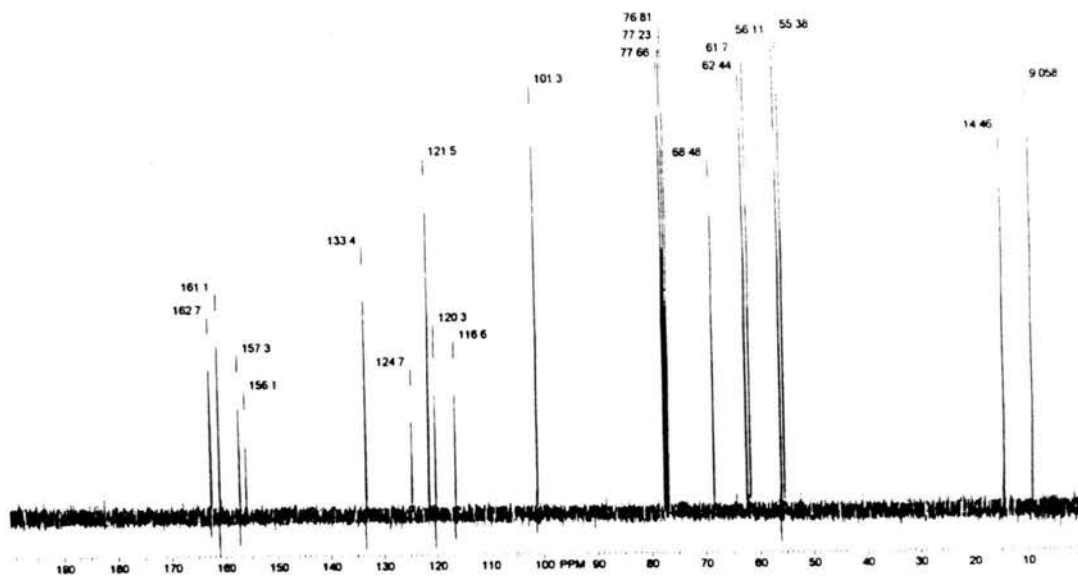
**3-Carboethoxy-(2,2'-carbonyl)-9,11-methoxy-10-methyltetrahydro  
isoquinoline (194).**

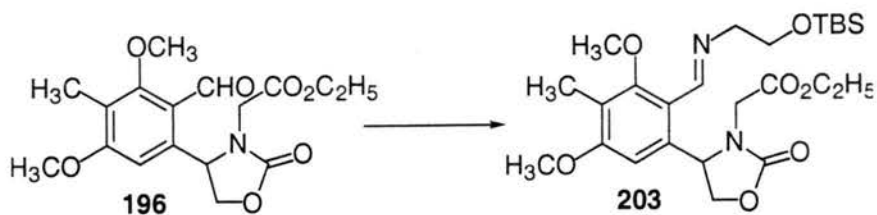
Sodium hydride (105 mg, 2.4 mmol) was added to aldehyde **196** (770 mg, 2.19 mmol) in 5 mL of DMF at RT. After 30 min the reaction was quenched by pouring over ice. HCl (1 M, 25 mL) was added and the mixture extracted with  $\text{CH}_2\text{Cl}_2$  (3 x 25 ml). The combined organic layers were washed with 1 M HCl, water and brine and then dried over  $\text{MgSO}_4$ . Concentration *in vacuo* gave 557 mg (76%) of **194** as yellow plates. m.p= 155-158 °C (recryst. EtOAc) TLC (3/1 EtOAc/Hex)  $R_f = 0.47$  (UV and PMA).  $^1\text{H-NMR}$  (300 MHz) ( $\text{CDCl}_3$ )  $\delta$  1.34 (t,  $J = 6.9$  Hz, 3H); 2.11 (s, 3H); 3.73 (s, 3H); 3.85 (s, 3H); 4.34 (m, 2H); 4.77 (dd,  $J = 3.6, 8.4$  Hz, 1H); 4.97 (t,  $J = 8.4$  Hz, 1H); 5.08 (dd,  $J = 3.6, 8.4$  Hz, 1H); 6.36 (s, 1H); 7.50 (s, 1H).  $^{13}\text{C-NMR}$  (75 MHz) ( $\text{CDCl}_3$ )  $\delta$  9.1, 14.5, 55.4, 56.1, 61.7, 62.4, 68.5, 101.3, 116.6, 120.3, 121.5, 124.7, 133.4, 156.1, 157.3, 161.1, 162.7. IR (NaCl, neat) 2941, 1767, 1716, 1603, 1564, 1444, 1413, 1312, 1276, 1216, 1129, 1038  $\text{cm}^{-1}$ .

EXPERIMENT: DL-LB11752.100



EXPERIMENT: DL-LB11752.101

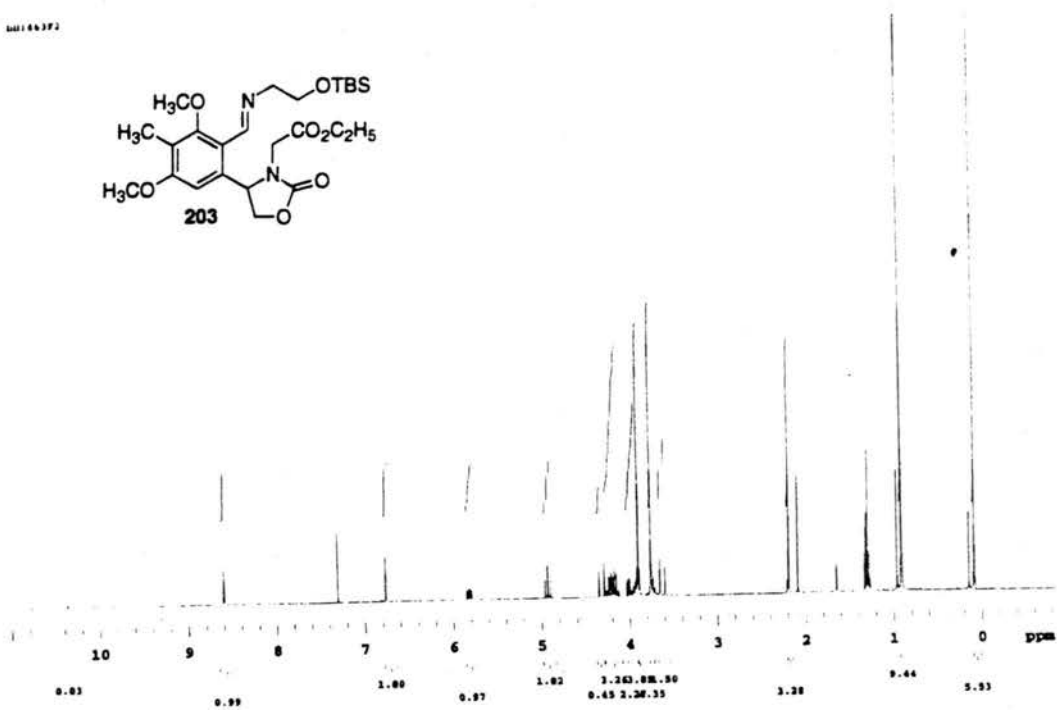
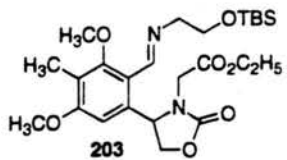


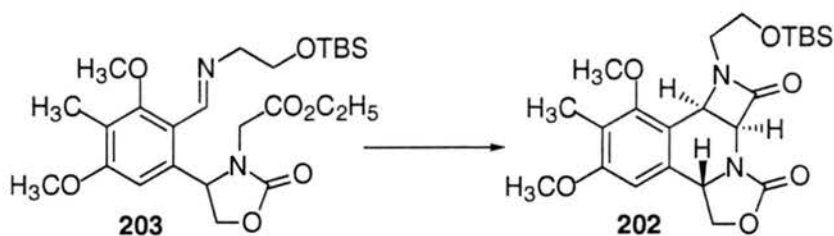


**1-(Carboethoxy)methyl-5-(2'-*N*-(*O*-*tert*-butyldimethylsilylhydroxy ethyl)aldimine-3',5'-dimethoxy-4'-methyl)phenyloxazolidin-2-one (203).**

Magnesium sulfate (282 mg, 2.34 mmol) and *O*-*tert*-butyldimethylsilyl-protected ethanolamine (47 mL, 2.34 mmol) was added to aldehyde **196** (164 mg, 0.47 mmol) in 4 mL of CH<sub>2</sub>Cl<sub>2</sub>. The reaction was stirred for 16 h and then filtered and concentrated. The crude product was chromatographed (3/1 EtOAc/Hex) to give 229 mg (96%) of **203** as a yellow oil. TLC (3/1 EtOAc/Hex) R<sub>f</sub> = 0.71 (UV and dragendorff). <sup>1</sup>H-NMR (300 MHz) (CDCl<sub>3</sub>) δ 0.11 (s, 3H); 0.14 (s, 3H); 0.84 (s, 9H); 1.22 (t, J= 7.2 Hz, 3H); 2.12 (s, 3H); 3.56 (d, J= 17.7 Hz, 1H); 3.69 (s, 3H); 3.69 (m, 1H); 3.83 (s, 3H); 3.83-3.93 (m, 2H); 3.94 (dd, J= 6.3, 9.0 Hz, 1H); 4.12-4.17 (m, 3H); 4.25 (d, J= 17.7 Hz, 1H); 4.86 (t, J= 9.0 Hz, 1H); 5.75 (dd, J= 6.3, 9.0 Hz, 1H); 6.70 (s, 1H); 8.54 (s, 1H).

MS166372





**3 $\alpha$ ,4 $\alpha$ ,5 $\beta$ -2,2'-carbonyl-3,4-N-(*O*-*tert*-butyldimethylsilylhydroxy ethyl)azetidinone-9,11-methoxy-10-methyltetrahydroisoquinoline (202).**

To imine **203** (726.0 mg, 1.43 mmol) in 20 mL of THF was added *n*-BuLi (2.6 mL, 2.86 mmol) at -78 °C. The reaction was allowed to warm up to RT and stir for 8 h. The reaction was quenched with water and the aqueous phase washed with ethyl acetate. The combined organic layers were concentrated and purified by chromatography (3/1 EtOAc/Hex) to give 245 mg (37%) of **202** as a yellow oil. TLC (3/1 EtOAc/Hex)  $R_f$  = 0.33 (UV and dragendorff).  $^1\text{H-NMR}$  (300 MHz) ( $\text{CDCl}_3$ )  $\delta$  0.005 (s, 3H); 0.016 (s, 3H); 0.85 (s, 9H); 2.14 (s, 3H); 2.91 (dt,  $J$ = 5.7, 14.1 Hz, 1H); 3.34-3.43 (m, 1H); 3.59-3.66 (m, 2H); 3.73 (s, 3H); 3.83 (s, 3H); 4.56 (dd,  $J$ = 4.5, 8.7 Hz, 1H); 4.80 (t,  $J$ = 8.7 Hz, 1H); 4.93 (dd,  $J$ = 4.5, 8.7 Hz, 1H); 4.99 (d,  $J$ = 5.3 Hz, 1H); 5.46 (d,  $J$ = 5.3 Hz, 1H); 6.36 (s, 1H).  $^{13}\text{C-NMR}$  (75 MHz) ( $\text{CDCl}_3$ )  $\delta$  165.8, 159.6, 159.1, 156.3, 133.8, 120.0, 117.1, 102.3, 67.6, 61.6, 59.7, 59.3, 56.0, 52.2, 47.7, 43.4, 26.0, 18.4, 9.5, -5.2. IR (NaCl, neat) 2929, 1770, 1608, 1580, 1464, 1418, 1333, 1306, 1126, 1102, 837  $\text{cm}^{-1}$ .

100 MHz 1H NMR (CDCl3) 200

0.267

0.246

0.237 0.275  
0.268 0.266

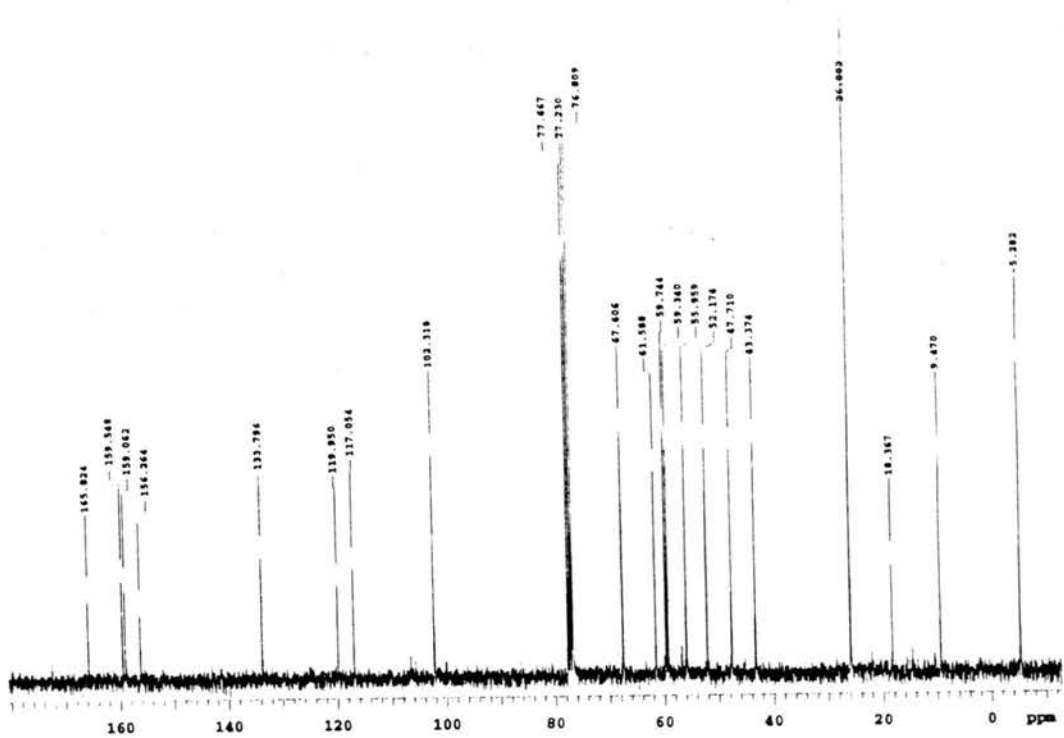
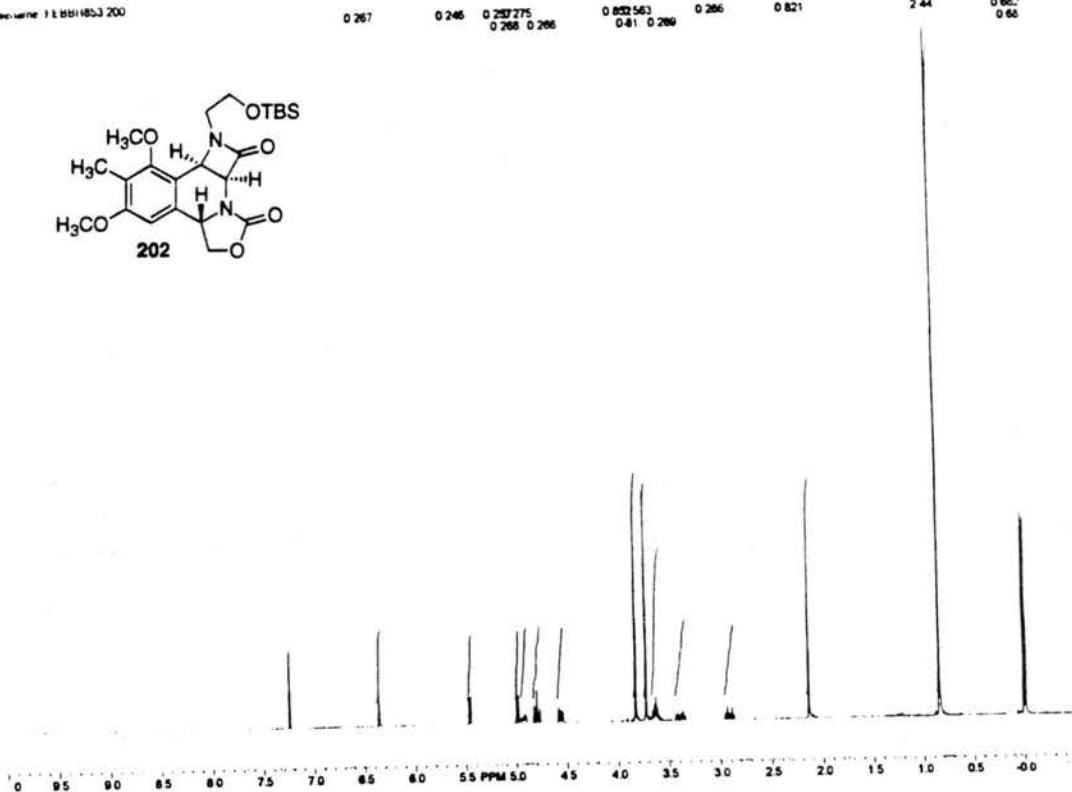
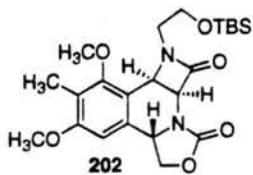
0.832 0.563  
0.81 0.269

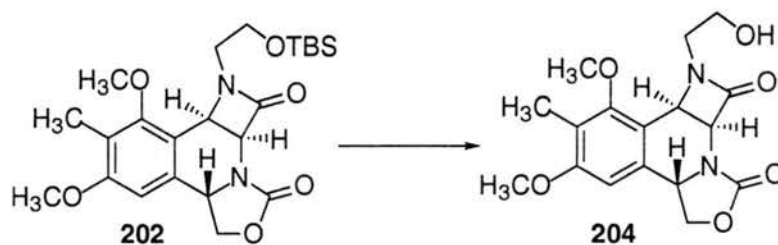
0.266

0.821

2.44

0.667  
0.66

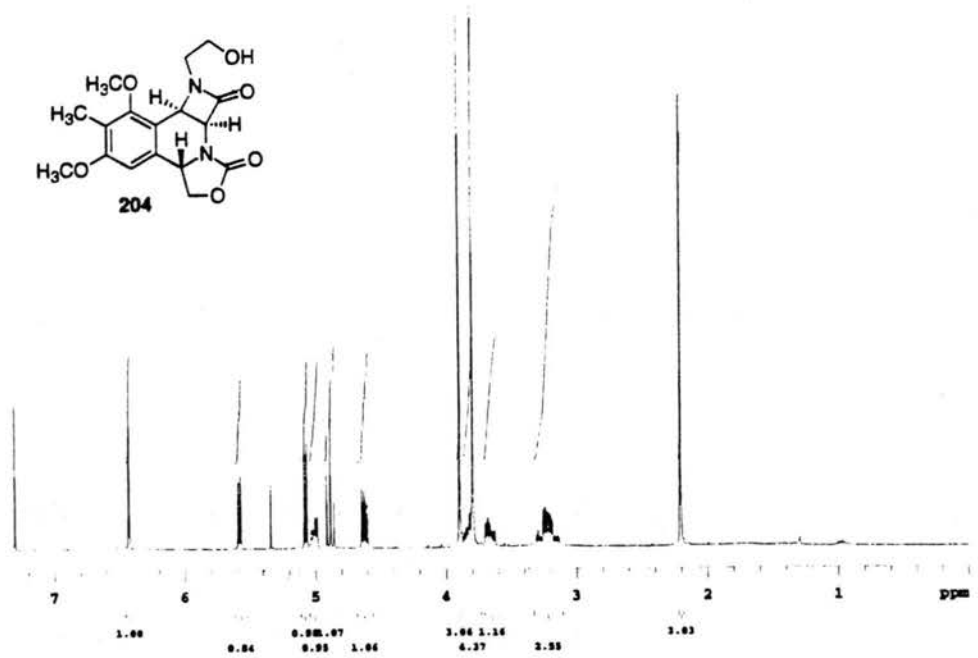
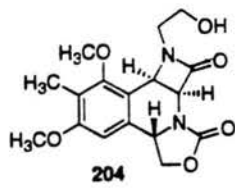




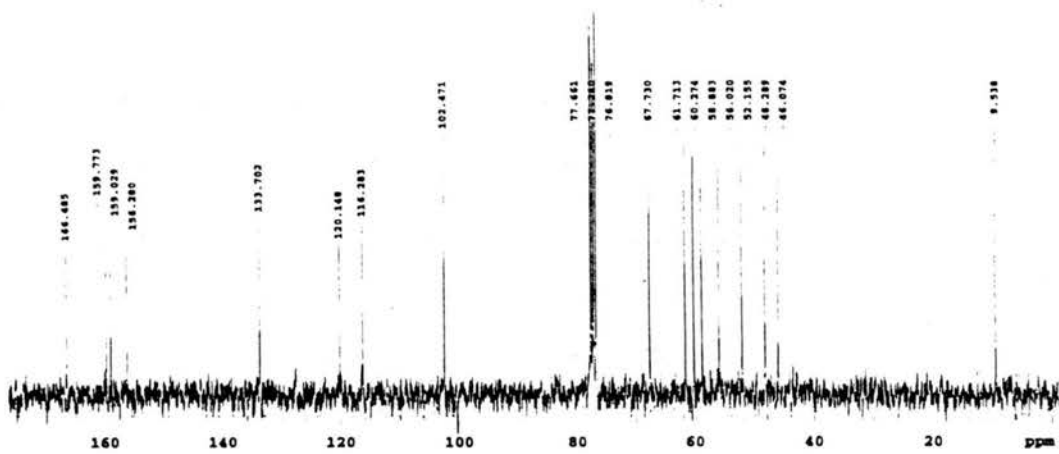
**3 $\alpha$ ,4 $\alpha$ ,5 $\beta$ -2,2'-carbonyl-3,4-N-(hydroxyethyl)azetidinone-9,11-methoxy-10-methyltetrahydroisoquinoline (204).**

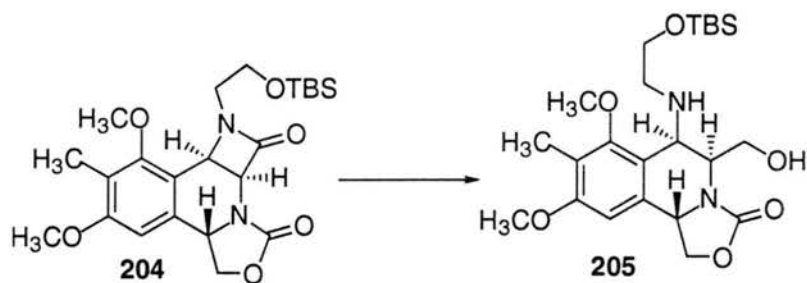
A solvent system of HOAc:H<sub>2</sub>O:THF (3:1:1, 3 mL) was added to  $\beta$ -lactam **202** (38 mg, 0.082 mmol) and the reaction was allowed to stir for 6 h. NaHCO<sub>3</sub> (sat.) was added and the reaction was extracted with CH<sub>2</sub>Cl<sub>2</sub>. The crude product was chromatographed (10/1 CH<sub>2</sub>Cl<sub>2</sub>/ MeOH) to give 14.8 mg (52%) of **204** as crystals. m.p.= 159-161 °C (recryst. CHCl<sub>3</sub>). TLC (10/1 CH<sub>2</sub>Cl<sub>2</sub>/MeOH) R<sub>f</sub> = 0.43 (UV and PMA). <sup>1</sup>H-NMR (300 MHz) (CDCl<sub>3</sub>)  $\delta$  1.64 (br s, 1H, D<sub>2</sub>O exch.); 2.21 (s, 3H); 3.28 (ddd, J= 3.6, 6.0, 14.4 Hz, 1H); 3.26 (ddd, J= 3.6, 6.0, 14.4 Hz, 1H); 3.67 (ddd, J= 3.6, 6.6, 12.0 Hz, 1H); 3.80 (s, 3H); 3.83 (ddd, J= 3.6, 6.6, 12.6 Hz, 1H); 3.90 (s, 3H); 4.63 (dd, J= 4.5, 8.4 Hz, 1H); 4.89 (t, J= 8.4 Hz, 1H); 5.01 (dd, J= 4.5, 8.4 Hz, 1H); 5.08 (d, J= 5.4 Hz, 1H); 5.58 (d, J=5.4 Hz, 1H); 6.43 (s, 1H). <sup>13</sup>C-NMR (75 MHz) (CDCl<sub>3</sub>)  $\delta$  166.5, 159.8, 159.0, 156.3, 133.7, 120.2, 116.3, 102.5, 67.7, 61.7, 60.3, 58.9, 56.0, 52.2, 48.3, 46.1, 9.5. IR (NaCl, neat) 3414, 2931, 1607, 1414, 1331, 1306, 1226, 1126, 1055 cm<sup>-1</sup>. See Appendix 2 for X-ray structure.

UN142191



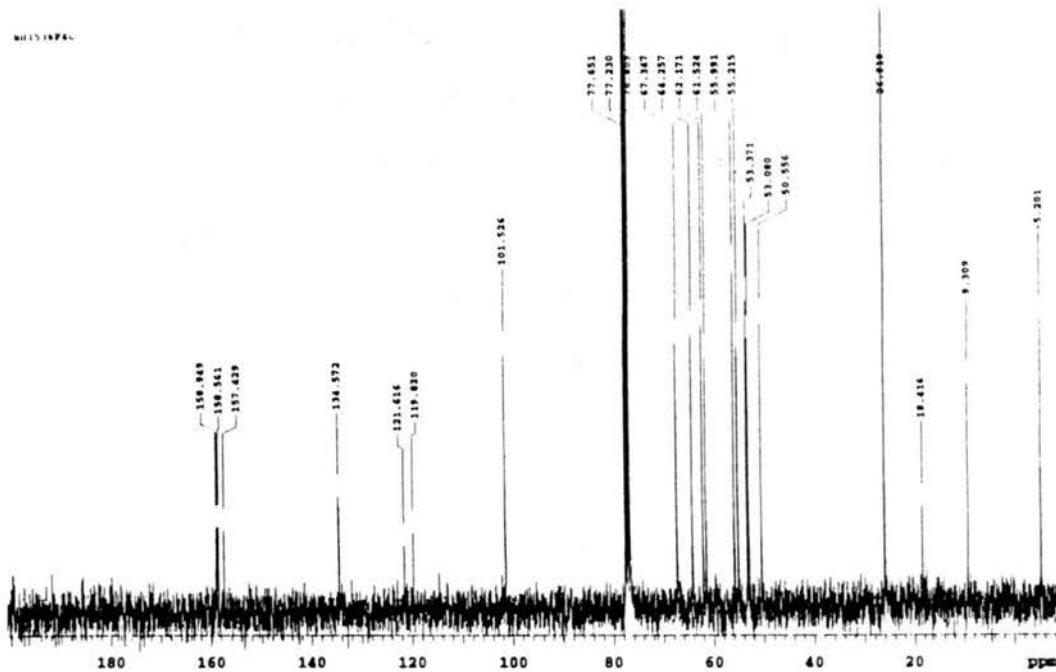
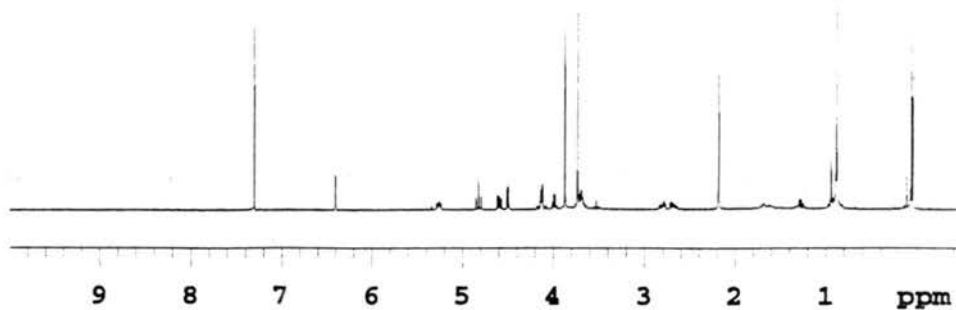
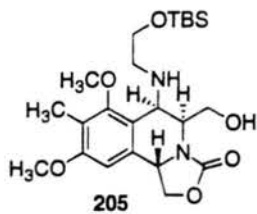
UN142191

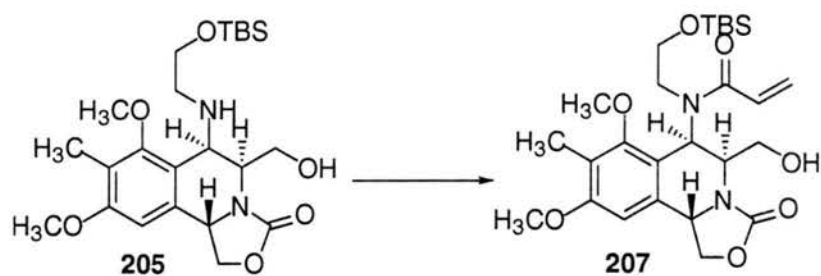




**3 $\alpha$ ,4 $\alpha$ ,5 $\beta$ -2,2'-carbonyl-3-hydroxymethyl-4-N-(O-*tert*-butyldimethylsilylhydroxyethyl)amine-9,11-methoxy-10-methyltetrahydroisoquinoline (205).**

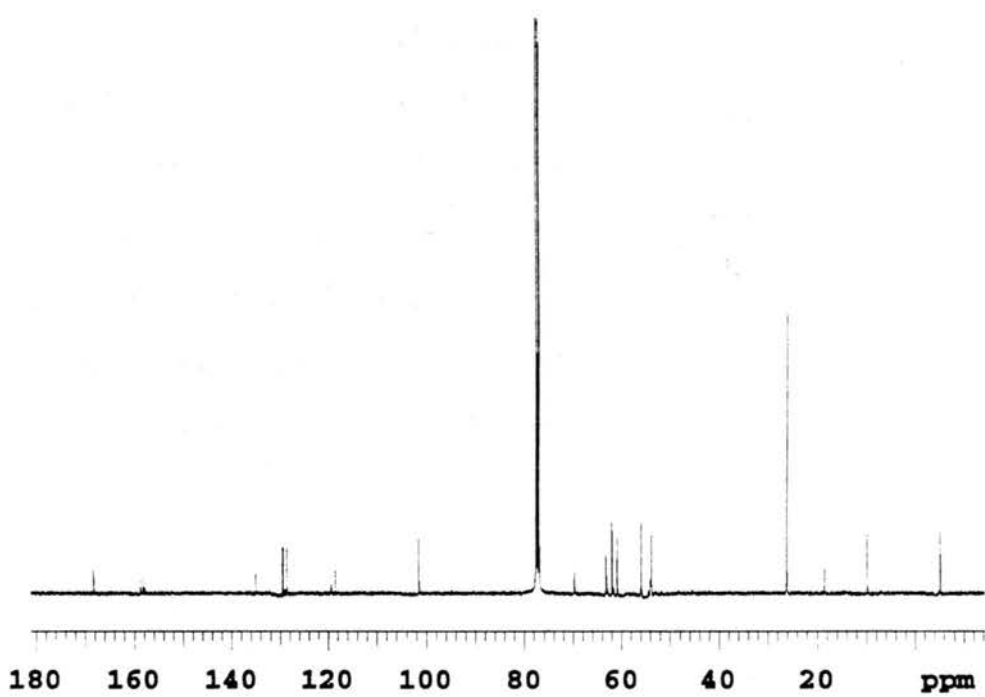
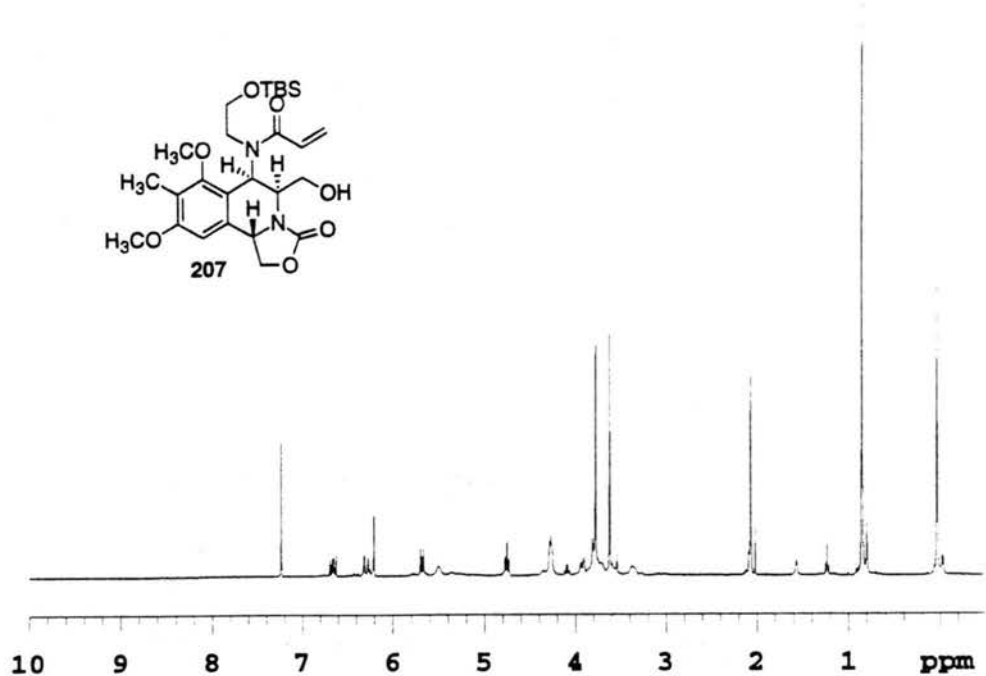
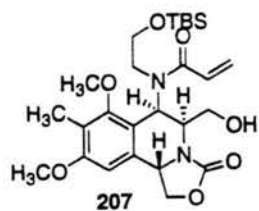
In a flame-dried 10 mL flask under argon, borane-THF complex (1M, 270  $\mu$ L, 0.27 mmol) was added to **204** (132.4 mg, 0.29 mmol) in 8.0 mL of THF at -10  $^{\circ}$ C. The reaction was allowed to warm up to RT and stir overnight. NaHCO<sub>3</sub> (sat.) was then added to quench the reaction. The crude product was washed with Rochelle's salt (sat. K<sup>+</sup>-Na<sup>+</sup> tartrate soln.) and extracted with CH<sub>2</sub>Cl<sub>2</sub>. The organic layer was separated, dried and concentrated. The crude reaction was purified by chromatography (10/1 CH<sub>2</sub>Cl<sub>2</sub>/MeOH) to afford 50.8 mg (38%) of **205** as a white solid. m.p.= 145-147  $^{\circ}$ C (recryst. MeOH). TLC (3/1 EtOAc/Hex) R<sub>f</sub> = 0.39 (UV and dragendorff). <sup>1</sup>H-NMR (300 MHz) (CDCl<sub>3</sub>)  $\delta$  0.044 (2, 3H); 0.065 (s, 3H); 0.88 (s, 9H); 2.19 (s, 3H); 1.65 (br s, 2H, D<sub>2</sub>O exch.) 2.64-2.84 (m, 2H); 3.63-3.76 (m, 2H); 3.73 (s, 3H); 3.87 (s, 3H); 3.99 (q, J= 5.0 Hz, 1H); 4.13 (ddd, J= 4.7, 10.8, 15.5 Hz, 2H); 4.50 (d, J= 5.1 Hz, 1H); 4.59 (dd, J= 5.6, 8.9 Hz, 1H); 4.82 (t, J= 8.4 Hz, 1H); 5.26 (dd, J= 5.4, 8.1 Hz, 1H); 6.40 (s, 1H). <sup>13</sup>C-NMR (75 MHz) (CDCl<sub>3</sub>)  $\delta$  159.0, 158.6, 157.4, 134.6, 121.6, 119.8, 101.5, 67.4, 64.3, 62.2, 61.5, 60.0, 55.2, 53.4, 53.1, 50.6, 26.0, 18.4, 9.3, -5.2. IR (NaCl, neat) 3379, 2928, 1747, 1464, 1410, 1125 cm<sup>-1</sup>. HRMS calcd for (FAB) for C<sub>23</sub>H<sub>39</sub>N<sub>2</sub>O<sub>6</sub>Si (M+H) 467.2577; 467.2573 found.

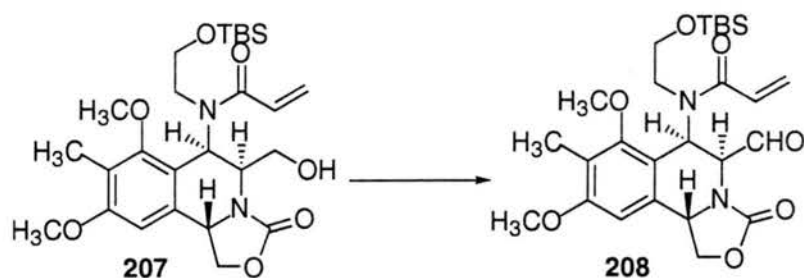




**3 $\alpha$ ,4 $\alpha$ ,5 $\beta$ -2,2'-carbonyl-3-hydroxymethyl-4-N-(*O*-*tert*-butyldimethylsilylhydroxyethyl-N-acryloyl)amine-9,11-methoxy-10-methyltetrahydroisoquinoline (207).**

In a flame-dried one neck flask under argon charged with amino alcohol **205** (45.4 mg, 0.097 mmol) was added chlorotrimethylsilane (15  $\mu$ L, 0.116 mmol) and triethylamine (16  $\mu$ L, 0.116 mmol) in THF (1 mL) at RT. The reaction, which usually took 15 min, was monitored by TLC (3/1 EtOAc/Hex). Upon complete formation of the TMS ether, triethylamine (16  $\mu$ L, 0.116 mmol) and acryloyl chloride (9.4  $\mu$ L, 0.116 mmol) were added and the reaction stirred at RT for 30 min. The reaction was quenched with the addition of water and the aqueous layer washed with ethyl acetate. The combined organic layers were concentrated to give 48.6 mg of a yellow oil. Column chromatography (EtOAc) gave 25.4 mg (50%) of **207** as an oil. TLC (3/1 EtOAc/Hex)  $R_f$  = 0.13 (UV and dragendorff).  $^1\text{H-NMR}$  (300 MHz) ( $\text{CDCl}_3$ )  $\delta$  0.022 (s, 6H); 0.84 (s, 9H); 2.06 (s, 3H); 3.18 (br s, 1H,  $\text{D}_2\text{O}$  exch.); 3.31-3.40 (m, 1H); 3.61-3.70 (m, 1H); 3.69 (s, 3H); 3.76-3.88 (m, 3H); 3.84 (s, 3H); 3.99 (dd,  $J$ = 3.1, 12.3 Hz, 1H); 4.32-4.36 (m, 2H); 4.39-4.44 (m, 1H); 4.82 (t,  $J$ = 8.4 Hz, 1H); 5.56 (br s, 1H); 5.75 (dd,  $J$ = 1.8, 10.6 Hz, 1H); 6.28 (s, 1H); 6.36 (dd,  $J$ = 1.8, 16.7 Hz, 1H); 6.73 (dd,  $J$ = 10.6, 16.7 Hz, 1H).  $^{13}\text{C-NMR}$  (75 MHz) ( $\text{CDCl}_3$ )  $\delta$  168.3, 158.7, 158.2, 157.9, 135.1, 129.4, 128.5, 119.4, 118.5, 101.4, 69.7, 63.1, 61.9, 60.8, 55.8, 53.9, 53.7, 26.1, 18.4, 14.4, 9.7, -5.25, -5.28. IR (NaCl, neat) 3395, 2944, 2862, 1755, 1641, 1600, 1462, 1410, 1118  $\text{cm}^{-1}$ . HRMS (FAB) calcd for  $\text{C}_{26}\text{H}_{41}\text{N}_2\text{O}_7\text{Si}$  ( $\text{M}+\text{H}$ ) 521.2683; found 521.2684.

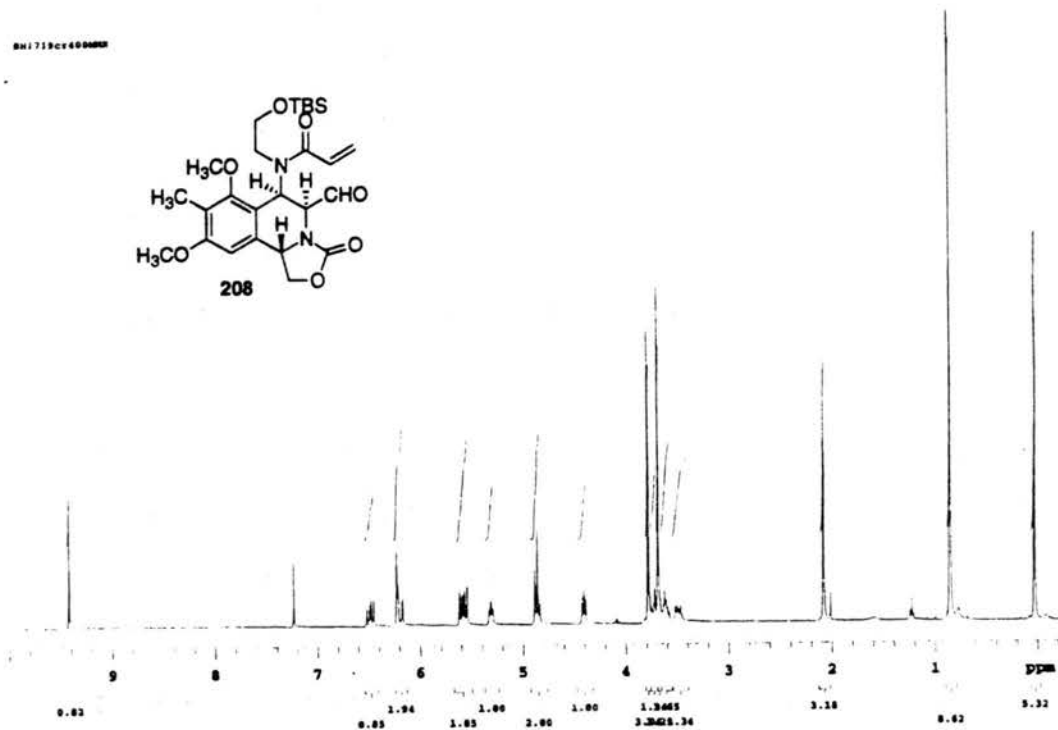
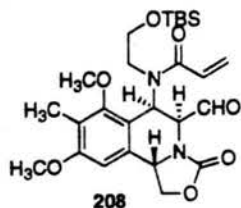




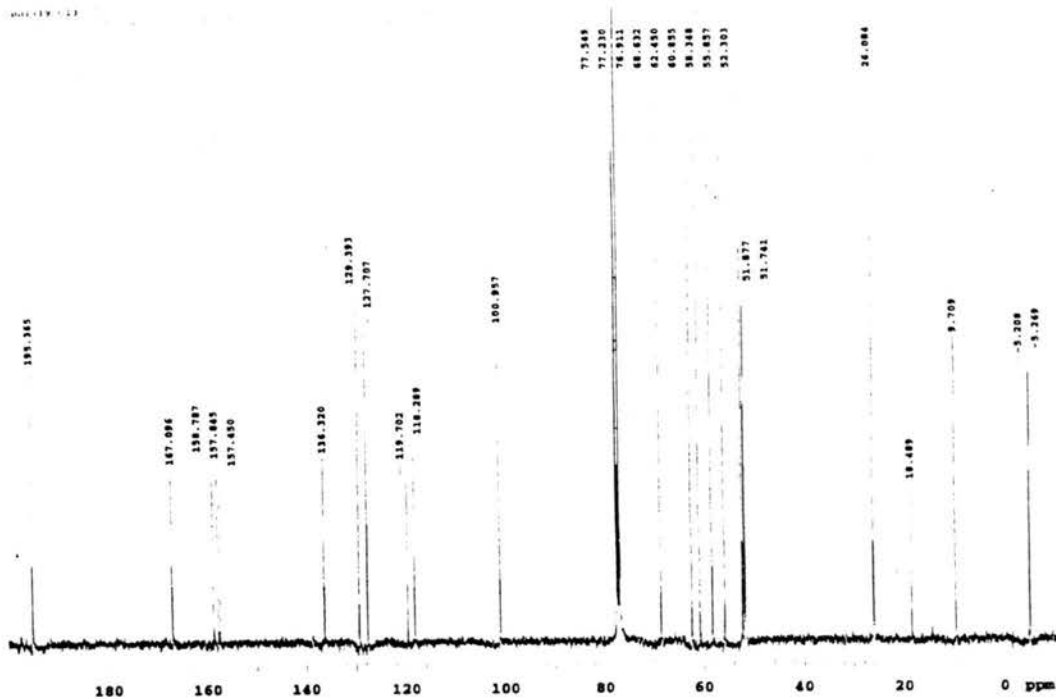
**3 $\alpha$ ,4 $\alpha$ ,5 $\beta$ -2,2'-carbonyl-3-formyl-4-N-(*O*-*tert*-butyldimethylsilyl)hydroxyethyl-N-acryloyl)amine-9,11-methoxy-10-methyltetrahydroisoquinoline (208).**

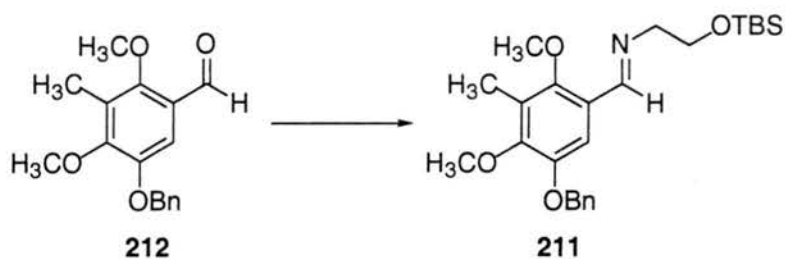
To a solution of **207** (7.7 mg, 0.015 mmol) in 1 mL of CH<sub>2</sub>Cl<sub>2</sub> was added Dess-Martin periodinane (25.4 mg, 0.060 mmol) at RT. The reaction stirred at RT and was quenched with the addition of Na<sub>2</sub>S<sub>2</sub>O<sub>3</sub>·5 H<sub>2</sub>O (60 mg, 0.24 mmol) in 0.5 mL of 1M NaHCO<sub>3</sub>. The quenched reaction was extracted with CH<sub>2</sub>Cl<sub>2</sub> and the organic layer dried and concentrated to give 7.1 mg (91%) of **208** as a clear oil. TLC (3/1 EtOAc/Hex) R<sub>f</sub> = 0.42 (UV and DNP). <sup>1</sup>H-NMR (300 MHz) (CDCl<sub>3</sub>)  $\delta$  0.017 (s, 6H); 0.84 (s, 9H); 2.07 (s, 3H); 3.46-3.52 (m, 1H); 3.58-3.65 (m, 2H); 3.68 (s, 3H); 3.71-3.77 (m, 1H); 3.78 (s, 3H); 4.40 (dd, J= 4.8, 6.3 Hz, 1H); 4.86 (t, J= 6.3 Hz, 1H); 4.87 (d, J= 7.8 Hz, 1H); 5.31 (dd, J= 4.8, 6.0 Hz, 1H); 5.58 (dd, J= 8.1, 14.7 Hz, 1H); 5.60 (d, J= 8.1 Hz, 1H); 6.19 (d, J= 12.6 Hz, 1H); 6.22 (s, 1H); 6.48 (dd, J= 7.8, 12.6 Hz, 1H); 9.42 (s, 1H). <sup>13</sup>C-NMR (75 MHz) (CDCl<sub>3</sub>)  $\delta$  195.37, 167.10, 158.79, 157.85, 157.45, 136.32, 129.39, 127.71, 119.70, 118.29, 100.96, 68.63, 62.45, 60.86, 58.35, 55.86, 52.30, 51.88, 51.74, 26.08, 18.49, 9.71, -5.21, -5.27. IR (NaCl, neat) 2930, 2857, 1760, 1732, 1608, 1470, 1416, 1257, 1104, 837 cm<sup>-1</sup>. HRMS (FAB) calcd for C<sub>26</sub>H<sub>39</sub>N<sub>2</sub>O<sub>7</sub>Si (M+H) 519.2526; found 519.2522.

001719c400000



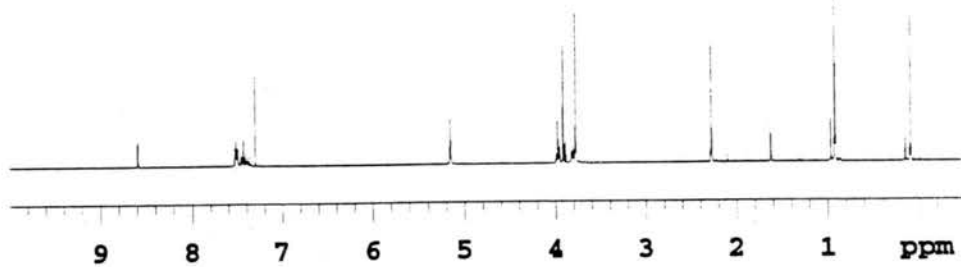
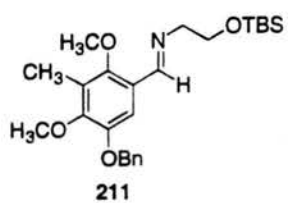
001719c400000

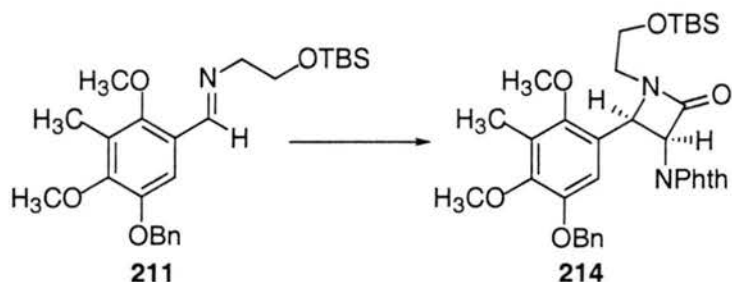




**2,4-methoxy-3-methyl-5-benzyloxy-N-(*O*-*tert*-butyldimethylsilyl hydroxyethyl)aldimine (211).**

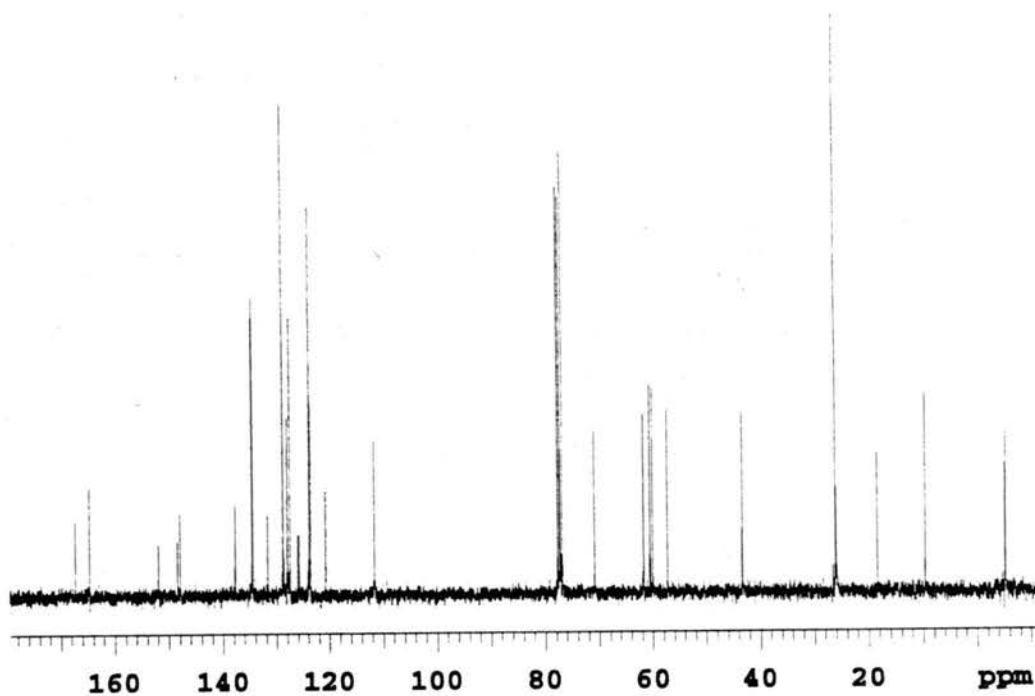
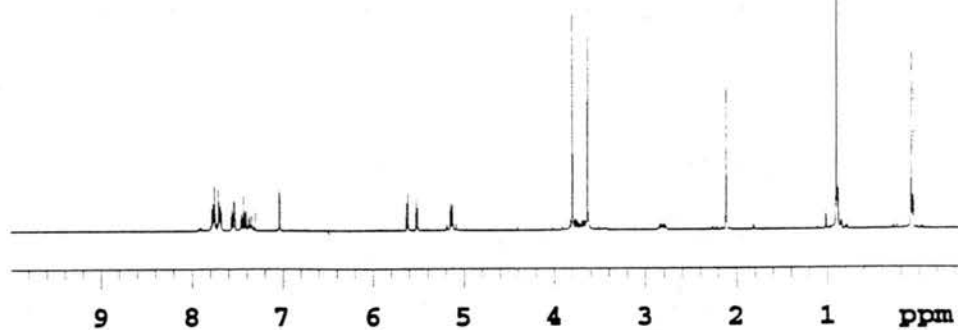
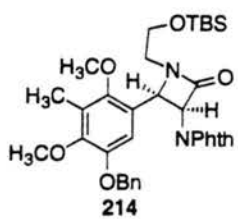
To a solution of aldehyde **212** (4.0 g, 14.0 mmol) in 40 mL of  $\text{CH}_2\text{Cl}_2$  was added  $\text{MgSO}_4$  (8.4 g, 70.0 mmol) and *O*-*tert*-butyldimethylsilyl-protected ethanol amine (3.67 g, 21.0 mmol). The reaction was monitored by  $^1\text{H-NMR}$  spectroscopy and after 1 h was complete. The mixture was then filtered and the crude product purified by running it through a short plug of silica gel with EtOAc as the eluent to give 6.65 g (97%) of **211** as a yellow oil. The material was directly carried on to the next step without further purification.  $^1\text{H-NMR}$  (300 MHz) ( $\text{CDCl}_3$ )  $\delta$  0.09 (s, 6H); 0.92 (s, 9H); 2.27 (s, 3H); 3.78 (s, 3H); 3.81 (t,  $J = 5.7$  Hz, 2H); 3.91 (s, 3H); 3.97 (t,  $J = 5.7$  Hz, 2H); 5.15 (s, 2H); 7.37-7.52 (m, 6H); 8.60 (s, 1H).



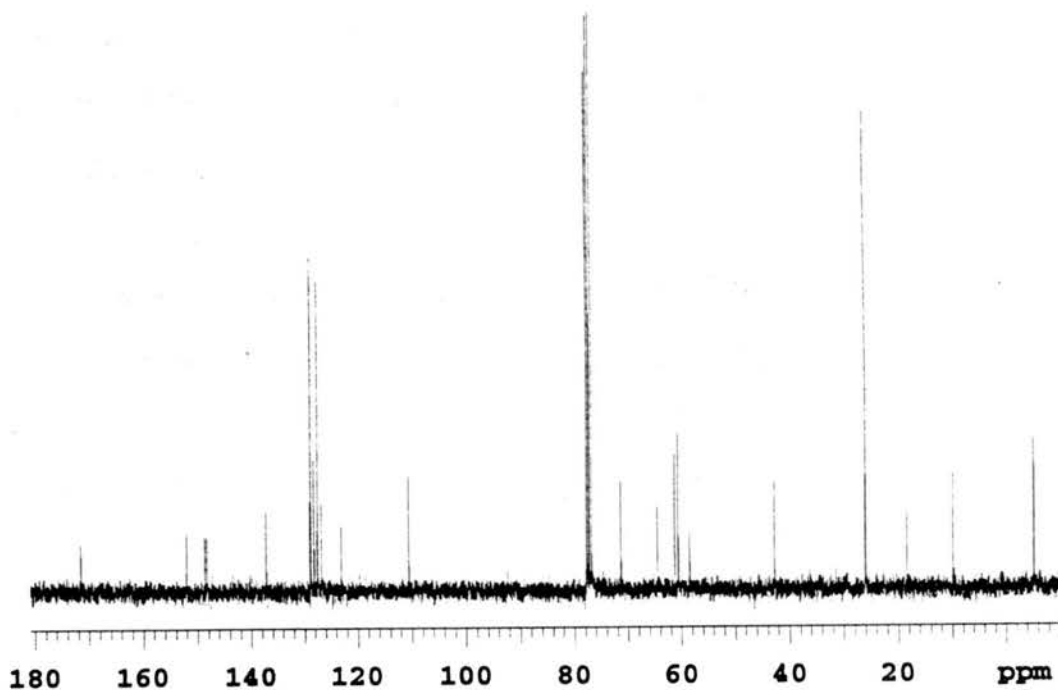
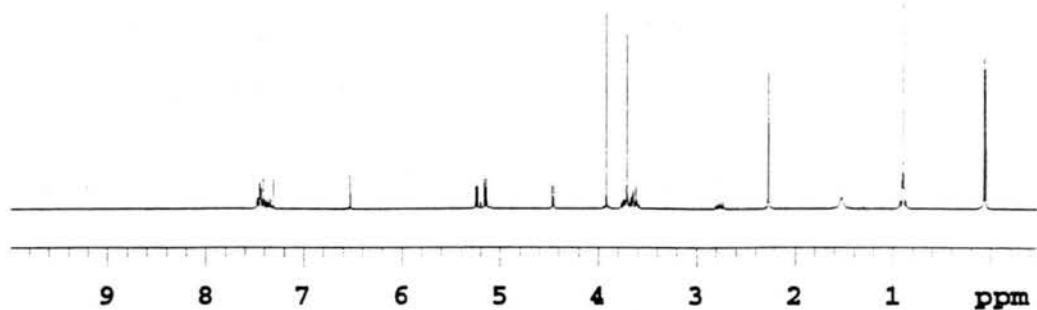
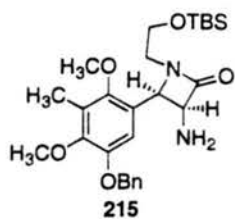


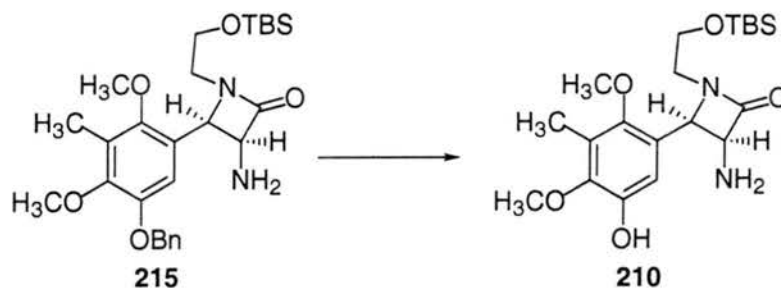
**1-*O*-*tert*-butyldimethylsilylhydroxyethyl-3-*N*-(phthalimide)amine-4-(2',4'-methoxy-3'-methyl-5'-benzyloxy)phenyl-2-azetidinone (214).**

Triethylamine (1.94 mL, 13.91 mmol) was added dropwise to a solution of the acid chloride of *N*-phthalamide protected glycine (2.07 g, 9.27 mmol) in 26.5 mL of CH<sub>2</sub>Cl<sub>2</sub> at -78 °C under Ar. The reaction was allowed to stir at -78 °C for 15 min and then imine **211** (3.04 g, 6.18 mmol) in 9.5 mL of CH<sub>2</sub>Cl<sub>2</sub> was added and the reaction warmed up to 0 °C. After stirring for 2 h at 0 °C the reaction was quenched with NH<sub>4</sub>Cl. The quenched reaction was extracted with CH<sub>2</sub>Cl<sub>2</sub> and the organic layer dried and concentrated. After column chromatography (1/1 EtOAc/Hex) 3.11 g (80%) of **214** was obtained as a white solid. m.p.= 114-116 °C (recryst. EtOAc). TLC (1/1 EtOAc/Hex) R<sub>f</sub> = 0.53 (UV and PMA). <sup>1</sup>H-NMR (300 MHz) (CDCl<sub>3</sub>) δ 0.058 (s, 3H); 0.080 (s, 3H); 0.90 (s, 9H); 2.11 (s, 3H); 2.77-2.85 (m, 1H); 3.64 (s, 3H); 3.62-3.82 (m, 3H); 3.80 (s, 3H); 5.10 (1/2 ABq, J= 12.0 Hz, 1H); 5.17 (1/2 ABq, J= 12.0 Hz, 1H); 5.52 (d, J= 5.1 Hz, 1H); 5.62 (d, J= 5.1 Hz, 1H); 7.04 (s, 1H); 7.32-7.45 (m, 3H); 7.56-7.53 (m, 2H); 7.68-7.78 (m, 4H). <sup>13</sup>C-NMR (75 MHz) (CDCl<sub>3</sub>) δ 167.3, 164.6, 151.9, 148.3, 147.9, 137.7, 134.5, 131.6, 128.8, 127.9, 127.4, 125.8, 123.7, 120.7, 111.6, 70.8, 61.7, 60.5, 60.4, 60.0, 57.2, 43.3, 26.0, 18.4, 9.6, -5.2, -5.3. IR (NaCl, neat) 2930, 1770, 1723, 1384, 1232, 1087 cm<sup>-1</sup>. HRMS (FAB) calcd for C<sub>35</sub>H<sub>43</sub>N<sub>2</sub>O<sub>7</sub>Si (M+H) 631.2840; found 631.2844.



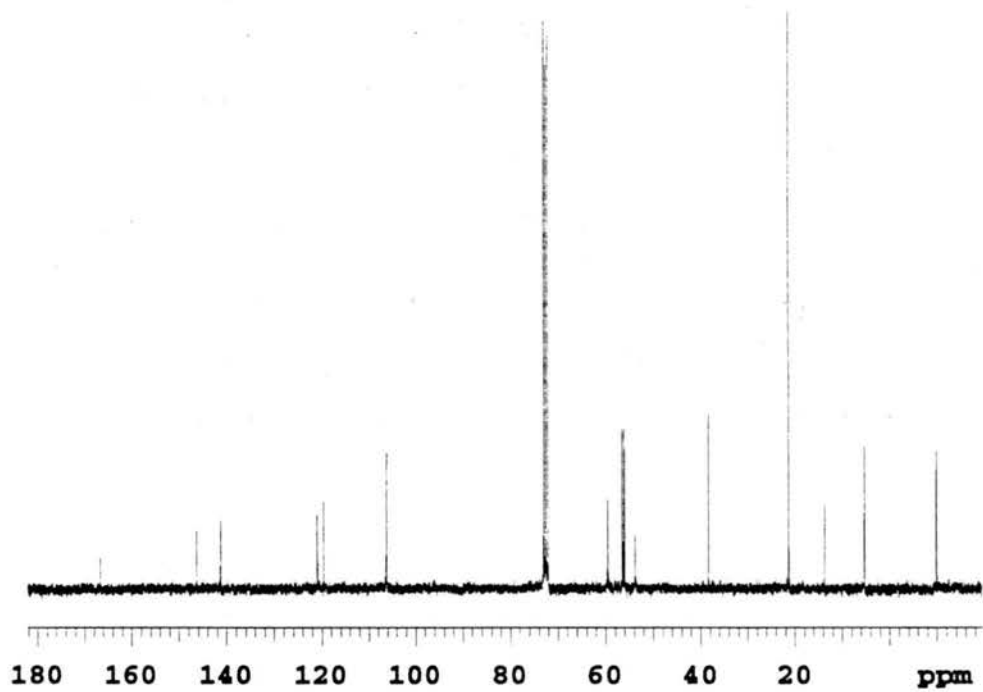
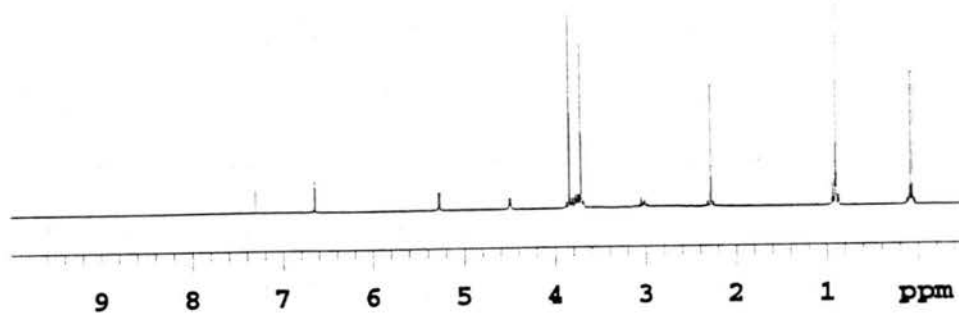
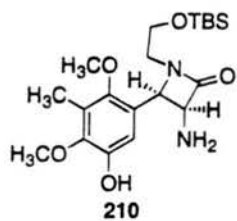


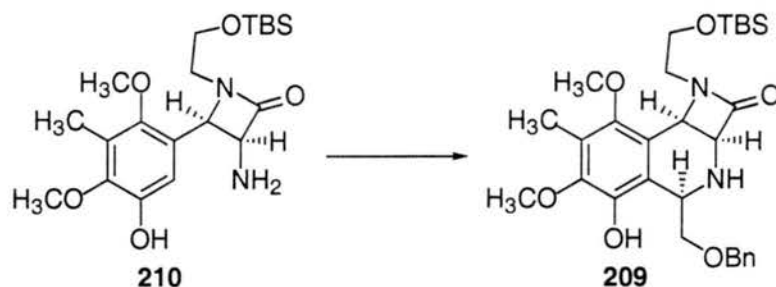




**1-*O*-*tert*-butyldimethylsilylhydroxyethyl-3-amino-4-(2',4'-methoxy-3'-methyl-5'-hydroxy)phenyl-2-azetidinone (210).**

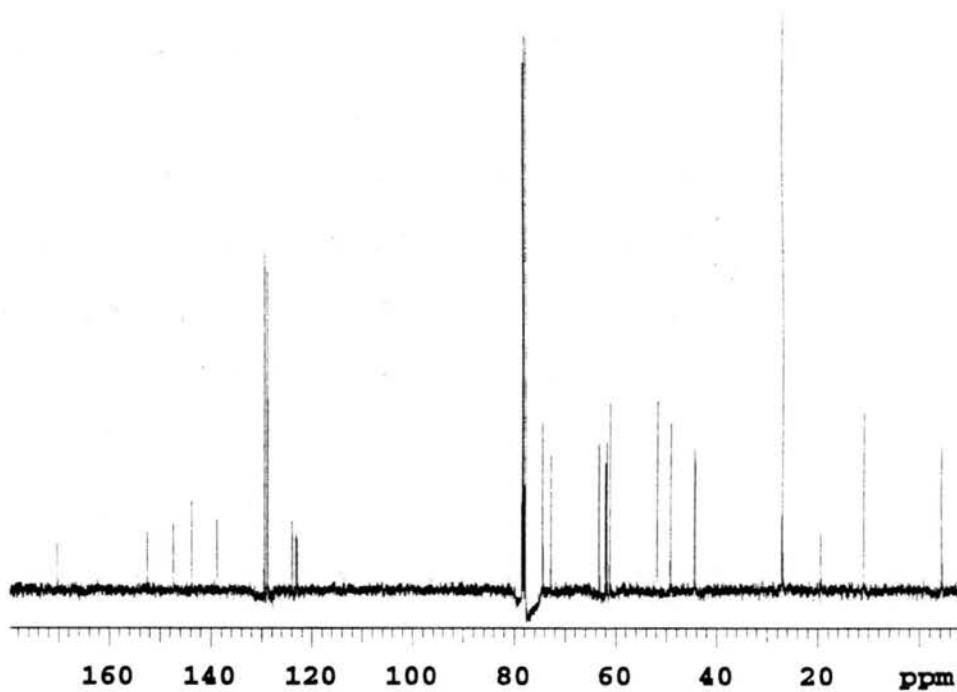
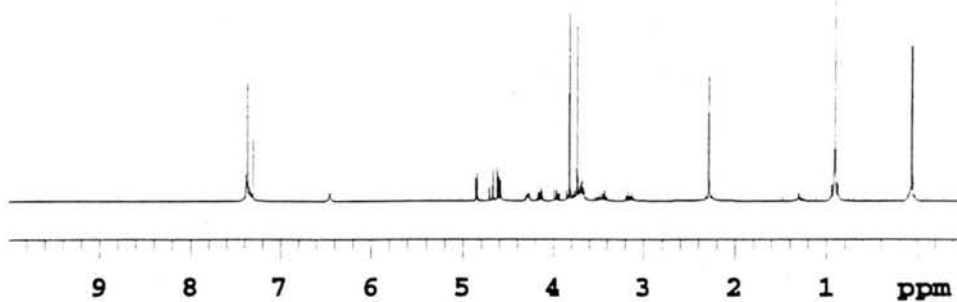
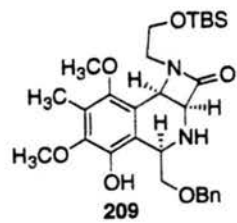
To a degassed solution of **215** (2.00 g, 3.99 mmol) in EtOH (50 mL) in a pressure tube was added 5% Pd/C (425 mg, 0.20 mmol, 0.05 eq). The reaction was then pressurized with H<sub>2</sub> to 50 psi and the reaction stirred overnight at RT. The reaction was then degassed with argon and concentrated. The residue was taken up in EtOAc and filtered through celite. The crude product was purified by column chromatography (5% MeOH in EtOAc) to give 1.57 g (96%) of **210** as a white foam. TLC (EtOAc) R<sub>f</sub> = 0.17 (UV and dragendorff). <sup>1</sup>H-NMR (300 MHz) (CDCl<sub>3</sub>) δ 0.062 (s, 3H); 0.082 (s, 3H); 0.90 (s, 9H); 2.29 (s, 3H); 2.98-3.08 (m, 1H); 3.69-3.83 (m, 3H); 3.72 (s, 3H); 3.85 (s, 3H); 4.49 (d, J= 5.1 Hz, 1H); 5.27 (d, J= 5.1 Hz, 1H); 6.66 (s, 1H). <sup>13</sup>C-NMR (75 MHz) (CDCl<sub>3</sub>) δ 171.37, 150.99, 145.99, 145.88, 125.61, 124.27, 110.94, 64.24, 61.25, 60.84, 60.68, 58.45, 42.97, 25.99, 18.35, 9.94, -5.23, -5.31. IR (NaCl, neat) 3332, 2929, 1747, 1455, 1416, 1360, 1255, 1230, 1114, 1063, 1010, 836 cm<sup>-1</sup>. HRMS (FAB) calcd for C<sub>20</sub>H<sub>34</sub>N<sub>2</sub>O<sub>5</sub>Si (M<sup>+</sup>) 410.2237; found 410.2231.

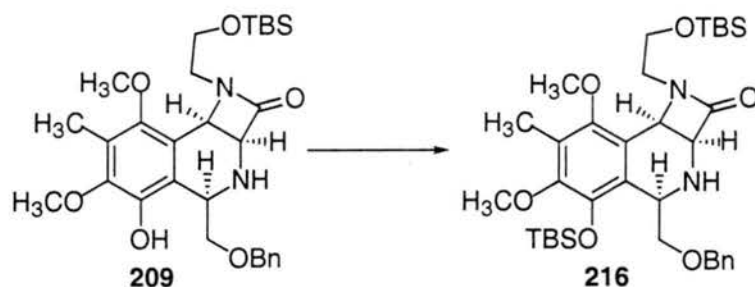




**3 $\alpha$ ,4 $\alpha$ -3,4-N-(*O*-*tert*-butyldimethylsilylhydroxyethyl)azetidinone-8-hydroxy-9,11-methoxy-10-methyltetrahydroisoquinoline (209).**

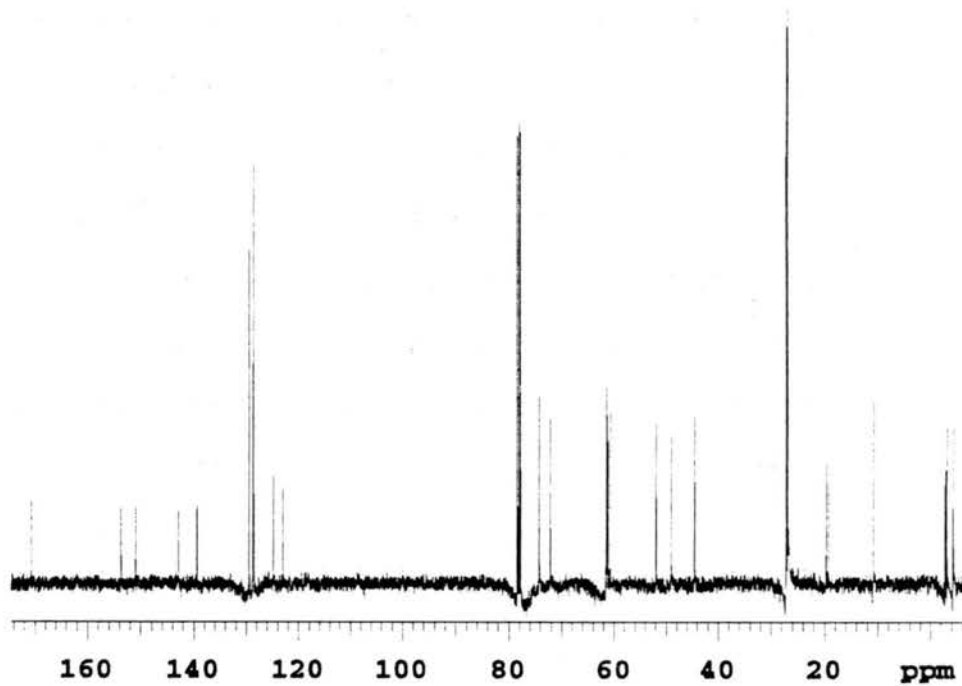
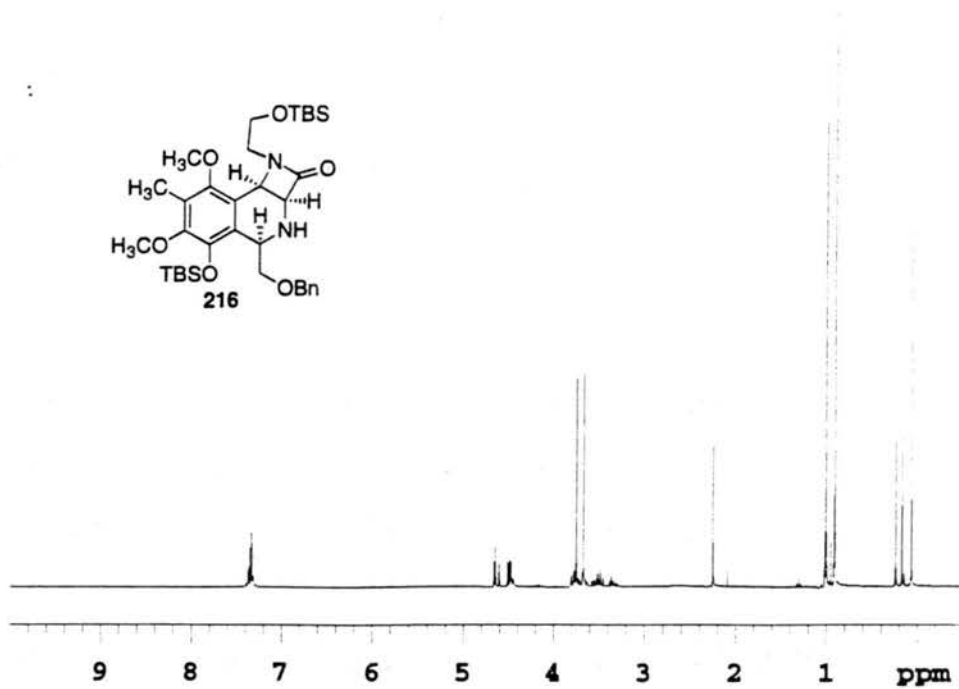
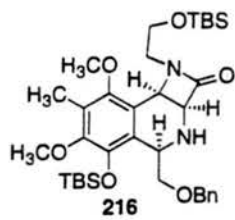
Freshly distilled benzyloxyacetaldehyde (630  $\mu$ L, 4.48 mmol) was added to a solution of **210** (1.53 g, 3.73 mmol) in MeOH (75 mL), stirred at RT for 30 min and then heated at 50  $^{\circ}$ C for 23 h. The reaction was then allowed cooled to RT and concentrated. The crude product was purified by column chromatography (3/1 EtOAc/Hex then EtOAc) to give 1.74 g (86%) of **209** as a yellow oil. TLC (EtOAc)  $R_f$  = 0.44 (UV and dragendorff).  $^1\text{H-NMR}$  (300 MHz) ( $\text{CDCl}_3$ )  $\delta$  0.049 (s, 3H); 0.063 (s, 3H); 0.91 (s, 9H); 2.28 (s, 3H); 2.49 (br s, 1H,  $\text{D}_2\text{O}$  exch.); 3.15 (dt,  $J$ = 6.0, 13.8 Hz, 1H); 3.45 (m, 1H); 3.68 (dt,  $J$ = 2.4, 6.3 Hz, 2H); 3.73 (s, 3H); 3.82 (s, 3H); 3.96 (dd,  $J$ = 6.6, 9.6 Hz, 1H); 4.15 (dd,  $J$ = 4.5, 9.6 Hz, 1H); 4.29 (dd,  $J$ = 4.5, 6.6 Hz, 1H); 4.59 (d,  $J$ = 5.1 Hz, 1H); 4.60 (1/2 ABq,  $J$ = 12.0 Hz, 1H); 4.69 (1/2 ABq,  $J$ = 12.0 Hz, 1H); 4.85 (d,  $J$ = 5.1 Hz, 1H); 6.45 (br s, 1H,  $\text{D}_2\text{O}$  exch.); 7.30-7.42 (m, 5H).  $^{13}\text{C-NMR}$  (75 MHz) ( $\text{CDCl}_3$ )  $\delta$  169.42, 151.68, 146.48, 142.91, 137.96, 128.62, 128.06, 127.98, 123.07, 122.25, 122.09, 73.49, 71.90, 62.37, 61.16, 60.82, 60.26, 50.88, 48.22, 43.39, 26.05, 18.43, 9.98, -5.22, -5.25. IR (NaCl, neat) 3326, 2929, 1747, 1463, 1416, 1258, 1110, 1065, 1007, 836  $\text{cm}^{-1}$ . HRMS (FAB) calcd for  $\text{C}_{29}\text{H}_{43}\text{N}_2\text{O}_6\text{Si}$  ( $\text{M}+\text{H}$ ) 543.2890; found 543.2864.

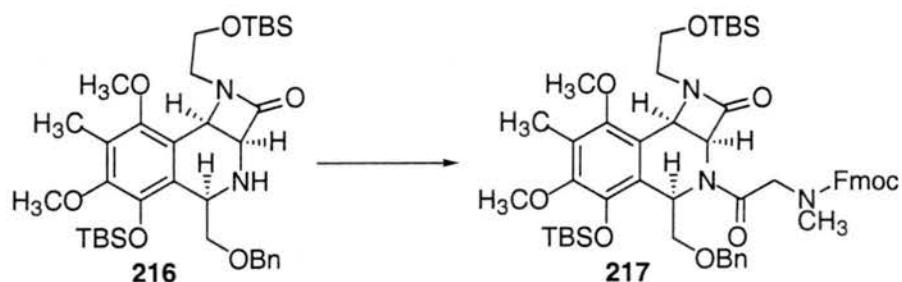




**3 $\alpha$ ,4 $\alpha$ -3,4-N-(O-*tert*-butyldimethylsilylhydroxyethyl)azetidinone-8-O-(*tert*-butyldimethylsilyl)hydroxy-9,11-methoxy-10-methyltetrahydroisoquinoline (216).**

*tert*-Butyldimethylsilyl chloride (1.18 g, 7.86 mmol) and NEt<sub>3</sub> (1.10 mL, 7.86 mmol) was added to amino phenol **209** (1.42 g, 2.62 mmol) in 3 mL of THF at RT. The reaction was stirred for 12 h and then water was added and the reaction was extracted with EtOAc. The organic layer was separated, dried over MgSO<sub>4</sub> and concentrated *in vacuo*. Column chromatography (1/1 EtOAc/ Hex) of the crude product gave 1.66 g (97%) of **216** as an oil. TLC (3/1 EtOAc/Hex) R<sub>f</sub> = 0.53 (UV and dragendorff). <sup>1</sup>H-NMR (300 MHz) (CDCl<sub>3</sub>)  $\delta$  0.063 (s, 6H); 0.17 (s, 3H); 0.24 (s, 3H); 0.91 (s, 9H); 1.01 (s, 9H); 2.25 (s, 3H); 2.60 (br s, 1H); 3.34 (dt, J= 6.3, 13.5 Hz, 1H); 3.48 (t, J= 9.9 Hz, 2H); 3.54 (dd, J= 6.3, 13.5 Hz, 1H); 3.65 (dd, J= 6.3, 9.9 Hz, 1H); 3.67 (s, 3H); 3.75 (s, 3H); 3.79 (dd, J= 3.3, 9.0 Hz, 1H); 4.44 (dd, J= 3.3, 9.0 Hz, 1H); 4.48 (d, J= 5.1 Hz, 1H); 4.49 (d, J= 12.0 Hz, 1H); 4.63 (d, J= 12.0 Hz, 1H); 4.65 (d, J= 5.1 Hz, 1H); 7.30-7.37 (m, 5H). <sup>13</sup>C-NMR (75 MHz) (CDCl<sub>3</sub>)  $\delta$  169.8, 152.8, 150.0, 142.0, 138.5, 128.6, 127.83, 127.78, 127.7, 123.9, 122.0, 73.4, 71.3, 60.6, 60.5, 60.2, 59.9, 51.1, 48.2, 43.7, 26.3, 26.1, 18.8, 18.5, 10.0, -3.7, -4.0, -5.15, -5.21. IR (NaCl, neat) 3346, 2917, 1760, 1461, 1411, 1353, 1254, 1108 cm<sup>-1</sup>. HRMS (FAB) calcd for C<sub>35</sub>H<sub>57</sub>N<sub>2</sub>O<sub>6</sub>Si<sub>2</sub> (M+H) 657.3755; found 657.3740.



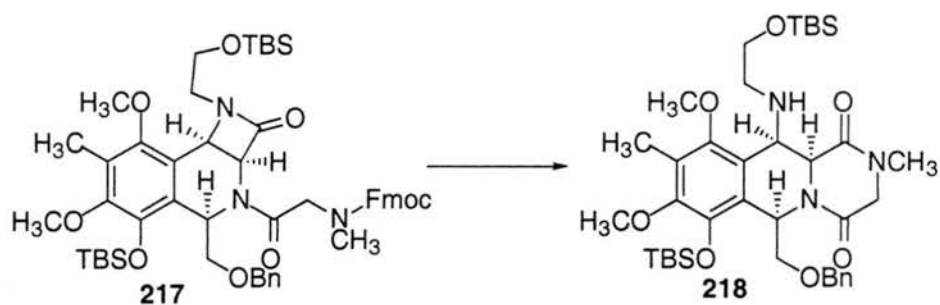


**3 $\alpha$ ,4 $\alpha$ -2-((N-methyl-N-fluorenylmethoxycarbonyl)amino)acetate-3,4-N-(O-*tert*-butyldimethylsilylhydroxyethyl)azetidione-8-O-(*tert*-butyldimethylsilyl)hydroxy-9,11-methoxy-10-methyltetrahydroisoquinoline (217).**

To prepare the acid chloride of *N*-Fmoc-sarcosine, oxalyl chloride (58  $\mu$ L, 0.67 mmol) and DMF (5.2  $\mu$ L, 0.067 mmol) were added to a solution of *N*-Fmoc-sarcosine (193 mg, 0.62 mmol) in 5 mL of  $\text{CH}_2\text{Cl}_2$  at RT. The reaction was allowed to stir for 1 h at RT and then hexanes (5 mL) was added. The heterogeneous mixture was pushed through a plug of glass wool and concentrated. The acid chloride was suspended in 2 mL of  $\text{CH}_2\text{Cl}_2$  and cooled to 0  $^\circ\text{C}$ . Amine **216** (370.4 mg, 0.56 mmol) was added in 3 mL of  $\text{CH}_2\text{Cl}_2$  followed by DMAP (75 mg, 0.62 mmol). The reaction was warmed up to RT and stirred for 2 h. Water was then added and the reaction extracted with  $\text{Et}_2\text{O}$ . The organic layer was separated, dried over  $\text{MgSO}_4$  and concentrated *in vacuo*. Column chromatography (1/1 EtOAc/ Hex) of the crude product gave 475 mg (89%) of **217** as a white foam.  $^1\text{H-NMR}$  (300 MHz) ( $\text{DMSO-d}_6$ , 120  $^\circ\text{C}$ )  $\delta$  0.028 (s, 3H); 0.03 (s, 3H); 0.16 (s, 3H); 0.22 (s, 3H); 0.86 (s, 9H); 0.99 (s, 9H); 2.22 (s, 3H); 2.88 (s, 3H); 2.91 (br s, 1H); 3.34 (dd,  $J = 3.6, 9.9$  Hz, 1H); 3.35 (dd,  $J = 6.0, 13.5$  Hz, 1H); 3.48 (dd,  $J = 6.0, 13.5$  Hz, 1H); 3.62 (dd,  $J = 3.6, 9.9$  Hz, 1H); 3.664 (s, 3H); 3.665 (d,  $J = 5.7$  Hz, 1H); 3.70 (s, 3H); 4.19 (d,  $J = 12.0$  Hz, 1H); 4.25-4.37 (m, 5H); 4.92 (br d,  $J = 12.9$  Hz, 1H); 5.04 (d,  $J = 5.4$  Hz, 1H); 5.23 (d,  $J = 5.4$  Hz, 1H); 5.96 (m, 1H); 7.05-7.08 (m, 2H); 7.19-7.31 (m, 5H); 7.36-7.41 (m, 2H); 7.64-7.66 (m, 2H); 7.83 (d,  $J = 7.5$  Hz, 2H). IR (NaCl, neat) 2928, 1758,

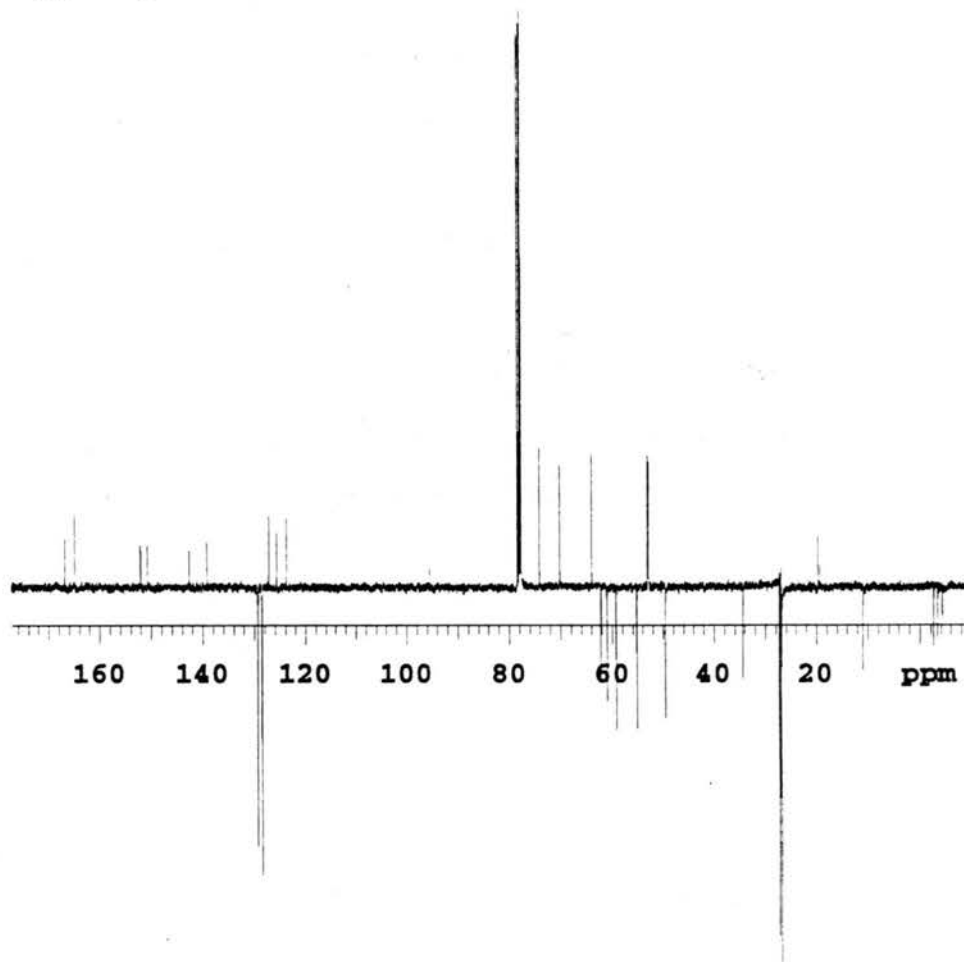
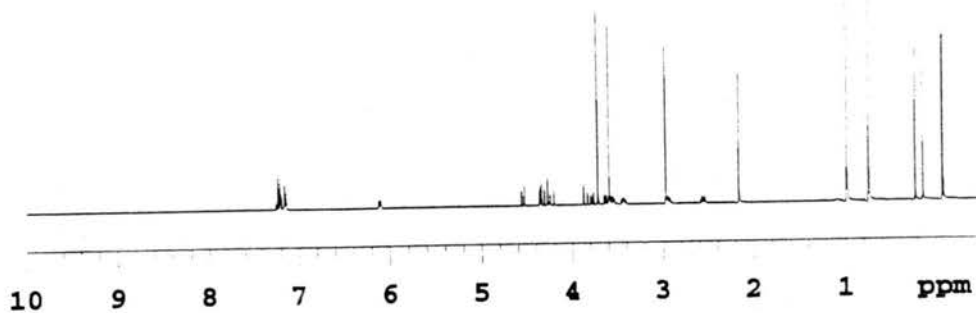
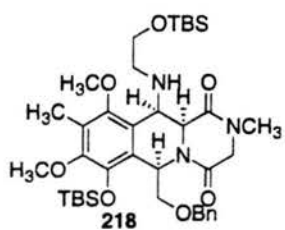
1710, 1461, 1408, 1361, 1255, 1074, 837  $\text{cm}^{-1}$ . HRMS (FAB) calcd for  $\text{C}_{53}\text{H}_{72}\text{N}_3\text{O}_9\text{Si}_2$   
(M+H) 950.4807; 950.4799 found.

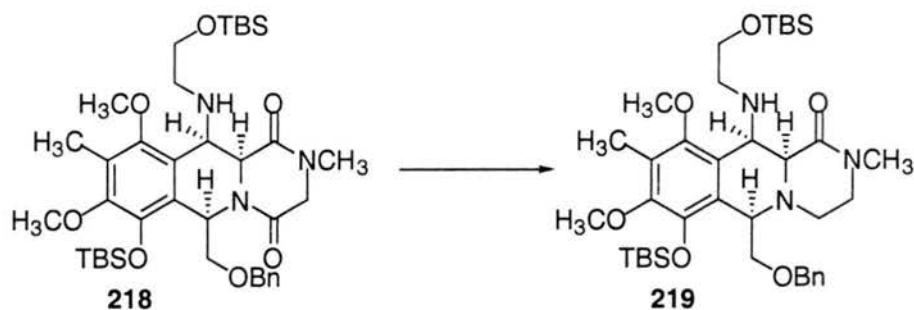




### Diketopiperazine (218).

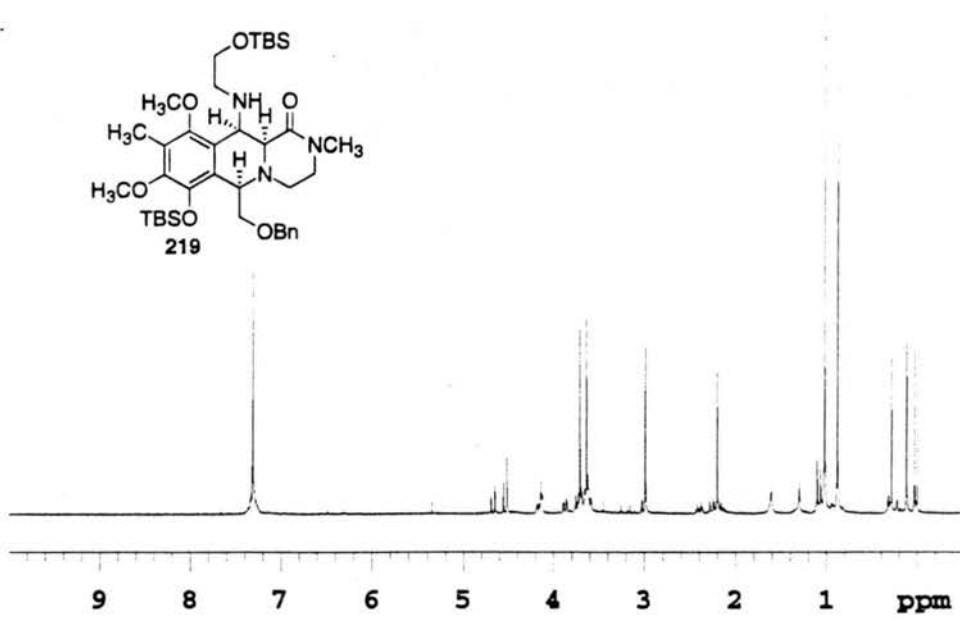
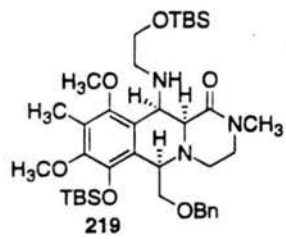
To a solution of **217** (650 mg, 0.68 mmol) in 9.5 mL of CH<sub>3</sub>CN was added piperidine (0.5 mL) at RT. The reaction stirred for 30 min and was then concentrated. The product was purified by column chromatography (1/1 EtOAc/Hex) to give 495 mg of **218** as a clear oil. TLC (3/1 EtOAc/Hex) R<sub>f</sub> = 0.53 (UV and dragendorff). <sup>1</sup>H-NMR (300 MHz) (CDCl<sub>3</sub>) δ -0.04 (s, 3H); -0.01 (s, 3H); 0.22 (s, 3H); 0.30 (s, 3H); 0.82 (s, 9H); 1.06 (s, 9H); 1.12 (br s, 1H, D<sub>2</sub>O exch.); 2.24 (s, 3H); 2.63 (dt, J= 4.5, 11.4 Hz, 1H); 2.98-3.05 (m, 1H); 3.05 (s, 3H); 3.51 (ddd, J= 4.1, 8.1, 9.9 Hz, 1H); 3.60-3.65 (m, 1H); 3.67 (s, 3H); 3.70 (dd, J= 8.1, 10.2 Hz, 1H); 3.80 (s, 3H); 3.86 (dd, J= 3.3, 10.2 Hz, 1H); 3.93 (1/2 ABq, J= 16.8 Hz, 1H); 4.31 (1/2 ABq, J= 16.8 Hz, 1H); 4.35 (d, J= 2.1 Hz, 1H); 4.37 (1/2 ABq, J=12.6 Hz, 1H); 4.43 (s, 1H); 4.63 (1/2 ABq, J= 12.6 Hz, 1H); 6.18 (dd, J= 3.3, 8.1 Hz, 1H); 7.22-7.32 (m, 5H). <sup>13</sup>C-NMR (100 MHz) (CDCl<sub>3</sub>) δ 166.0, 164.1, 151.2, 149.9, 141.8, 128.4, 128.5, 127.72, 127.66, 126.4, 124.9, 122.9, 73.3, 69.4, 63.2, 61.3, 60.2, 58.4, 54.4, 52.2, 52.1, 48.7, 33.5, 26.4, 26.0, 18.8, 18.4, 10.1, -3.46, -4.24, -5.12, -5.19. IR (NaCl, neat) 2931, 1668, 1455, 1410, 1337, 1256, 1009, 1068, 832, 781 cm<sup>-1</sup>. HRMS (FAB) calcd for C<sub>38</sub>H<sub>62</sub>N<sub>3</sub>O<sub>7</sub>Si<sub>2</sub> (M+H) 728.4126; found 728.4117.

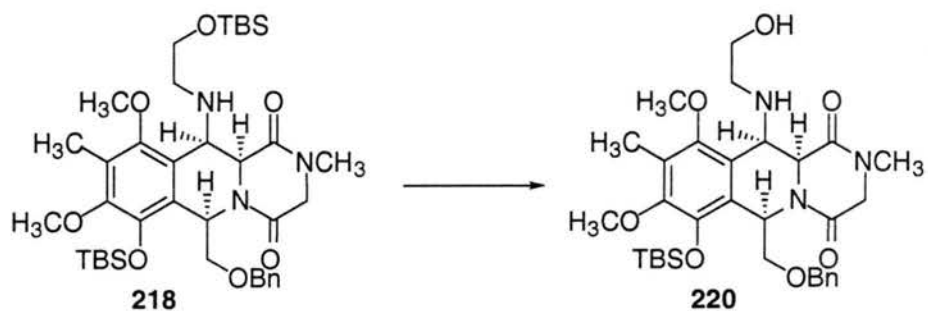




### Lactam (**219**).

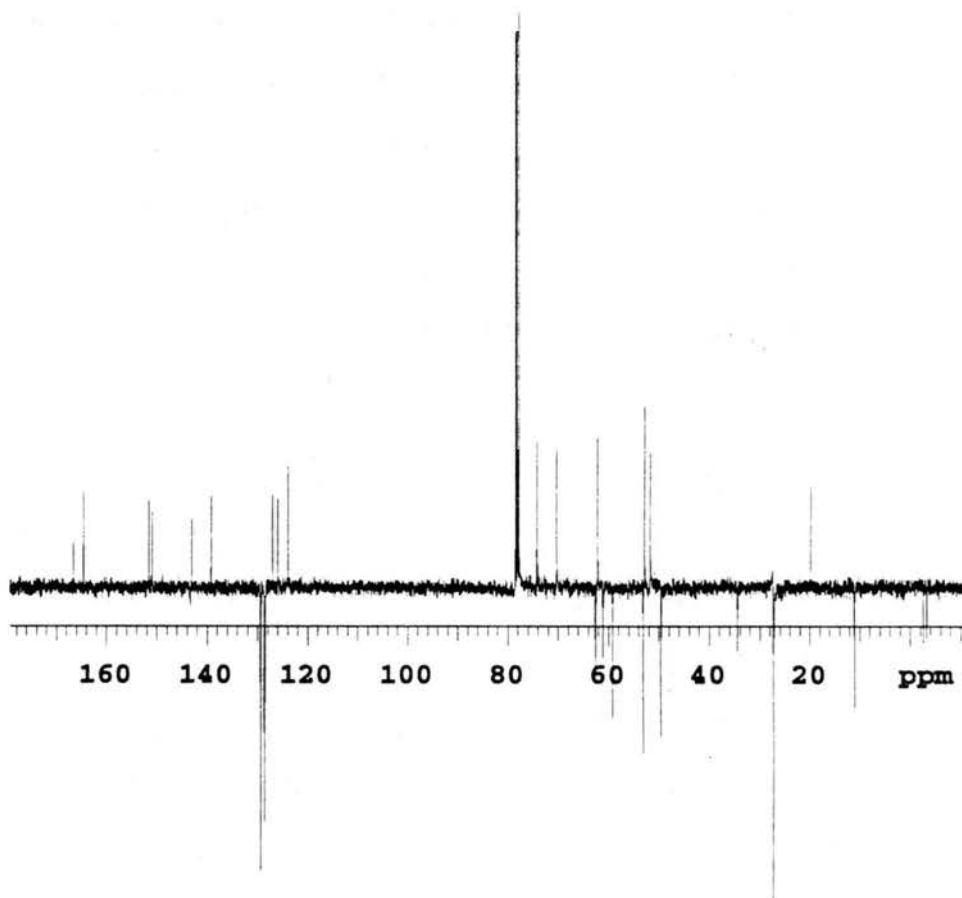
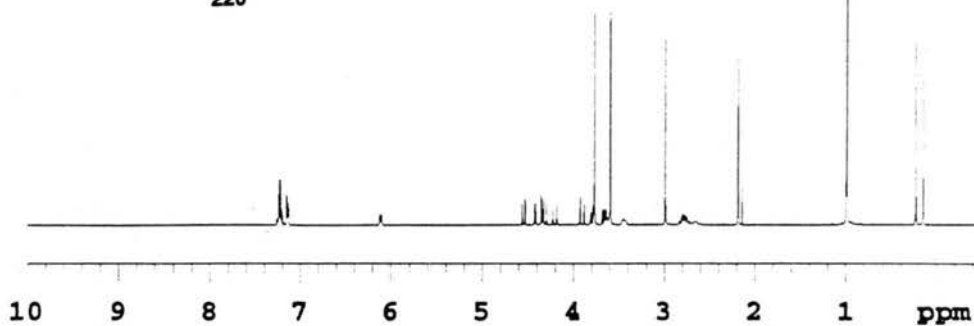
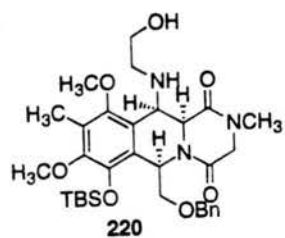
Lithium aluminum hydride (1 M in THF, 26  $\mu$ L, 0.026 mmol) was added to diketopiperazine **218** (15.6 mg, 0.021 mmol) in 0.5 mL of THF at 0  $^{\circ}$ C. The reaction was stirred for 1 h at 0  $^{\circ}$ C and was then quenched by the addition of H<sub>2</sub>O. The reaction was extracted with EtOAc and the combined organic layers were dried over MgSO<sub>4</sub> and concentrated. Purification by PTLC (3/1 EtOAc/Hex) gave 1.6 mg of **218** and 1.4 mg (9%) of **219** as an oil. TLC (3/1 EtOAc/Hex) R<sub>f</sub> = 0.17 (UV and anisaldehyde). <sup>1</sup>H-NMR (300 MHz) (CDCl<sub>3</sub>)  $\delta$  -0.001 (s, 3H); 0.03 (s, 3H); 0.12 (s, 3H); 0.28 (s, 3H); 0.88 (s, 9H); 1.03 (s, 9H); 1.32 (br s, 1H); 2.20 (s, 3H); 2.23-2.28 (m, 1H); 2.39 (dt, J = 3.9, 13.2 Hz, 1H); 2.99 (s, 3H); 3.58-3.66 (m, 4H); 3.64 (s, 3H); 3.69-3.76 (m, 2H); 3.71 (s, 3H); 3.87 (dd, J = 2.4, 9.9 Hz, 1H); 4.13-4.18 (m, 3H); 4.52 (s, 1H); 4.53 (d, J = 12.6 Hz, 1H); 4.67 (d, J = 12.6 Hz, 1H); 7.25-7.33 (m, 5H). IR (NaCl, neat) 2931, 1668, 1456, 1406, 1254, 1068, 1002, 836 cm<sup>-1</sup>. HRMS (FAB) calcd for C<sub>38</sub>H<sub>62</sub>N<sub>3</sub>O<sub>6</sub>Si<sub>2</sub> (M-H) 712.4177; found 712.4187.

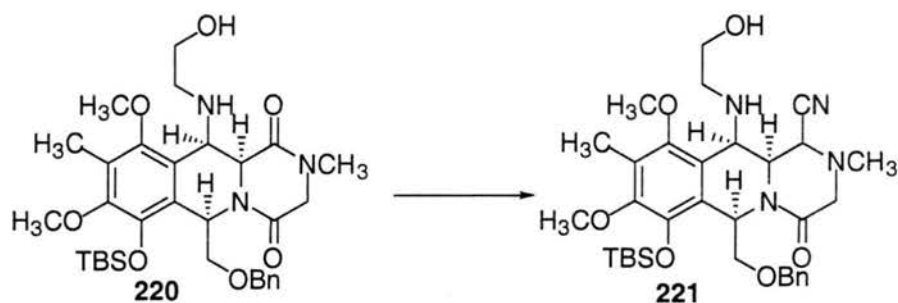




### Amino alcohol (**220**).

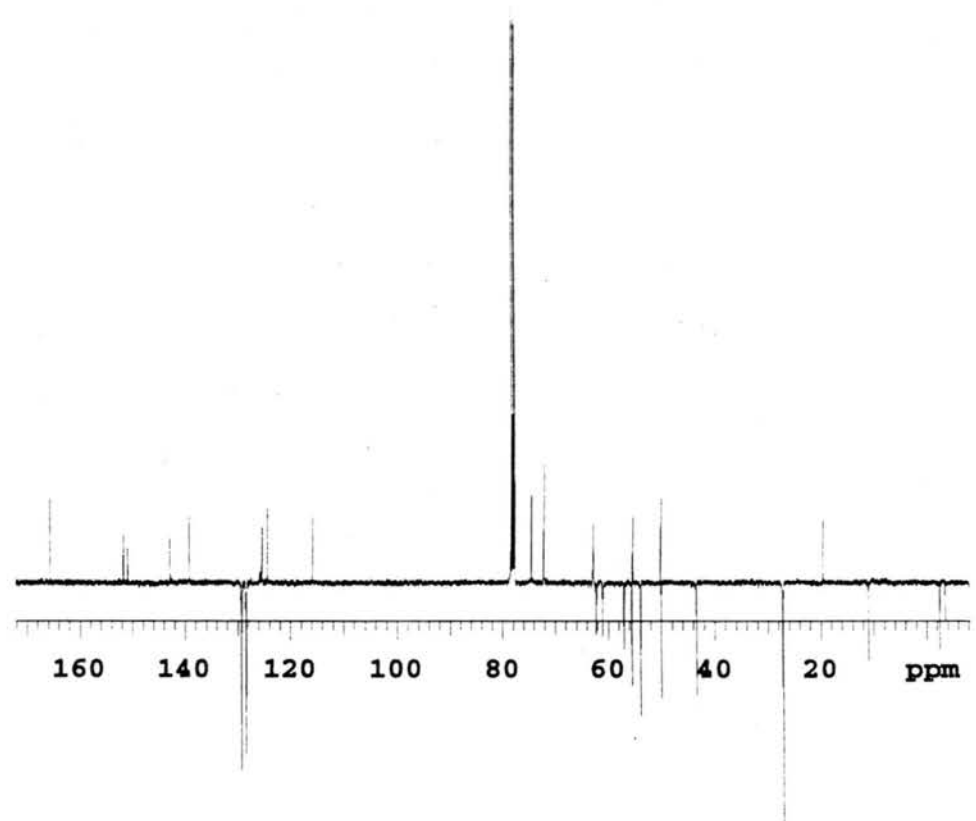
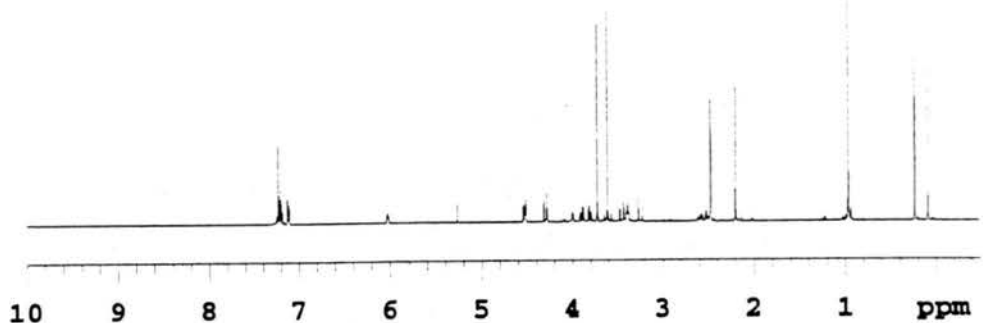
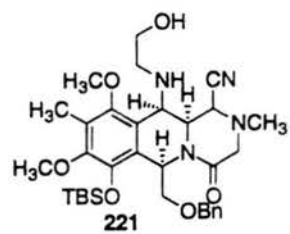
*O*-TBS protected diketopiperazine **218** (840 mg, 1.15 mmol) was stirred in 20 mL of a HOAc:THF:H<sub>2</sub>O (3:1:1) solvent system overnight at RT. The reaction was concentrated, and the residue taken up in EtOAc and washed with H<sub>2</sub>O followed by NaHCO<sub>3</sub> (sat.). The organic layer was separated, dried over MgSO<sub>4</sub> and concentrated to give 692 mg of crude product, which was chromatographed (10/1 CH<sub>2</sub>Cl<sub>2</sub>/ MeOH) to give 571 mg of **220**. TLC (10/1 CH<sub>2</sub>Cl<sub>2</sub>/ MeOH) R<sub>f</sub> = 0.50 (UV and dragendorff). <sup>1</sup>H-NMR (300 MHz) (CDCl<sub>3</sub>) δ -0.15 (s, 3H); 0.24 (s, 3H); 0.99 (s, 9H); 2.18 (s, 3H); 2.65 (br s, 1H, D<sub>2</sub>O exch.); 2.74 (ddd, J= 2.7, 2.7, 9.9 Hz, 1H); 2.85 (ddd, J= 2.7, 3.9, 9.9 Hz, 1H); 2.99 (s, 3H); 3.42-3.46 (m, 1H); 3.59 (s, 3H); 3.60-3.65 (m, 1H); 3.66 (dd, J= 5.7, 7.8 Hz, 1H); 3.77 (s, 3H); 3.80 (dd, J= 2.4, 7.8 Hz, 1H); 3.91 (1/2 ABq, J= 12.9 Hz, 1H); 4.20 (1/2 ABq, J= 12.9 Hz, 1H); 4.31 (1/2 ABq, J= 9.6 Hz, 1H); 4.35 (d, J= 1.8 Hz, 1H); 4.42 (m, 1H); 4.54 (1/2 ABq, J= 9.6 Hz, 1H); 6.11 (dd, J= 2.4, 5.7 Hz, 1H); 7.13-7.15 (m, 2H); 7.20-7.24 (m, 3H). <sup>13</sup>C-NMR (100 MHz) (CDCl<sub>3</sub>) δ 165.7, 163.7, 150.7, 150.0, 142.2, 138.3, 128.5, 127.8, 127.7, 126.1, 125.1, 123.1, 73.3, 69.4, 61.7, 61.3, 60.2, 58.3, 52.3, 52.0, 50.8, 48.7, 33.6, 26.3, 18.8, 10.1, -3.5, -4.2. IR (NaCl, neat) 3446, 2933, 1667, 1455, 1410, 1339, 1257, 1117, 1069, 832 cm<sup>-1</sup> HRMS (FAB) calcd for C<sub>32</sub>H<sub>48</sub>N<sub>3</sub>O<sub>7</sub>Si<sub>2</sub> (M+H) 614.3262; found 614.3266.

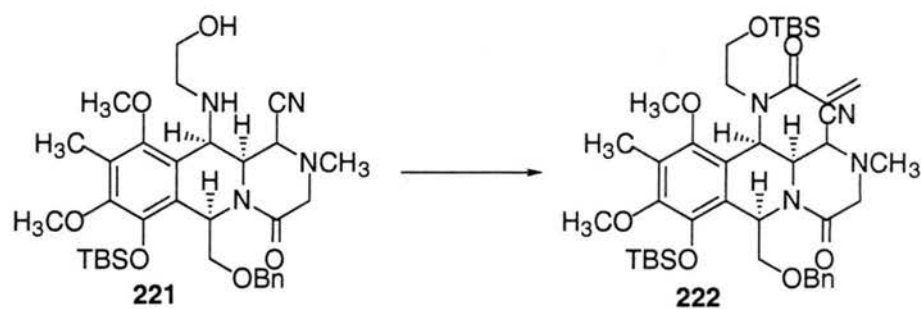




### Amino nitrile (221).

LiAl(OEt)<sub>3</sub> (341  $\mu$ L, 0.34 mmol, in THF), which was prepared by adding 1 eq of EtOH (abs.) to a 1 M solution of LiAlH<sub>4</sub> (THF, Aldrich), was added to diketopiperazine **220** (170 mg, 0.28 mmol) in THF (6 mL) at 0 °C. The reaction stirred for 30 min and then a solution of NaCN (1 M, 3 mL) was added and the reaction allowed to warm up to RT and stirred for 1 h. Rochelle's salt was added (sat. K<sup>+</sup>-Na<sup>+</sup> tartrate soln.) and the reaction extracted with EtOAc. The quenched reaction was extracted with EtOAc and the organic layer dried over MgSO<sub>4</sub> and concentrated. The crude product was purified by column chromatography (5% MeOH in CH<sub>2</sub>Cl<sub>2</sub>) to give 151 mg (85%) of **221** as an oil. TLC (10/1 CH<sub>2</sub>Cl<sub>2</sub>/ MeOH) R<sub>f</sub> = 0.23 (UV and anisaldehyde). <sup>1</sup>H-NMR (400 MHz) (CDCl<sub>3</sub>)  $\delta$  0.086 (s, 3H); 0.23 (s, 3H); 0.96 (s, 9H); 2.20 (s, 3H); 2.47 (s, 3H); 2.49-2.53 (m, 1H); 2.56-2.62 (m, 1H); 3.12 (br s, 2H); 3.25 (1/2 ABq, J= 12.3 Hz, 1H); 3.38-3.41 (m, 2H); 3.45 (1/2 ABq, J= 12.3 Hz, 1H); 3.62 (s, 3H); 3.73 (s, 3H); 3.81 (dd, J= 2.4, 7.5 Hz, 1H); 3.90 (dd, J= 3.9, 7.5 Hz, 1H); 4.00 (br d, J= 2.1 Hz, 1H); 4.28 (s, 1H); 4.30 (1/2 ABq, J= 9.3 Hz, 1H); 4.51-4.53 (m, 1H); 4.53 (1/2 ABq, J= 9.3 Hz, 1H); 6.02 (dd, J= 2.4, 3.9 Hz, 1H); 7.11-7.13 (m, 2H); 7.18-7.25 (m, 3H). <sup>13</sup>C-NMR (100 MHz) (CDCl<sub>3</sub>)  $\delta$  164.8, 150.9, 150.1, 142.0, 138.4, 128.5, 127.62, 127.56, 124.6, 123.6, 115.0, 73.7, 71.4, 62.0, 61.4, 60.2, 56.2, 54.7, 54.6, 53.0, 49.3, 49.2, 42.6, 26.3, 18.8, 10.1, -3.5, -4.4. IR (NaCl, neat) 3349, 2938, 2860, 1654, 1459, 1411, 1255, 1101, 1066, 1107, 837 cm<sup>-1</sup>. HRMS (FAB) calcd for C<sub>33</sub>H<sub>49</sub>N<sub>4</sub>O<sub>6</sub>Si (M+H) 625.3421; found 625.3425.

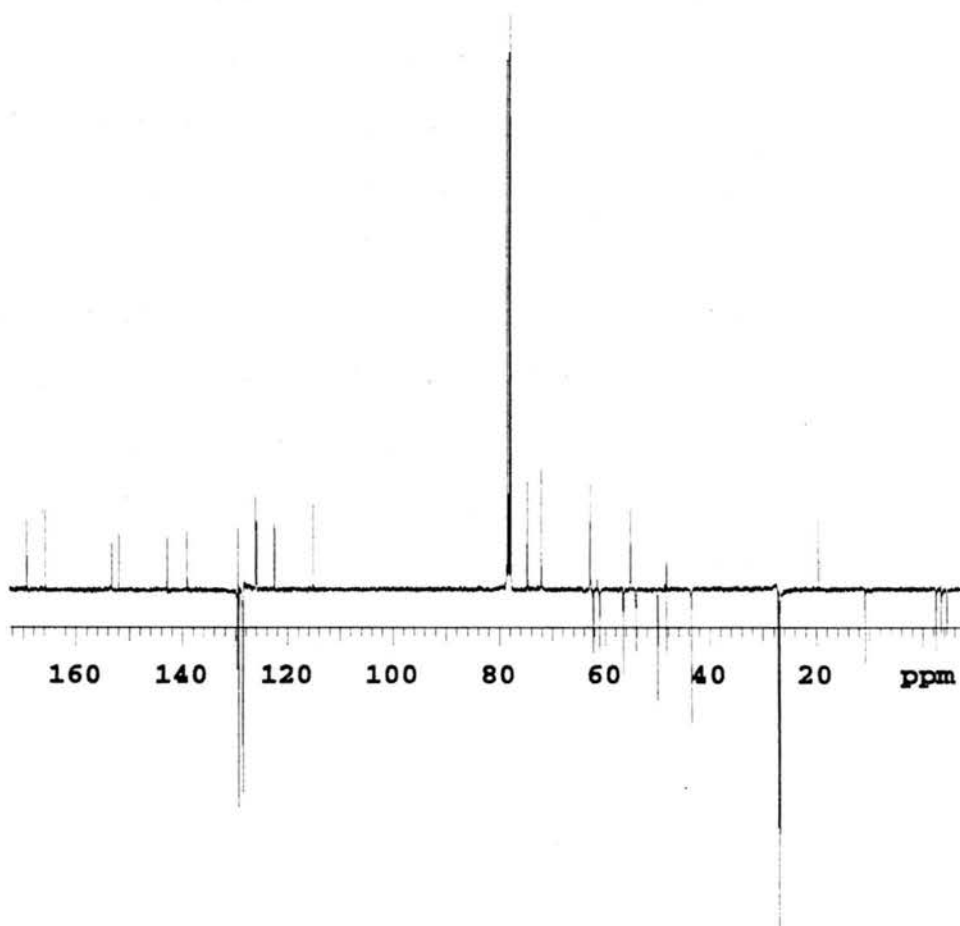
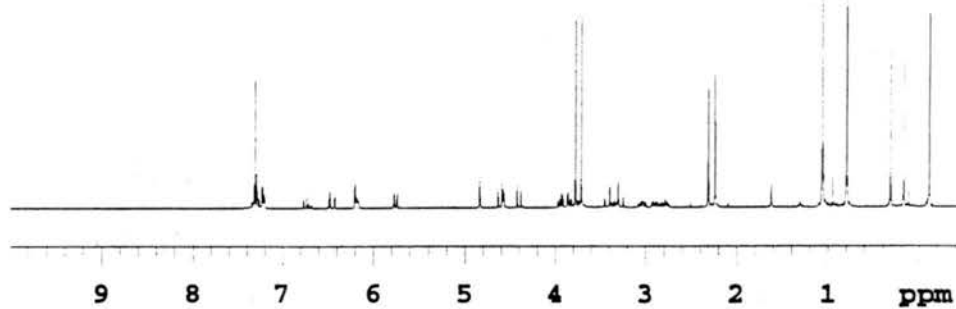
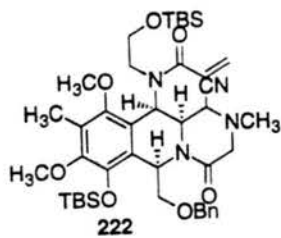


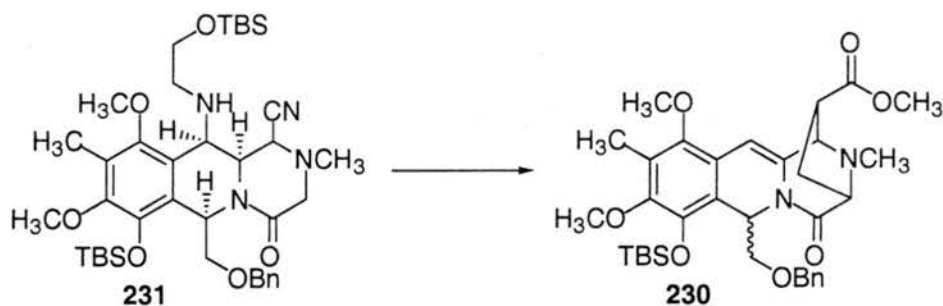


**$\alpha,\beta$ -unsaturated amide (222).**

*tert*-Butyldimethylsilyl chloride (18 mg, 0.12 mmol) and  $\text{NEt}_3$  (17  $\mu\text{L}$ , 0.12 mmol) were added to amino alcohol **221** (62 mg, 0.10 mmol) in 100  $\mu\text{L}$  of THF at RT and the reaction was allowed to stir overnight at RT. Next, acryloyl chloride (9.5  $\mu\text{L}$ , 0.12 mmol) was added followed by another portion of  $\text{NEt}_3$  (17  $\mu\text{L}$ , 0.12 mmol) at RT. The reaction was stirred for 1 h and then  $\text{H}_2\text{O}$  was added and the quenched reaction was extracted with EtOAc. The organic layer was dried, concentrated and purified by column chromatography (2/1 Hex/ EtOAc) to give 61 mg of **222** as white needles. m.p.= 119-121  $^\circ\text{C}$  (EtOH). TLC (1/1 Hex/ EtOAc)  $R_f$  = 0.53 (UV and anisaldehyde (red)).  $^1\text{H-NMR}$  (400 MHz) ( $\text{CDCl}_3$ )  $\delta$  -0.194 (s, 3H); -0.191 (s, 3H); 0.10 (s, 3H); 0.24 (s, 3H); 0.72 (s, 9H); 0.99 (s, 9H); 2.16 (s, 3H); 2.23 (s, 3H); 2.71 (ddd,  $J$ = 3.6, 3.6, 6.6 Hz, 1H); 2.81 (ddd,  $J$ = 3.9, 6.0, 11.4 Hz, 1H); 2.96 (ddd,  $J$ = 4.5, 6.0, 7.5 Hz, 1H); 3.20 (1/2 ABq,  $J$ = 12.6 Hz, 1H); 3.27 (ddd,  $J$ = 4.5, 6.3, 11.4 Hz, 1H); 3.34 (1/2 ABq,  $J$ = 12.6 Hz, 1H); 3.64 (s, 3H); 3.70 (s, 3H); 3.77 (dd,  $J$ = 2.4, 7.5 Hz, 1H); 3.87 (dd,  $J$ = 3.9, 7.5 Hz, 1H); 4.32 (1/2 ABq,  $J$ = 9.0 Hz, 1H); 4.50 (d,  $J$ = 2.7 Hz, 1H); 4.53 (1/2 ABq,  $J$ = 9.0 Hz, 1H); 4.76 (s, 1H); 5.67 (dd,  $J$ = 1.7, 7.5 Hz, 1H); 6.09 (dd,  $J$ = 2.4, 3.9 Hz, 1H); 6.12 (d,  $J$ = 2.7 Hz, 1H); 6.37 (dd,  $J$ = 1.7 Hz, 12.3 Hz, 1H); 6.65 (dd,  $J$ = 7.5, 12.3 Hz, 1H); 7.13-7.15 (m, 2H); 7.19-7.26 (m, 3H).  $^{13}\text{C-NMR}$  (100 MHz) ( $\text{CDCl}_3$ )  $\delta$  168.4, 164.9, 152.4, 151.0, 142.0, 138.2, 128.7, 128.6, 128.5, 127.6, 125.2, 125.0, 121.7, 114.2, 73.8, 71.2, 61.9, 61.4, 60.1, 55.6, 54.2, 53.20, 53.17, 49.1, 47.40, 47.35, 42.6, 26.3, 26.0, 18.7, 18.4, 9.9, -3.4, -4.4, -5.5. IR (NaCl, neat) 2932, 2858, 2360, 2342, 1666, 1651,

1610, 1476, 1424, 1254, 1099, 1010, 839  $\text{cm}^{-1}$ . HRMS (FAB) calcd for  $\text{C}_{42}\text{H}_{65}\text{N}_4\text{O}_7\text{Si}_2$   
(M+H) 793.4392; found 793.4375.

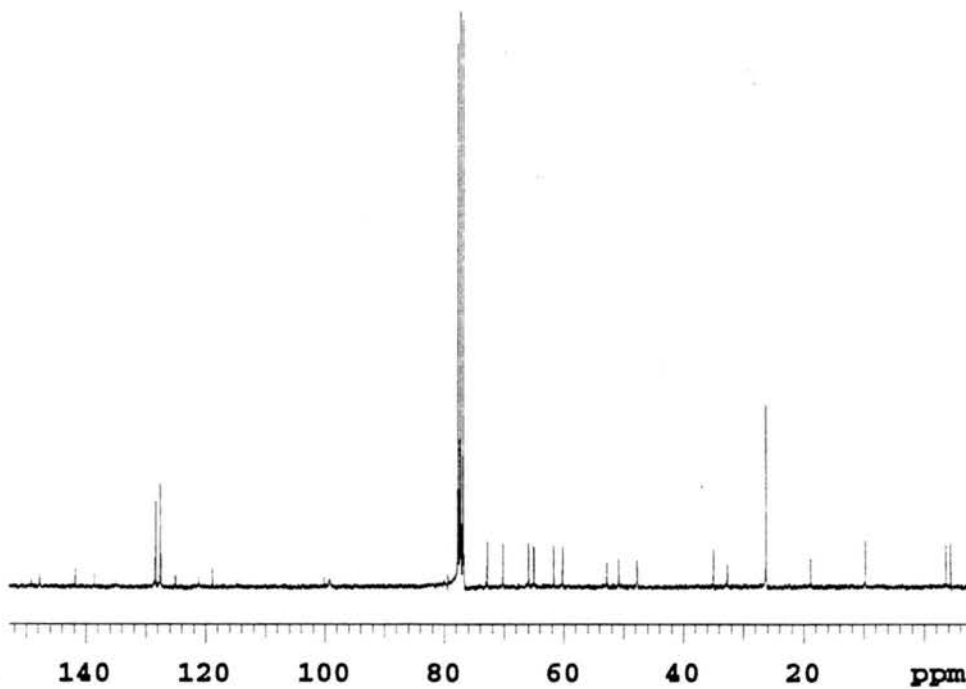
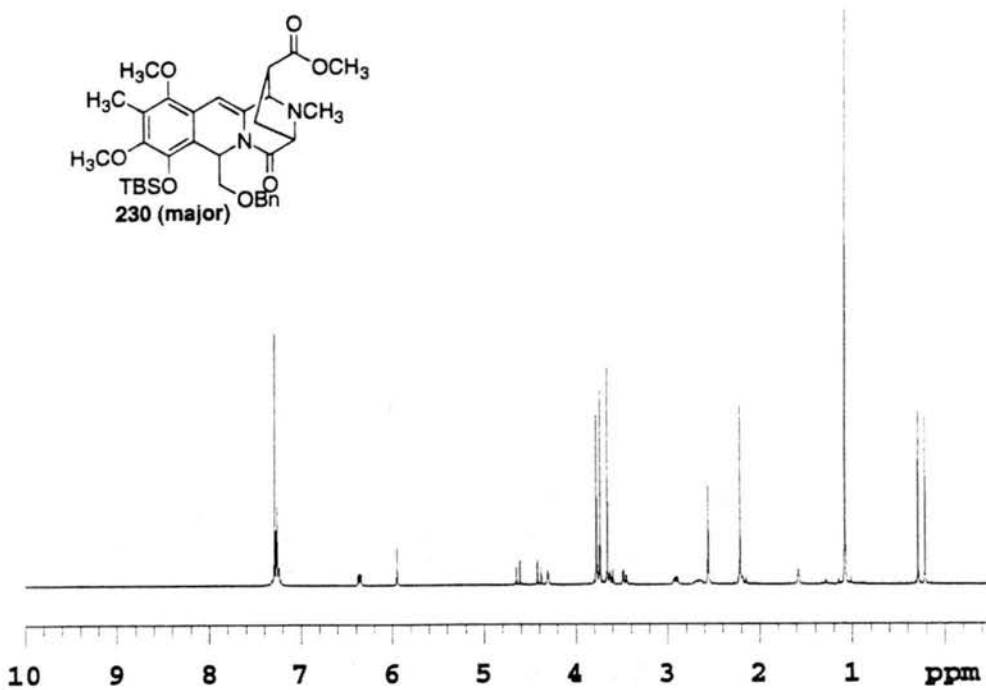
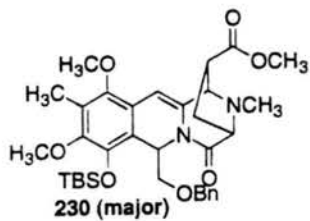


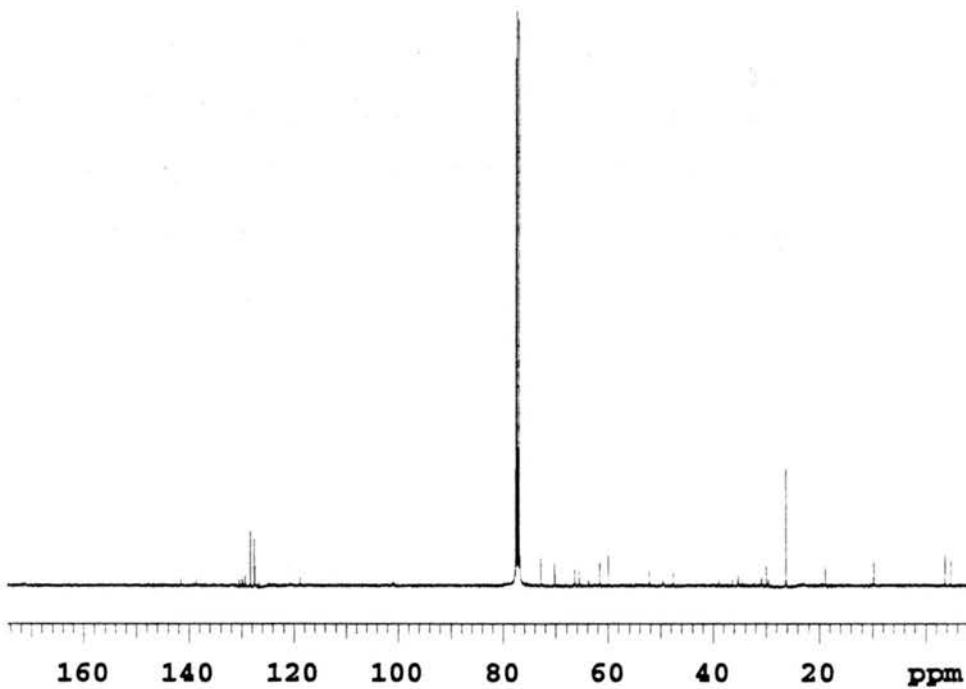
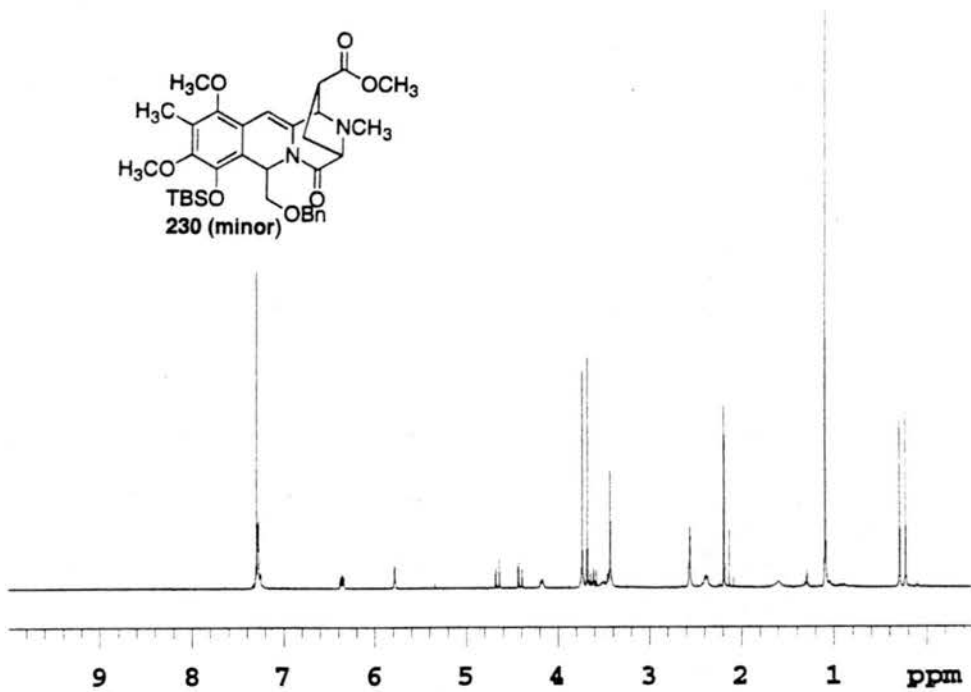
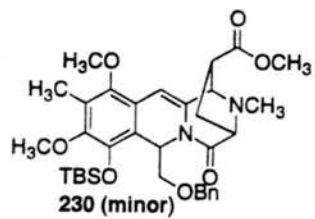


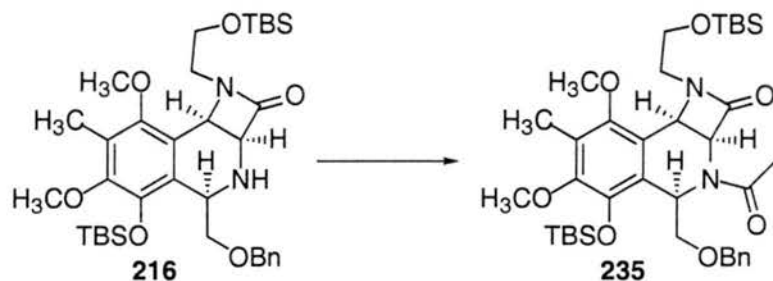
**Methyl-5,7,8,9,10,11-hexahydro-1,3-methoxy-2-methyl-4-O-(*tert*-butyldimethylsilyl)-5-benzoxymethyl-7-oxo-8,11-iminoazepino[1,2-*b*]isoquinoline-10-carboxylate (230).**

To aminonitrile **231** (9.5 mg, 0.013 mmol) in 0.2 mL of EtOH was added AgNO<sub>3</sub> (2.6 mg, 0.15 mmol) at RT. The reaction stirred for 10 min and was then cooled to 0 °C. Methyl acrylate (5.8 μL, 0.65 mmol) followed by K<sub>2</sub>CO<sub>3</sub> (2 mg, 0.015 mmol) was added and the reaction was allowed to stir at 0 °C and was then warmed up to RT. The reaction stirred for 12 h at RT. The reaction was filtered through celite and the crude product purified by PTLC (1/1 EtOAc/Hex) to afford 5.1 mg (63%) of **230** obtained as an oil in a 2:3 mixture of diastereomers. **Diastereomer A (major):** TLC (1/1 Hex/ EtOAc) R<sub>f</sub> = 0.47 (UV and PMA). <sup>1</sup>H-NMR (300 MHz) (CDCl<sub>3</sub>) δ 0.21 (s, 3H); 0.29 (s, 3H); 1.08 (s, 9H); 1.60 (s, 1H); 2.15-2.19 (m, 1H); 2.21 (s, 3H); 2.56 (s, 3H); 2.61-2.71 (m, 1H); 2.91 (dd, J= 4.7, 9.8 Hz, 1H); 3.47 (dd, J= 3.9, 10.5 Hz, 1H); 3.63 (dd, J= 7.8, 10.5 Hz, 1H); 3.66 (s, 3H); 3.74 (s, 3H); 3.78 (s, 3H); 4.31 (br s, 1H); 4.40 (1/2 ABq, J= 11.7 Hz, 1H); 4.63 (1/2 ABq, J= 11.7 Hz, 1H); 5.95 (s, 1H); 6.36 (dd, J= 3.9, 7.8 Hz, 1H); 7.24-7.29 (m, 5H). <sup>13</sup>C-NMR (100 MHz) (CDCl<sub>3</sub>) δ 149.2, 147.7, 141.7, 138.5, 134.9, 128.4, 127.5, 125.0, 121.1, 118.8, 110.2, 99.2, 79.4, 72.8, 70.2, 65.9, 65.0, 61.7, 60.2, 52.8, 50.8, 47.7, 35.0, 32.7, 26.2, 18.8, 9.7, -3.7, -4.5. IR (NaCl, neat) 2947, 1739, 1688, 1635, 1462, 1353, 1244, 1071, 1005, 837 cm<sup>-1</sup>. HRMS (FAB) calcd for C<sub>34</sub>H<sub>47</sub>N<sub>2</sub>O<sub>7</sub>Si (M+H) 623.3153; found 623.3144.

**Diastereomer B (minor):** TLC (1/1 Hex/ EtOAc)  $R_f = 0.23$  (UV and PMA).  $^1\text{H-NMR}$  (300 MHz) ( $\text{CDCl}_3$ )  $\delta$  0.22 (s, 3H); 0.29 (s, 3H); 1.09 (s, 9H); 2.18 (s, 3H); 2.35-2.43 (m, 1H); 2.49 (t,  $J = 7.2$  Hz, 1H); 2.68 (t,  $J = 7.2$  Hz, 1H); 3.21 (dt,  $J = 7.2, 10.5$  Hz, 1H); 3.42 (s, 3H); 3.41-3.46 (m, 1H); 3.52-3.64 (m, 3H); 3.67 (s, 3H); 3.73 (s, 3H); 4.12-4.23 (m, 2H); 4.40 (1/2 ABq,  $J = 11.7$  Hz, 1H); 4.64 (1/2 ABq,  $J = 11.7$  Hz, 1H); 5.77 (br s, 1H); 6.35 (dd,  $J = 4.2, 7.8$  Hz, 1H); 7.22-7.37 (m, 5H). IR (NaCl, neat) 2933, 1739, 1687, 1636, 1463, 1358, 1257, 1074, 1008, 835  $\text{cm}^{-1}$ . HRMS (FAB) calcd for  $\text{C}_{34}\text{H}_{47}\text{N}_2\text{O}_7\text{Si}$  (M+H) 623.3153; found 623.3146.

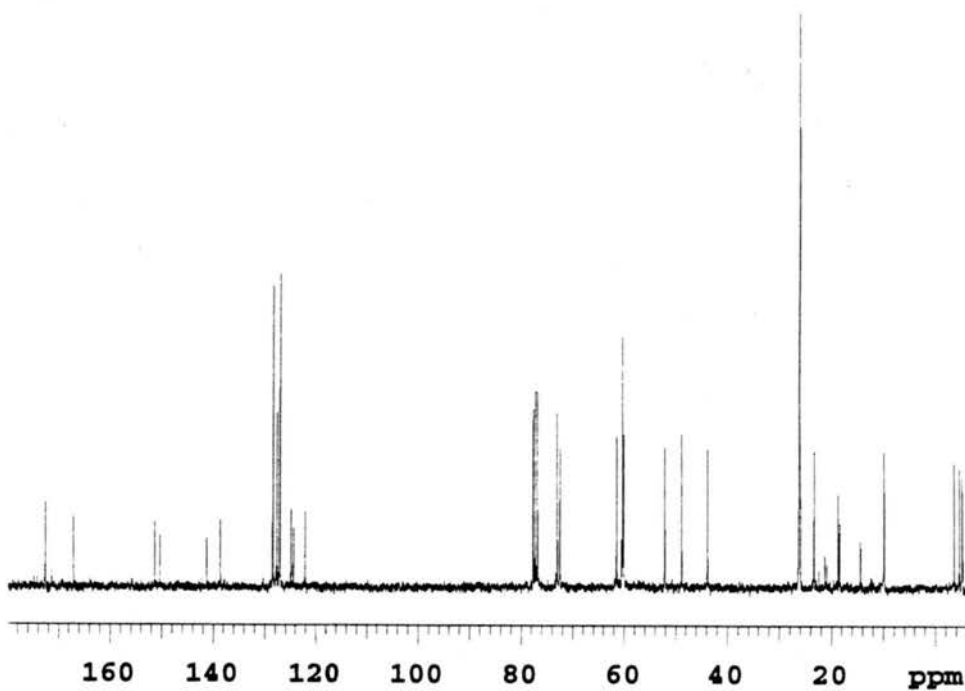
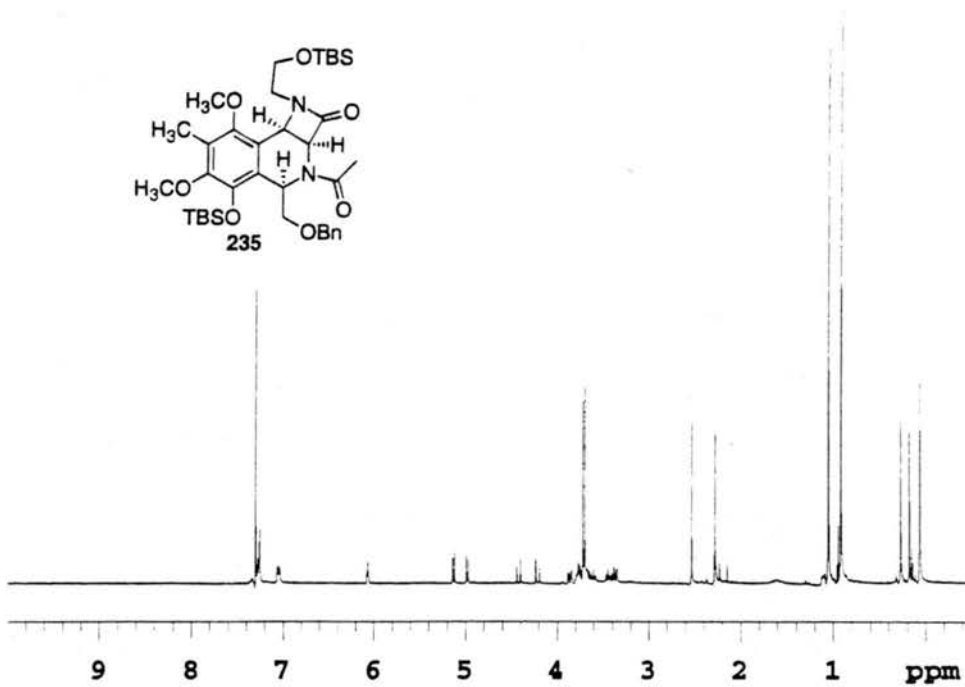
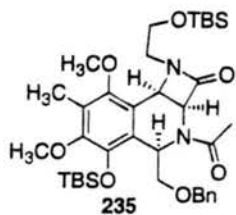


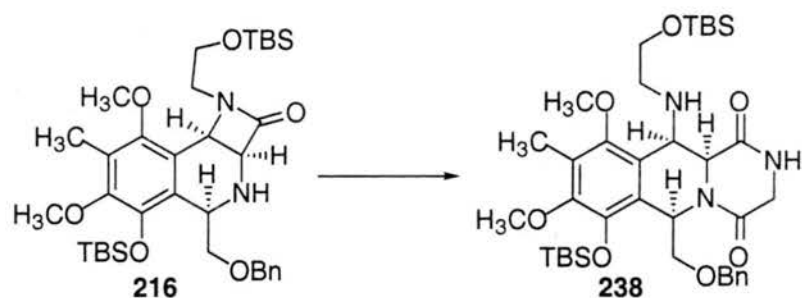




**3 $\alpha$ ,4 $\alpha$ -2-acetyl-3,4-N-(*O*-*tert*-butyldimethylsilylhydroxyethyl)azetidione-8-*O*-(*tert*-butyldimethylsilyl)hydroxy-9,11-methoxy-10-methyltetrahydroisoquinoline (235).**

Pyridine (0.48 mL, 5.94 mmol) and acetic anhydride (2.5 mL, 26.4 mmol) were added to  $\beta$ -lactam **216** (121 mg, 0.18 mmol) at RT. The reaction stirred for 24 h and was then concentrated. The crude product was purified by chromatography (1/1 EtOAc/Hex) to give 116 mg (92%) of **235** as an oil. TLC (1/1 EtOAc/Hex)  $R_f$  = 0.60 (UV and anisaldehyde).  $^1\text{H-NMR}$  (300 MHz) ( $\text{CDCl}_3$ )  $\delta$  0.07 (s, 3H); 0.08 (s, 3H); 0.19 (s, 3H); 0.28 (s, 3H); 0.93 (s, 9H); 1.06 (s, 9 H); 2.29 (s, 3H); 2.54 (s, 3H); 3.36 (dd,  $J$ = 2.1, 9.6 Hz, 1H); 3.40-3.47 (m, 1H); 3.58-3.68 (m, 2H); 3.70 (s, 3H); 3.72 (s, 3H); 3.74-3.79 (m, 1H); 3.86 (dd,  $J$ = 2.1, 9.6 Hz, 1H); 4.22 (1/2 ABq,  $J$ = 12.6 Hz, 1H); 4.42 (1/2 ABq,  $J$ = 12.6 Hz, 1H); 4.99 (d,  $J$ = 5.4 Hz, 1H); 5.13 (d,  $J$ = 5.4 Hz, 1H); 6.07 (m, 1H); 7.04-7.07 (m, 2H); 7.26-7.29 (m, 3H).  $^{13}\text{C-NMR}$  (100 MHz) ( $\text{CDCl}_3$ )  $\delta$  172.6, 167.1, 151.4, 150.4, 141.2, 138.6, 128.4, 127.6, 127.1, 124.9, 124.4, 73.0, 72.5, 61.5, 60.6, 60.4, 60.1, 52.1, 48.8, 43.8, 26.2, 26.0, 23.3, 18.7, 18.4, 9.9, -3.6, -4.6, -5.2, -5.3. IR (NaCl, neat) 2933, 1760, 1662, 1463, 1391, 1257, 1082, 837  $\text{cm}^{-1}$ .

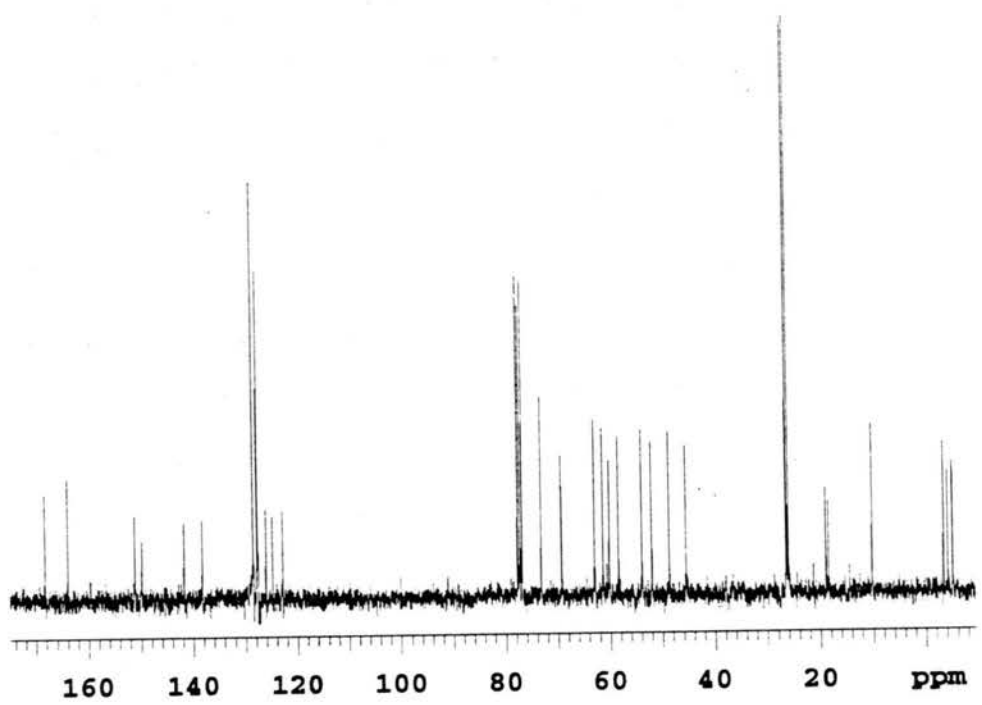
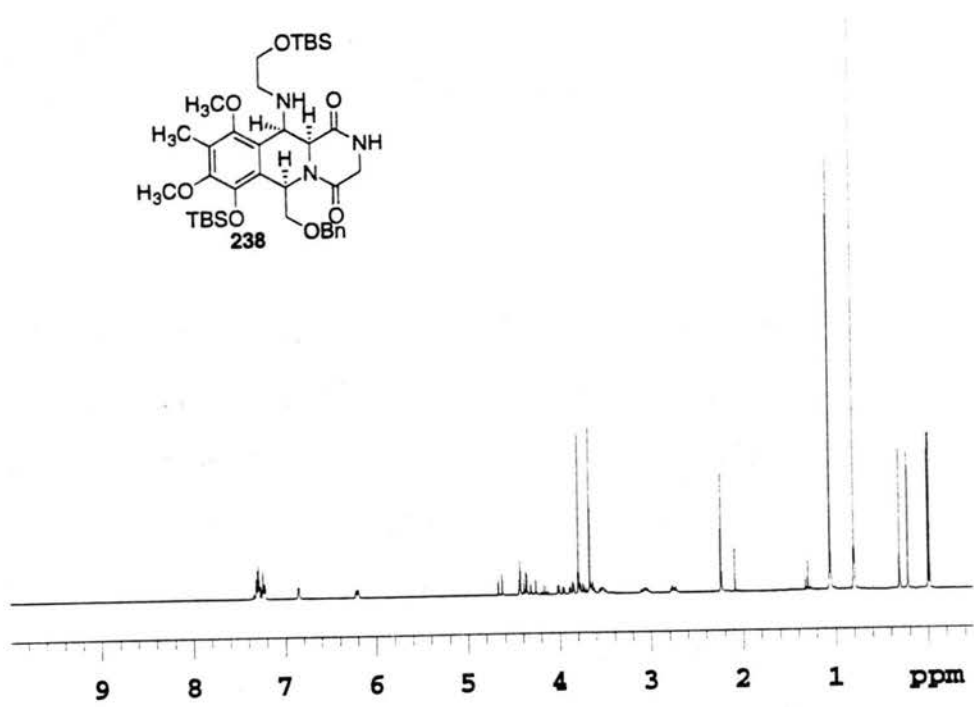
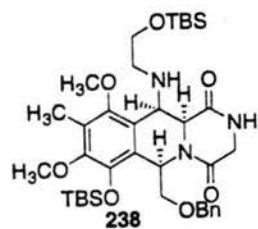


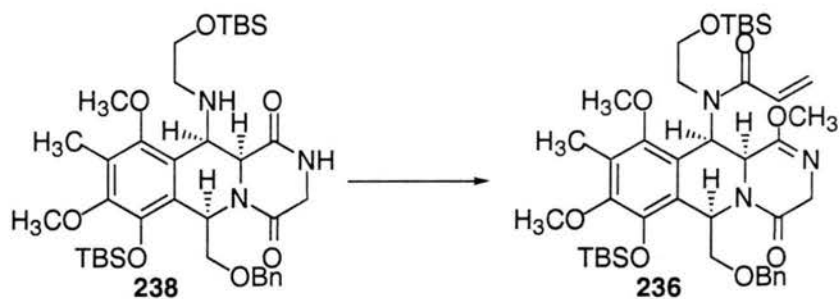


### Diketopiperazine (238).

To prepare the acid chloride of *N*-Fmoc-glycine, oxalyl chloride (69  $\mu\text{L}$ , 0.80 mmol) and DMF (6.2  $\mu\text{L}$ , 0.08 mmol) were added to a solution of *N*-Fmoc-glycine (220 mg, 0.74 mmol) in 6 mL of  $\text{CH}_2\text{Cl}_2$  at RT. The reaction was allowed to stir for 1 h at RT and then hexanes (6 mL) was added. The heterogeneous mixture was pushed through a plug of glass wool and concentrated. The acid chloride was resuspended in 3 mL of  $\text{CH}_2\text{Cl}_2$  and cooled to 0  $^\circ\text{C}$ . Amine **216** (441.0 mg, 0.67 mmol) was added in 3 mL of  $\text{CH}_2\text{Cl}_2$  followed by DMAP (94 mg, 0.74 mmol). The reaction was warmed up to RT and stirred for 2 h. Water was then added and the reaction extracted with  $\text{CH}_2\text{Cl}_2$ . The organic layer was separated, dried over  $\text{MgSO}_4$  and concentrated *in vacuo*. Column chromatography (1/1 Hex/EtOAc,  $R_f = 0.65$  (UV and PMA)) of the crude product gave 533 mg (89%) of the amide. Piperidine (100  $\mu\text{L}$ ) was added to the amide (90.8 mg, 0.097 mmol) in 1.9 mL of  $\text{CH}_3\text{CN}$  and the reaction stirred at RT. After 2 h the reaction was concentrated and purified by column chromatography to yield 43 mg (53% for two steps) of **238** as a white foam. TLC (EtOAc)  $R_f = 0.49$  (UV and anisaldehyde).  $^1\text{H-NMR}$  (300 MHz) ( $\text{CDCl}_3$ )  $\delta$  -0.018 (s, 3H); -0.001 (s, 3H); 0.22 (s, 3H); 0.31 (s, 3H); 0.80 (s, 9H); 1.06 (s, 9H); 1.27 (br s, 1H); 2.24 (s, 3H); 2.75 (dt,  $J = 4.2, 11.4$  Hz, 1H); 3.07 (ddd,  $J = 4.2, 8.4, 11.4$  Hz, 1H); 3.53 (ddd,  $J = 4.2, 8.4, 10.2$  Hz, 1H); 3.62-3.69 (m, 1H); 3.67 (s, 3H); 3.74 (dd,  $J = 7.8, 10.2$  Hz, 1H); 3.80 (s, 3H); 3.87 (dd,  $J = 3.3, 10.2$  Hz, 1H); 3.98 (d,  $J = 3.3, 16.8$  Hz, 1H); 4.29 (d,  $J = 16.8$  Hz, 1H); 4.36 (d,  $J = 2.1$  Hz, 1H); 4.41 (1/2 ABq,  $J = 12.0$  Hz, 1H); 4.43 (d,  $J = 2.1$  Hz, 1H); 4.65 (1/2 ABq,  $J = 12.0$  Hz, 1H); 6.21 (dd,  $J = 3.3, 7.8$  Hz,

1H); 6.85 (m, 1H); 7.22-7.32 (m, 5H). <sup>13</sup>C-NMR (100 MHz) (CDCl<sub>3</sub>) δ 168.2, 163.9, 151.1, 149.8, 141.7, 138.2, 128.5, 127.7, 126.1, 124.8, 122.8, 73.2, 69.3, 63.0, 61.4, 60.2, 58.4, 53.9, 52.0, 48.7, 45.5, 26.4, 26.1, 18.9, 18.4, 10.2, -3.4, -4.2, -5.07, -5.14. IR (NaCl, neat) 3241, 2934, 1671, 1456, 1411, 1331, 1256, 1075, 1008, 834 cm<sup>-1</sup>.

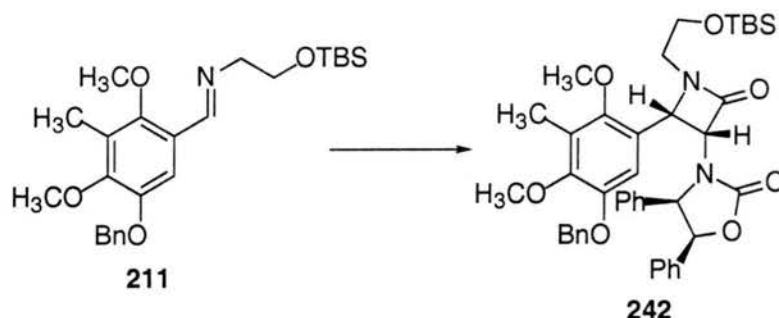




### Lactim ether (236).

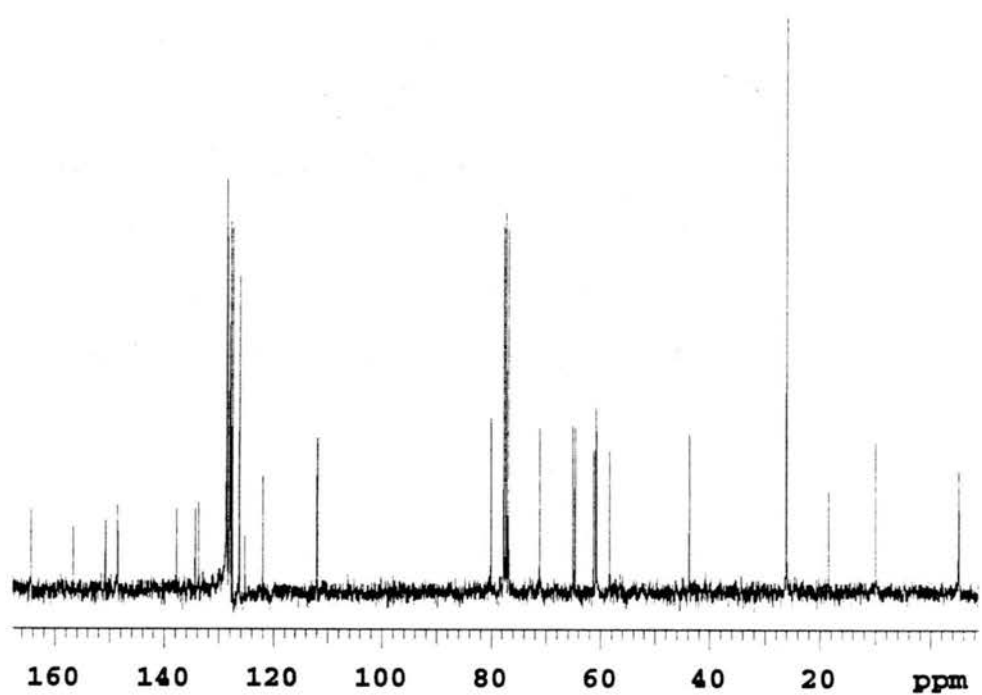
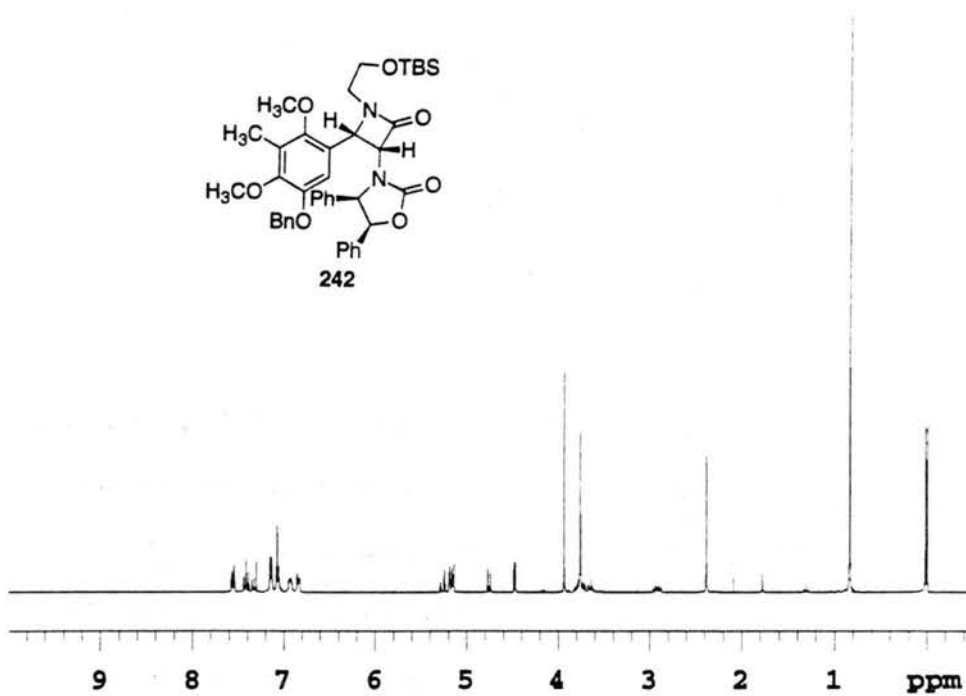
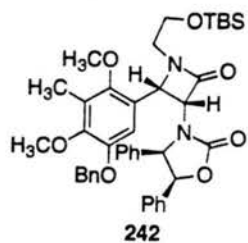
Acryloyl chloride (3.2  $\mu\text{L}$ , 0.40 mmol) and  $\text{NEt}_3$  (5.6  $\mu\text{L}$ , 0.040 mmol) was added to amine **238** (23.6 mg, 0.033 mmol) in 0.5 mL of THF. After 30 min  $\text{H}_2\text{O}$  was added and the quenched reaction was extracted with EtOAc. The crude product was purified by chromatography (EtOAc,  $R_f = 0.13$ ). To the diketopiperazine (86 mg, 0.11 mmol) in 1 mL of  $\text{CH}_2\text{Cl}_2$  was added  $\text{Me}_3\text{OBF}_4$  (50 mg, 0.34 mmol) and  $\text{Na}_2\text{CO}_3$  (58 mg, 0.55 mmol) at RT. The reaction stirred at RT for 1 h and then  $\text{H}_2\text{O}$  was added. The quenched reaction was extracted with  $\text{CH}_2\text{Cl}_2$  and the combined organic layers concentrated. The crude product was purified by chromatography (EtOAc) to give 39 mg (34% for two steps) of **236** as a yellow foam. TLC (1/1 Hex/ EtOAc)  $R_f = 0.47$  (UV and PMA).  $^1\text{H-NMR}$  (300 MHz) ( $\text{DMSO-d}_6$ , 120  $^\circ\text{C}$ )  $\delta$  -0.14 (s, 3H); 0.023 (s, 3H); 0.19 (s, 3H); 0.27 (s, 3H); 0.76 (s, 9H); 1.03 (s, 9H); 2.17 (s, 3H); 3.35-3.45 (m, 2H); 2.58 (s, 3H); 2.59-2.83 (m, 3H); 3.66 (s, 3H); 3.69 (s, 3H); 3.79 (dd,  $J = 3.3, 10.2$  Hz, 1H); 3.86 (dd,  $J = 7.2, 10.2$  Hz, 1H); 3.99 (dd,  $J = 2.1, 21.0$  Hz, 1H); 4.09 (dd,  $J = 2.1, 21.0$  Hz, 1H); 4.33 (1/2 ABq,  $J = 12.6$  Hz, 1H); 4.49 (1/2 ABq,  $J = 12.6$  Hz, 1H); 4.81 (br s, 1H); 5.66-5.69 (m, 1H); 6.10 (dd,  $J = 3.3, 7.2$  Hz, 1H); 6.15-6.21 (m, 1H); 6.84 (br s, 1H); 7.12 (m, 2H); 7.24-7.27 (m, 3H). IR (NaCl, neat) 2930, 1705, 1659, 1462, 1413, 1254, 1077, 835  $\text{cm}^{-1}$ . HRMS (FAB) calcd for  $\text{C}_{41}\text{H}_{64}\text{N}_3\text{O}_8\text{Si}_2$  (M+H) 782.4232; found 782.4233.

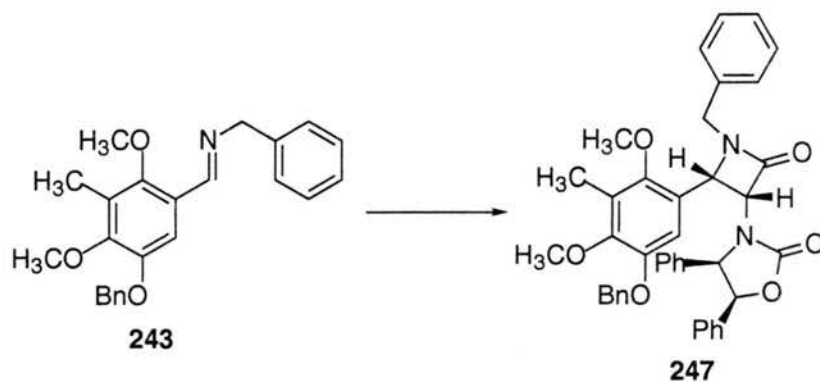




### **$\beta$ -Lactam (242).**

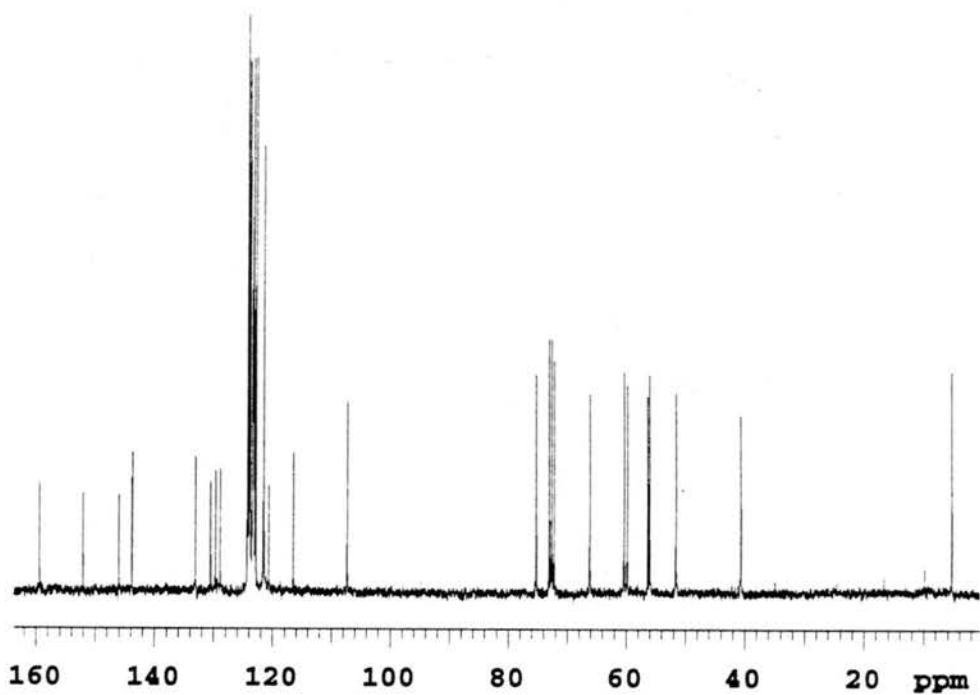
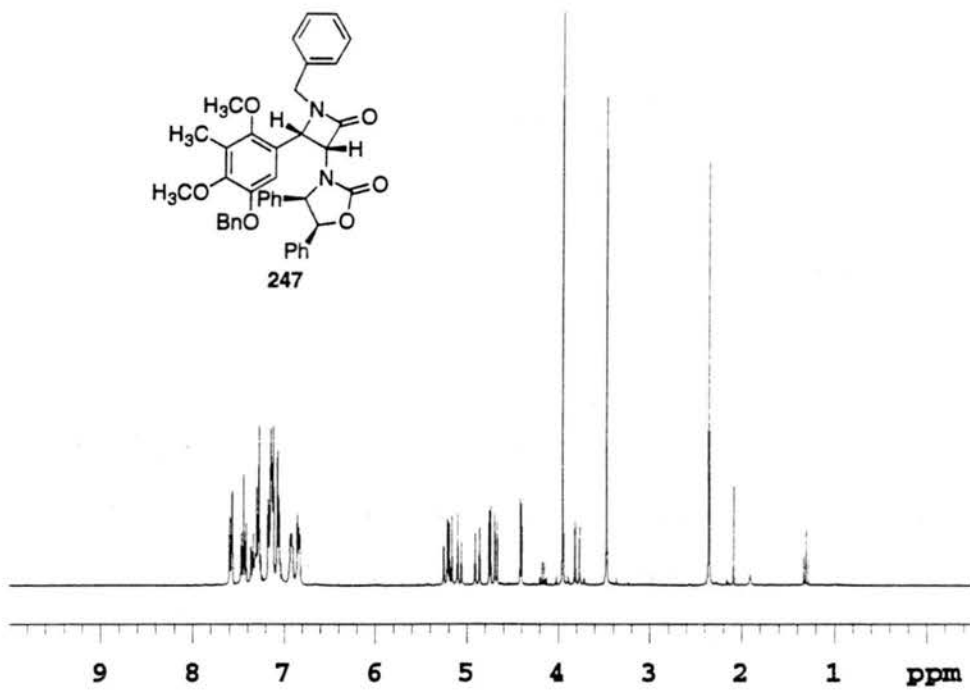
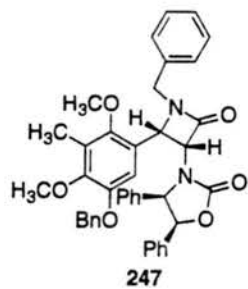
The acid chloride of chiral oxazolidine **241** (145 mg, 0.49 mmol) was prepared with the addition of oxalyl chloride (75  $\mu$ L, 0.87 mmol) and a drop of DMF in 1.5 mL of  $\text{CH}_2\text{Cl}_2$ . The reaction stirred for 1 h and was then concentrated *in vacuo*. Triethylamine (114  $\mu$ L, 0.82 mmol) was added dropwise to a solution of the acid in 1.5 mL of  $\text{CH}_2\text{Cl}_2$  at  $-78^\circ\text{C}$  under Ar. The reaction was allowed to stir at  $-78^\circ\text{C}$  for 15 min and then imine **211** (187 mg, 0.38 mmol) in 0.6 mL of  $\text{CH}_2\text{Cl}_2$  was added and the reaction warmed up to  $0^\circ\text{C}$ . After stirring for 2 h at  $0^\circ\text{C}$  the reaction was quenched with  $\text{NH}_4\text{Cl}$ . The quenched reaction was extracted with  $\text{CH}_2\text{Cl}_2$  and the organic layer dried and concentrated. After column chromatography (2/1 Hex/EtOAc) 250 mg (91%) of **242** was obtained as a clear oil. TLC (2/1 Hex/EtOAc)  $R_f = 0.25$  (UV and PMA).  $^1\text{H-NMR}$  (300 MHz) ( $\text{CDCl}_3$ )  $\delta$  -0.001 (s, 3H); 0.019 (s, 3H); 0.83 (s, 9H); 2.38 (s, 3H); 2.87-2.96 (m, 1H); 3.60-3.68 (m, 1H); 3.71-3.82 (m, 2H); 3.76 (s, 3H); 3.94 (s, 3H); 4.55 (d,  $J = 4.8$  Hz, 1H); 4.76 (d,  $J = 8.1$  Hz, 1H); 5.15 (d,  $J = 4.8$  Hz, 1H); 5.17 (d,  $J = 12.3$  Hz, 1H); 5.18 (d,  $J = 8.1$  Hz, 1H); 5.27 (d,  $J = 12.3$  Hz, 1H); 6.83-6.86 (m, 2H); 6.92-6.95 (m, 2H); 7.06-7.08 (m, 4H); 7.14-7.16 (m, 3H); 7.33-7.44 (m, 3H); 7.55-7.58 (m, 2H).  $^{13}\text{C-NMR}$  (75 MHz) ( $\text{CDCl}_3$ )  $\delta$  164.3, 156.6, 150.7, 148.5, 148.4, 137.7, 134.3, 133.6, 128.6, 128.5, 128.1, 128.0, 127.9, 127.5, 126.2, 125.2, 121.9, 111.9, 80.0, 71.1, 65.0, 64.6, 61.3, 60.8, 60.7, 58.3, 43.7, 26.0, 18.4, 9.9, -5.1, -5.2. IR (NaCl, neat) 2930, 1767, 1486, 1457, 1413, 1360, 1232, 1084, 834  $\text{cm}^{-1}$ .

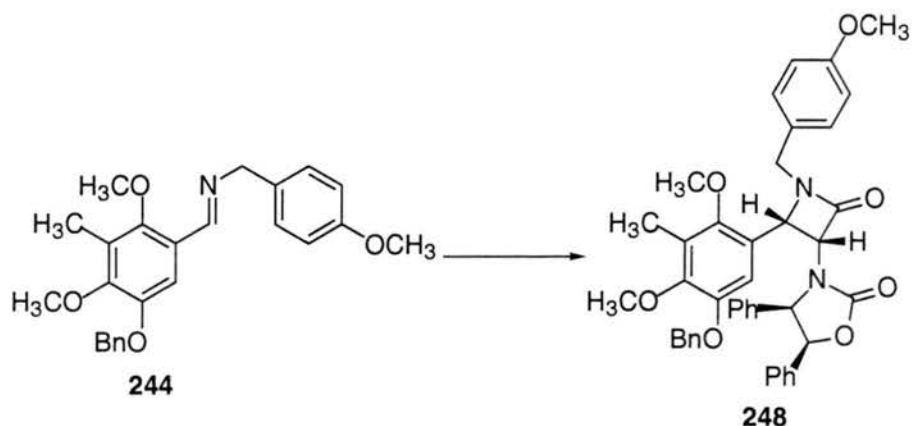




### **$\beta$ -Lactam (247).**

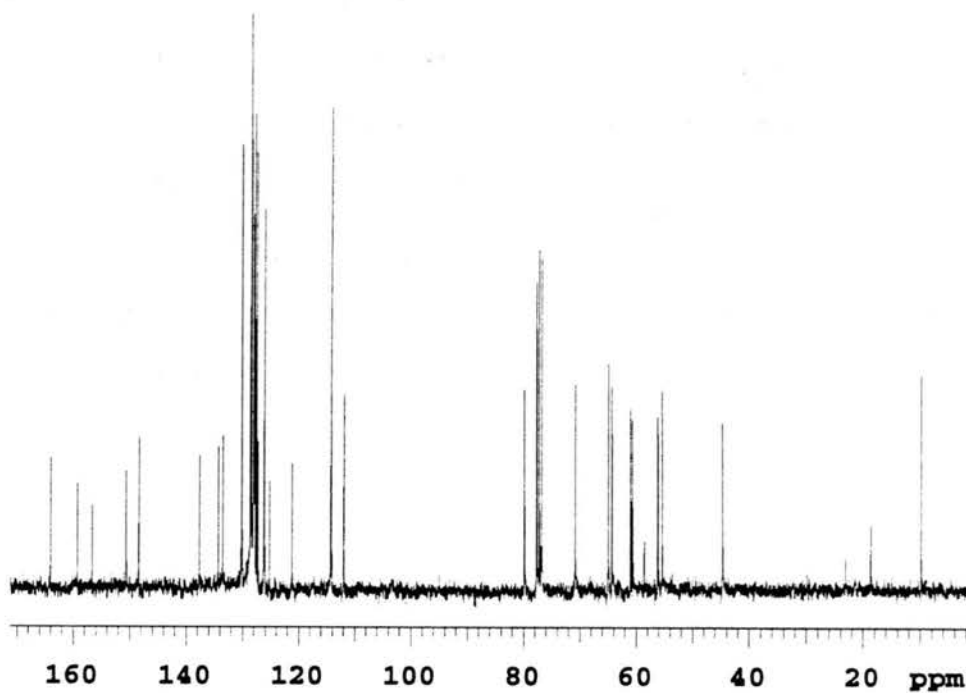
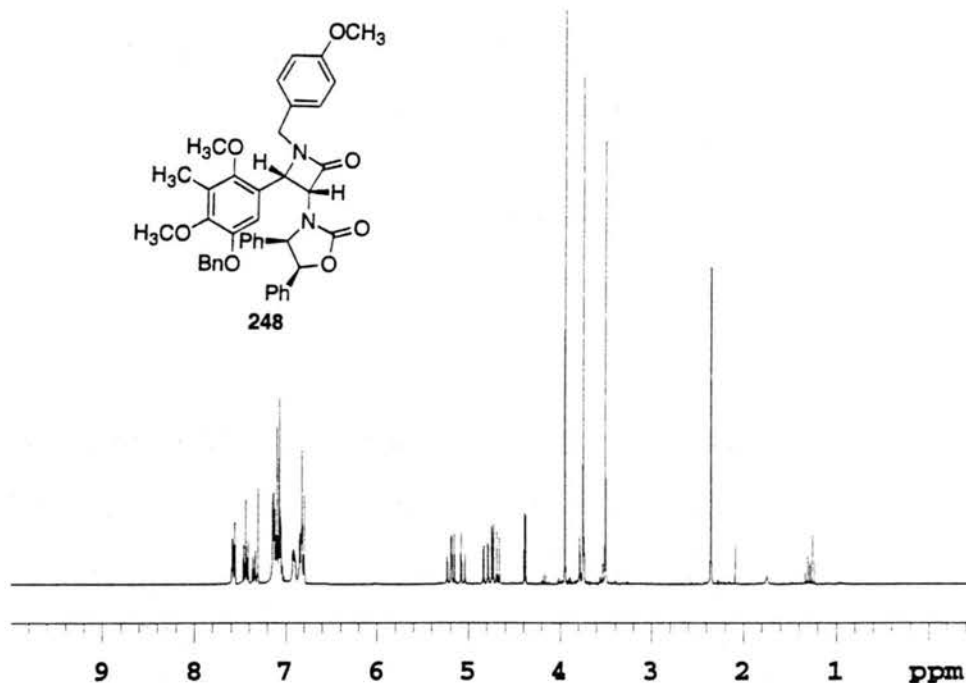
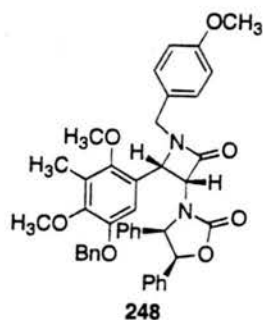
The Staudinger protocol used for **242** was followed using oxazolidine **241** (402 mg, 1.35 mmol), imine **243** (390 mg, 1.04 mmol) and  $\text{NEt}_3$  (312  $\mu\text{L}$ , 2.24 mmol). After 2 h at 0  $^\circ\text{C}$  the reaction was quenched with  $\text{NH}_4\text{Cl}$ , and the crude reaction purified by column chromatography (1/1 Hex/ EtOAc) to give 634 mg (93%) of **247** as a yellow oil. TLC (1/1 Hex/ EtOAc)  $R_f = 0.44$  (UV and PMA).  $^1\text{H-NMR}$  (300 MHz) ( $\text{CDCl}_3$ )  $\delta$  2.36 (s, 3H); 3.48 (s, 3H); 3.79 (d,  $J = 14.7$  Hz, 1H); 3.95 (s, 3H); 4.41 (d,  $J = 5.1$  Hz, 1H); 4.68 (d,  $J = 8.4$  Hz, 1H); 4.75 (d,  $J = 5.1$  Hz, 1H); 4.89 (d,  $J = 14.7$  Hz, 1H); 5.08 (d,  $J = 12.3$  Hz, 1H); 5.18 (d,  $J = 8.4$  Hz, 1H); 5.23 (d,  $J = 12.3$  Hz, 1H); 6.83-6.86 (m, 2H); 6.91-6.94 (m, 2H); 7.06-7.08 (m, 3H); 7.12-7.18 (m, 6H); 7.27-7.37 (m, 4H); 7.45 (t,  $J = 7.5$  Hz, 2H); 7.58 (t,  $J = 7.5$  Hz, 2H).  $^{13}\text{C-NMR}$  (75 MHz) ( $\text{CDCl}_3$ )  $\delta$  164.0, 156.6, 150.6, 148.3, 137.6, 135.1, 134.3, 133.5, 128.9, 128.8, 128.6, 128.5, 128.4, 128.1, 128.0, 127.93, 127.86, 127.7, 127.5, 127.1, 125.3, 121.1, 111.9, 79.9, 70.8, 65.0, 64.4, 60.9, 60.6, 56.2, 45.3, 9.9. IR (NaCl, neat) 2936, 1766, 1488, 1454, 1415, 1351, 1231, 1127, 1078, 1006, 698  $\text{cm}^{-1}$ .

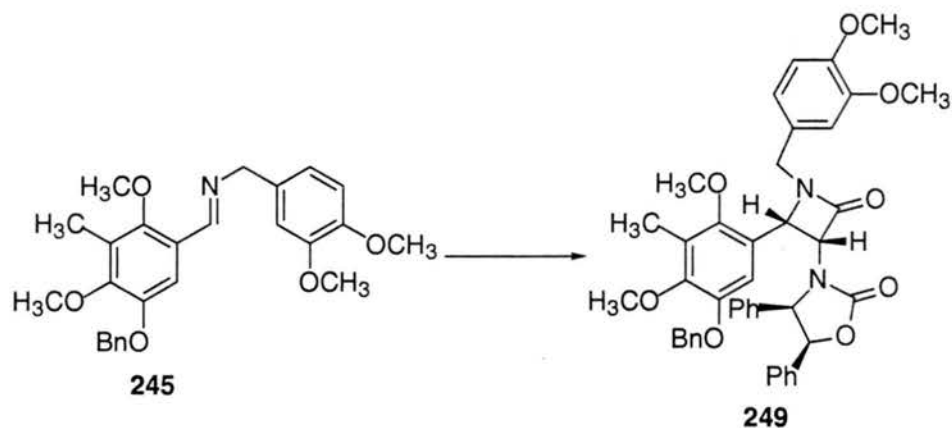




### **$\beta$ -lactam (248).**

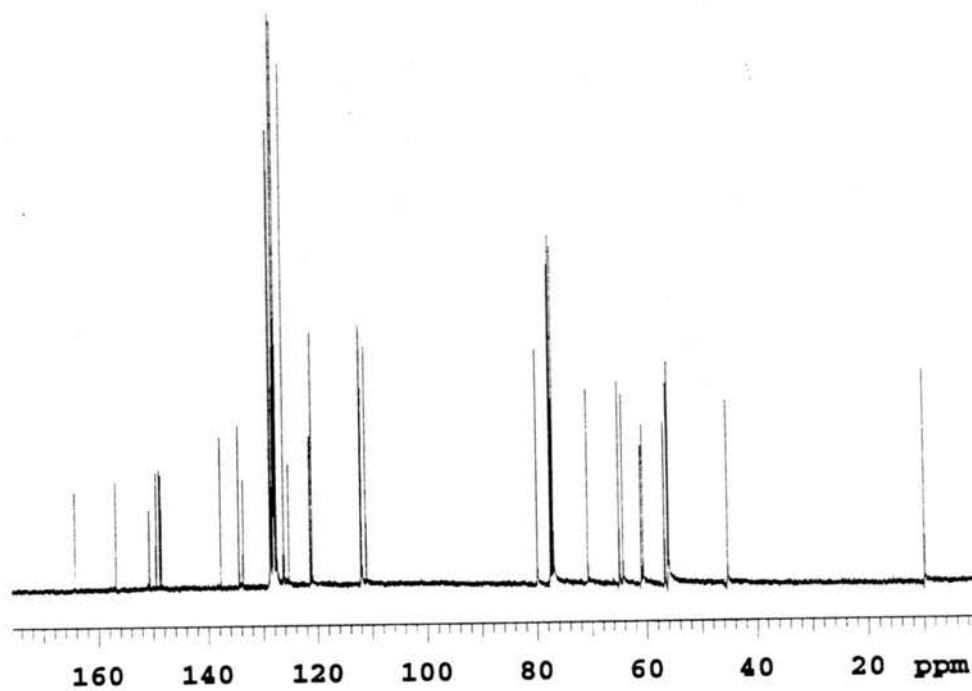
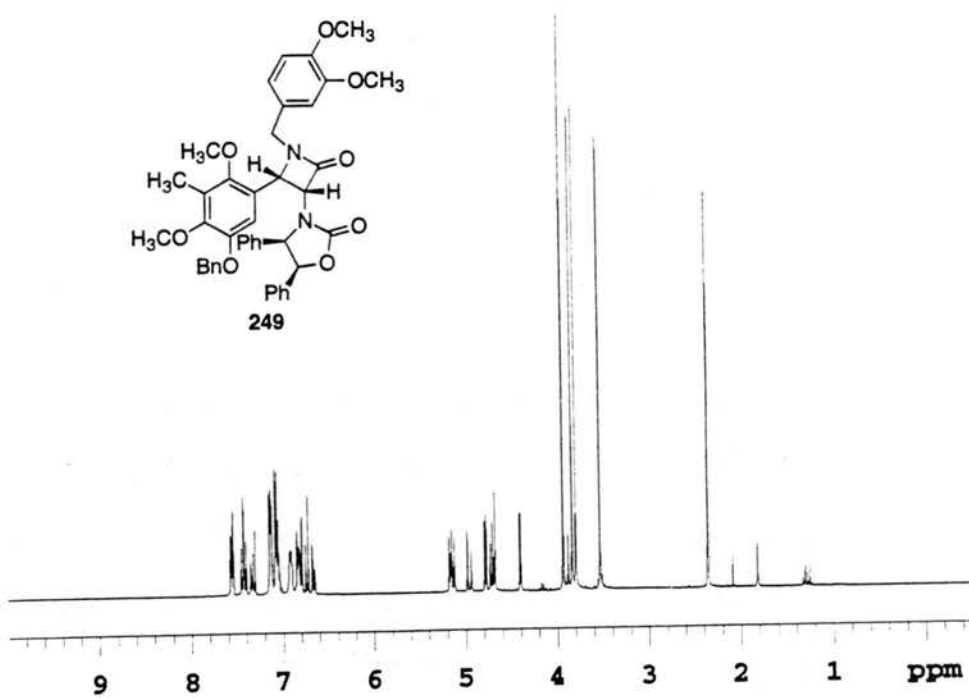
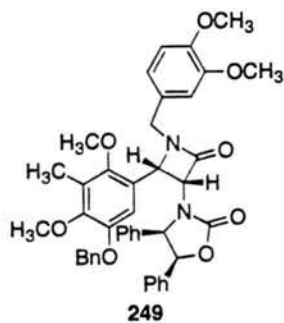
The Staudinger protocol used for **242** was followed using oxazolidine **241** (336 mg, 1.13 mmol), imine **244** (418 mg, 1.03 mmol) and  $\text{NEt}_3$  (237  $\mu\text{L}$ , 1.70 mmol). After 2 h at 0  $^\circ\text{C}$  the reaction was quenched with  $\text{NH}_4\text{Cl}$ , and the crude reaction purified by column chromatography (1/1 Hex/ EtOAc) to give 549 mg (78%) of **248** as a white foam. TLC (1/1 Hex/ EtOAc)  $R_f = 0.42$  (UV and PMA).  $^1\text{H-NMR}$  (300 MHz) ( $\text{CDCl}_3$ )  $\delta$  2.35 (s, 3H); 3.50 (s, 3H); 3.75 (s, 3H); 3.76 (d,  $J = 14.7$  Hz, 1H); 3.95 (s, 3H); 4.38 (d,  $J = 5.1$  Hz, 1H); 4.68 (d,  $J = 8.4$  Hz, 1H); 4.74 (d,  $J = 5.1$  Hz, 1H); 4.81 (d,  $J = 14.7$  Hz, 1H); 5.06 (d,  $J = 13.6$  Hz, 1H); 5.17 (d,  $J = 8.4$  Hz, 1H); 5.21 (d,  $J = 13.6$  Hz, 1H); 6.80-6.85 (m, 4H); 6.90-6.93 (m, 2H); 7.05-7.15 (m, 9H); 7.34-7.36 (m, 1H); 7.41-7.47 (m, 2H); 7.56-7.59 (m, 2H).  $^{13}\text{C-NMR}$  (75 MHz) ( $\text{CDCl}_3$ )  $\delta$  164.0, 159.2, 156.6, 150.6, 148.4, 137.6, 134.3, 133.5, 130.1, 128.6, 128.5, 128.4, 128.0, 127.9, 127.8, 127.5, 127.2, 126.1, 125.2, 121.2, 114.2, 111.9, 79.9, 70.8, 65.0, 64.3, 61.0, 60.6, 56.2, 55.4, 44.7, 9.9. IR (NaCl, neat) 2934, 1770, 1514, 1487, 1455, 1417, 1348, 1248, 1178, 1132, 1074, 1030  $\text{cm}^{-1}$ .

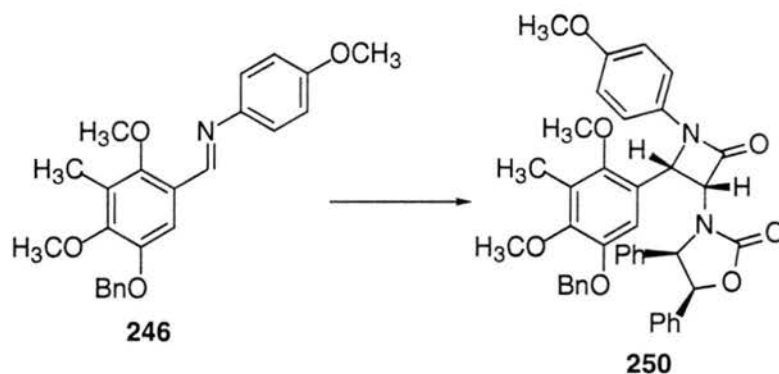




### **$\beta$ -lactam (249).**

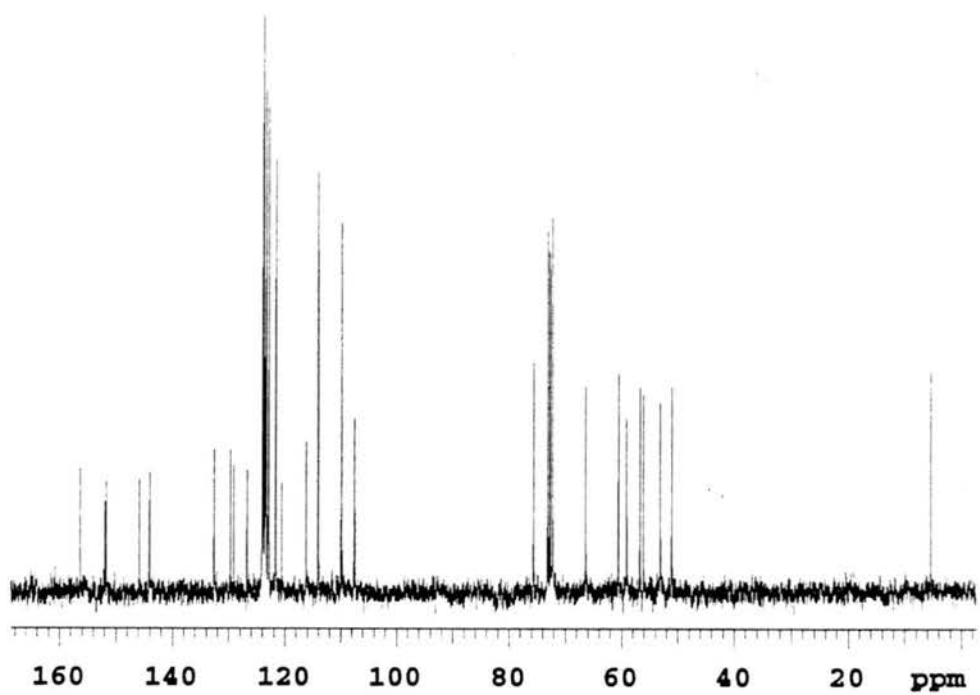
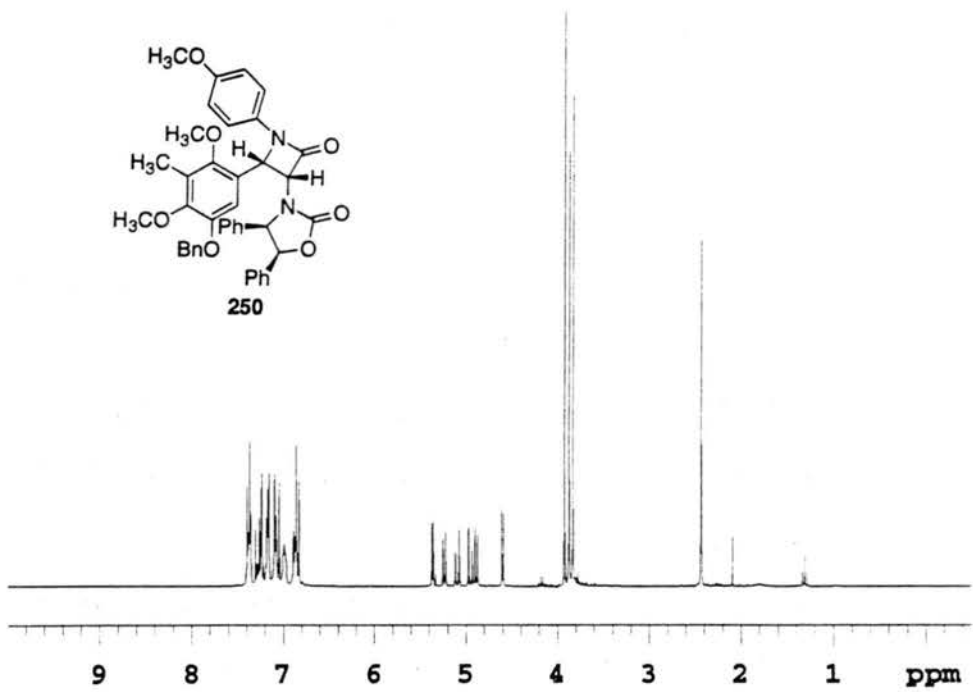
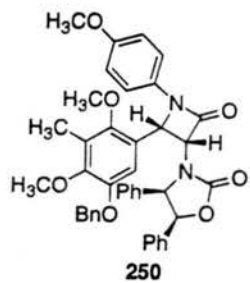
The Staudinger protocol used for **242** was followed using oxazolidine **241** (178 mg, 0.60 mmol), imine **245** (200 mg, 0.46 mmol) and  $\text{NEt}_3$  (140  $\mu\text{L}$ , 0.99 mmol). After 2 h at 0  $^\circ\text{C}$  the reaction was quenched with  $\text{NH}_4\text{Cl}$ , and the crude reaction purified by column chromatography (1/1 Hex/ EtOAc) to give 273 mg (83%) of **249** as a white foam. TLC (1/1 Hex/ EtOAc)  $R_f = 0.35$  (UV and PMA).  $^1\text{H-NMR}$  (300 MHz) ( $\text{CDCl}_3$ )  $\delta$  2.35 (s, 3H); 3.53 (s, 3H); 3.80 (s, 3H); 3.84 (s, 3H); 3.91 (d,  $J = 15.3$  Hz, 1H); 3.93 (s, 3H); 4.40 (d,  $J = 4.5$  Hz, 1H); 4.69 (d,  $J = 8.1$  Hz, 1H); 4.70 (d,  $J = 15.3$  Hz, 1H); 4.78 (d,  $J = 4.5$  Hz, 1H); 4.96 (d,  $J = 12.0$  Hz, 1H); 5.14 (d,  $J = 12.0$  Hz, 1H); 5.16 (d,  $J = 8.1$  Hz, 1H); 6.65-6.93 (m, 7H); 7.03-7.15 (m, 7H); 7.33-7.57 (m, 5H).  $^{13}\text{C-NMR}$  (75 MHz) ( $\text{CDCl}_3$ )  $\delta$  164.2, 156.7, 150.7, 149.4, 148.8, 148.5, 148.5, 137.7, 134.4, 133.6, 128.68, 128.65, 128.6, 128.2, 128.1, 128.0, 127.9, 127.6, 126.3, 125.3, 121.4, 121.1, 112.1, 112.0, 111.1, 79.9, 70.7, 65.0, 64.3, 61.0, 60.7, 56.7, 56.1, 56.0, 45.3, 9.8. IR (NaCl, neat) 2936, 1770, 1516, 1455, 1417, 1351, 1237, 1138, 1077, 1027  $\text{cm}^{-1}$ .

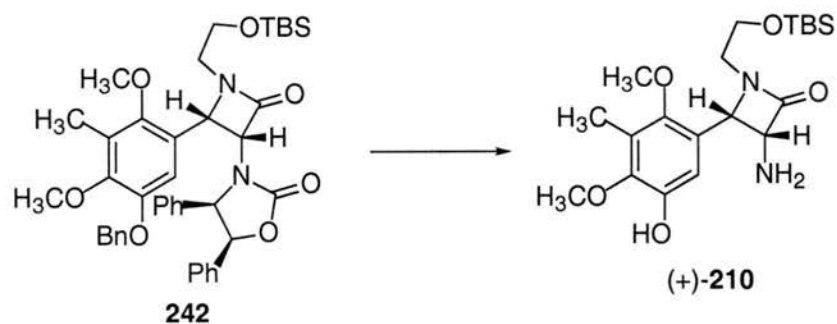




### **$\beta$ -lactam (250).**

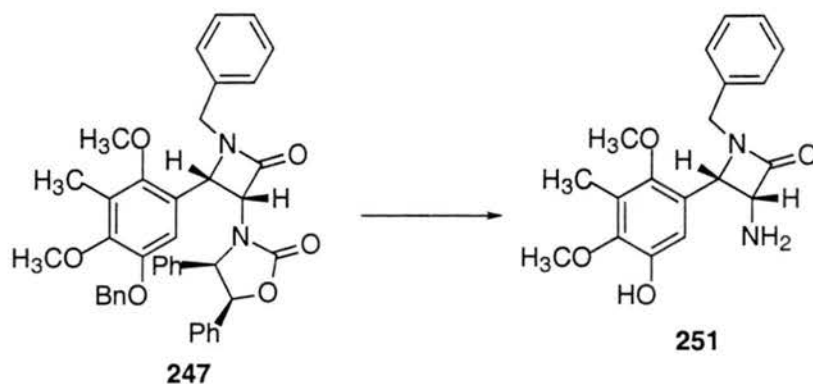
The Staudinger protocol used for **242** was followed using oxazolidine **241** (143 mg, 0.48 mmol), imine **246** (154 mg, 0.37 mmol) and  $\text{NEt}_3$  (111  $\mu\text{L}$ , 0.80 mmol). After 2 h at 0  $^\circ\text{C}$  the reaction was quenched with  $\text{NH}_4\text{Cl}$ , and the crude reaction purified by column chromatography (1/1 Hex/ EtOAc) to give 185 mg (75%) of **250** as a yellow oil. TLC (1/1 Hex/ EtOAc)  $R_f = 0.47$  (UV and PMA).  $^1\text{H-NMR}$  (300 MHz) ( $\text{CDCl}_3$ )  $\delta$  2.43 (s, 3H); 3.83 (s, 3H); 3.87 (s, 3H); 3.92 (s, 3H); 4.60 (d,  $J = 5.1$  Hz, 1H); 4.89 (d,  $J = 8.2$  Hz, 1H); 4.95 (d,  $J = 12.1$  Hz, 1H); 5.10 (d,  $J = 12.1$  Hz, 1H); 5.24 (d,  $J = 8.2$  Hz, 1H); 5.36 (d,  $J = 5.1$  Hz, 1H); 6.83-6.90 (m, 4H); 6.98-7.00 (m, 2H); 7.05 (s, 1H); 7.08-7.10 (m, 3H); 7.16-7.19 (m, 3H); 7.24-7.26 (m, 3H); 7.36-7.40 (m, 4H).  $^{13}\text{C-NMR}$  (75 MHz) ( $\text{CDCl}_3$ )  $\delta$  160.9, 156.5, 156.3, 150.4, 148.7, 148.6, 137.2, 134.2, 133.6, 131.3, 128.6, 128.5, 128.4, 128.2, 128.0, 127.9, 127.6, 127.5, 126.2, 125.1, 120.8, 118.6, 114.4, 112.1, 80.2, 70.9, 65.1, 63.7, 61.3, 60.7, 57.7, 55.6, 10.0. IR (NaCl, neat) 2935, 1760, 1512, 1416, 1387, 1247, 1130, 1081, 1033  $\text{cm}^{-1}$ .





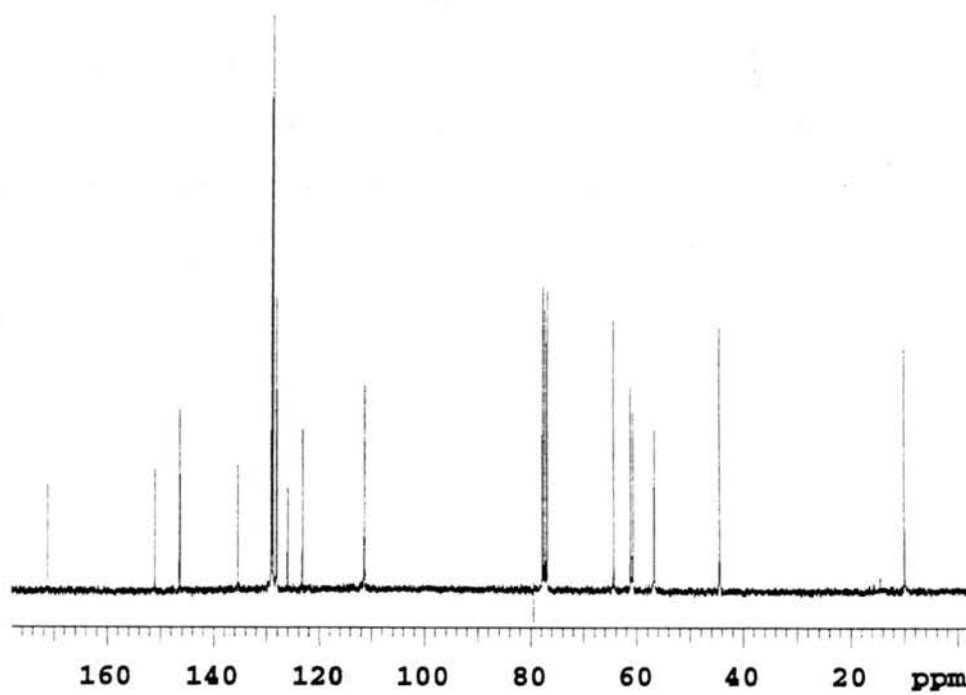
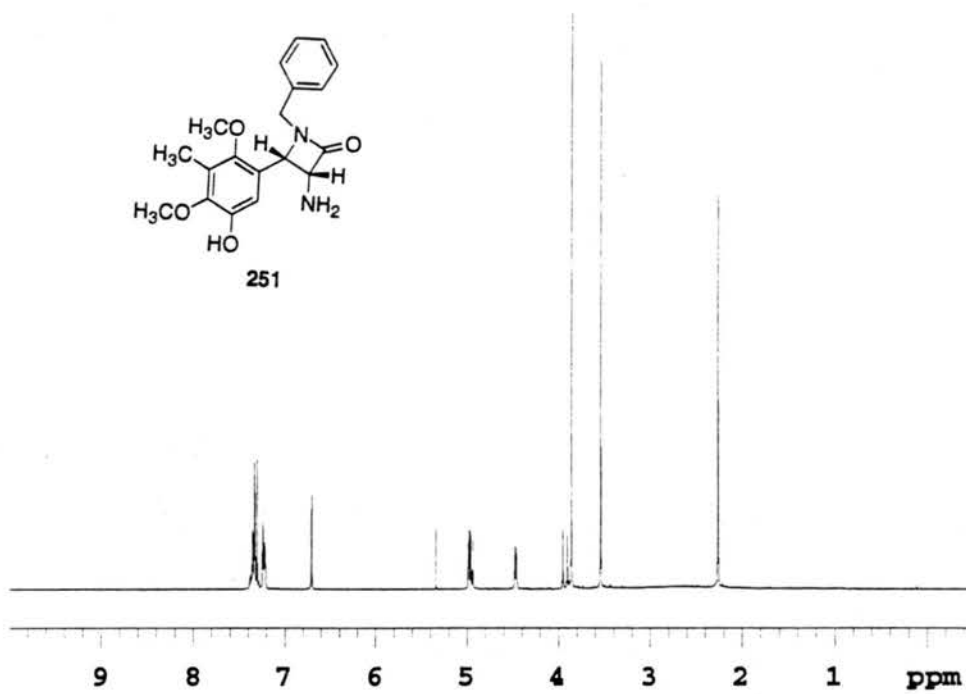
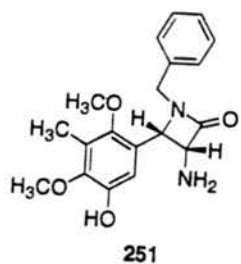
**(+)-1-*O*-*tert*-butyldimethylsilyloxyethyl-3-amino-4-(2',4'-methoxy-3'-methyl-5'-hydroxy)phenyl-2-azetidinone (210).**

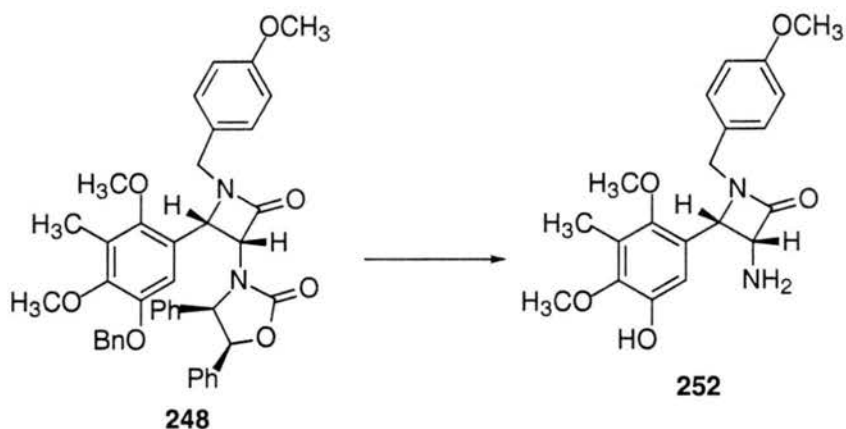
To a degassed solution of **242** (200 mg, 0.28 mmol) in 5.6 mL of MeOH/THF (1/1) was added 20% Pd(OH)<sub>2</sub> (116 mg, 0.17 mmol) and then pressurized with H<sub>2</sub> to 60 psi. The reaction stirred overnight at RT and was then filtered through celite and concentrated. The crude reaction mixture was purified by column chromatography (5% MeOH in EtOAc) to give 91 mg (74%) of **210** as a yellow oil. TLC and <sup>1</sup>H-NMR, <sup>13</sup>CNMR, IR and MS same as **210**. [ $\alpha$ ]<sub>D</sub><sup>25</sup> = +109.3 (CH<sub>2</sub>Cl<sub>2</sub>, c = 1.35).



**1-Benzyl-3-amino-4-(2',4'-methoxy-3'-methyl-5'-hydroxy)phenyl-2-azetidinone (251).**

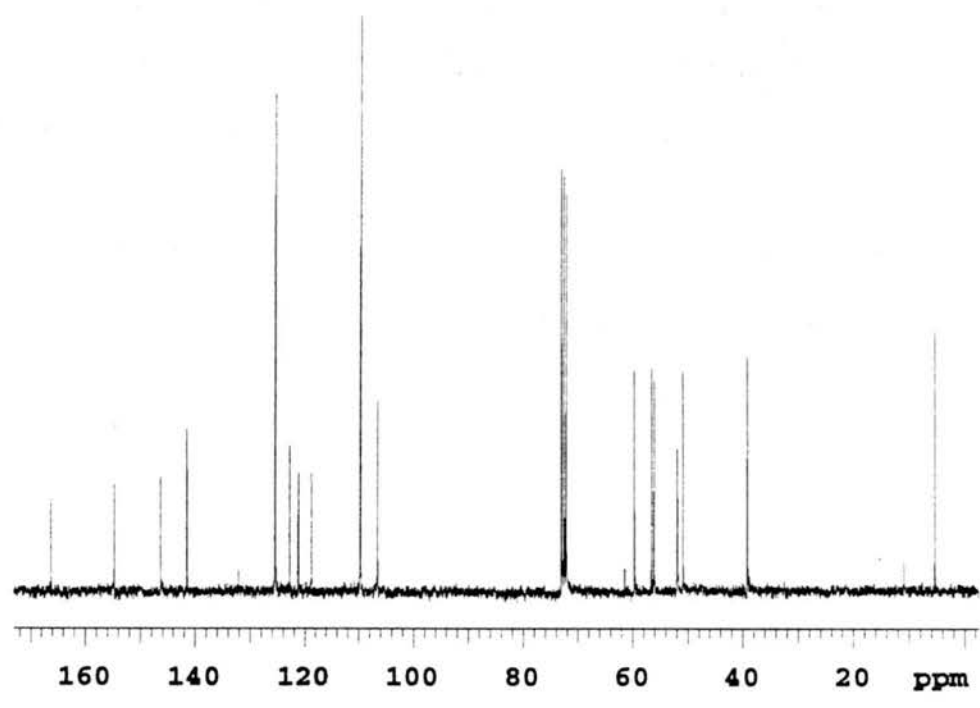
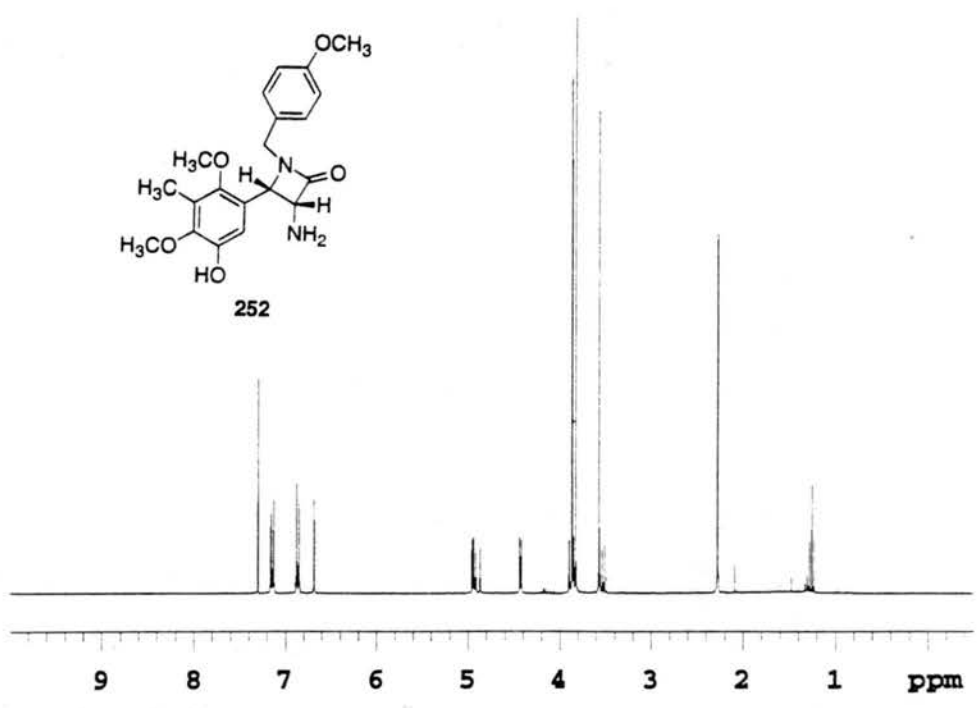
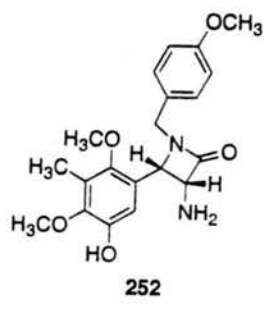
To a degassed solution of **247** (260 mg, 0.40 mmol) in 8.0 mL of MeOH/THF (1/1) was added 20% Pd(OH)<sub>2</sub> (167 mg, 0.24 mmol) and then pressurized with H<sub>2</sub> to 60 psi. The reaction stirred overnight at RT and was then filtered through celite and concentrated. The crude reaction mixture was purified by column chromatography (5% MeOH in EtOAc) to give 121 mg (74%) of **251** as a yellow oil. TLC (5% MeOH in EtOAc) R<sub>f</sub> = 0.38 (UV and PMA). <sup>1</sup>H-NMR (300 MHz) (CDCl<sub>3</sub>) δ 2.27 (s, 3H); 3.55 (s, 3H); 3.87 (s, 3H); 3.93 (d, J= 14.7 Hz, 1H); 4.47 (d, J= 5.1 Hz, 1H); 4.96 (d, J= 14.7 Hz, 1H); 4.97 (d, J= 5.1 Hz, 1H); 6.71 (s, 1H); 7.22-7.24 (m, 2H); 7.32-7.36 (m, 3H). <sup>13</sup>C-NMR (75 MHz) (CDCl<sub>3</sub>) δ 171.1, 150.9, 146.3, 146.2, 135.3, 129.0, 128.0, 125.9, 123.1, 111.2, 64.3, 61.1, 60.7, 56.6, 44.4, 9.9. IR (NaCl, neat) 3287, 2935, 1747, 1594, 1455, 1418, 1353, 1117, 997 cm<sup>-1</sup>.

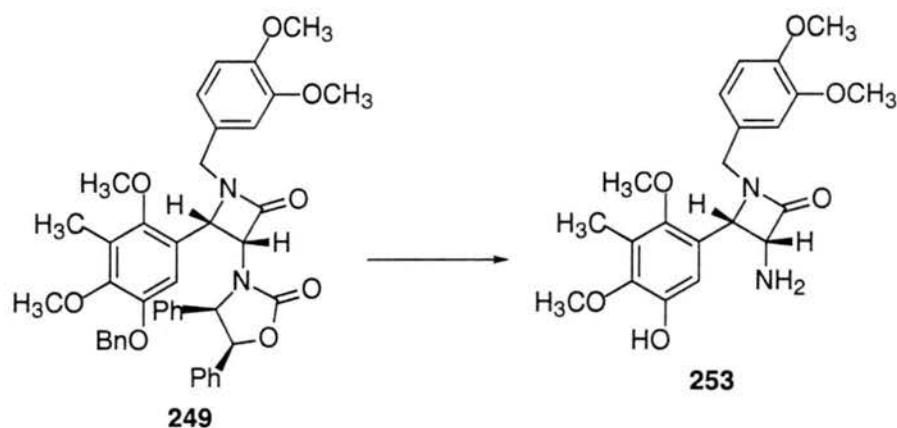




**1-(4'-Methoxy)benzyl-3-amino-4-(2',4'-methoxy-3'-methyl-5'-hydroxy)phenyl-2-azetidinone (252).**

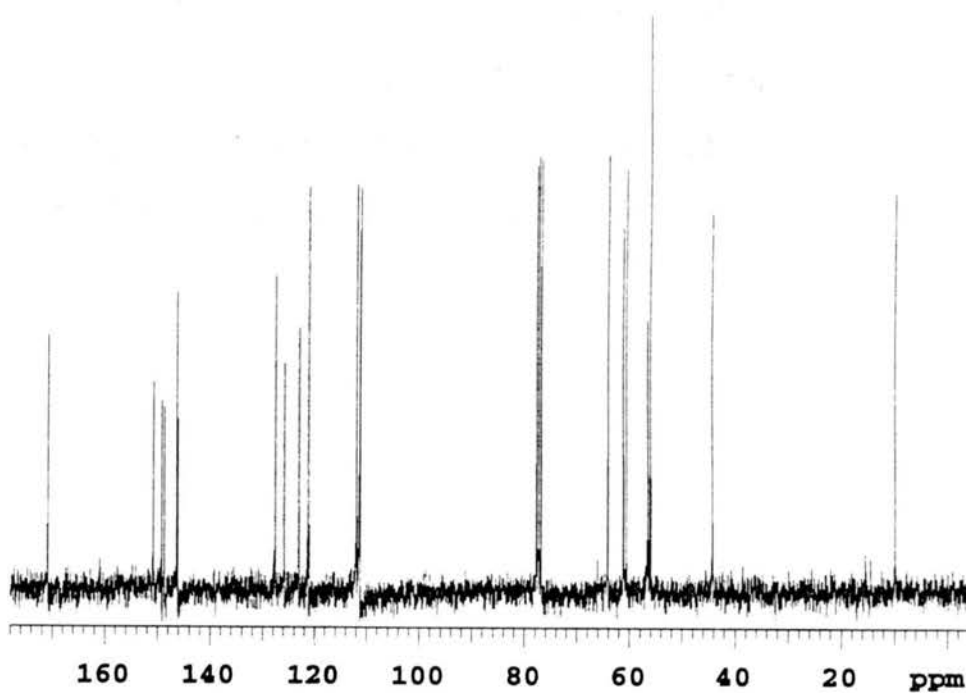
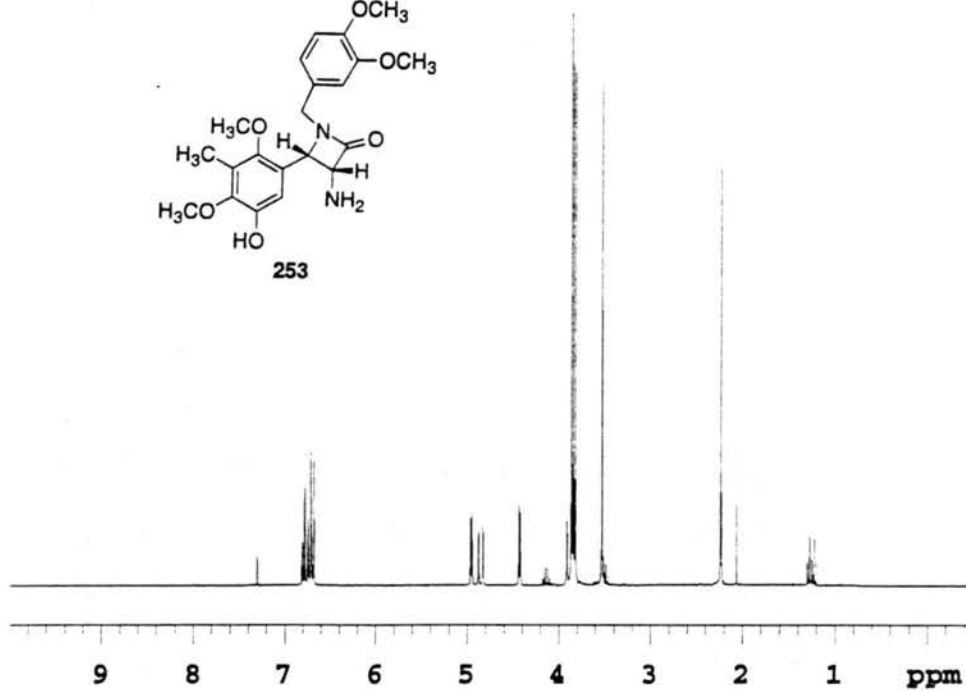
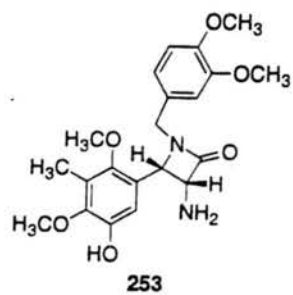
To a degassed solution of **248** (68 mg, 0.01 mmol) in 1.0 mL of MeOH/THF (1/1) was added 20% Pd(OH)<sub>2</sub> (42 mg, 0.06 mmol) and then pressurized with H<sub>2</sub> to 60 psi. The reaction stirred overnight at RT and was then filtered through celite and concentrated. The crude reaction mixture was purified by column chromatography (5% MeOH in EtOAc) to give 31 mg (81%) of **252** as a yellow oil. TLC (5% MeOH in EtOAc) R<sub>f</sub> = 0.31 (UV and dragendorff). <sup>1</sup>H-NMR (300 MHz) (CDCl<sub>3</sub>) δ 2.27 (s, 3H); 3.57 (s, 3H); 3.82 (s, 3H); 3.86 (s, 3H); 3.87 (d, J= 14.7 Hz, 1H); 4.43 (d, J= 5.1 Hz, 1H); 4.89 (d, J= 14.7 Hz, 1H); 4.95 (d, J= 5.1 Hz, 1H); 6.69 (s, 1H); 6.87 (d, J= 8.4 Hz, 2H); 7.15 (d, J= 8.4 Hz, 2H). <sup>13</sup>C-NMR (75 MHz) (CDCl<sub>3</sub>) δ 166.2, 154.6, 146.2, 141.5, 141.4, 125.4, 122.7, 121.1, 118.7, 109.6, 106.5, 59.7, 56.5, 56.1, 51.9, 50.9, 39.2, 5.3. IR (NaCl, neat) 3335, 2936, 1746, 1612, 1514, 1456, 1421, 1357, 1247, 1177, 1122, 1051, 1009 cm<sup>-1</sup>.

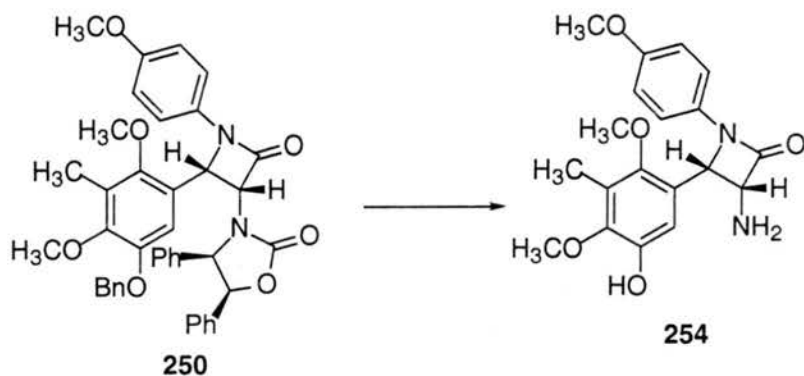




**1-(3',4'-Methoxy)benzyl-3-amino-4-(2',4'-methoxy-3'-methyl-5'-hydroxy)phenyl-2-azetidinone (253).**

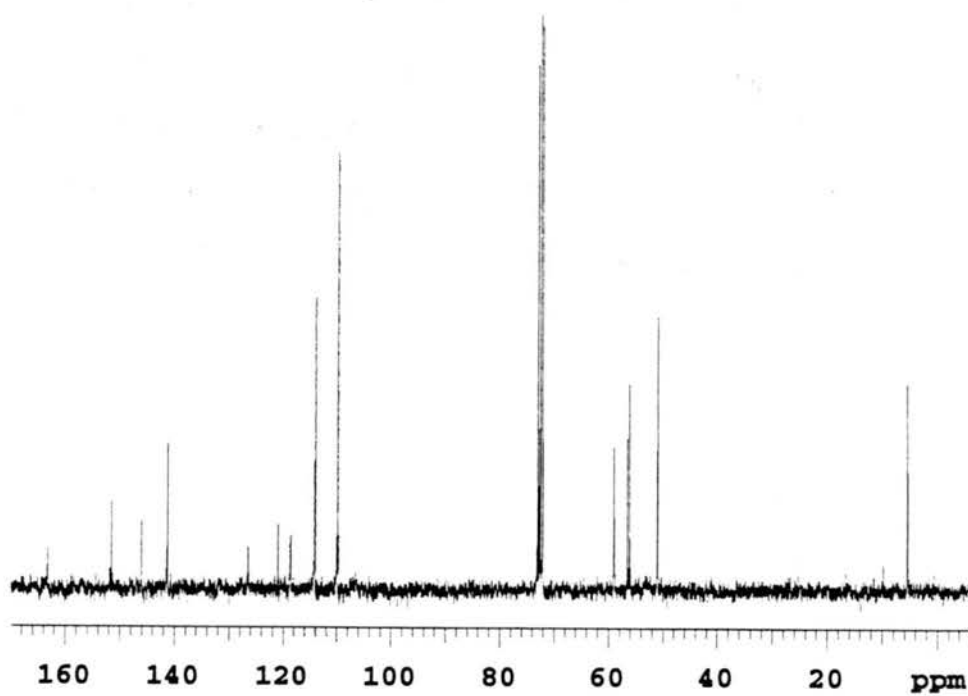
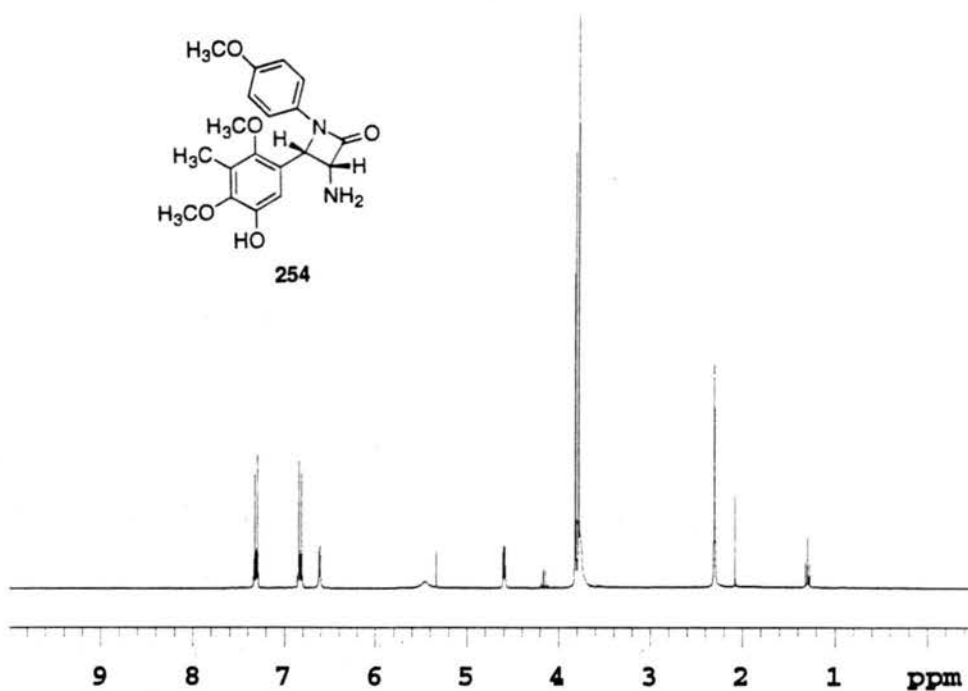
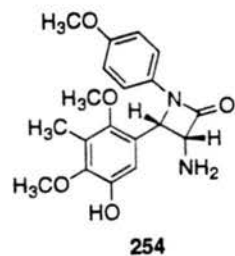
To a degassed solution of **249** (135 mg, 0.18 mmol) in 3.6 mL of MeOH/THF (1/1) was added 20% Pd(OH)<sub>2</sub> (79 mg, 0.11 mmol) and then pressurized with H<sub>2</sub> to 60 psi. The reaction stirred overnight at RT and was then filtered through celite and concentrated. The crude reaction mixture was purified by column chromatography (5% MeOH in EtOAc) to give 67 mg (92%) of **253** as a yellow oil. TLC (5% MeOH in EtOAc) R<sub>f</sub> = 0.27 (UV and PMA). <sup>1</sup>H-NMR (300 MHz) (CDCl<sub>3</sub>) δ 2.24 (s, 3H); 3.53 (s, 3H); 3.82 (s, 3H); 3.85 (s, 3H); 3.87 (s, 3H); 3.89 (d, J= 14.7 Hz, 1H); 4.43 (d, J= 5.1 Hz, 1H); 4.85 (d, J= 14.7 Hz, 1H); 4.96 (d, J= 5.1 Hz, 1H); 6.69 (s, 1H); 6.68-6.81 (m, 3H). <sup>13</sup>C-NMR (75 MHz) (CDCl<sub>3</sub>) δ 170.8, 150.8, 149.2, 148.7, 146.3, 146.2, 127.6, 125.8, 123.0, 121.1, 111.9, 111.3, 111.2, 64.1, 61.2, 60.6, 56.5, 56.1, 56.0, 44.3, 9.9. IR (NaCl, neat) 3337, 2938, 1732, 1594, 1516, 1455, 1360, 1260, 1238, 1122, 1027 cm<sup>-1</sup>.

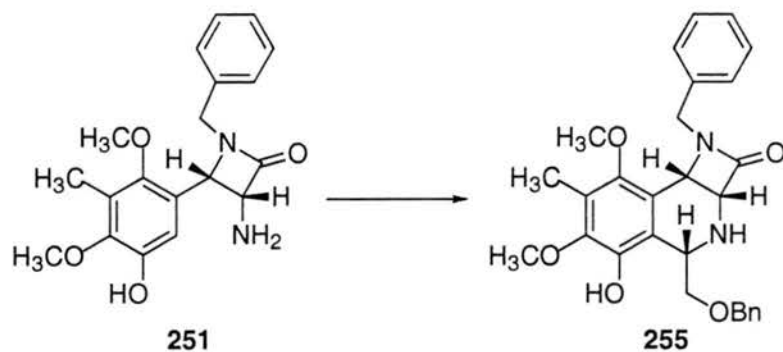




**1-(4'-Methoxy)phenyl-3-amino-4-(2',4'-methoxy-3'-methyl-5'-hydroxy)phenyl-2-azetidinone (254).**

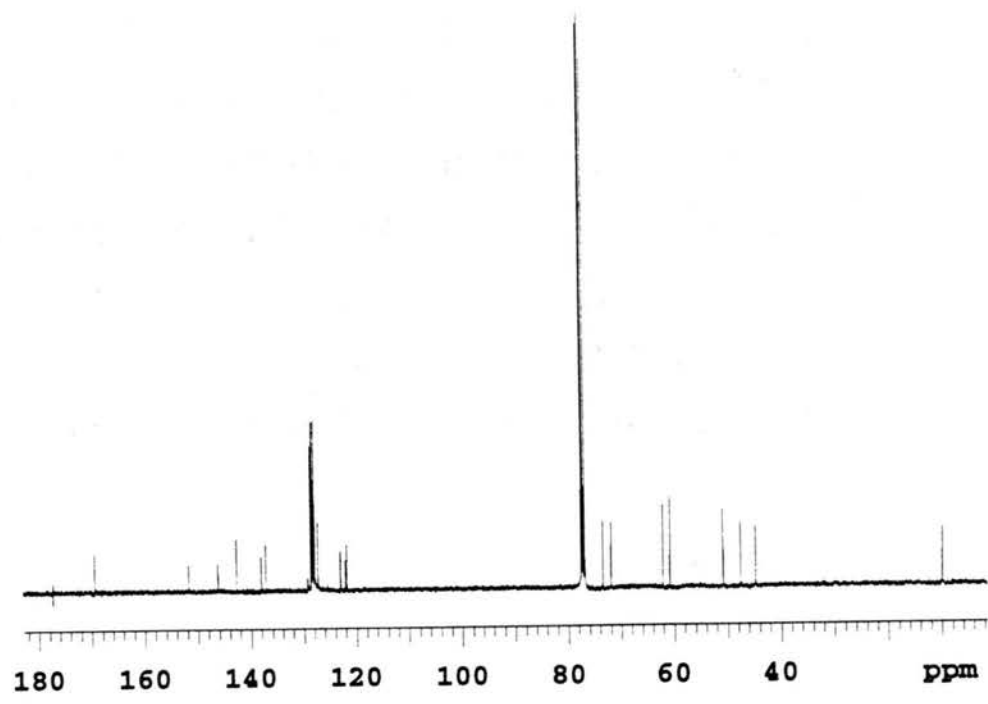
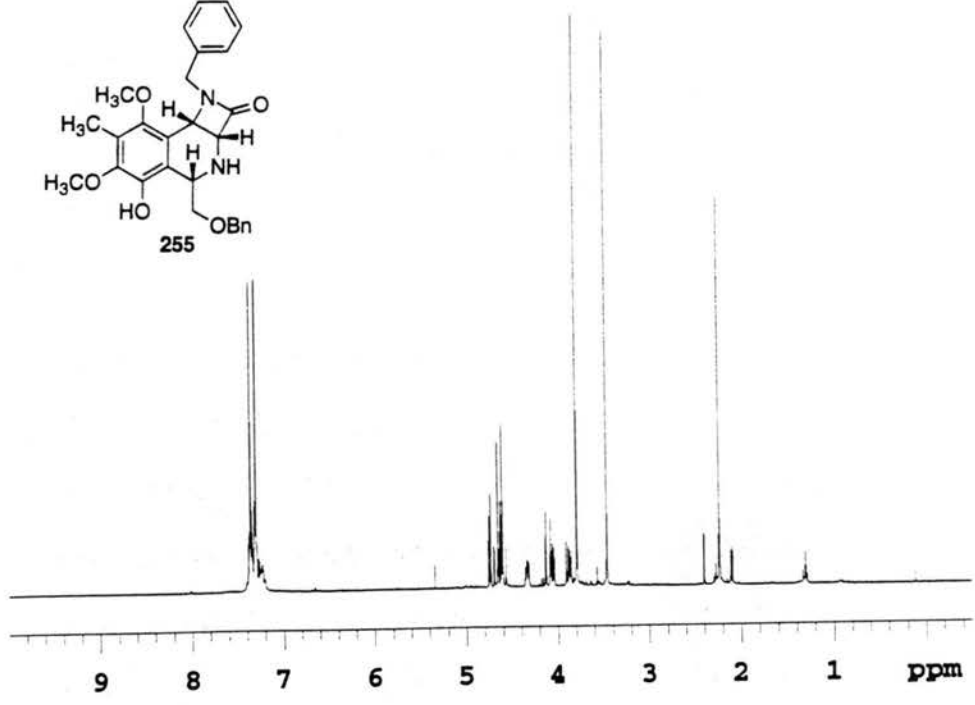
To a degassed solution of **250** (87 mg, 0.13 mmol) in 2.6 mL of MeOH/THF (1/1) was added 20% Pd(OH)<sub>2</sub> (54 mg, 0.78 mmol) and then pressurized with H<sub>2</sub> to 60 psi. The reaction stirred overnight at RT and was then filtered through celite and concentrated. The crude reaction mixture was purified by column chromatography (10/ EtOAc/MeOH) to give 24 mg (52%) of **254** as a yellow oil. TLC (10/1 EtOAc/MeOH) R<sub>f</sub> = 0.55 (UV and PMA). <sup>1</sup>H-NMR (300 MHz) (CDCl<sub>3</sub>) δ 2.30 (s, 3H); 3.77 (br s, 3H); 3.79 (s, 3H); 3.82 (s, 3H); 4.59 (d, J= 5.4 Hz, 1H); 5.46 (br s, 1H); 6.61 (s, 1H); 6.82-6.85 (m, 2H); 7.30-7.37 (m, 2H). <sup>13</sup>C-NMR (75 MHz) (CDCl<sub>3</sub>) δ 163.2, 151.5, 146.1, 141.4, 141.3, 126.5, 120.9, 118.6, 114.1, 109.9, 50.0, 56.6, 56.2, 51.0, 5.5. IR (NaCl, neat) 3349, 2938, 1739, 1594, 1512, 1454, 1392, 1299, 1246, 1123, 1038, 1002, 830 cm<sup>-1</sup>.

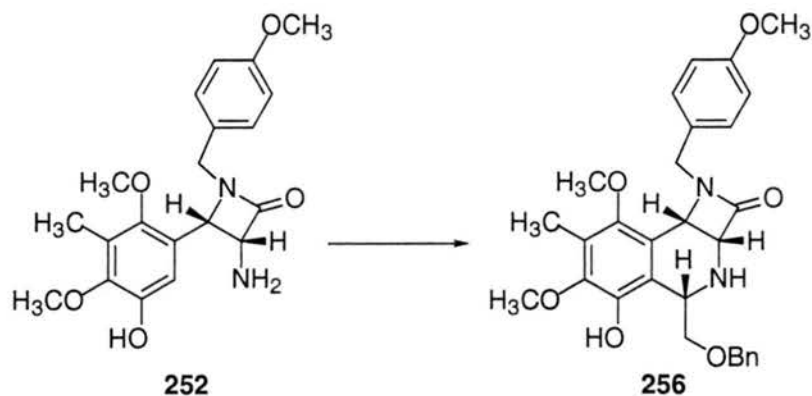




**3 $\alpha$ ,4 $\alpha$ -3,4-N-(benzyl)azetidinone-8-hydroxy-9,11-methoxy-10-methyltetrahydroisoquinoline (255).**

Freshly distilled benzyloxyacetaldehyde (31  $\mu$ L, 0.22 mmol) was added to a solution of **251** (63 mg, 0.18 mmol) in MeOH (1.8 mL), stirred at RT for 30 min and then heated at 50  $^{\circ}$ C for 23 h. The reaction was then allowed cooled to RT and concentrated. The crude product was purified by column chromatography (1/1 EtOAc/Hex then EtOAc) to give 13 mg (15%) of **255** as a yellow oil. TLC (EtOAc)  $R_f$  = 0.36 (UV and PMA).  $^1$ H-NMR (300 MHz) ( $\text{CDCl}_3$ )  $\delta$  2.23 (s, 3H); 3.46 (s, 3H); 3.74 (s, 3H); 3.88 (dd,  $J$ = 7.0, 9.5 Hz, 1H); 4.06 (dd,  $J$ = 4.4, 9.5 Hz, 1H); 4.11 (d,  $J$ = 15.4 Hz, 1H); 4.34 (dd,  $J$ = 4.4, 7.0 Hz, 1H); 4.59 (d,  $J$ = 11.7 Hz, 1H); 4.63 (d,  $J$ = 5.1 Hz, 1H); 4.68 (d,  $J$ = 11.7 Hz, 1H); 4.75 (d,  $J$ = 5.1 Hz, 1H); 7.20-7.41 (m, 10H).  $^{13}$ C-NMR (75 MHz) ( $\text{CDCl}_3$ )  $\delta$  169.5, 151.8, 146.2, 142.7, 138.1, 137.3, 128.6, 128.5, 128.3, 128.02, 127.98, 127.3, 123.0, 122.0, 121.9, 73.5, 72.0, 62.2, 60.8, 50.8, 47.6, 44.8, 9.9. IR (NaCl, neat) 3334, 2928, 1744, 1453, 1410, 1067  $\text{cm}^{-1}$ .





**3 $\alpha$ ,4 $\alpha$ -3,4-N-(4'-methoxybenzyl)azetidinone-8-hydroxy-9,11-methoxy-10-methyltetrahydroisoquinoline (256).**

Freshly distilled benzyloxyacetaldehyde (28  $\mu$ L, 0.20 mmol) was added to a solution of **252** (61 mg, 0.16 mmol) in MeOH (1.6 mL), stirred at RT for 30 min and then heated at 50  $^{\circ}$ C for 23 h. The reaction was then allowed cooled to RT and concentrated. The crude product was purified by column chromatography (3/1 EtOAc/Hex then EtOAc) to give 37 mg (46%) of **256** as a yellow oil. TLC (EtOAc)  $R_f$  = 0.43 (UV and PMA).  $^1\text{H-NMR}$  (300 MHz) ( $\text{CDCl}_3$ )  $\delta$  2.24 (s, 3H); 2.70 (br s, 1H,  $\text{D}_2\text{O}$  exch.); 3.51 (s, 3H); 3.79 (s, 3H); 3.81 (s, 3H); 3.89 (dd,  $J$  = 6.9, 9.6 Hz, 1H); 4.04 (d,  $J$  = 15.0 Hz, 1H); 4.08 (dd,  $J$  = 4.2, 9.6 Hz, 1H); 4.31 (dd,  $J$  = 4.2, 6.9 Hz, 1H); 4.53 (d,  $J$  = 15.0 Hz, 1H); 4.58 (d,  $J$  = 4.2, 9.6 Hz, 1H); 4.59 (d,  $J$  = 5.1 Hz, 1H); 4.67 (d,  $J$  = 12.0 Hz, 1H); 4.73 (d,  $J$  = 5.1 Hz, 1H); 6.38 (br s, 1H,  $\text{D}_2\text{O}$  exch.); 6.84 (d,  $J$  = 8.7 Hz, 2H); 7.23 (d,  $J$  = 8.7 Hz, 2H); 7.31-7.37 (m, 5H).  $^{13}\text{C-NMR}$  (75 MHz) ( $\text{CDCl}_3$ )  $\delta$  169.3, 158.8, 151.7, 146.2, 142.7, 138.0, 129.6, 129.4, 128.6, 128.01, 127.95, 123.0, 122.0, 121.9, 113.8, 73.5, 71.9, 62.2, 60.9, 60.8, 55.4, 50.8, 47.4, 44.1, 9.9. IR (NaCl, neat) 3326, 2929, 1738, 1605, 1514, 1437, 1406, 1247, 1113, 1067, 734  $\text{cm}^{-1}$ .

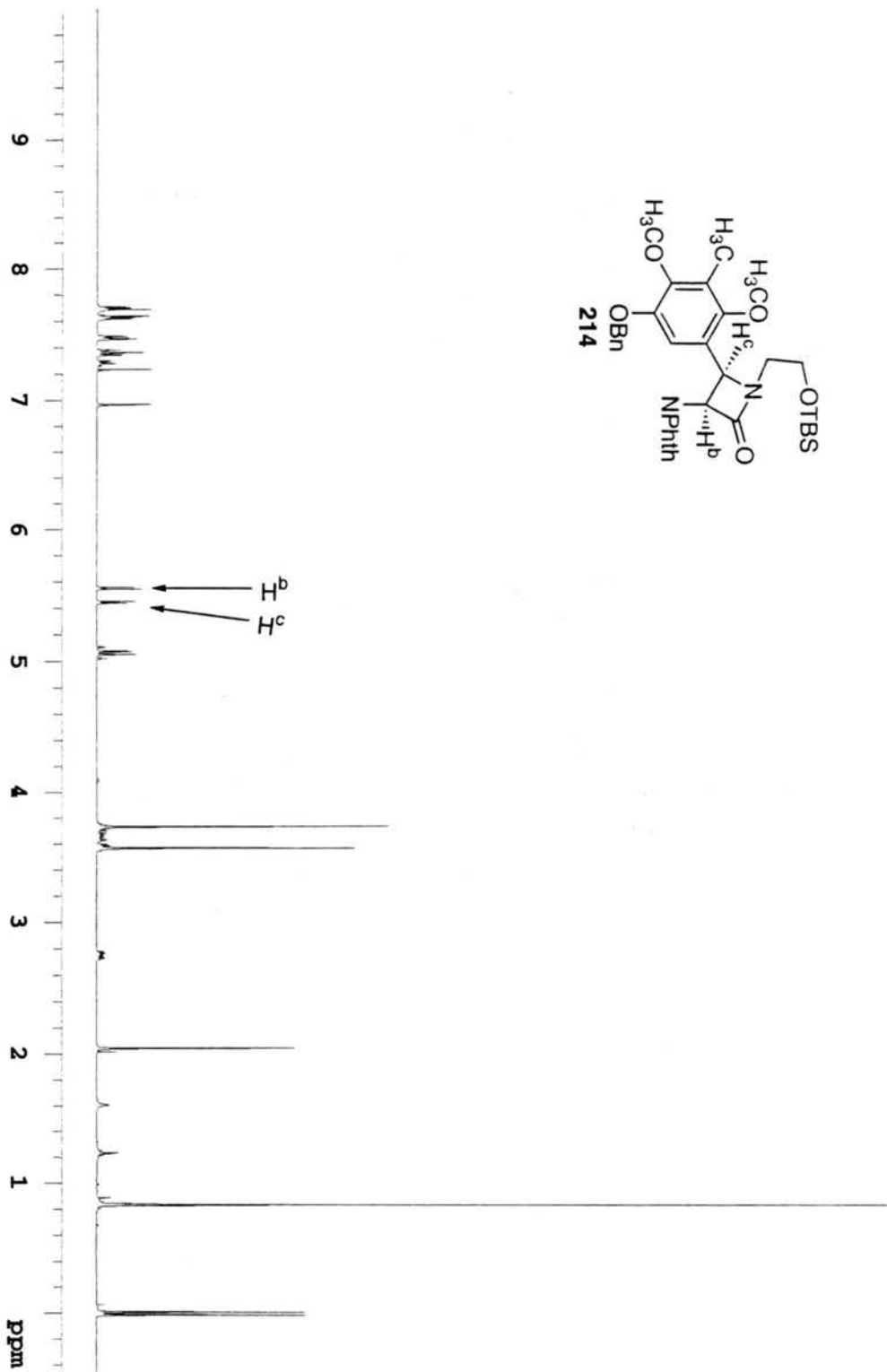
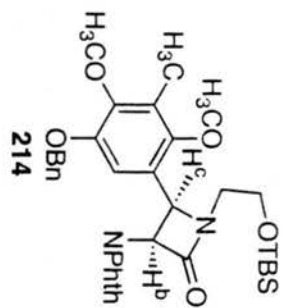


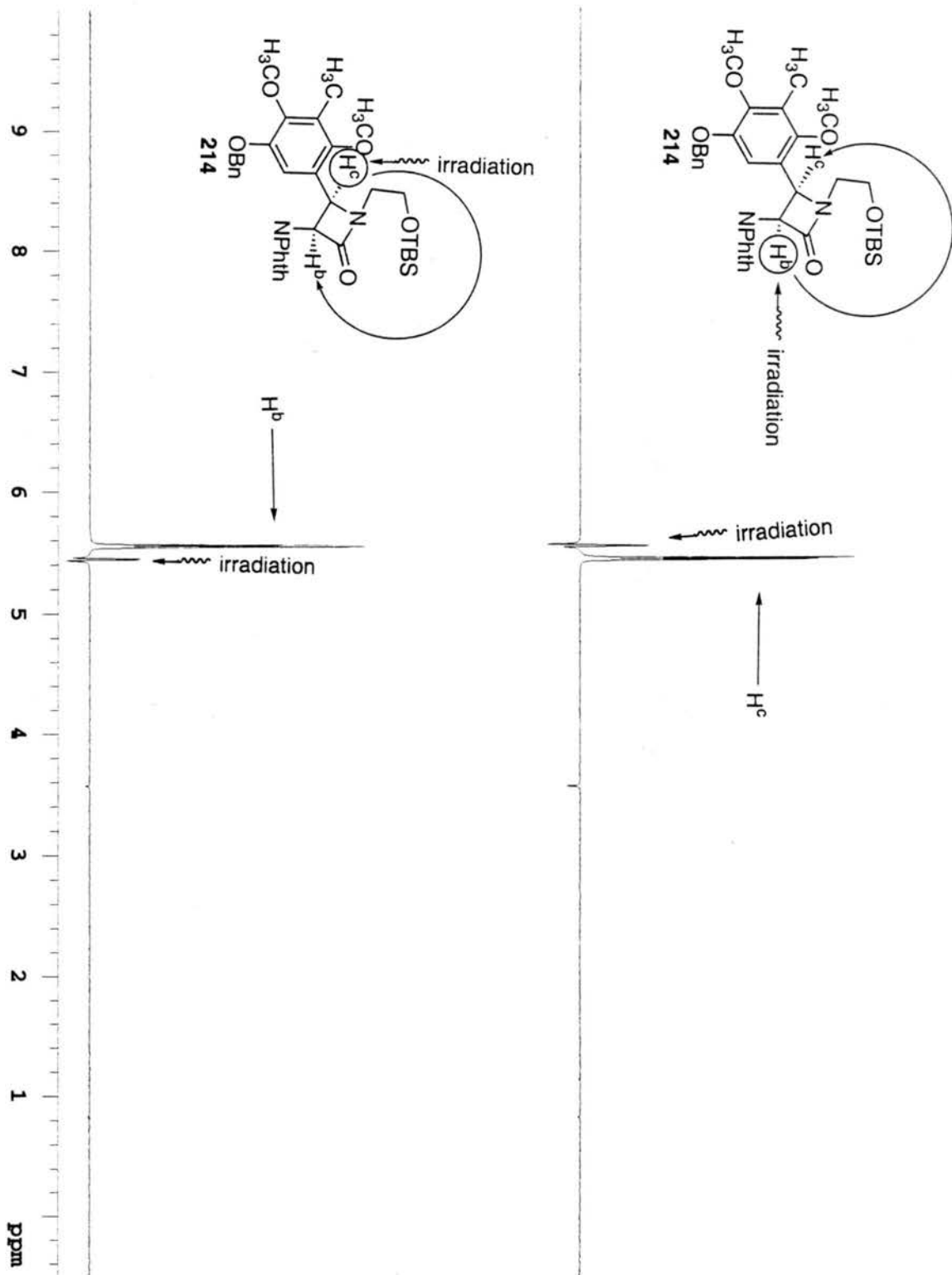
## **Appendix 1**

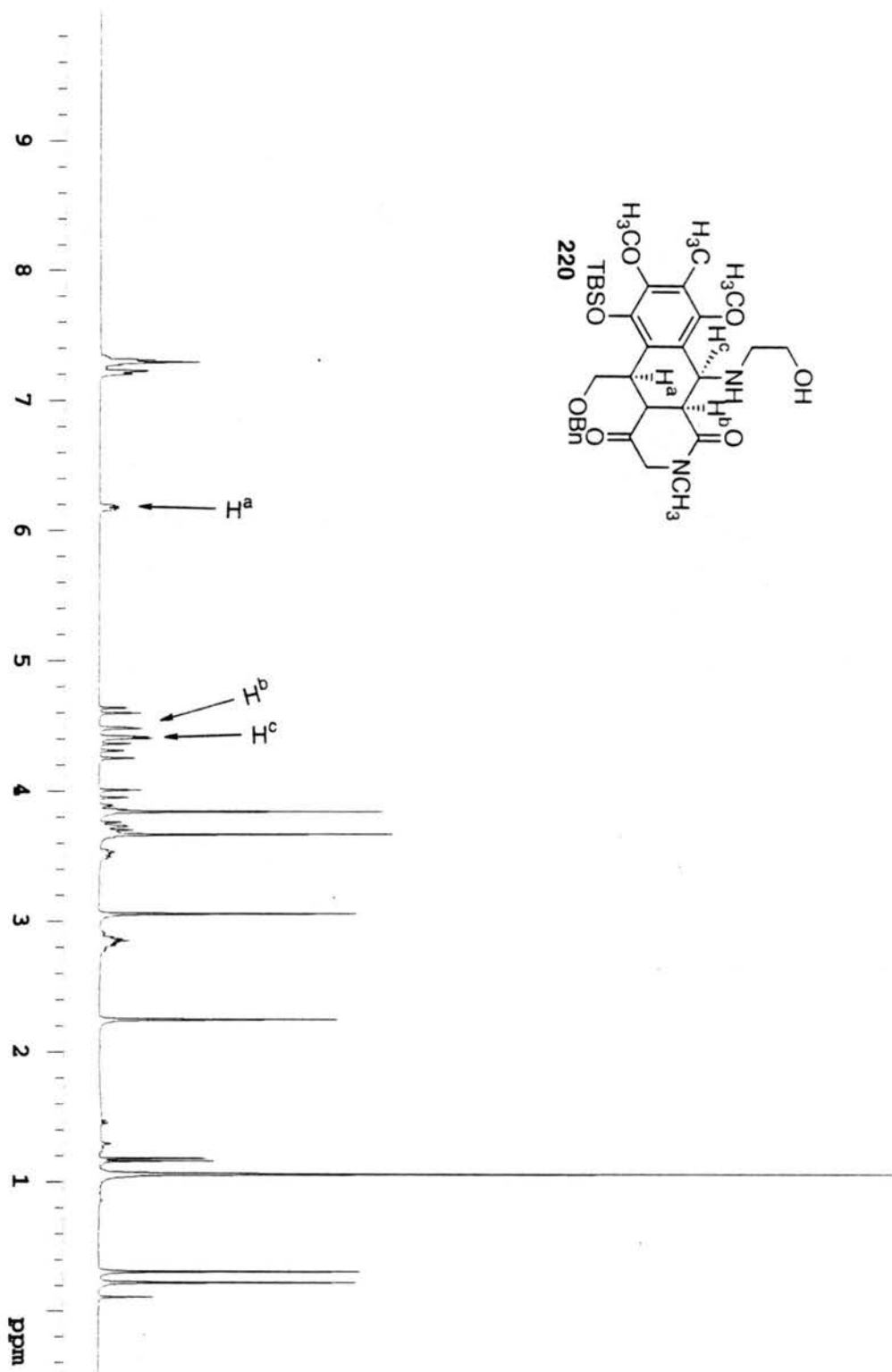
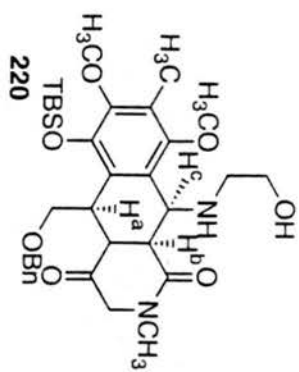
### Nuclear Overhauser Effect Experiments

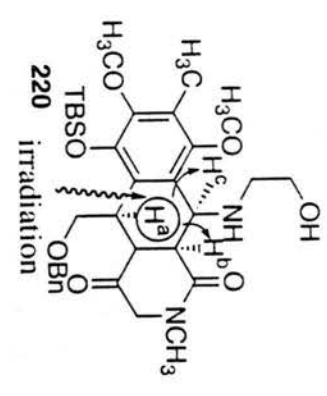
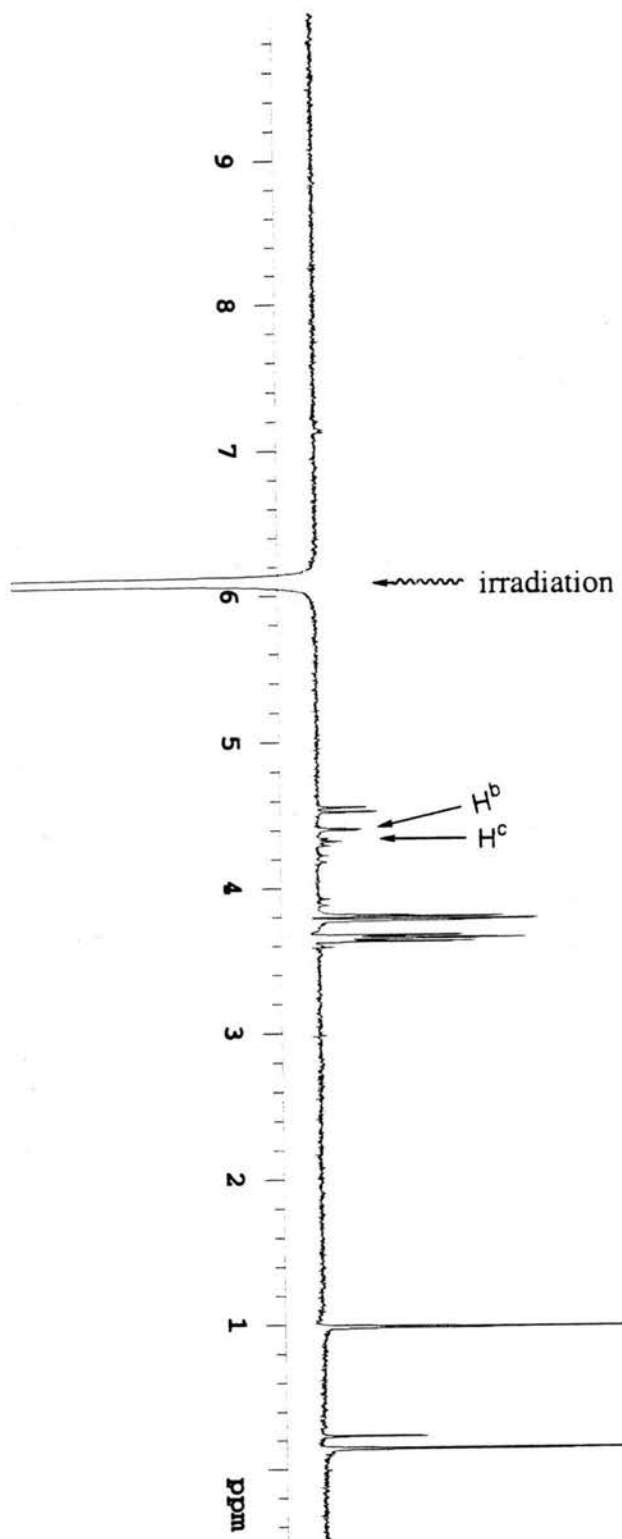
Included are the nOe experiments for the following compounds:

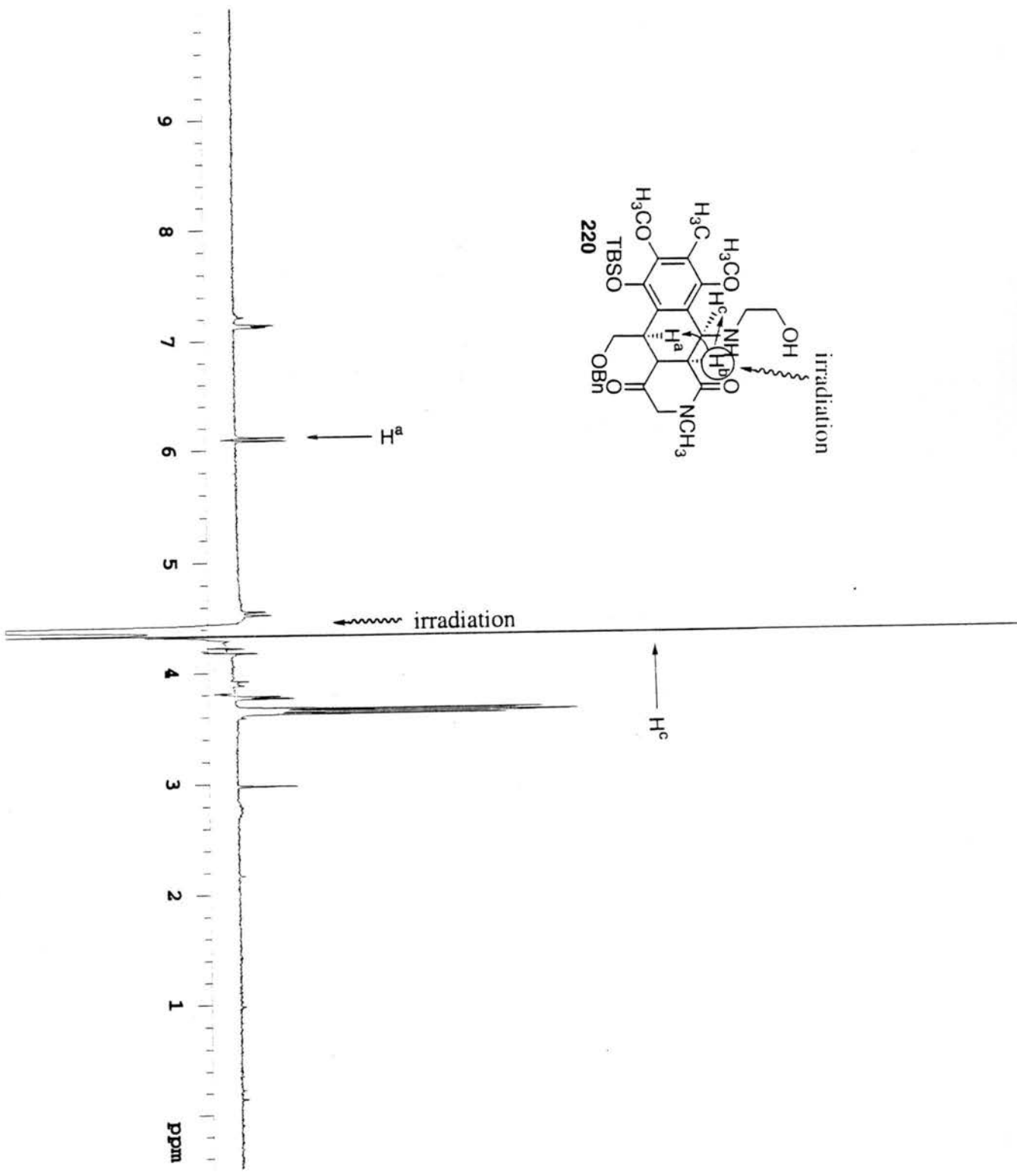
**214, 220, 235**

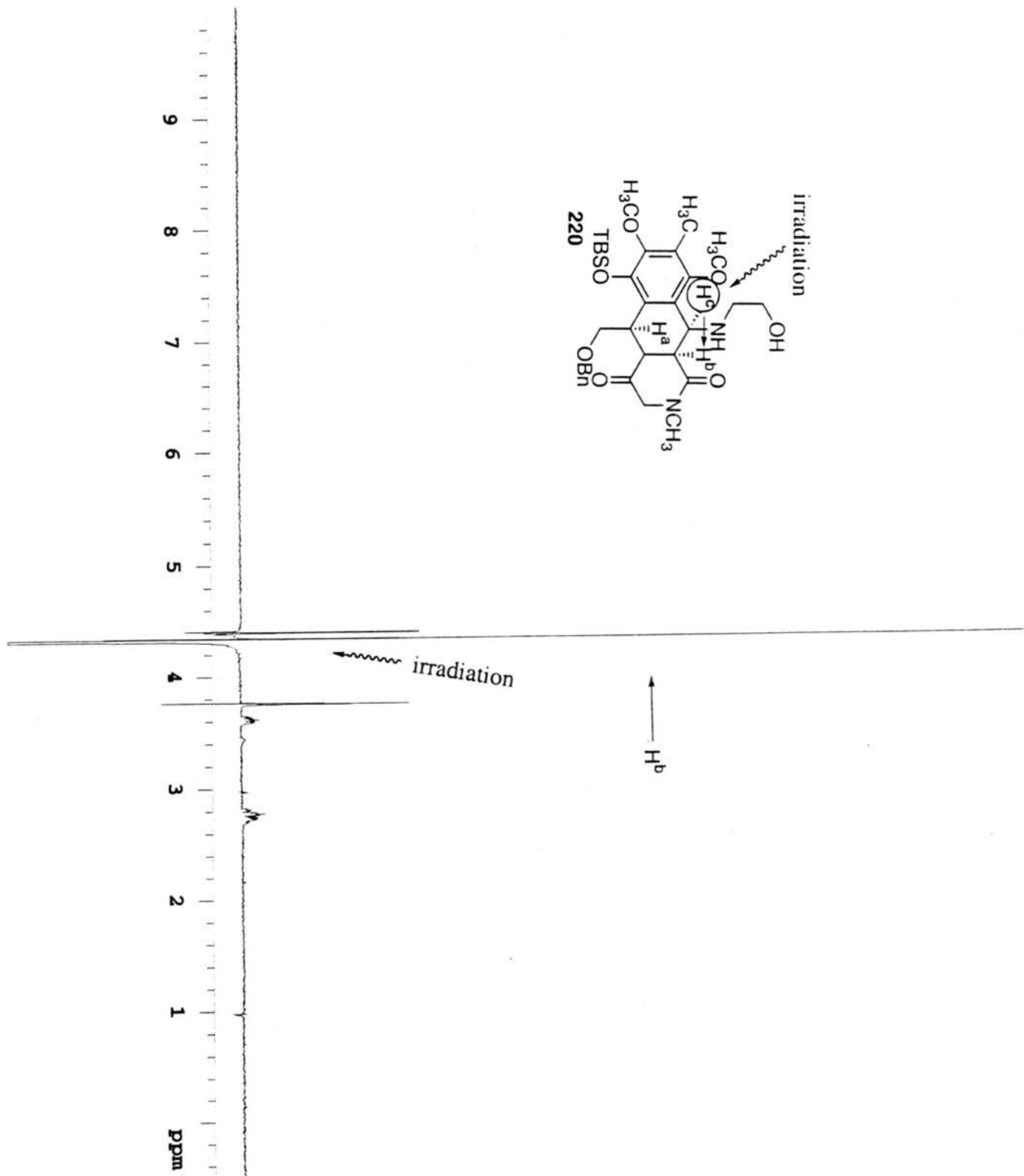
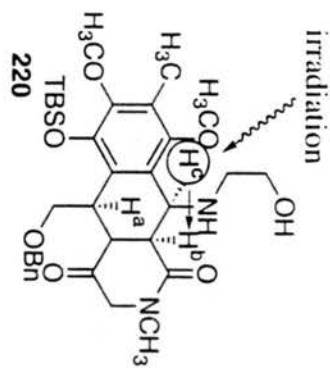




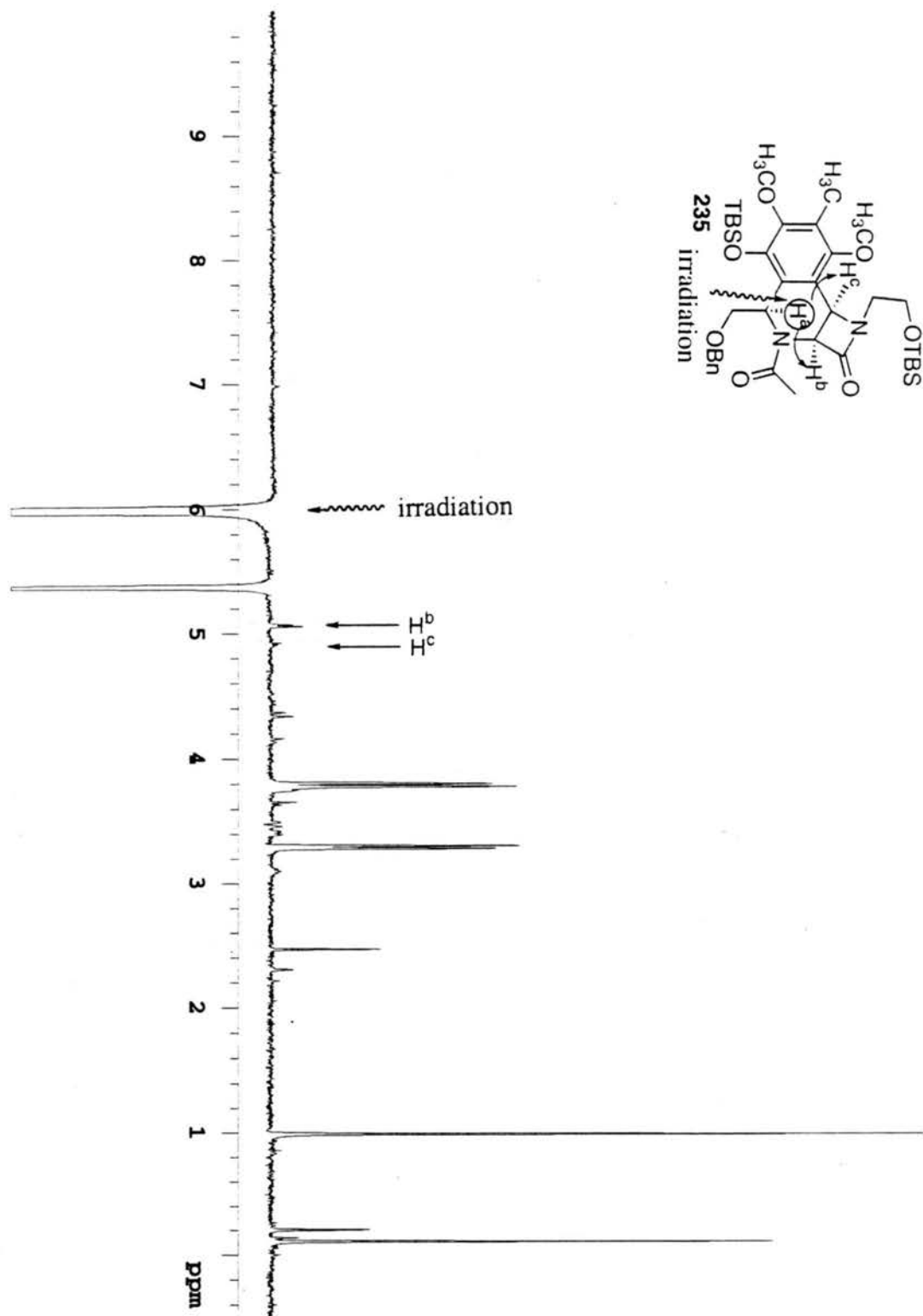


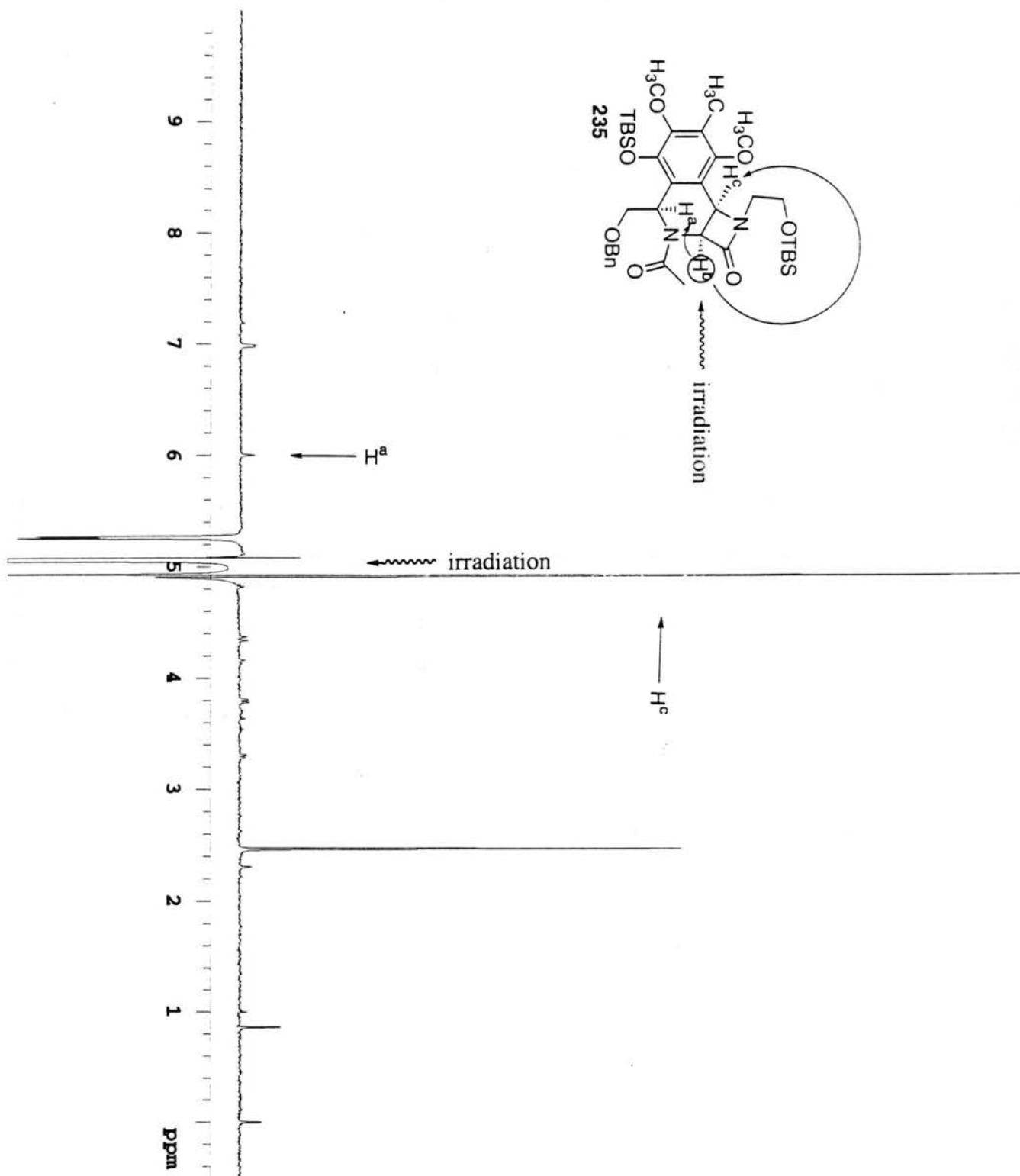


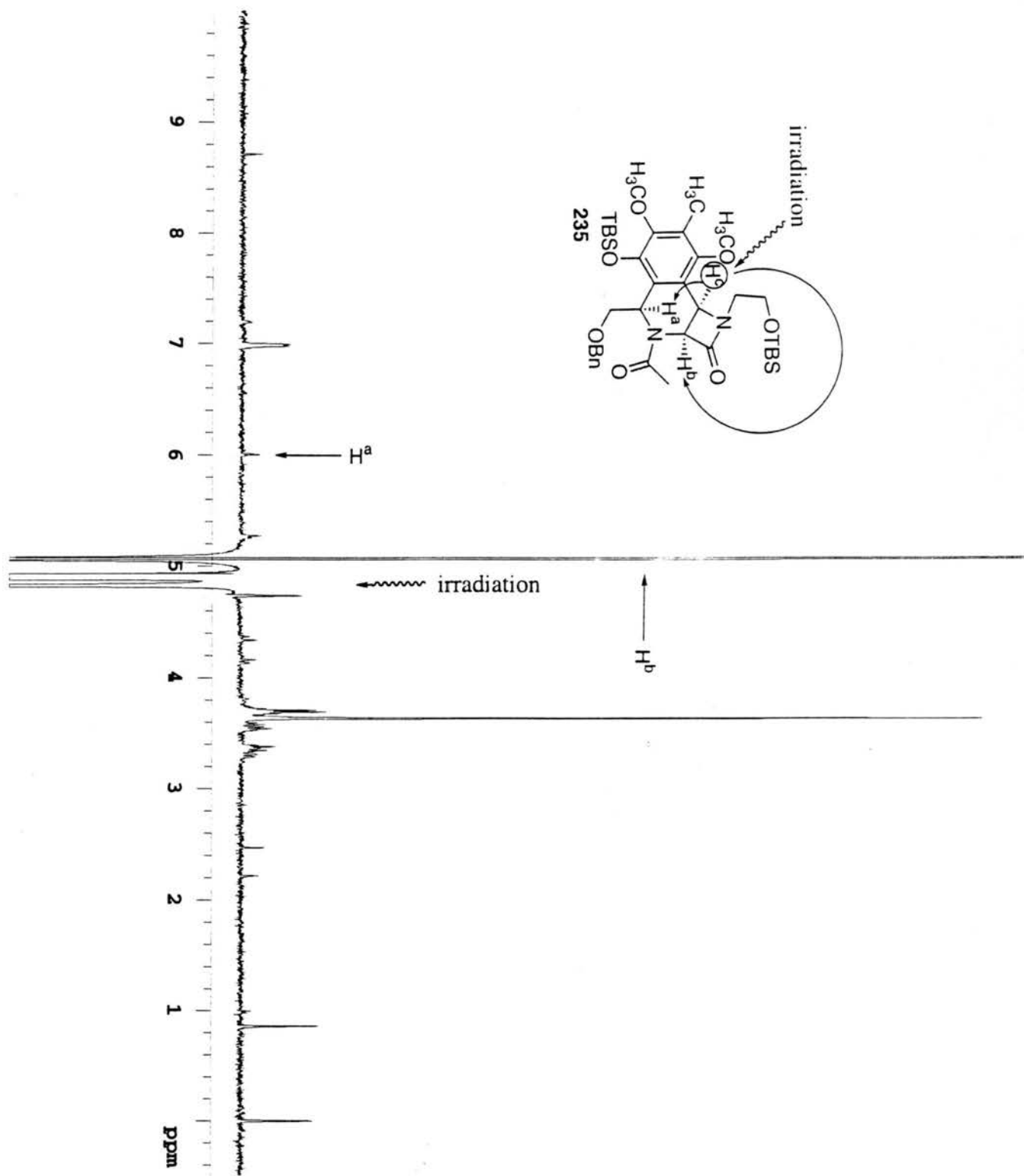












## **Appendix 2**

X-ray crystal structure of **204**.

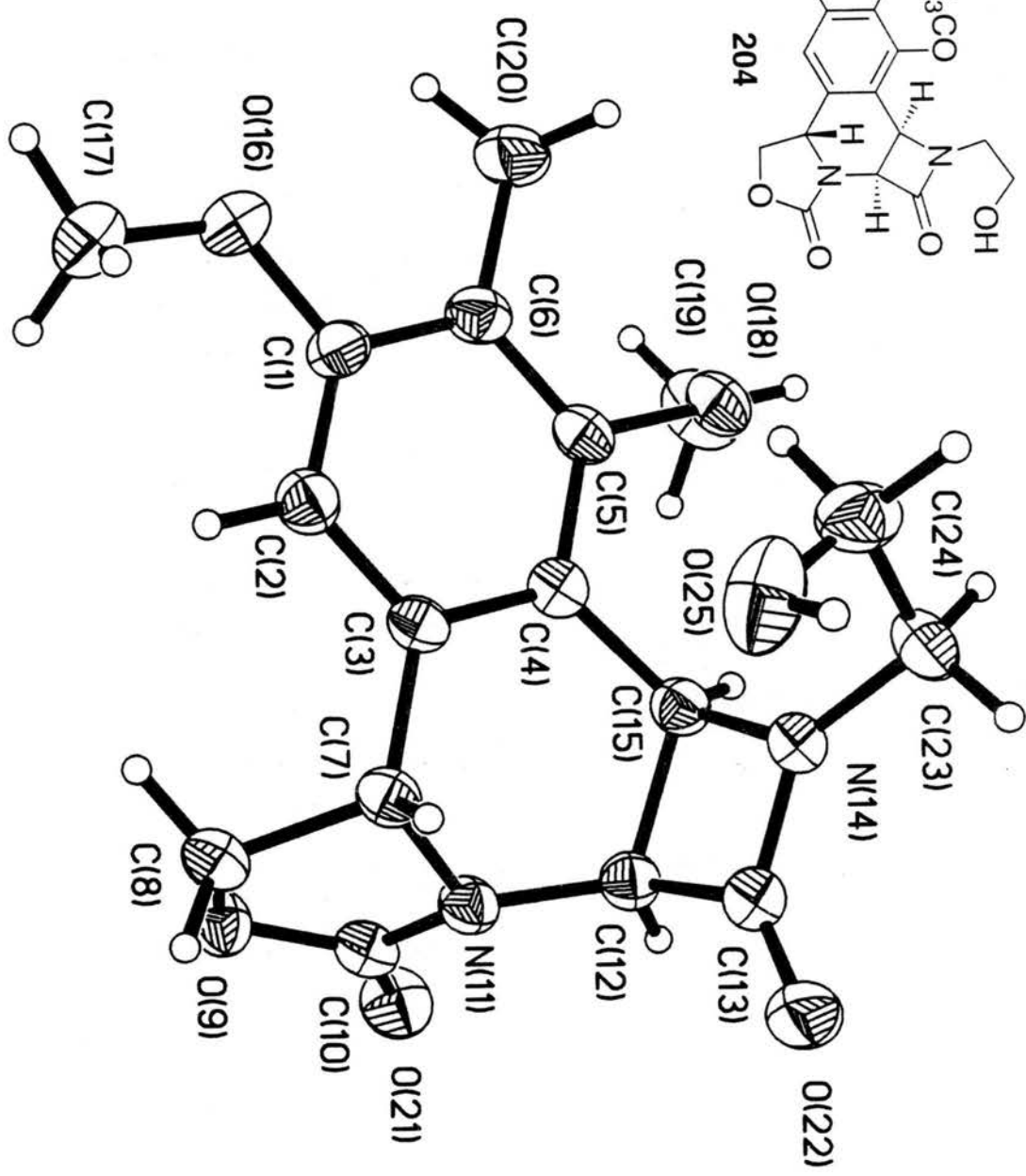
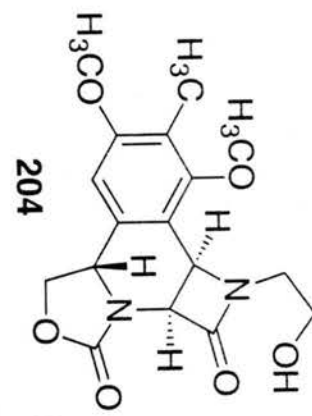


Table 1. Crystal data and structure refinement for 1.

Identification code	rwsad
Empirical formula	$C_{17}H_{20}N_2O_6$
Formula weight	348.35
Temperature	167(2) K
Wavelength	0.71073 Å
Crystal system	Monoclinic
Space group	C2/c
Unit cell dimensions	$a = 30.4982(10)$ Å $\alpha = 90^\circ$ $b = 6.2371(2)$ Å $\beta = 100.4390(13)^\circ$ $c = 18.2966(6)$ Å $\gamma = 90^\circ$
Volume, Z	$3422.8(2)$ Å <sup>3</sup> , 8
Density (calculated)	$1.352$ Mg/m <sup>3</sup>
Absorption coefficient	$0.103$ mm <sup>-1</sup>
F(000)	1472
Crystal size	.08 x .10 x .25 mm
$\theta$ range for data collection	$1.36$ to $28.25^\circ$
Limiting indices	$-40 \leq h \leq 28$ , $-8 \leq k \leq 7$ , $-24 \leq l \leq 19$
Reflections collected	10737
Independent reflections	4121 ( $R_{int} = 0.0495$ )
Absorption correction	<del>None</del> SADABS (Tr. factor: 0.544 - 0.483)
Refinement method	Full-matrix least-squares on $F^2$
Data / restraints / parameters	4120 / 0 / 227
Goodness-of-fit on $F^2$	1.036
Final R indices [ $I > 2\sigma(I)$ ]	$R1 = 0.0616$ , $wR2 = 0.1552$
R indices (all data)	$R1 = 0.1066$ , $wR2 = 0.1847$
Extinction coefficient	$0.0006(4)$
Largest diff. peak and hole	$0.452$ and $-0.393$ eÅ <sup>-3</sup>

Table 2. Atomic coordinates [ $\times 10^4$ ] and equivalent isotropic displacement parameters [ $\text{\AA}^2 \times 10^3$ ] for 1.  $U(\text{eq})$  is defined as one third of the trace of the orthogonalized  $U_{ij}$  tensor.

	x	y	z	$U(\text{eq})$
C(1)	1691(1)	4775(4)	-1930(1)	32(1)
C(2)	1744(1)	4936(4)	-1161(1)	31(1)
C(3)	1486(1)	6392(3)	-840(1)	26(1)
C(4)	1170(1)	7656(4)	-1295(1)	26(1)
C(5)	1120(1)	7439(4)	-2069(1)	28(1)
C(6)	1375(1)	6011(4)	-2402(1)	31(1)
C(7)	1537(1)	6591(4)	4(1)	27(1)
C(8)	2015(1)	6452(4)	451(1)	30(1)
O(9)	2168(1)	8656(3)	518(1)	34(1)
C(10)	1810(1)	9975(4)	391(1)	30(1)
N(11)	1428(1)	8790(3)	211(1)	28(1)
C(12)	1016(1)	9749(4)	-141(1)	29(1)
C(13)	590(1)	8605(4)	-24(1)	33(1)
N(14)	470(1)	8161(3)	-749(1)	29(1)
C(15)	867(1)	9164(4)	-980(1)	29(1)
O(16)	1934(1)	3404(3)	-2289(1)	44(1)
C(17)	2217(1)	1882(6)	-1852(2)	58(1)
O(18)	784(1)	8596(3)	-2510(1)	34(1)
C(19)	941(1)	10546(5)	-2797(2)	50(1)
C(20)	1301(1)	5748(5)	-3239(1)	42(1)
O(21)	1842(1)	11913(3)	445(1)	41(1)
O(22)	415(1)	8234(3)	519(1)	46(1)
C(23)	79(1)	7116(4)	-1173(1)	37(1)
C(24)	183(1)	4874(5)	-1408(2)	45(1)
O(25)	355(1)	3566(3)	-790(1)	56(1)

Table 3. Bond lengths [Å] and angles [°] for 1.

C(1)-O(16)	1.373(3)	C(1)-C(2)	1.391(3)
C(1)-C(6)	1.403(3)	C(2)-C(3)	1.398(3)
C(3)-C(4)	1.398(3)	C(3)-C(7)	1.530(3)
C(4)-C(5)	1.404(3)	C(4)-C(15)	1.504(3)
C(5)-O(18)	1.385(3)	C(5)-C(6)	1.395(3)
C(6)-C(20)	1.516(3)	C(7)-N(11)	1.477(3)
C(7)-C(8)	1.539(3)	C(8)-O(9)	1.449(3)
O(9)-C(10)	1.352(3)	C(10)-O(21)	1.215(3)
C(10)-N(11)	1.369(3)	N(11)-C(12)	1.435(3)
C(12)-C(13)	1.530(3)	C(12)-C(15)	1.564(3)
C(13)-O(22)	1.232(3)	C(13)-N(14)	1.340(3)
N(14)-C(23)	1.453(3)	N(14)-C(15)	1.490(3)
O(16)-C(17)	1.428(3)	O(18)-C(19)	1.441(3)
C(23)-C(24)	1.513(4)	C(24)-O(25)	1.415(4)
O(16)-C(1)-C(2)	123.8(2)	O(16)-C(1)-C(6)	114.7(2)
C(2)-C(1)-C(6)	121.6(2)	C(1)-C(2)-C(3)	120.1(2)
C(2)-C(3)-C(4)	119.8(2)	C(2)-C(3)-C(7)	121.0(2)
C(4)-C(3)-C(7)	119.2(2)	C(3)-C(4)-C(5)	118.9(2)
C(3)-C(4)-C(15)	122.1(2)	C(5)-C(4)-C(15)	119.0(2)
O(18)-C(5)-C(6)	119.4(2)	O(18)-C(5)-C(4)	118.1(2)
C(6)-C(5)-C(4)	122.4(2)	C(5)-C(6)-C(1)	117.3(2)
C(5)-C(6)-C(20)	121.1(2)	C(1)-C(6)-C(20)	121.5(2)
N(11)-C(7)-C(3)	110.4(2)	N(11)-C(7)-C(8)	98.8(2)
C(3)-C(7)-C(8)	116.4(2)	O(9)-C(8)-C(7)	104.5(2)
C(10)-O(9)-C(8)	109.1(2)	O(21)-C(10)-O(9)	122.7(2)
O(21)-C(10)-N(11)	127.5(2)	O(9)-C(10)-N(11)	109.7(2)
C(10)-N(11)-C(12)	121.4(2)	C(10)-N(11)-C(7)	109.9(2)
C(12)-N(11)-C(7)	119.5(2)	N(11)-C(12)-C(13)	116.0(2)
N(11)-C(12)-C(15)	114.8(2)	C(13)-C(12)-C(15)	85.8(2)
O(22)-C(13)-N(14)	132.7(2)	O(22)-C(13)-C(12)	134.8(2)
N(14)-C(13)-C(12)	92.5(2)	C(13)-N(14)-C(23)	132.2(2)
C(13)-N(14)-C(15)	96.0(2)	C(23)-N(14)-C(15)	131.7(2)
N(14)-C(15)-C(4)	115.6(2)	N(14)-C(15)-C(12)	85.7(2)
C(4)-C(15)-C(12)	115.6(2)	C(1)-O(16)-C(17)	118.0(2)
C(5)-O(18)-C(19)	113.1(2)	N(14)-C(23)-C(24)	111.9(2)
O(25)-C(24)-C(23)	111.9(2)		

Symmetry transformations used to generate equivalent atoms:

Table 4. Anisotropic displacement parameters [ $\text{\AA}^2 \times 10^3$ ] for 1.

The anisotropic displacement factor exponent takes the form:

$$-2\pi^2 [ (ha^*)^2 U_{11} + \dots + 2hka^* b^* U_{12} ]$$

	U11	U22	U33	U23	U13	U12
C(1)	30(1)	35(1)	33(1)	-9(1)	9(1)	0(1)
C(2)	32(1)	29(1)	31(1)	-1(1)	2(1)	1(1)
C(3)	28(1)	25(1)	23(1)	-1(1)	2(1)	-4(1)
C(4)	28(1)	24(1)	25(1)	2(1)	4(1)	-2(1)
C(5)	31(1)	28(1)	24(1)	3(1)	0(1)	-2(1)
C(6)	33(1)	35(1)	25(1)	-1(1)	6(1)	-4(1)
C(7)	30(1)	25(1)	25(1)	0(1)	3(1)	-3(1)
C(8)	33(1)	31(1)	25(1)	2(1)	3(1)	-3(1)
O(9)	29(1)	32(1)	38(1)	-2(1)	1(1)	-4(1)
C(10)	33(1)	31(1)	26(1)	-2(1)	2(1)	-4(1)
N(11)	28(1)	26(1)	27(1)	-4(1)	1(1)	0(1)
C(12)	30(1)	28(1)	30(1)	-6(1)	2(1)	1(1)
C(13)	29(1)	38(1)	31(1)	-5(1)	3(1)	3(1)
N(14)	26(1)	33(1)	27(1)	-3(1)	2(1)	0(1)
C(15)	30(1)	28(1)	26(1)	0(1)	2(1)	2(1)
O(16)	41(1)	52(1)	39(1)	-12(1)	10(1)	11(1)
C(17)	54(2)	65(2)	53(2)	-18(2)	1(2)	25(2)
O(18)	36(1)	36(1)	27(1)	5(1)	-3(1)	1(1)
C(19)	62(2)	42(2)	42(2)	17(1)	0(1)	-3(1)
C(20)	47(2)	52(2)	26(1)	-2(1)	8(1)	0(1)
O(21)	43(1)	28(1)	48(1)	-5(1)	3(1)	-7(1)
O(22)	37(1)	73(1)	31(1)	-6(1)	10(1)	-6(1)
C(23)	32(1)	43(2)	34(1)	-2(1)	-5(1)	-2(1)
C(24)	44(2)	48(2)	44(2)	-17(1)	15(1)	-16(1)
O(25)	41(1)	40(1)	90(2)	7(1)	18(1)	1(1)

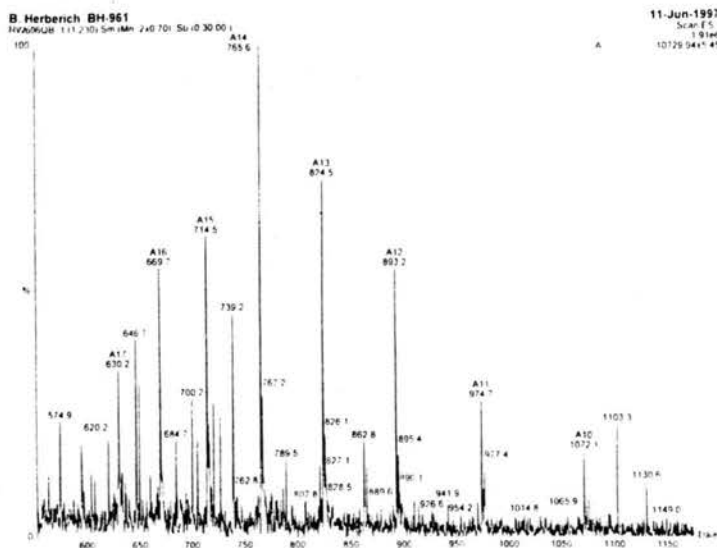
Table 5. Hydrogen coordinates ( $\times 10^4$ ) and isotropic displacement parameters ( $\text{\AA}^2 \times 10^3$ ) for 1.

	x	y	z	U(eq)
H(2A)	1955(1)	4055(4)	-853(1)	37
H(7A)	1341(1)	5530(4)	197(1)	32
H(8A)	2017(1)	5813(4)	947(1)	36
H(8B)	2207(1)	5577(4)	184(1)	36
H(12A)	1006(1)	11327(4)	-48(1)	35
H(15A)	787(1)	10459(4)	-1300(1)	34
H(17A)	2369(1)	1012(6)	-2175(2)	87
H(17B)	2038(1)	950(6)	-1590(2)	87
H(17C)	2439(1)	2640(6)	-1488(2)	87
H(19A)	691(1)	11293(5)	-3103(2)	75
H(19B)	1166(1)	10201(5)	-3100(2)	75
H(19C)	1075(1)	11470(5)	-2382(2)	75
H(20A)	1510(1)	4683(5)	-3369(1)	62
H(20B)	1349(1)	7125(5)	-3470(1)	62
H(20C)	994(1)	5266(5)	-3420(1)	62
H(23A)	-35(1)	7981(4)	-1621(1)	45
H(23B)	-157(1)	7046(4)	-868(1)	45
H(24A)	-93(1)	4213(5)	-1686(2)	53
H(24B)	403(1)	4953(5)	-1744(2)	53
H(25A)	146(1)	2905(3)	-650(1)	84

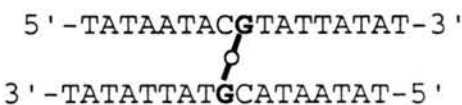
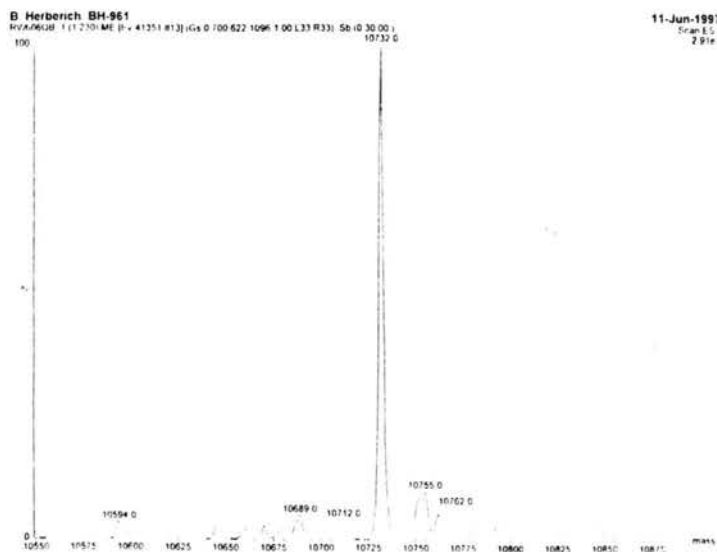
## **Appendix 3**

Mass Spectrum of Bioxalomycin  $\alpha_2$ -DNA Adduct

Spectrum 1.



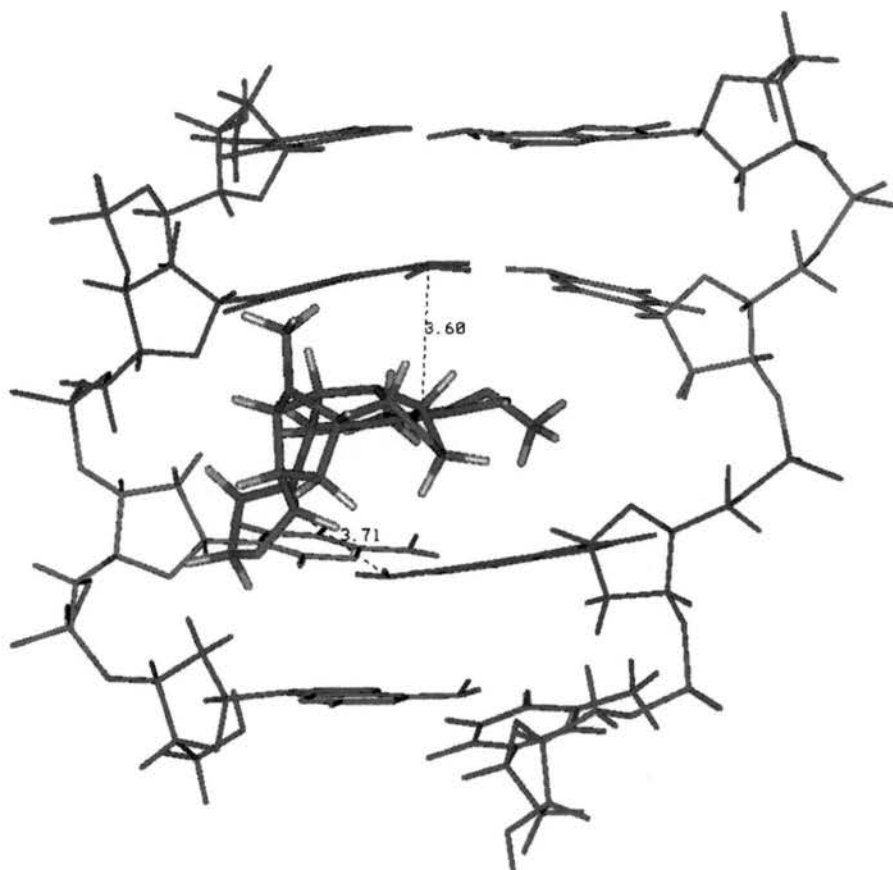
Spectrum 2.



**Spectrum 1.** Electrospray negative ion mass spectral analysis of multiply charged cross-linked adducts, which are labeled A10-A17. **Spectrum 2.** Maximum entropy software on the measured mass spectrum in spectrum 1 gave the molecular ion peak of  $10732 \pm 5.5$ .

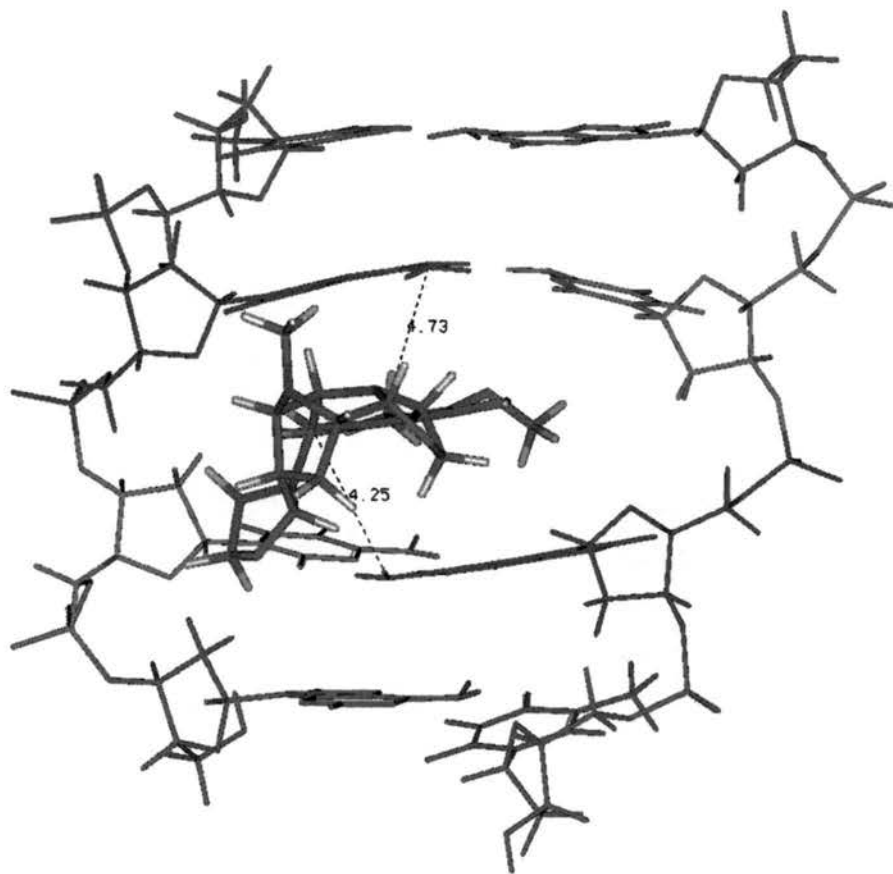
## **Appendix 4**

Molecular Modeling of Bioxalomycin  $\alpha_2$ -DNA Binding



Intercalation of  $d(ACGT)_2$  by bioxalomycin  $\alpha_2$ . Distances shown to C-3a (3.71 Å) and C-9 (3.60 Å).





Intercalation of  $d(ACGT)_2$  by bioxalomycin  $\alpha_2$ . Distances shown to C-7 (4.73 Å) and C-13b (4.25 Å).



## Appendix 5

### Publication

1. *DNA Interstrand Cross-Link Formation Induced by Bioxalomycin  $\alpha_2$* , Williams, R. M.; Herberich, B. *J. Am. Chem. Soc.* **1998**, *120*, 10272~10273.

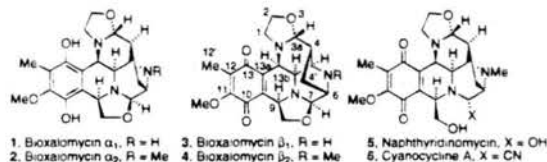
## DNA Interstrand Cross-Link Formation Induced by Bioxalomycin $\alpha_2$

Robert M. Williams\* and Brad Herberich

Department of Chemistry  
Colorado State University  
Fort Collins, Colorado 80523

Received June 12, 1998

The Bioxalomycins (1–4) are antitumor antibiotics isolated from *Streptomyces viridostanicus* subsp. "litoralis";<sup>1</sup> Bioxalomycin  $\alpha_2$  (2), the main component of the mixture, possesses activity against Gram-positive and Gram-negative bacteria, including potent activity against methicillin-resistant *Staphylococcus aureus* (MRSA).<sup>2</sup> Subsequent biological evaluation demonstrated that these compounds also exhibit activity against a panel of tumor cell lines. Ellestad and co-workers at Lederle Laboratories have demonstrated that bioxalomycin  $\beta_2$  is identical with the well-known antibiotic naphthyridinomycin.<sup>3</sup> The antitumor activity of this class of compounds is believed to arise from their ability to inhibit DNA synthesis.<sup>4</sup> Previous work on the antibiotic naphthyridinomycin (5) and cyanocycline A (6)<sup>3</sup> demonstrated that these substances inhibit DNA synthesis via alkylation of DNA in the minor groove in GC-rich regions.<sup>4d</sup> In addition, the obligate reductive activation of these substances through reduction of the quinone moiety to the semiquinone radical anion species results in redox cycling of molecular oxygen with the production of superoxide; downstream Fenton–Haber–Weiss redox cycling culminates in oxidative damage and DNA strand scission.<sup>5</sup>



Remers and co-workers,<sup>4c</sup> as well as Cox and co-workers,<sup>4b,f</sup> have carried out molecular mechanics calculations on the interac-

(1) Zaccardi, J.; Alluri, M.; Ashcroft, J.; Berman, V.; Korshalla, J. D.; Morton, G. O.; Siegel, M.; Tsao, R.; Williams, D. R.; Maiese, W.; Ellestad, G. A. *J. Org. Chem.* **1994**, *59*, 4045–4047.

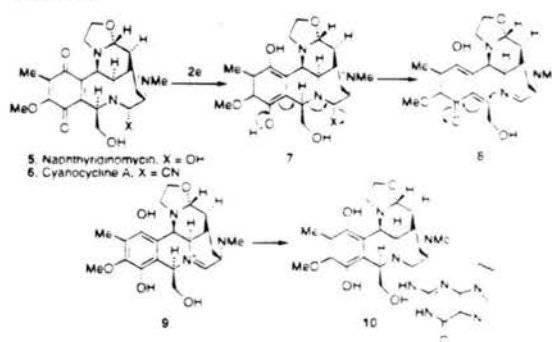
(2) Singh, M. P.; Peterson, P. J.; Jacobus, N. V.; Maiese, W. M.; Greenstein, M.; Steinberg, D. A. *Antimicrob. Agents Chemother.* **1994**, *38*, 1808–1812.

(3) The structure previously portrayed in the literature as naphthyridinomycin (5) is actually incorrect. Ellestad et al.<sup>1</sup> have shown that structure 5 is an artifact of isolation where the oxazolidine ring has been hydrolytically ring-opened. Naphthyridinomycin is therefore identical to bioxalomycin  $\beta_2$ . For isolation and structural elucidation of naphthyridinomycin and the related compound cyanocycline, see: (a) Sygusch, J.; Brisse, F.; Hanessian, S. *Tetrahedron Lett.* **1974**, 4021–4023. (b) Sygusch, J.; Brisse, F.; Hanessian, S. *Acta Crystallogr.* **1976**, *B32*, 1139–1142. (c) Kluepfel, D.; Baker, H. A.; Pantoni, G.; Sengal, S. N.; Sidorowicz, A.; Singh, K.; Vezina, C. *J. Antibiot.* **1975**, *28*, 497–502. (d) Hayashi, T.; Noto, T.; Nawata, Y.; Okazaki, H.; Sawada, M.; Ando, K. *J. Antibiot.* **1982**, *35*, 771–777. (e) Zmijewski, M. J., Jr.; Goebel, M. *J. Antibiot.* **1982**, *35*, 524–526.

(4) (a) Singh, K.; Sun, S.; Kluepfel, D. *Dev. Ind. Microbiol.* **1976**, *17*, 209–221. (b) Cox, M. B.; Arjunan, P.; Arora, S. K. *J. Antibiot.* **1991**, *44*, 885–894. (c) Hill, G. C.; Wunz, T. P.; MacKenzie, N. E.; Gooley, P. R.; Remers, W. A. *J. Med. Chem.* **1991**, *34*, 2079–2088. (d) Zmijewski, M. J., Jr.; Miller-Hatch, K.; Mikolajczak, M. *Chem.-Biol. Interact.* **1985**, *52*, 361–375. (e) Zmijewski, M. J., Jr.; Miller-Hatch, K.; Goebel, M. *Antimicrob. Agents Chemother.* **1982**, *21*, 787–793. A partial intercalative approach of naphthyridinomycin has been considered; however, the unnatural enantiomer was modeled in this study, see: (f) Arora, S. K.; Cox, M. B. *J. Biomol. Struct. Dynam.* **1988**, *6*, 489–502. For related studies on the covalent alkylation of DNA by saframycin A, see: (g) Ishiguro, K.; Takahashi, K.; Yazawa, K.; Sakiyama, S.; Arai, T. *J. Biol. Chem.* **1981**, *256*, 2162–2167.

(5) Breen, A. P.; Murphy, J. A. *Free Radical Biol. Med.* **1995**, *18*, 1033–1076.

## Scheme 1



tion of naphthyridinomycin with DNA and have postulated a mode for covalent monoadduct formation in the minor groove (Scheme 1). Two-electron reduction of the quinone moiety to the hydroquinone (7) was proposed by Zmijewski<sup>4d</sup> to facilitate expulsion of the cyano group (in the case of cyanocycline) or water (in the case of naphthyridinomycin) from C7 to form the iminium species 9; subsequent nucleophilic capture by the exocyclic amine of guanine provides the monoalkylation adduct 10 with the R-stereochemistry at C7.

Additional modeling of the possible formation of covalent adducts at C3a and C7 forced these workers to conclude that: "The geometry of naphthyridinomycin does not permit interstrand cross-linking involving both C3a and C7, but formation of cross-link to protein appears possible".<sup>4c</sup> Herein, we describe the first experimental evidence for DNA interstrand cross-link formation mediated by this class of compounds.

Incubating the 5'-<sup>32</sup>P end-labeled A–B oligomer (Figure 1) with bioxalomycin  $\alpha_2$  at 37 °C for 12 h resulted in band-shifted products of slower mobility for the cross-linked DNA (Figure 1, C, lane 2).<sup>6,8</sup> The cross-linked DNA product was separated by denaturing polyacrylamide gel electrophoresis (DPAGE) (Figure 1, A, lane 2 and Figure 1, B, lane 2). Following isolation, both native and cross-linked materials were subjected to Fe(II)/EDTA footprinting reactions<sup>7</sup> (Figure 1, A and B). As expected, native DNA subjected to Fe(II)-EDTA digestion yields an equimolar assortment of all fragment sizes up to and including the full-length strand (Figure 1, A, lane 5 and Figure 1, B, lane 5). On the other hand, analogous treatment of the cross-linked product yields short fragments corresponding to cleavage at or to the radiolabeled side of the alkylated residue (Figure 1, A, lane 6 and Figure 1, B, lane 6). The observed cleavage patterns show that, for cross-linking of the native duplex, the drug patterns dG10 (oligo A) to dG25 (oligo B) demonstrating a <sup>3</sup>CG<sup>3</sup> specificity. Further evidence for this specificity was obtained by using duplex bearing inosine substituted at the dG25 on oligomer B. Incubation of the 2'-deoxy inosine-substituted duplex, where dG25 is substituted with 2'-deoxy inosine, abolished cross-link formation (Figure 1, C, lane 3). This result implicates that the alkylation events occur at the exocyclic amine at C2 of guanosine in the minor groove of DNA.

(6) The doubling seen for the cross-link product is presumed to be due to orientational isomerism of the drug with respect to the cross-linkable site. For a related example of this phenomenon, see: Williams, R. M.; Rajski, S. R.; Rollins, S. B. *Chem. Biol.* **1997**, *4*, 127–137.

(7) Weidner, M. F.; Millard, J. T.; Hopkins, P. B. *J. Am. Chem. Soc.* **1989**, *111*, 9270–9272.

(8) (a) Tomasz, M. *Chem. Biol.* **1995**, *2*, 575–579. (b) Verdine, G. L. Ph.D. Thesis, Columbia University, 1986. (c) Tomasz, M.; Lipman, R. *J. Am. Chem. Soc.* **1979**, *101*, 6063–6067.

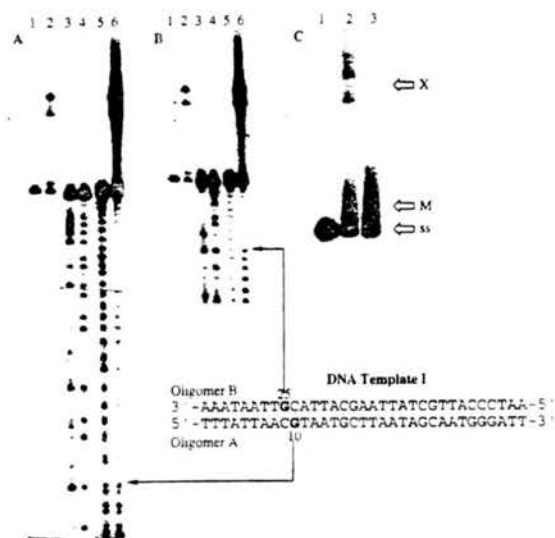


**Figure 1.** Autoradiograms A and B: Fe(II)-EDTA footprinting of cross-linked template 1 ( $^{32}\text{P}$ -labeled at the 5' terminus of oligo A and B, respectively). Lanes 1 and 2, standard DNA, cross-linked template 1; lanes 3 and 4, Maxam-Gilbert G, G+A, respectively; lane 5, 1.5 mM Fe(II)-EDTA control; lane 6, cross-linked product after 1.5 mM Fe(II)-EDTA digestion. Autoradiogram C: Bioxalomyacin  $\alpha_2$  reactions with dG25 substitution in oligomer B. Lane 1 is the native DNA template control. Lane 2 is the cross-linked DNA product. Lane 3 is the reaction of template 1 with bioxalomyacin  $\alpha_2$  where inosine has been substituted at dG25. The cross-linked product at X is where the drug spans dG10 (A) to dG25 (B); ss refers to single-stranded DNA; M is monoalkylated DNA.

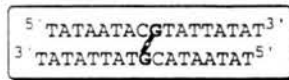


**Figure 2.**

Since earlier molecular modeling suggested that the complete naphthridinomycin molecule could not cross-link DNA, we endeavored to secure experimental evidence for the molecular mass of the cross-linked DNA. We have isolated the gel-purified cross-link from the self-complementary DNA substrate depicted in Figure 2 and have obtained electrospray mass spectral data for the product; the observed mass was  $10732 \pm 5.5$ . The calculated mass for a bioxalomyacin cross-link was 10766; the difference in the calculated and observed mass corresponds to a loss of the hydroxymethyl moiety at C9. This facile fragmentation has been observed in related hydroxymethyl-substituted isoquinolines.<sup>9</sup> In addition, the electrospray mass spectrum of cyanocycline (6) observed under the same conditions gave the molecular ion peak (calcd mass 426.2) minus the  $\text{CH}_2\text{OH}$  fragment (obsd mass 395.1) without detection of the parent ion peak.<sup>10</sup>

Several bis-electrophilic species can be envisioned to arise from the bioxalomyacin framework. Zmijewski proposed a mechanism

(9) Williams, R. M.; Glinka, T.; Flanagan, M. E.; Gallegos, R.; Coffman, H.; Pei, D. *J. Am. Chem. Soc.* **1992**, *114*, 733-740.

(Scheme 1) that accounts for alkylation at C3a or C7 of bioxalomyacin  $\alpha_2$ .<sup>46</sup> Another mechanism for DNA cross-linking by naphthridinomycin was postulated by Moore<sup>11</sup> wherein it was proposed that a quinone methide, formed from the deprotonation of the dihydroquinone, is the alkylating agent. This would place the alkylation sites at C13b and C9 of bioxalomyacin  $\alpha_2$ . We have found that cyanocycline (6) cross-links, in low yield, a similar DNA template, but *only in the presence of dithiothreitol* (which reduces the quinone to the dihydroquinone). This experimental result lends further support for the importance of the dihydroquinone moiety in activating the electrophilic sites. Based on this experimental observation, it can be envisioned that an *ortho*-quinone methide species would result in alkylation at C13b and C7 via a partial intercalative presentation of the drug.<sup>12</sup> Previous modeling work in this area<sup>46,47</sup> apparently only considered approach of the drug from the right-hand sector toward the minor groove in a "face on" approach and did not consider a partial intercalative approach. Positions C3a and C9 are also possible but seem unlikely in view of the well-established importance of the carbinolamine (C7 for bioxalomyacin) or functionally equivalent derivatives of the carbinolamine in DNA alkylation by these drugs.<sup>48</sup> Identification of the exact molecular structure of the bioxalomyacin  $\alpha_2$ -mediated cross-link is currently being pursued in this laboratory.

These results point to the possible significance of benzylic (C13b) oxidation in this family of antitumor antibiotics and that similar DNA interstrand and/or DNA-protein cross-linking behavior might be anticipated for the structurally related marine antitumor antibiotics, the ecteinascidins.<sup>13</sup> Efforts are underway to examine these issues and to determine the exact molecular structure of the cross-linked species and if such a reaction occurs *in vivo*.

**Acknowledgment.** This work was supported by the National Institutes of Health (CA43969). Natural bioxalomyacin  $\alpha_2$  was kindly provided by Dr. George Ellestad (Lederle Labs). Cyanocycline was kindly provided by Professor Steve Gould (Oregon State University). Mass spectra were obtained on instruments supported by NIH Grant GM49631.

**Supporting Information Available:** Experimental procedures for cross-link formation, digestion, and mass spectral analysis of the isolated cross-linked product including data for a 7-deazaguanosine-substituted DNA substrate (7 pages, print/PDF). See any current masthead page for ordering information and Web access instructions.

JA982049Z

(10) The electrospray mass spectrum of bioxalomyacin  $\alpha_2$  yielded a molecular ion ( $m/z$ : 418.0 (M-H)). Based on the observation that cyanocycline, which is in the quinone form, loses  $\text{CH}_2\text{OH}$  as the major fragmentation pathway, we suspect that the cross-linked adduct has undergone a dihydroquinone to quinone autooxidation.

(11) Moore, H. W. *Science* **1977**, *197*, 527-532.

(12) We have carried out preliminary molecular mechanics calculations (Silicon Graphics Indigo I1zx, Biosym Insight/Discover) on bioxalomyacin noncovalently bound to DNA in an effort to determine likely modes of association of the drug with DNA that would result in an appropriate presentation of two electrophilic sites that would culminate in DNA cross-linking. We have found that there is excellent presentation of the putative electrophilic sites at C7 and C13b if the aromatic portion of the drug partially intercalates into the DNA helix.

(13) (a) Rinehart, K. L.; Holt, T. G.; Fregeau, N. L.; Stroh, J. G.; Keifer, P. A.; Sun, F.; Li, L. H.; Marun, D. G. *J. Org. Chem.* **1990**, *55*, 4512-4515. (b) Wright, A. E.; Forleo, D. A.; Gunawardana, G. P.; Gunasekera, S. P.; Koehn, F. E.; McConnell, O. J. *J. Org. Chem.* **1990**, *55*, 4508-4512.

## **Appendix 6**

Research Proposal

## **Abstract**

The goal of this proposal is to develop a methodology to regulate protein-protein interactions utilizing a small ligand as a switch. One of the proteins will be a mutant that has a decreased binding affinity to the other protein of interest. A library of ligands will then be added to the two proteins and screened for the reemergence of protein-protein binding. The selected proteins will then undergo further mutagenesis to improve the complementation of the ligand with the protein. Following this additional round of mutagenesis another assay to select for protein pairs that have the highest response rates to the ligand will be conducted.

## **Background and Significance**

Protein-protein interactions play a central role in a wide variety of processes in the cell. Some of these processes are DNA replication, transcription, translation, cell growth, and signal transduction. Regulation of these processes is a very powerful tool and is the goal of many industrial and academic research groups. The most common route followed to control these processes is to develop a ligand that inhibits activity through binding reversibly or irreversibly to a protein. This route has been relatively unsuccessful in down regulating protein-protein interactions due to the difficulty in finding ligands that effectively block protein-protein interactions. An alternate approach involves the design of a variant of the native protein that does not bind to its substrate due to a mutation. It is desired that the mutation produces a small cavity in the binding domain, but does not introduce a conformational change in the protein. The cavity in the binding domain would abolish binding by eliminating critical interactions. These interactions would most likely include hydrophobic interactions, but could also include hydrogen or ionic bonds. The loss of binding affinity of the protein for its substrate could be regained by the addition of a small ligand that can fill the cavity and reestablish the critical interactions for binding.

We propose to test this approach by developing a strategy to regulate the binding between human growth hormone (hGH) and human growth hormone binding protein (hGHbp). The methodology will use a mutant of the hGHbp that has a decreased binding affinity to hGH. A substitution of tryptophan 104 to alanine in hGHbp (W104A-hGHbp) has shown to decrease binding by a factor of >2500.<sup>1</sup> In the presence of a library of tryptophan analogs the binding between hGH and W104A-hGHbp will be screened using the yeast two-hybrid system<sup>2</sup> and the tryptophan analogs that reconstitute binding will be selected. To increase the shape complementarity of the tryptophan analog to W104A-hGHbp, DNA shuffling of *W104A-hGHbp* will be carried out.<sup>3</sup>

The development of the protein-protein regulatory system will provide insight into the molecular forces that govern protein-protein and protein-ligand interactions. A further understanding of protein-ligand interactions will help contribute to the rational design of potential drugs. In addition this methodology would provide an additional powerful tool for the temporal control of engineered proteins introduced into a host.<sup>4</sup> The binding of the engineered protein would depend on the presence of the ligand to reconstitute an important protein-protein interaction(i.e. binding of an insulin variant to the insulin receptor). Finally if the methodology is successful in reestablishing protein-protein interactions, it could be extended to the screening of possible drugs for genetic diseases. If a genetic disease was the result of a loss of a protein-protein interaction due to a point mutation, the yeast two-hybrid system could be used to screen possible ligands.

### **Research Design and Methods**

The protein-protein interaction that will be investigated is between the human growth hormone (hGH) and the extracellular domain of its receptor (hGHbp).<sup>1</sup> The hGHbp/hGH complex exists as a 2:1 complex with a dissociation constant ( $K_d$ ) of 0.3 nM

corresponding to a binding free energy of  $-12.3 \text{ kcal mol}^{-1}$ .<sup>5</sup> Alanine mutagenesis of the binding domain of hGHbp has identified a number of residues that are important in binding to hGH.<sup>1b</sup> The most critical residue is tryptophan 104 and the W104A mutant (W104A-hGHbp) demonstrated a >2500 fold loss of binding to hGH ( $K_d > 1\mu\text{M}$ ,  $>4.5 \text{ kcal mol}^{-1}$ ). The mutation forms a  $150 \text{ \AA}$  hole, which decreases lipophilic interactions and results in the great loss of affinity for binding. This position is specific for tryptophan and even the substitution of phenylalanine, which contains an aromatic sidechain, for W104 decreases binding 110 fold.

Since the binding is very specific for tryptophan, the library of ligands used to fill this cavity will be based on a tryptophan or indole scaffold. The Available Chemicals Directory<sup>6</sup> will be searched to find many possible analogs as a starting point, examples that are available from Aldrich are shown in Figure 1.

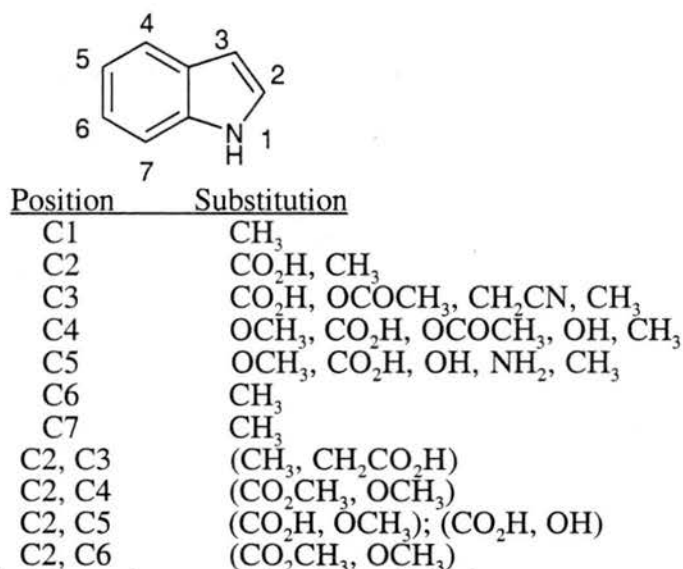
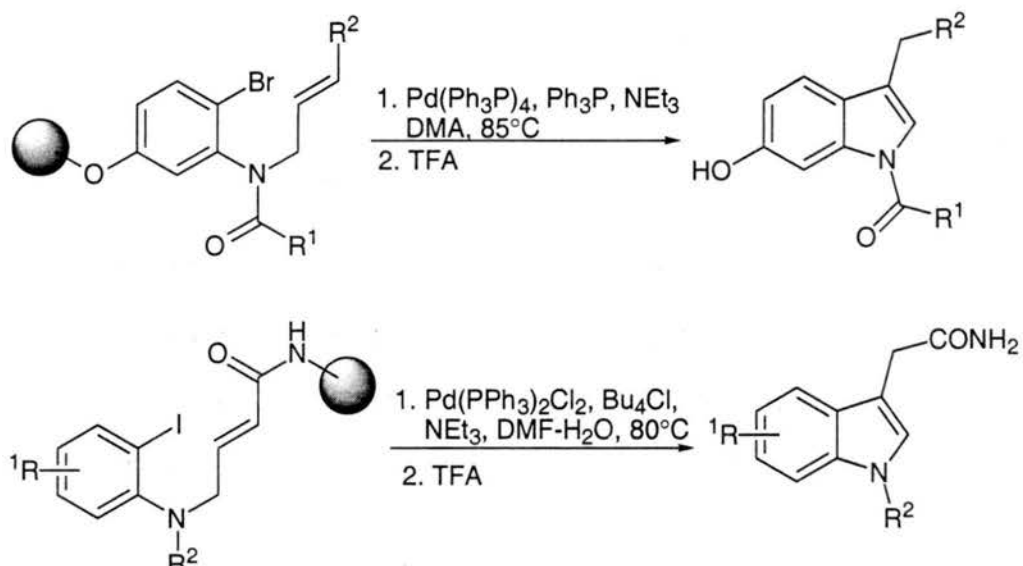


**Figure 1.** A sample of indole analogs available from Aldrich.

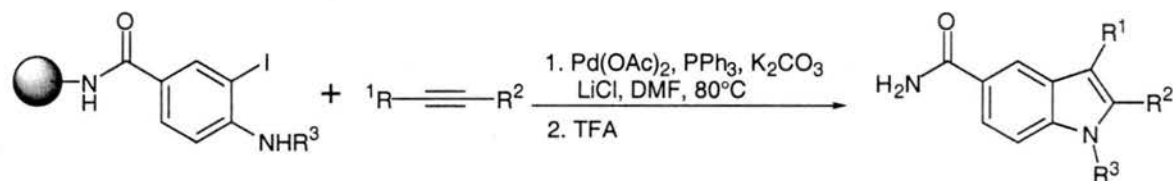
Once lead structures are identified, sublibraries around this framework can be synthesized. There are two general strategies for the construction of indoles on solid

support. The first strategy uses an intramolecular Heck reaction to form the indole ring system.<sup>7</sup> Using this methodology variation can be achieved at C3 or, by changing the attachment of the polymer support, substituents at positions C4-7 can be introduced.



**Scheme 1.** Solid phase syntheses of indole derivatives based on an intramolecular Heck reaction.

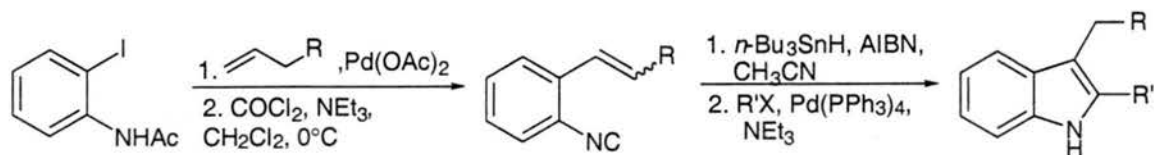
The other strategy uses an intramolecular palladium heteroannulation between an alkyne and a resin-bound *o*-iodoaniline.<sup>8</sup> This approach allows different substitutions at the C1 and C2 positions. The functional groups that have been substituted at C1 and C2 include alkyl, arene, alcohol, ester, trimethylsilyl, and amino moieties.



**Scheme 2.** Palladium catalyzed heteroannulation of an *o*-iodoaniline and an alkyne to give an indole framework.

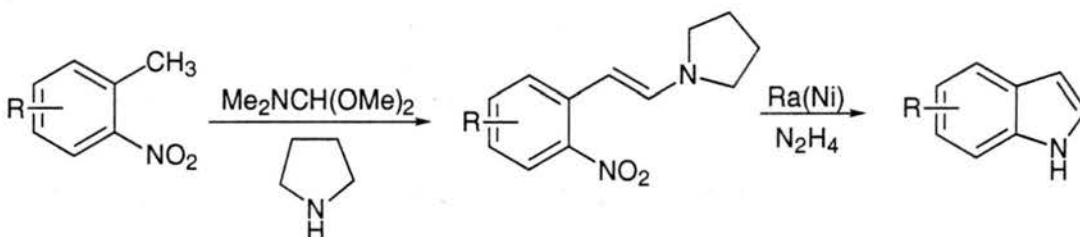
In addition to these syntheses of indole analogs on solid-support, libraries of indoles have been synthesized in solution. A synthesis of 2,3-disubstituted indoles that can

prepare a wide range of indole derivatives has been developed by Fukuyama.<sup>9</sup> In this approach the C2 substituent is introduced by a Heck reaction while the C3 substituent is introduced via a Stille coupling.



**Scheme 3.** Synthesis of 2,3-disubstituted indoles by Fukuyama.

Substitution at positions 4-7 of indole can be accomplished by synthesizing the indole framework from the appropriately substituted 2-nitrotoluene.<sup>10</sup> This synthesis is versatile and can accommodate electron donating (alkoxy) and electron withdrawing (halogens, esters) groups on the aromatic ring.



**Scheme 4.** Synthesis of substituted indoles at positions 4-7

The ligands and proteins will be screened using the yeast two-hybrid system developed by Fields.<sup>2</sup> This assay uses plasmids that contain fusion proteins between the DNA binding domain of GAL4 (residues 1-147) and the transcription activation domain of GAL4 (residues 768-881) and the two proteins of interest X and Y (Figure 2). The fusion proteins are ligated into plasmids, which are introduced into yeast. The yeast are grown on plates that contain 5-bromo-4-chloro-3-indoyl- $\beta$ -D-galactopyranoside (X-gal) and  $\beta$ -galactosidase activity is monitored by a colorimetric assay. If the two proteins interact, transcription of the GAL1-*lacZ* gene will occur, resulting in  $\beta$ -galactosidase activity. The

yeast two-hybrid assay was chosen since it is a library based screen that has been demonstrated to be highly sensitive.<sup>11</sup> In addition the magnitude of  $\beta$ -galactosidase activity is proportional to the binding affinity of the two fusion proteins.<sup>12</sup> This is important since one goal is to engineer a protein-ligand pair that has a high binding affinity, which will result in a high rate of response to the addition of a ligand. If the yeast two hybrid system does not work as an assay, an alternative *in vitro* screening assay is monovalent phage display.<sup>13</sup>

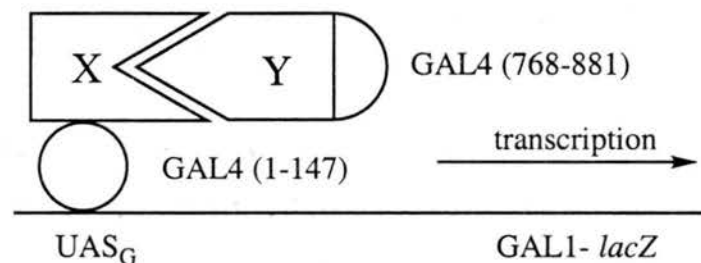
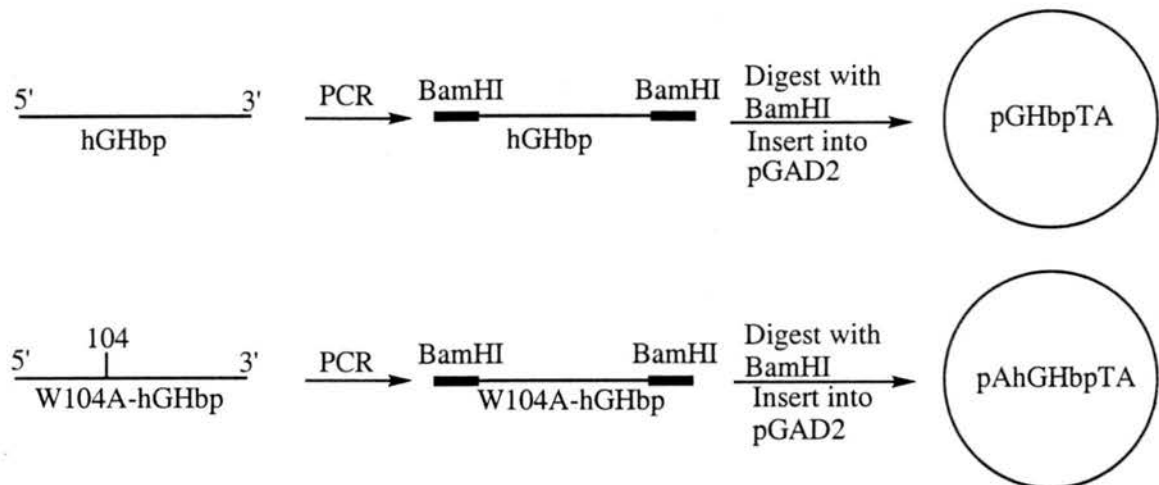


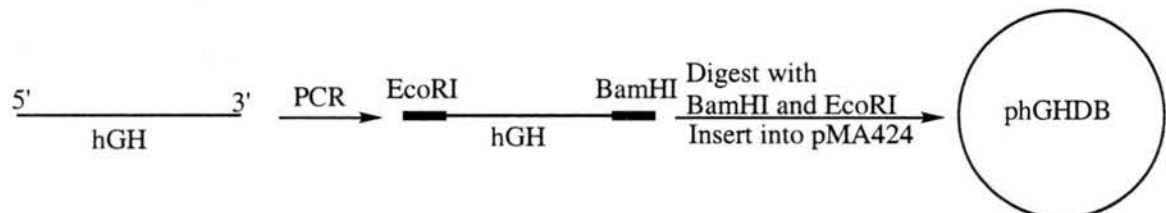
**Figure 2.** A general scheme of the yeast two-hybrid system developed by Fields.

In the yeast-two hybrid system, the first step will be to construct the fusion proteins of hGHbp and hGH with the transcriptional activation domain and DNA binding domain of GAL4, respectively. The hGHbp and W104A-hGHbp proteins will be joined to the transcriptional activation domain of GAL4 to give the two fusion products hGHbp-GALTA and W104A-hGHbp-GALTA, by inserting the two DNA fragments into pGAD2.<sup>2b</sup> This plasmid contains the sequence for the GAL4 transcription activation domain followed by a unique BamHI restriction site and a *LEU2* selectable marker. The gene fragment encoding the extracellular domain of hGHbp corresponding to residues 1-238 of hGHbp and W104A-hGHbp will be prepared using PCR of the respective cDNA<sup>14</sup> (available in the Schultz lab) with primers that include BamHI restriction sites. The cDNA of hGHbp and W104A-hGHbp will then be digested with BamHI and inserted into pGAD2 to give pHGHbpTA and pAhGHbpTA.



**Scheme 5.** The preparation of plasmids pGHbpTA and pAhGHbpTA. The sense and antisense primers are CGCGGATCCGCGGTATGGATCTCTGGCAGCTGCTG and CGCGGATCCGCGTTGGCTCATCTGAGGAAGTGTTAC, respectively.

The human growth hormone will be fused to the DNA binding domain of GAL4 by inserting it into pMA424.<sup>15</sup> This plasmid contains the DNA binding domain of GAL4 followed by EcoRI and BamHI restriction sites and a yeast *HIS3* selection maker. The hGH protein will be prepared using PCR of the cloned gene<sup>16</sup> (available in the Schultz lab) with sense and antisense primers that contain EcoRI and BamHI restriction sites, respectively. The PCR product will then be digested with BamHI and EcoRI and inserted into pMA424 to give pHGDB.

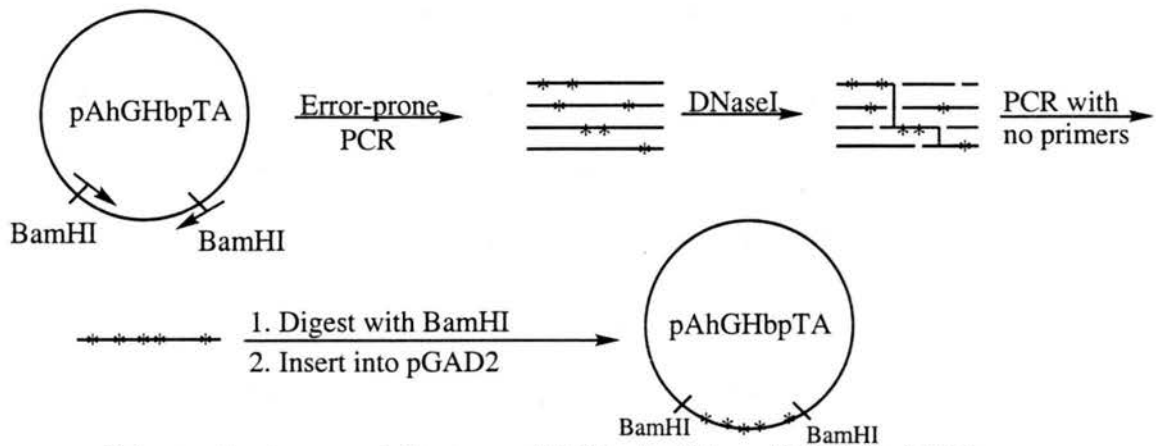


**Scheme 6.** The preparation of pHGDB. The sense and antisense primers are CCGGAATCCGGATGTTCCCAACTATAACCACTATCTCG and CGCGGATCCGCGCTAGAAGCCACAGCTGCCCTCCACAG, respectively.

The plasmids will be introduced into the yeast strain GGY1::171,<sup>17</sup> which is His<sup>-</sup> and Leu<sup>-</sup>. The yeast will be grown on plates lacking histidine and leucine and in the

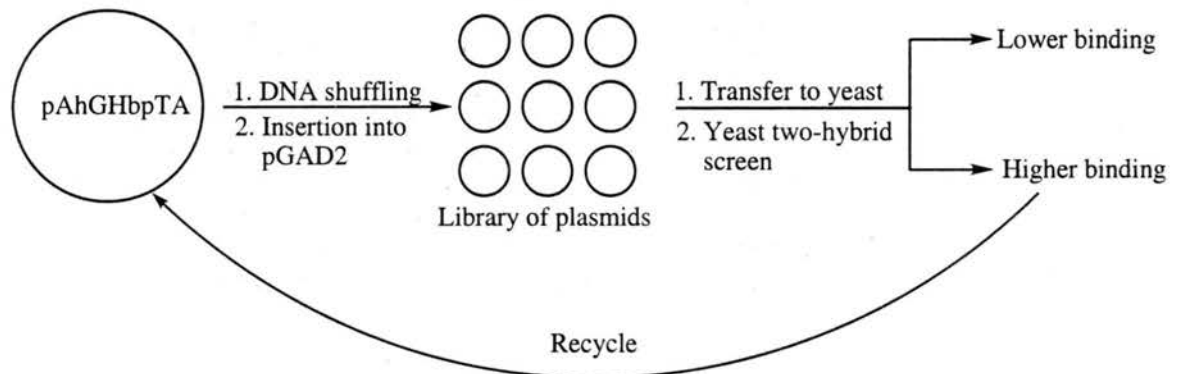
presence of X-gal. The absence of leucine and histidine in the growth media serves as a control to insure only the yeast colonies that contain both plasmids are grown. The yeast that contain pHGbpTA and pHGDB will serve as the positive control. These yeast should turn blue due to transcription of the *GAL1-lacZ* gene and  $\beta$ -galactosidase activity. On the other hand the yeast that contain pAhGHbpTA and pHGDB and in the absence of ligands, should not demonstrate any  $\beta$ -galactosidase activity and will serve as the negative control.

To screen for possible ligands, the yeast colonies that contain the pAhGHbpTA and pHGDB will then be grown on plates or in microtiter wells that contain a ligand. The ligands that are able to fill the cavity in the binding domain between W104A-hGHbp and hGH and reestablish  $\beta$ -galactosidase activity will be selected. It is our expectation that the first round of selection may not produce ligands that have a high binding affinity to W104A-hGHbp. The use of tryptophan analogs provide ligands that are designed to fill the cavity in the binding domain between W104A-hGHbp and hGH, but not to bind substantially to W104A-hGHbp itself. An important feature of our strategy is the tailoring of the protein to the ligand. To increase the binding affinity of the ligand to W104A-hGHbp, it will be mutagenized by DNA shuffling<sup>3</sup> as this technique has been proven to greatly enhance the rate of a protein for a selected trait.<sup>18</sup>



**Scheme 7.** A general diagram of DNA shuffling of *W104A-hGHbp*.

Random point mutations will be introduced into *W104A-hGHbp* using error prone PCR.<sup>19</sup> The pool of DNA will then be digested with DNase I to give 100 bp fragments. The fragments will be reconstructed by a PCR process with no primers, instead homogenous sections of the different DNA strands will serve as the primers. The new fragments will then be digested with BamHI and ligated back into pGAD2F.



**Scheme 8.** DNA shuffling followed by the yeast two-hybrid system assay should produce ligands that have a high binding affinity to *W104A-hGHbp* and reestablish the binding affinity between *W104A-hGHbp* and hGH.

Because of the new round of mutagenesis the new *W104A-hGHbp-GALTA* fusion protein may be able to bind to the hGH-GAL4DB fusion protein in the absence of a ligand. At this point it will be important to eliminate these false positives.<sup>20</sup> *pAhGHbpTA* will be transformed into the yeast with no other plasmid, with pGHDB, and with pGHDB and a

ligand. If the transcription activation hybrid by itself or with the DNA binding hybrid in the absence of a ligand displays  $\beta$ -galactosidase activity, the transcription activation hybrid will be eliminated from consideration. The rounds of DNA shuffling followed by selection will be continued until a ligand-hGHbp pair is found to exhibit a quick response to the ligand. This will be measured against the  $\beta$ -galactosidase activity found using the hybrid system with native hGH and hGHbp. The selected hGHbp mutant protein will then undergo DNA shuffling against the wild-type hGHbp and screened with the ligand to eliminate any non-necessary mutations.

---

### Literature Citations

<sup>1</sup> (a) Cunningham, B. C.; Wells, J. A. High resolution epitope mapping of hGH-receptor interactions by alanine-scanning mutagenesis. *Science* **1989**, *244*, 1081-1085. (b) Bass, S. H.; Mulkerrin, M. G.; Wells, J. A. A systematic mutational analysis of hormone-binding determinants in the human growth hormone receptor. *Proc. Natl. Acad. Sci. U.S.A.* **1991**, *88*, 4498-4502. (c) Clackson, T.; Wells, J. A. A hot spot of binding energy in a hormone-receptor interface. *Science* **1995**, *267*, 383-386. (d) Atwell, S.; Ultsch, M.; De Vos, A. M.; Wells, J. A. Structural plasticity in a remodeled protein-protein interface. *Science* **1997**, *278*, 1125-1128. (e) Wells, J. A.; Cunningham, B. C.; Fuh, G.; Lowman, H. B.; Bass, S. H.; Mulkerrin, M. G.; Ultsch, M.; DeVos, A. M. The molecular basis for growth hormone-receptor interactions. *Rec. Prog. Horm. Res.* **1993**, *48*, 253-275. (f) Fuh, G.; Cunningham, B. C.; Fukunaga, R.; Nagata, S.; Goeddel, D. V.; Wells, J. A. Rational design of potent antagonists to the human growth hormone receptor. *Science* **1992**, *256*, 1677-1680. (g) Cunningham, B. C.; Jhurani, P.; Ng, P.; Wells, J. A. Receptor and antibody epitopes in human growth hormone identified by homolog-scanning. *Science* **1989**, 1330-1336.

<sup>2</sup> (a) Fields, S.; Song, O.-K. A novel genetic system to detect protein-protein interactions. *Nature* **1989**, *340*, 245-246. (b) Chien, C.-T.; Bartel, P. L.; Sternglanz, R.; Fields, S. The yeast two-hybrid system: a method to identify and clone genes for proteins that interact with a protein of interest. *Proc. Natl. Acad. Sci. U.S.A.* **1991**, *88*, 9578-9582.

<sup>3</sup> (a) Stemmer, W. P. C. Rapid evolution of a protein *in vitro* by DNA shuffling. *Nature* **1994**, *370*, 389-391. (b) Stemmer, W. P. C. DNA shuffling by random fragmentation and reassembly: *in vitro* recombination for molecular evolution. *Proc. Natl. Acad. Sci. U.S.A.* **1994**, *91*, 10747-10751.

<sup>4</sup>(a) Gossen, M.; Bujard, H. Tight control of gene expression in mammalian cells by tetracycline-responsive promoters. *Proc. Natl. Acad. Sci. U.S.A.* **1992**, *89*, 5547-5551. (b) Furth, P. A.; St. Onge, L.; Boger, H.; Gruss, P.; Gossen, M.; Kistner, A.; Bujard, H.; Henninghausen, L. Temporal control of gene expression in transgenic mice by a tetracycline-responsive promoter. *Proc. Natl.*

*Acad. Sci. U.S.A.* **1994**, *91*, 9302-9306. (c) No, D.; Yao, T.-Y.; Evans, R. M. Ecdysone-inducible gene expression in mammalian cells and transgenic mice. *Proc. Natl. Acad. Sci. U.S.A.* **1996**, *93*, 3346-3351. (d) Io, S. N.; Biggar, S. R.; Spencer, D. M.; Schreiber, S. L.; Crabtree, G. R. Dimeric ligands define a role for transcriptional activation domains in reinitiation. *Nature* **1996**, *382*, 822-826. (e) Kistner, A.; Gossen, M.; Zimmerman, F.; Jerecic, J.; Ullmer, C.; Lubbert, H.; Bujard, H. Doxycycline-mediated quantitative and tissue-specific control of gene expression in transgenic mice. *Proc. Natl. Acad. Sci. U.S.A.* **1996**, *93*, 10933-10938. (f) Belshaw, P. J.; Ho, S. N.; Crabtree, G. R.; Schreiber, S. L. Controlling protein association and subcellular localization with a synthetic ligand that induces the dimerization of proteins. *Proc. Natl. Acad. Sci. U.S.A.* **1996**, *93*, 4604-4607. (g) Spencer, D. M.; Wandless, T. J.; Schreiber, S. L.; Crabtree, G. R. Controlling signal transduction with synthetic ligands. *Science* **1993**, *262*, 1019-1024. (h) Riveria, V. M.; Clackson, T.; Natesan, S.; Pollock, R.; Amara, J. F.; Keenan, T.; Magari, S. R.; Phillips, T.; Courage, N. L.; Cerasoli, Jr., F.; Holt, D. A.; Gilman, M. A humanized system for pharmacologic control of gene expression. *Nat. Med.* **1996**, *2*, 1028-1032.

<sup>5</sup>De Vos, A. M.; Ultsch, M.; Kossiakoff, A. A. Human growth hormone and extracellular domain of its receptor: crystal structure of the complex. *Science* **1992**, *255*, 306-312.

<sup>6</sup>The Available Chemicals Directory (ACD) is distributed by Molecular Design Ltd. San Leandro, CA.

<sup>7</sup>(a) Yun, W.; Mohan, R. Heck reaction on solid support: synthesis of indole analogs. *Tetrahedron Lett.* **1996**, *37*, 7189-7192. (b) Zhang, H.-C.; Maryanoff, B. E. Construction of indole and benzofuran systems on the solid phase via palladium-mediated cyclizations. *J. Org. Chem.* **1997**, *62*, 1804-1809.

<sup>8</sup>(a) Fagnola, M. C.; Candiani, I.; Visentin, G.; Cabri, W.; Zarini, F.; Mongelli, N.; Bedeschi, A. Solid-phase synthesis of indoles using the palladium-catalysed coupling of alkynes with iodoaniline derivatives. *Tetrahedron Lett.* **1997**, *38*, 2307-2310. (b) Zhang, H.-C.; Brumfield, K. K.; Maryanoff, B. E. Synthesis of trisubstituted indoles on the solid phase via palladium-mediated heteroannulation of internal alkynes. *Tetrahedron Lett.* **1997**, *38*, 2439-2442. (c) Collini, M. D.; Ellingboe, J. W. The solid phase synthesis of tri-substituted indoles. *Tetrahedron Lett.* **1997**, *38*, 7963-7966. (d) Zhang, H.-C.; Brumfield, K. K.; Jaroskova, L.; Maryanoff, B. E. Facile substitution of resin-bound indoles via the Mannich reaction. *Tetrahedron Lett.* **1998**, *39*, 4449-4452.

<sup>9</sup>Fukuyama, T.; Chen, X.; Peng, G. A novel tin-mediated indole synthesis. *J. Am. Chem. Soc.* **1994**, *116*, 3127-3128.

<sup>10</sup>Batcho, A. D.; Leimgruber, W. Indoles from 2-methylnitrobenzenes by condensation with formamide acetals followed by reduction: 4-benzyloxyindole. *Org. Syn. Coll. Vol. VII* 34-41.

<sup>11</sup>Li, B.; Fields, S. Identification of mutations in p53 that affect its binding to SV40 large T antigen by using the yeast two-hybrid system. *FASEB*, **1993**, *7*, 957-963.

<sup>12</sup>Holt, K. H.; Olson, A. L.; Moye-Rowley, W. S.; Pessin, J. E. Phosphatidylinositol 3-kinase activation is mediated by high-affinity interactions between distinct domains within the p110 and p85 subunits. *Mol. Cell Biol.* **1994**, *14*, 42-49.

<sup>13</sup>(a) Smith, G. P. Filamentous fusion phage: novel expression vectors that display cloned antigens on the virion surface. *Science* **1985**, *228*, 1315-1317. (b) Lowman, H. B.; Bass, S. H.; Simpson, N.; Wells, J. A. Selecting high-affinity binding proteins by monovalent phage

---

display. *Biochemistry* 1991, 30, 10832-10838. (c) For a review see: Smith, G. P.; Petrenko, V. A. Phage Display. *Chem. Rev.* 1997, 97, 391-410.

<sup>14</sup>(a) Leung, D. W.; Spencer, S. A.; Cachianes, G.; Hammonds, R. G.; Collins, C.; Henzel, W. J.; Barnard, R.; Waters, M. J.; Wood, W. I. Growth hormone receptor and serum binding protein: purification, cloning, and expression. *Nature*, 1987, 330, 537-543. (b) Fuh, G.; Mulkerrin, M. G.; Bass, S.; McFarland, N.; Brochier, M.; Bourell, J. H.; Light, D. R.; Wells, J. A. The human growth receptor. *J. Biol. Chem.* 1990, 265, 3111-3115.

<sup>15</sup>Ma, J.; Ptashne, M. A new class of yeast transcriptional activators. *Cell*, 1987, 51, 113-119.

<sup>16</sup>Goeddel, D. V.; Heyneker, H. L.; Hozumi, T.; Arentzen, R.; Itakura, K.; Yansura, D. G.; Ross, M. J.; Miozzari, G.; Crea, R.; Seeburg, P. H. Direct expression in *Escherichia coli* of a DNA sequence coding for human growth hormone. *Nature* 1979, 281, 544-548.

<sup>17</sup>Gill, G.; Ptashne, M. Mutants of GAL4 protein altered in an activation function. *Cell* 1987, 51, 121-126.

<sup>18</sup>(a) Cramer, A.; Whitehorn, E. A.; Tate, E.; Stemmer, W. P. C. Improved green fluorescent protein by molecular evolution using DNA shuffling. *Nat. Biotech.* 1996, 14, 315-319. (b) Cramer, A.; Dawes, G.; Rodriguez, Jr., E.; Silver, S.; Stemmer, W. P. C. Molecular evolution of an arsenate detoxification pathway by DNA shuffling. *Nat. Biotech.* 1997, 15, 436-438. (c) Zhang, J.-H.; Dawes, G.; Stemmer, W. P. C. Directed evolution of a fucosidase from a galactosidase by DNA shuffling and screening. *Proc. Natl. Acad. Sci. USA* 1997, 94, 4504-4509 (d) Cramer, A.; Raillard, S.-A.; Bermudez, E.; Stemmer, W.P.C. DNA shuffling of genes from diverse species accelerates directed evolution. *Nature* 1998, 391, 288-291

<sup>19</sup>Leung, D. W.; Chen, E.; Goeddel, D. V. A method for random mutagenesis of a defined DNA segment using a modified polymerase chain reaction. *Technique* 1989, 1, 11-15.

<sup>20</sup>Bartel, P.; Chien, C.-T.; Sternglanz, R.; Fields, S. Elimination of false positives that arise in using the two-hybrid system. *Biotechniques* 1993, 14, 920-924.